SPbGASU
1832

ARCHITECTURE & ENGINEERING

Volume 10
Issue 3
September, 2025

By Architects. For Architects.
By Engineers. For Engineers.

Architecture
Civil and Structural Engineering
Mechanics of Materials
Building and Construction
Urban Planning and Development
Transportation Issues in Construction
Geotechnical Engineering and Engineering Geology
Designing, Operation and Service
of Construction Site Engines

eISSN: 2500-0055
http://aej.spbgasu.ru/

Architecture and Engineering

Volume 10 Issue 3 (2025)

ISSN: 2500–0055

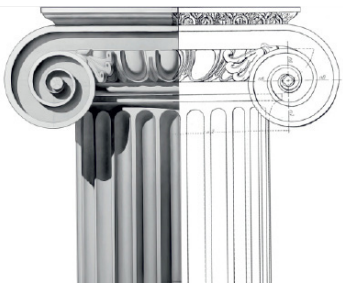

CONTENTS

Architecture and Engineering
peer-reviewed scientific journal
Start date: 2016/03
4 issues per year

Founder, Publisher:
Saint Petersburg State University of Architecture and Civil Engineering

Indexing:
Scopus, Russian Science Citation Index, Directory of Open Access Journals (DOAJ), Google Scholar, Index Copernicus, Ulrich's Periodicals Directory, WorldCat, Bielefeld Academic Search Engine (BASE), Library of University of Cambridge and CyberLeninka

Corresponding address:
4 Vtoraya Krasnoarmejskaja Str.,
St. Petersburg, 190005, Russia

Website: http://aej.spbgasu.ru/
Phone: +7(812) 316 48 49
Email: aejeditorialoffice@gmail.com

Date of issue: October 02, 2025

The Journal was re-registered by the Federal Service for Supervision of Communications, Information Technologies and Mass Communications (Roskomnadzor) on May 31, 2017;
registration certificate of media organization El No. FS77–70026

DOI: 10.23968/2500-0055-2025-10-3-3-14

ARCHITECTURAL DESIGNS INSPIRED BY NATURE AND MATHEMATICAL MODELS

Aslı Taş[1]*, Güneş Mutlu Avinç[2]

[1]Nevşehir Hacı Bektaş Veli University, Nevşehir, Turkey
[2]Muş Alparslan University, Muş, Turkey

*Corresponding author's email: aslydz@gmail.com

Abstract

Introduction: This paper explores how nature-inspired mathematical models and principles are applied in architectural design and how these approaches contribute to innovative and sustainable solutions. Architectural structures incorporating nature-inspired and mathematical models have been widely studied in the literature. However, research examining the relationship between nature and mathematics specifically within the field of architecture remains limited. Addressing this gap, the study investigates the interplay between mathematics and nature in architectural design. Its contribution lies in providing a holistic examination of mathematical models in architecture. Within the scope of the study, five examples demonstrating different mathematical theorems were analyzed. **Methods:** The structures were evaluated using qualitative content analysis, while the mathematical models were identified through visual content analysis. The findings are summarized in a table. **Conclusion:** Architecture is profoundly shaped by the relationship between nature and mathematics. Analyzing the mathematics inherent in nature and applying these principles in design serves as a guide for creating aesthetically pleasing, sustainable, and innovative buildings.

Keywords: mathematical model, nature-inspired architecture, golden ratio, fractal geometry, mathematics in architecture.

Introduction

Humans are inspired by and learn from nature in all their creations. However, this influence is not unidirectional, as humans also attribute order to nature (Peker, 2017). The search for order within the apparent chaos of nature reflects human efforts to understand and reconstruct the physical world. In this process, mathematics serves as a tool to interpret the complexity and patterns of nature. Ancient philosophers argued that the fundamental structure of the universe is rooted in mathematics and that this serves as the creative element of nature (Cooper, 1997). This perspective has influenced architecture since antiquity. Architecture materializes humanity's relationship with nature by embodying mathematical order and harmony in the physical environment. From prehistoric times through Ancient Greece, Rome, the Renaissance, and Modern Architecture, mathematical principles derived from nature have shaped architectural design.

The relationship between architecture and mathematics is evident in the direct application of fundamental mathematical concepts — such as proportion, symmetry, and geometry — to building design. Architects employ mathematics to achieve structures that are balanced aesthetically and functionally. Throughout history, mathematical principles have provided stability and harmony in architectural forms. Furthermore, the mathematics of nature enables the imitation of natural forms and the integration of buildings with their surroundings. In this way, the mathematics of nature has long served as a source of inspiration for both aesthetic and functional aspects of architecture (Aejaz and Yasmeen, 2023; Kavurmacıoğlu and Arıdağ, 2013).

The use of mathematics and geometry in architecture is not only a compositional tool but also a language of representation, employed throughout history to convey cultural, spiritual, and even cosmic meanings in architectural works. As Salvadori (1968) emphasizes, although architecture is grounded in the physical world, its connection with abstract mathematical principles is indispensable. No architectural work can exist without mathematical foundations such as measurements, proportions, and geometry. For instance, the use of geometry to express cosmic themes in ancient Greek and Roman architecture illustrates how the mathematical order inherent in nature influences architectural design (Ostwald and Williams, 2015). The direct relationship between the mathematical order found in nature and its application in architecture demonstrates how mathematics has shaped both the visual and structural language of buildings across cultures

and historical periods. During the Renaissance, architects, artists, and designers extensively explored the relationship between mathematics and nature. They documented the golden section ratios and applied them in remarkable works, including sculptures, paintings, and architectural designs (Akhtaruzzaman and Shafie, 2011).

Mathematical models represent the structure and organization of forms found in nature and have been employed in architectural design for centuries (Nowak, 2015). The golden ratio, one of nature's mathematical properties, can be observed across a wide range of length scales, from the galactic to the atomic (Marples and Williams, 2022). Using Fibonacci numbers, the golden ratio forms a golden spiral that appears ubiquitously in nature, such as in shells, pine cones, the arrangement of seeds in a sunflower head, and even in galaxies. Adolf Zeising, a mathematician and philosopher, concluded that the golden ratio operates as a universal law when studying natural phenomena (Akhtaruzzaman and Shafie, 2011). Fractal geometry, in turn, explains many natural formations, from the branching structures of plants to the rings of Saturn, reflecting the self-similarity inherent in nature. Examples of fractal structures include blood vessels, lungs, river networks, lightning, tree branches, rocky coastlines, and weather patterns (Bovill, 1996; Hacısalihoğlu, 2015). The concept of tessellation, important in aesthetics, mathematics, chemistry, and molecular science, refers to the covering of a plane without overlaps or gaps. Various tessellation patterns can be observed in self-organizing systems in biology and nanotechnology (Cheng et al., 2018). Similarly, the Voronoi diagram describes a self-organizing system of biological structures, as seen in dragonfly wings, turtle shells, honeycombs, and sea urchin shells (Nowak, 2015). Natural examples such as tree branches, rocks, and Romanesco broccoli also exhibit Voronoi structures (Kornev, 2018; Zhao et al., 2016). Modern design increasingly relies on mathematical models to understand the principles of self-organization in biological structures. The use of computational geometry in architecture and urban planning offers new opportunities for designing structures and elements that integrate these natural processes and patterns (Nowak, 2015).

To summarize the information presented so far, the relationship between architecture and mathematics is grounded in the use of proportion, symmetry, geometry, and mathematical models in building design. Concepts such as the golden ratio, fractal geometry, and tessellation have been widely employed in architecture to achieve both aesthetic and structural balance. Throughout history, the mathematics of nature has inspired the imitation of natural forms in architecture and facilitated the harmonious integration of buildings with their surroundings. Since the Renaissance, mathematical proportions have gained particular importance for ensuring both structural stability and visual appeal. Fractal and geometric forms observed in nature are now reinterpreted and applied in architecture through computational design techniques. From this perspective, the present study examines the use of mathematical models — including the golden ratio, fractal geometry, tessellation, Voronoi diagrams, and the Sierpiński Triangle — in architectural design. The relationship between mathematics, nature, and architecture is explored through a selection of building examples. A unique aspect of this study is the presentation of a method for evaluating the interplay between nature and mathematics, highlighting how buildings incorporate mathematical models in facades, floor plans, and three-dimensional forms. For this purpose, abstractions were created based on photographs of buildings obtained from various websites and books. Traces of mathematical models were identified across different dimensions, reflecting patterns inspired by nature. These patterns relate to nature not only at the structural level but also in terms of spatial organization.

Mathematical Models and Principles Used in Architectural Design

Mathematical principles are frequently employed in architecture to achieve aesthetic appeal, structural efficiency, and harmony with nature. These principles contribute to the modeling of natural systems and the design of architectural structures. Mathematical models have been applied in architecture in various forms since antiquity. Among these, the golden ratio is the most widely recognized and utilized. The golden ratio, or golden proportion, represents an irrational number approximately equal to 1.6180339887 and is denoted by the Greek letter phi (φ). Due to its unique and intriguing properties, the golden ratio — also referred to as the golden section — has been extensively studied by researchers and mathematicians (Akhtaruzzaman and Shafie, 2011). It generally describes the mathematical proportion between sizes and shapes (Fig. 1). Valued for its

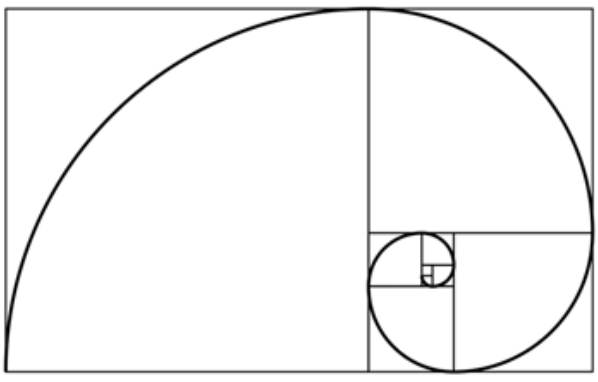

Fig. 1. Golden ratio (drawn by the authors)

aesthetic appeal, it is believed to impart beauty and harmony in nature and art (Bergil, 1993). According to the architectural theorist Neufert, the golden ratio functions as an architectural ratio and is considered an inherent law in architecture. Le Corbusier, meanwhile, viewed it as a natural rhythm reflected in the human organism. The golden ratio is applied across various art forms to create visual balance and harmony. In architecture, it has been used in both floor plans and facades. Prominent historical examples include the Pyramid of Cheops and the Parthenon, which exemplify the application of golden ratio principles (Peker, 2017).

Fractal geometry represents a form of complex, repetitive, and continuous patterns (Fig. 2) (Bovill, 1996). It is used to describe structures that cannot be defined by Euclidean geometry. The forms of natural objects rarely correspond to the rigid shapes of Euclidean geometry, which is insufficient for explaining the complexity of natural structures. Consequently, the geometry of nature is best described by fractal geometry (Mandelbrot, 1982). A defining characteristic of fractal structures is their self-similarity across different scales. Regardless of scale, the degree of irregularity in a fractal remains consistent, producing ordered complexity within apparent randomness. This property allows fractals to be used effectively to describe and analyze natural forms. In architecture, fractal principles are applied to examine the complexity, repetition, and self-similarity of floor plans and facades (Hagerhall et al., 2004).

Tessellation refers to the complete covering of a plane with repeating geometric shapes (Fig. 3) (Grünbaum and Shephard, 1987). Tessellations, which have been employed in engineering, art, and architecture since antiquity, can be categorized into three main types: regular, semi-regular, and irregular. Regular tessellations are created from shapes such as squares, rectangles, and triangles, while semi-regular tessellations arise from combining different polygons at a common vertex. Irregular tessellations are formed by arranging groups of shapes in different combinations. In architecture, tessellations are widely applied in exterior claddings and ceramic surfaces, serving both aesthetic and structural purposes (Gazi and Korkmaz, 2015).

Voronoi diagrams, originating in the 17th century and first formally illustrated by Georgy Voronoi in 1903, represent another important mathematical model (Fig. 4). As a data segmentation method, Voronoi diagrams are particularly suited for solving closest-point problems (Vassilev and Eades, 2013). Constructed from a set of points generating polygonal cells, this system defines and measures relationships between points in various fields. With advances in computational technologies, Voronoi diagrams have become a valuable tool in architectural design, yielding effective results in facades, spatial organization, urban planning, mapping, and analytical studies (Sack and Urrutia, 1999). Moreover, Voronoi diagrams are widely observed in nature, including in cell division, animal skin patterns, and leaf surfaces (Nowak and Rokicki, 2016).

The Sierpiński triangle, introduced by the Polish mathematician Wacław Sierpiński in 1915, exemplifies a self-replicating system of progressively

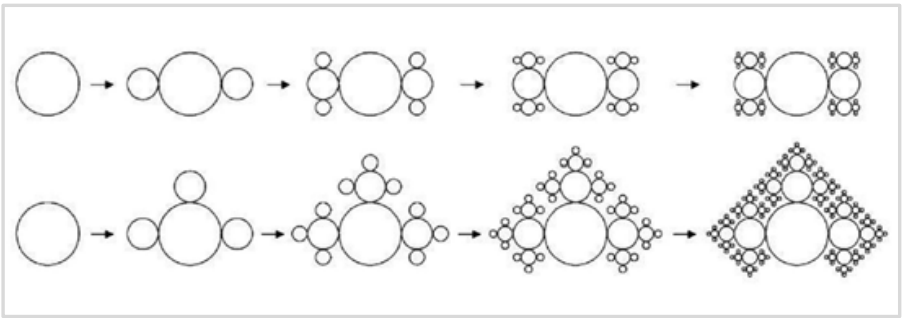

Fig. 2. Example of a fractal process (Rian et al., 2007)

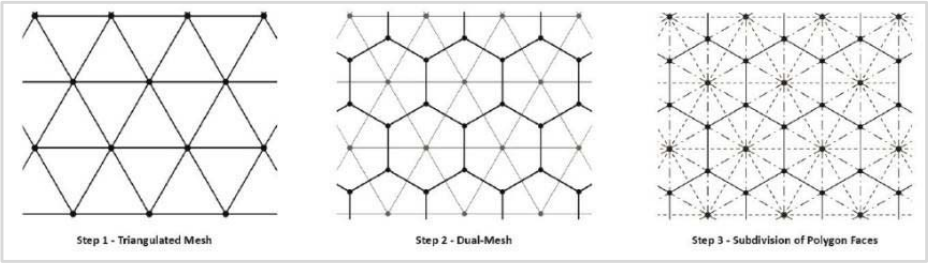

Fig. 3. Tessellation process (Chandra et al., 2015)

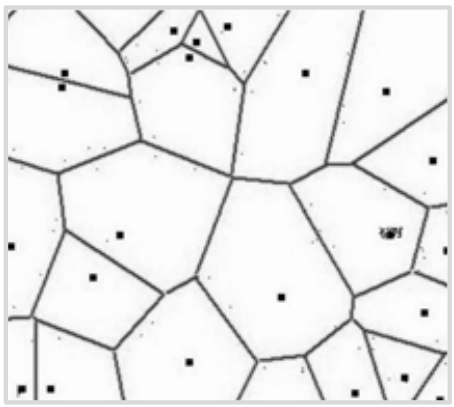

Fig. 4. Voronoi diagram (drawn by the authors)

smaller triangles (Fig. 5). The model begins with an equilateral triangle or square, and new triangles are generated by connecting the midpoints of each side. This process is repeated iteratively, creating a fractal structure (Bovill, 1996). The Sierpiński triangle offers both aesthetic and functional advantages in architectural design, particularly in modular systems, optimization of building components, and shading strategies.

Methods

The study employs a methodology combining qualitative and visual content analysis. Through qualitative content analysis, general information about the architectural characteristics of the selected buildings was obtained. Visual content analysis involved the examination of architectural drawings and photographs sourced from various websites. The buildings were evaluated in terms of their facades, plans, and architectural elements, with particular attention to five mathematical models and their relationship with nature. The results of these evaluations are presented in tables for each building. These findings are significant in demonstrating how the relationship between mathematics and nature is applied in architecture and the types of designs it inspires. More specifically, the purpose of applying visual content analysis was to determine how mathematical models inspired by nature are reflected in architectural design. This method made it possible to identify and classify the mathematical principles embedded in the form, plan, and facade design of the buildings, thereby presenting the role of mathematical models in architectural practice in a more systematic manner. Furthermore, the process has the potential to generate datasets that may be integrated into future AI-supported content recognition and manual classification systems.

The buildings examined in this study are the Villa at Garches (Le Corbusier), Arab World Institute (Jean Nouvel), Toronto Engineering School (ZAS Architects), Beijing National Aquatics Center (PTW Architects + CSCE + Arup), and Grand Egyptian Museum (Heneghan Peng Architects). These iconic structures were selected because they exemplify both the application of mathematical principles and a design philosophy in harmony with nature. The Villa at Garches demonstrates the use of the golden ratio, aligning with human scale and natural context. The Arab World Institute incorporates complex fractal patterns inspired by Islamic geometry and environmental factors. The facade of the Toronto Engineering School is shaped by intricate tessellations, reflecting a strong relationship with nature. The Beijing National Aquatics Center has a facade structure based on Voronoi diagrams, effectively embodying natural processes and forms. Finally, the Grand Egyptian Museum integrates Sierpiński triangles into its plan, facade, and architectural elements, forging strong connections with both nature and cultural heritage. Due to their close ties with nature and mathematical principles, these buildings form a suitable dataset for the study.

The scope of the study is illustrated in the flowchart presented in Fig. 6.

Results

In this section, the findings derived from the case study buildings are summarized in tabular form (Tables 1–6).

Villa at Garches

Also known as Villa Stein-de Monzie, the Villa at Garches was designed by Le Corbusier in France between 1927 and 1928. It is one of his most iconic works, exemplifying five key architectural principles: pilotis, horizontal ribbon windows, a free facade, an open plan, and a roof garden. The building is characterized by spaciousness, flexibility, and modern functionality. Importantly, Le Corbusier considered the golden ratio not merely as

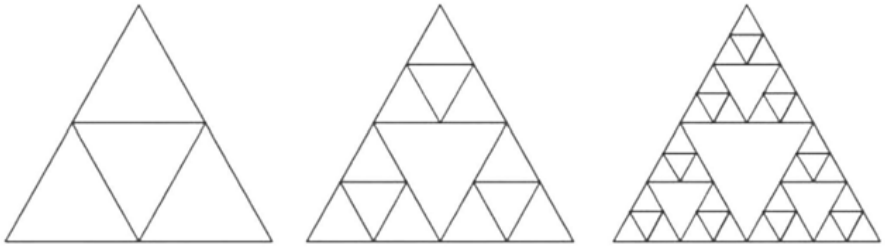

Fig. 5. Sierpiński triangle (drawn by the authors)

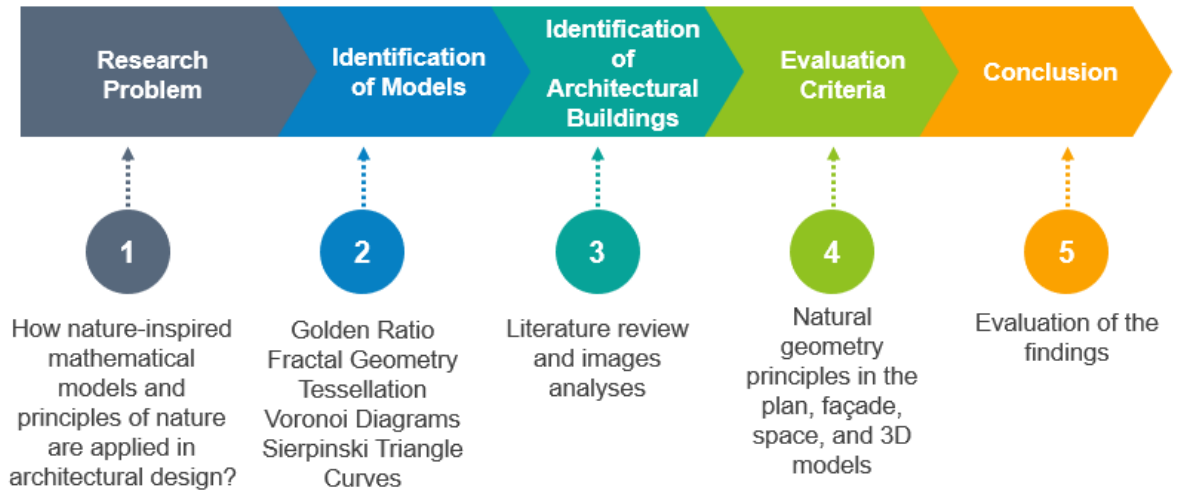

Fig. 6. Flowchart of the study

Table 1. **Villa at Garches — building analysis**

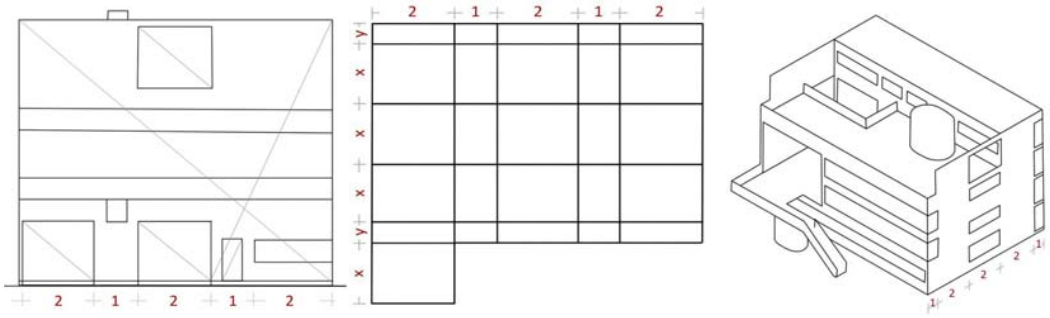

(drawn by the authors)

Relation of the facade to the golden ratio	**Relation of the plan to the golden ratio**	**Relation of the architectural elements to the golden ratio**
The harmony of horizontal and vertical facade proportions is organized according to the principles of the golden ratio. The placement of the windows, the spacing of the columns, and the overall dimensions of the facade are designed in accordance with this ratio.	The width, length, and height of the spaces are proportioned based on the golden ratio. This ensured that the rooms and spaces are harmonious, rhythmic, and fluid.	The stairs, window frames, columns, balcony projections, and eaves were designed according to the golden ratio principles.
Relation of the facade to nature	**Relation of the plan to nature**	**Relation of the architectural elements to nature**

(en.wikiarquitectura.com, 2017; Front Desk, 2014; Wood, 2025)

The windows are designed to optimize daylight. The rhythm of the facade masses resembles the layering and depth found in natural forms. The large windows visually integrate the exterior with the interior.	The building's plan presents a seamless integrity comparable to the fluidity observed in natural systems. The transitions between the interior and exterior spaces are continuous. Nature views are incorporated as active components of the interior, while the terraces strengthen the integration with the environment.	The thin delicate columns resemble tree trunks, while the openings between them allow the circulation of air and light like tree branches. The roof terrace establishes a direct interaction with nature. The continuity between the interior and exterior spaces, along with the inclusion of landscape elements on the roof, reinforces this relationship.

a mathematical principle but as a means to achieve aesthetic coherence and visual harmony. Through this application, the villa presents a design that is both balanced and visually satisfying (Herz-Fischler, 1984) (Table 1).

Arab World Institute

Designed by Jean Nouvel and completed in Paris in 1987, the Arab World Institute exemplifies a synthesis of modern and traditional design elements. Its most distinctive feature is the facade, composed of metallic panels that form a secondary wall. These panels are inspired by traditional mashrabiya motifs. By merging modern and traditional elements, the building seeks to create a symbolic bridge between Arab and Western cultures. Functionally, the Arab World Institute serves as a multidisciplinary research and cultural center, accommodating educational, cultural, and commercial activities. Architecturally and culturally, it has become an iconic landmark within its urban context (McKiernan, 2013) (Table 2).

Toronto Engineering School (Bergeron Center)

The Toronto Engineering School was designed by ZAS Architects in 2018 for the Faculty of Engineering at the University of Toronto, Ontario, Canada. The building is distinguished by its modern and dynamic facade design. It incorporates sustainable features,

Table 2. **Arab World Institute — building analysis**

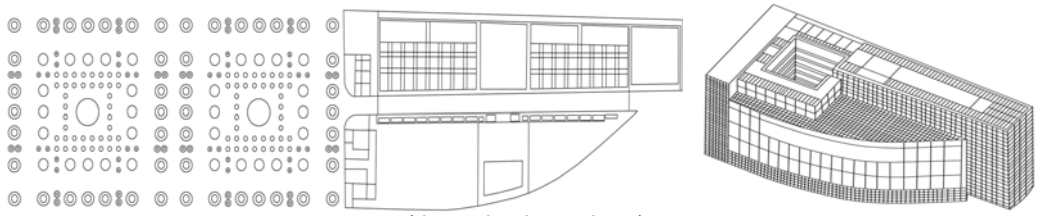

(drawn by the authors)

Relation of the facade to fractals	Relation of the plan to fractals	Relation of the architectural elements to fractals
The traditional motifs on the facade exhibit fractal characteristics, consisting of repeating patterns across multiple scales. The circular motifs intertwine to create a complex, multi-layered facade. The interplay of light and shadow follows fractal geometry principles, and the repetition of patterns at macro and micro scales generates a dynamic and rhythmic visual effect.	The building plan organizes various functional spaces symmetrically around a central axis. The layout expands outward from the center according to fractal principles, with each unit reflecting the larger order at smaller scales. The interior spatial hierarchy repeats at multiple scales, consistent with fractal geometry principles.	Numerous structural elements such as the shutters, interior columns, railings, as well as ceiling and floor coverings display fractal features. These elements contribute to a sense of balance, harmony, depth, and movement within the spaces. The facade shutters regulate daylight while producing fractal-like variations of light and shadow.

(Architecturestudio, 2025; cdn.sortiraparis.com, 2025; lookphotos, 2008)

Relation of the facade to nature	Relation of the plan to nature	Relation of the architectural elements to nature
The facade design mimics dynamic natural processes. Traditional mashrabiyas adapt to environmental conditions like organisms orient toward sunlight. Similar to plants opening and closing leaves for photosynthesis, the shutters adjust to control daylight, heating, and cooling. They also generate light patterns reminiscent of sunlight filtering through tree branches.	The building plan represents an architectural expression of organic forms and cycles observed in nature. The central courtyard functions as an inner garden, facilitating natural ventilation, daylight penetration, and energy efficiency. The plan exhibits a multi-layered, integrated system in which different functional spaces interact similarly to natural processes. Continuity between the interior and exterior spaces maintains a strong connection with nature.	Natural forms and patterns inform the design of the architectural elements. Natural materials are used for the flooring and walls, and the interior spaces incorporate water features and plants to create a microclimate that reinforces a connection with nature.

including a green roof, solar panels, and rainwater collection systems. The exposed structural systems transform the educational spaces into experimental environments. Overall, the Toronto Engineering School exemplifies a modern, innovative, sustainable, and flexible architectural approach. Environmentally responsive design strategies are a prominent feature of the building (URL-1) (Table 3).

Beijing National Aquatics Center (Water Cube)

Designed by PTW Architects, CSCE, and Arup and completed in 2008, the Beijing National Aquatics Center is located in Beijing, China. Its outer shell is inspired by the cellular structure of water molecules and the formation of foams in nature. Constructed for the 2008 Beijing Olympics, the building is recognized as an innovative and iconic example of contemporary architecture. It serves not only for competitive swimming but also for a variety of water sports. In 2010, the addition of a water park further expanded its use (Zou and Leslie-Carter, 2010) (Table 4).

Grand Egyptian Museum

The design by Heneghan Peng Architects was selected as the first-place winner among 1,557 entries in an international competition. The construction began in 2005, and the museum officially opened in 2023. Covering a total area of 480,000 square meters, it is one of the largest archaeological museums in the world. Its design integrates references to Egypt's cultural heritage with a contemporary architectural approach. The building is situated near the Pyramids of Giza. The museum's triangular and sloping surfaces are inspired by the pyramids themselves. In addition to its primary exhibition function, the museum also serves as a cultural and scientific center. The building is

Table 3. **Toronto Engineering School — building analysis**

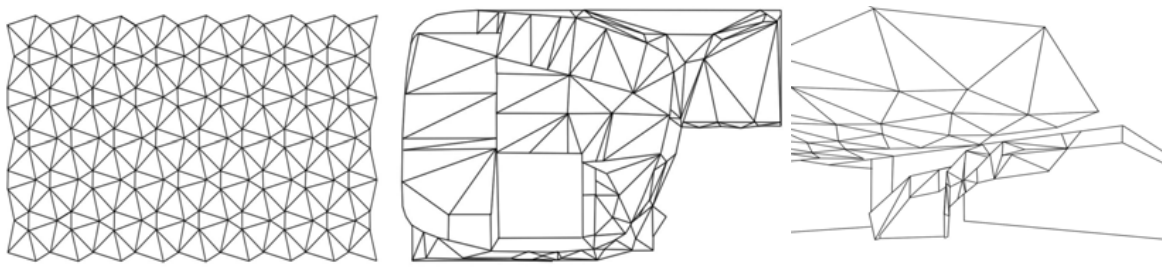

(drawn by the authors)

Relation of the facade to tessellation	Relation of the plan to tessellation	Relation of the architectural elements to tessellation
The facade cladding is designed according to the tessellation principles. Glass and metal panels repeat rhythmically along the facade. Beyond their aesthetic role, these panels contribute to daylight control, energy efficiency, and shading.	The tessellation principles are applied in the interior design. Tessellations in classrooms, laboratories, and open offices enhance spatial efficiency, and promote seamless, fluid circulation throughout the building.	Tessellation patterns are integrated into the ceiling panels, floor and wall coverings, and railings. These patterns add depth and dynamism to the spaces. The lighting elements are also designed in accordance with the tessellation principles.

(APA Facade Systems, 2025; images.adsttc.com, 2025)

Relation of the facade to nature	Relation of the plan to nature	Relation of the architectural elements to nature
The dynamic facade reflects patterns found in nature. The cladding system mimics natural shadow play and evokes leaf-like motifs. The curved and flexible structure of the facade embodies the fluidity of organic forms.	The building plan evokes intertwined natural organisms. The functional spaces are interconnected to reflect symbiotic relationships in nature. Natural ventilation and daylight penetration are maximized, and the building is sited in harmony with the existing topography.	Natural materials, such as stone and wood, are employed to create a warm interior environment. Shadow patterns generated by the facade panels reinforce a connection with natural phenomena. The terraces and courtyards incorporate vegetation to enhance the connection with nature.

Table 4. **Beijing National Acuatics Center — building analysis**

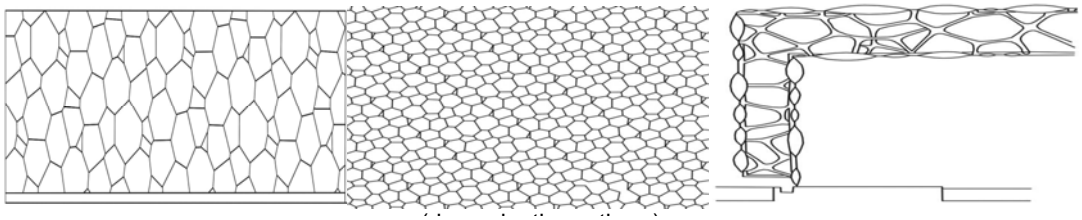

(drawn by the authors)

Relation of the facade to Voronoi diagrams	Relation of the plan to Voronoi diagrams	Relation of the architectural elements to Voronoi diagrams
The building's facade is inspired by Voronoi diagrams. The facade cells, arranged in an irregular organic pattern, are covered with ethylene-tetrafluoroethylene (ETFE) panels. Their arrangement according to Voronoi patterns creates dynamic light reflection and diffraction within the interior, producing a unique texture, multi-layered visual effects, and a sense of continuous movement.	The interior layout is also guided by Voronoi principles. The building plan organizes various functional spaces around a central core. The swimming pools and audience seating areas serve as primary functions, while service, circulation, and technical zones occupy supporting roles. The swimming pools and audience seating areas are designed according to Voronoi principles, promoting fluidity and efficient circulation throughout the space.	The structural elements and cladding also reflect Voronoi patterns. The cellular structure of these patterns is also maintained in the steel frame system, resulting in more balanced and stable load distribution throughout the structure.

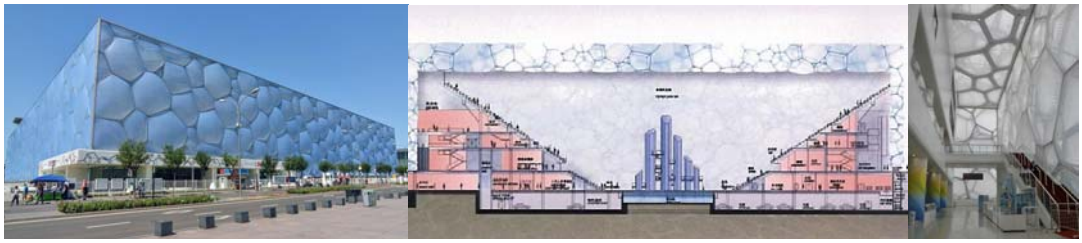

(Trubiano, 2013; w.litour.cn, 2025; Wordpress, 2025)

Relation of the facade to nature	Relation of the plan to nature	Relation of the architectural elements to nature
The facade draws inspiration from the geometric structures of water droplets and foams. These naturally irregular yet interconnected structures informed the design of the facade shell. The resulting cellular arrangement reflects the geometry, flexibility, and transparency of biological cell membranes.	The building plan evokes the fluidity and continuity of water, reflecting the symbiotic relationships observed among natural organisms. The building's interior is organized around the cooperative interaction of different functions, similar to an ecosystem. The water-related spaces are centrally located, reflecting the natural concept of gathering around a water source.	The ETFE panels emulate the lightness, flexibility, and strength of cell membranes. The transparency of the panels maximizes natural daylight penetration. They also provide temperature regulation and natural ventilation of the interior. This contributes to energy efficiency and sustainable performance.

distinguished by its integration of natural forms with cultural heritage and modern architecture, resulting in an original design (Attia et al., 2021) (Table 5).

The use of mathematical models and the relationship of the examined buildings with nature are summarized in Table 6. This table compares the buildings in terms of the mathematical models applied. As shown, nature-inspired mathematical models not only enhance aesthetic and structural optimization but also improve the integration of buildings with their surroundings. Such analyses are essential for understanding how mathematical models can be applied at different scales and incorporated into architectural design.

Conclusion

The relationship between mathematics and architecture in creating aesthetically pleasing and functional structures is based on nature-inspired mathematical models, such as the golden ratio, Voronoi diagrams, the Sierpiński triangle, curves, and parabolas. These mathematical principles, derived from observations of nature, have enabled architects to design structures that are simultaneously environmentally friendly, durable, aesthetically balanced, structurally sound, and lightweight.

Each mathematical model contributes to architecture in distinct ways. The golden ratio is employed to achieve proportionally balanced and visually harmonious building forms. Fractal geometry establishes relationships among complex, self-repeating patterns, supporting the design of dynamic and organic spaces. Tessellations are used to model intricate repeating patterns, ranging from traditional ornamentation to modern facade cladding. Voronoi

Table 5. **Grand Egyptian Museum — building analysis**

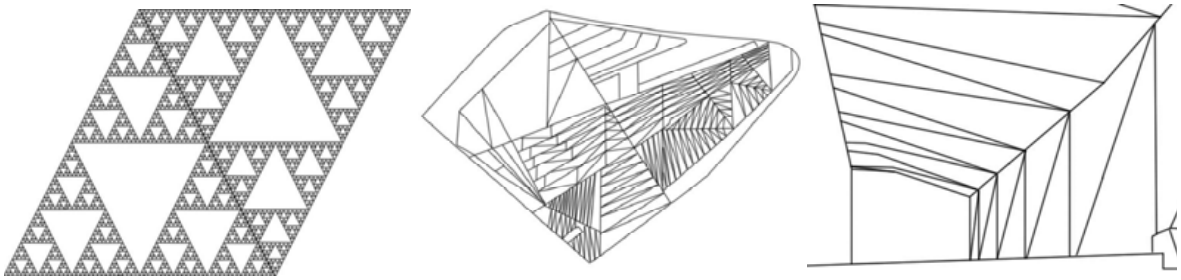

(drawn by the authors)

Relation of the facade to the Sierpiński triangle	Relation of the plan to the Sierpiński triangle	Relation of the architectural elements to the Sierpiński triangle
The building's facade is inspired by Sierpiński triangles and curved surfaces. The multi-layered, repetitive triangular structure is clearly articulated, simultaneously referencing the nearby Pyramids of Giza.	The Sierpiński triangle served as a reference for the museum's layout and interior design. Triangular and polygonal forms were employed in the planning of the exhibition spaces, research centers, and other functional areas, maintaining the hierarchical structure characteristic of Sierpiński triangles.	Sierpiński triangles are incorporated throughout the interior spaces, structural elements, and roof components of the building. The stairs and walkways consist of repetitive triangular units, and triangular patterns are also applied to the facades of the exhibition halls.

(besix.com, 2025; Egypt Forward, 2025; orascom.com, 2025)

Relation of the facade to nature	Relation of the plan to nature	Relation of the architectural elements to nature
Inspired by the slopes and geometric structure of the Giza Pyramids, the building harmonizes with its natural and cultural surroundings. The curved surfaces of the facade allow daylight to enter the interior spaces at varying angles, introducing rhythm and dynamism reminiscent of natural processes. Additionally, the triangular forms on the facade echo crystalline and mineral structures found in nature.	The building's plan evolves in a manner similar to the growth of cellular structures in nature, exhibiting gradual and organic development. The circulation spaces feature soft and fluid transitions, reflecting the continuity and fluidity observed in natural systems. The layout of the exhibition spaces is additionally inspired by geological stratification.	The museum's structural system exhibits an organic design. The interior patterns and motifs are inspired by natural forms. The wall surfaces feature designs reminiscent of ancient Egyptian hieroglyphs. Stone and other natural elements are selected to harmonize with the environment. Additionally, natural landscaping and water features are incorporated into both interior and exterior spaces to provide cooling and enhance the sense of relaxation.

Table 6. **Study summary**

Building	Mathematical model	Application in design	Relation to nature
Villa at Garches	Golden ratio	Facade, plan, architectural elements	The spatial organization resembles the fluid structure of nature. The large windows enhance integration with the surrounding environment.
Arab World Institute	Fractal geometry	Facade, plan, light control	Light-shadow dynamics are generated through traditional mashrabiya motifs, imitating variable lighting effects observed in nature.
Toronto Engineering School	Tessellation	Facade cladding, interior design	The geometric patterns on the facade echo honeycomb structures.
Beijing National Aquatics Center	Voronoi diagram	Facade, structural system, light control	The outer shell mimics the irregular yet interconnected structure of water molecules.
Grand Egyptian Museum	Sierpiński triangle	Facade, plan, structural elements	The triangular forms reference the nearby pyramids, while the geometric patterns reflect crystalline and mineral structures found in nature.

diagrams reflect cellular structures in nature and are applied in architecture for various purposes from the efficient and organic organization of spaces to facade cladding. The Sierpiński triangle facilitates complex visual textures, structural stability, and surface optimization. Curves and parabolas are employed in architecture to achieve both aesthetic refinement and engineering efficiency. Collectively, these nature-inspired mathematical models enrich architectural design by providing both aesthetic appeal and functional innovation.

Architects are increasingly applying mathematical models to develop innovative and sustainable designs. The advancement of computational design tools facilitates this process, creating new opportunities. Integrating mathematics allows for the creation of buildings that emulate the organic, self-organizing systems observed in nature. The method employed in this study enabled the systematic analysis of nature-inspired mathematical models in architecture. Such approaches are valuable for structuring architectural design processes and for integration with digital design tools. With the ongoing development of artificial intelligence, content identification and coding can be made more efficient, reducing the need for manual classification and cataloging. Future studies may incorporate AI-supported systems to enable more comprehensive and automated evaluation of nature-inspired architectural designs. In conclusion, the evolving relationship between architecture and mathematics presents numerous opportunities for future advancements. This paper provides a comprehensive and contemporary analysis of the application of nature-inspired mathematical models and principles in architectural design.

References

Aejaz, S. and Yasmeen, A. (2023). The importance and applications of mathematics in architecture. *International Journal of Current Science (IJCSPUB)*, Vol. 13, Issue 1, pp. 848–887. DOI: 10.13140/RG.2.2.19605.29923.

Akhtaruzzaman, M. and Shafie, A. A. (2011). Geometrical substantiation of Phi, the golden ratio and the baroque of nature, architecture, design and engineering. *International Journal of Arts*, Vol. 1, No. 1, pp. 1–22. DOI: 10.5923/j.arts.20110101.01.

APA Facade Systems (2015). *The Bergeron Centre for Engineering Excellence, York University, Canada*. [online] Available at: https://www.apafacadesystems.com/wp-content/uploads/2017/09/York-University-Lassonde-School-of-Engineering-19_Easy-Resize.com_.jpg [Date accessed 12.08.2025].

Architecturestudio (2021). *Institut du Monde Arabe*. [online] Available at: https://architecturestudio.fr/wp-content/uploads/2021/07/architecturestudio_pastb1_4-2200x1483.jpeg [Date accessed 12.08.2025].

Attia, A. S., Hussein, M. T., and El Shaer, N. S. E. D. (2021). The Grand Egyptian Museum: implications for sustainability. *The International Journal of Tourism and Hospitality Studies*, Vol. 1, Issue 2, pp. 13–24. DOI: 10.21608/ijthsx.2021.82482.1009.

Bergil, M. S. (1993). *Doğada Bilimde Sanatta Altın Oran*. İstanbul: Arkeoloji ve Sanat Yayınları, 192 p.

Besix.com (2022). [online] Available at: https://www.besix.com/en/projects/grand-egyptian-museum [Date accessed 12.08.2025].

Bovill, C. (1996). *Fractal geometry in architecture and design*. Boston: Birkhauser Verlag, 195 p.

cdn.sortiraparis.com (2021). *Institut du Monde Arabe*. [online] Available at: https://cdn.sortiraparis.com/images/80/47294/197171-jardin-d-orient-a-l-institut-du-monde-arabe.jpg [Date accessed 11.08.2025].

Chandra, S., Körner, A., Koronaki, A., Spiteri, R., Amin, R., Kowli, S. and Weinstock, M. (2015). Computing curved-folded tessellations through straight-folding approximation. In: Samuelson, H., Bhooshan, S., Goldstein, R. (eds.). *SimAUD ,15: Proceedings of the Symposium on Simulation for Architecture & Urban Design*. San Diego: Society for Computer Simulation International, pp. 152–159.

Cheng, F., Wu, X.-J., Hu, Z., Lu, X., Ding, Z., Shao, Y., Xu, H., Ji, W., Wu, J., and Loh, K. P. (2018). Two-dimensional tessellation by molecular tiles constructed from halogen–halogen and halogen–metal networks. *Nature Communications*, Vol. 9, 4871. DOI: 10.1038/s41467-018-07323-6.

Cooper, J. M. (ed.) (1997). *Plato. Complete works*. Indianapolis, Cambridge: Hackett Publishing Company, 1808 p.

Egypt Forward (2023). *Grand Egyptian Museum*. [online] Available at: https://egyptfwd.org/Article/6/5718/The-completion-of-placing-more-than-50-of-the-heavy [Date accessed 11.08.2025].

en.wikiarquitectura.com (2017). *Villa Cook*. [online] Available at: https://en.wikiarquitectura.com/villa_cook_3-2/ [Date accessed 11.08.2025].

Front Desk (2014). *Le Corbusier - Villa Stein, Garches*. [online] Available at: https://frontdesk.co.in/forum/Thread-Le-Corbusier-Villa-Stein-Garches?pid=1177 [Date accessed 12.08.2025].

Gazi, A. and Korkmaz, K. (2015). Tesselasyon kullanarak genişleyebilen strüktür tasarımı. In: *Uluslararası Katılımlı 17. Makina Teorisi Sempozyumu*, İzmir, Turkey, June 14–17, 2015.

Grünbaum, B. and Shephard, G. C. (1987). *Tilings and patterns*. New York: W. H. Freeman and Company, 700 p.

Hacısalihoğlu, H. H. (2015). *Fraktal geometri*. Ankara: Seçkin Yayıncılık, 160 p.

Hagerhall, C. M., Purcell, T., and Taylor, R. (2004). Fractal dimension of landscape silhouette outlines as a predictor of landscape preference. *Journal of Environmental Psychology,* Vol. 24, Issue 2, pp. 247–255. DOI: 10.1016/j.jenvp.2003.12.004.

Herz-Fischler, R. (1984). Le Corbusier's "regulating lines" for the Villa at Garches (1927) and other early works. *Journal of the Society of Architectural Historians*, Vol. 43, Issue 1, pp. 53–59. DOI: 10.2307/989975.

images.adsttc.com (2018). *Toronto Engineering School*. [online] Available at: https://images.adsttc.com/media/images/5670/ca23/e58e/ce8c/5500/02b7/slideshow/ZAS_bergeron-055-Pano-Edit.jpg?1450232335 [Date accessed 11.08.2025].

Kavurmacıoğlu, Ö. and Arıdağ, L. (2013). Strüktür tasarımında geometri ve matematiksel model ilişkisi. *Beykent University Journal of Science and Engineering*, Vol. 6, Issue 2, pp. 59–76.

Kolarevic, B. (2003). *Architecture in the digital age: design and manufacturing*. New York, London: Taylor & Francis, 320 p.

Kornev, A. P. (2018). Self-organization, entropy and allostery. *Biochemical Society Transactions*, Vol. 46, Issue 3, pp. 587–597. DOI: 10.1042/BST20160144.

lookphotos (2008). *France, Paris, Institut du Monde Arabe (Arab World Institute) by architect Jean Nouvel and Architecture studio*. [online] Available at: https://www.lookphotos.com/en/images/71117694-France-Paris-Institut-du-Monde-Arabe-Arab-World-Institute-by-architect-Jean-Nouvel-and-Architecture-studio [Date accessed 10.08.2025].

Mandelbrot, B. (1982). *The fractal geometry of nature.* San Francisco: W. H. Freeman and Company, 460 p.

Marples, C. R. and Williams, P. M. (2022). The golden ratio in nature: a tour across length scales. *Symmetry*, Vol. 14, Issue 10, 2059. DOI: 10.3390/sym14102059.

McKiernan, M. (2013). Jean Nouvel, Arab World Institute, 1987. *Occupational Medicine*, Vol. 63, Issue 8, pp. 524–525. DOI: 10.1093/occmed/kqt123.

Nowak, A. (2015). Application of Voronoi diagrams in contemporary architecture and town planning. *Challenges of Modern Technology*, Vol. 6, No. 2, pp. 30–34.

Nowak, A. and Rokicki, W. (2016). On surface geometry inspired by natural systems in current architecture. *Journal Biuletyn of Polish Society for Geometry and Engineering Graphics*, Vol. 29, pp. 41–51.

orascom.com (2023). *Grand Egyptian Museum*. [online] Available at: https://orascom.com/wp-content/uploads/1202-1366x768.jpg [Date accessed 10.08.2025].

Ostwald, M. J. and Williams, K. (2015). Relationships between architecture and mathematics. *Architecture and Mathematics from Antiquity to the Future. Volume 1: Antiquity to the 1500s*, pp. 1–21. DOI: 10.1007/978-3-319-00137-1_1.

Peker, A. U. (2017). Altın oran ve mimarlık: efsane ve gerçekler. *BÜMED*, No. 231, pp. 46–47.

Rian, I. M., Park, J.-H., Ahn, H. U., and Chang, D. (2007). Fractal geometry as the synthesis of Hindu cosmology in Kandariya Mahadev temple, Khajuraho. *Building and Environment,* Vol. 42, Issue 12, pp. 4093–4107. DOI: 10.1016/j.buildenv.2007.01.028.

Sack, J. R. and Urrutia, J. (eds.) (1999). *Handbook of computational geometry*. Amsterdam: Elsevier Science B. V., 1075 p.

Salvadori, M. G. (1968). *Mathematics in architecture.* Englewood Cliffs: Prentice Hall, 173 p.

Trubiano, F. (2013). *Performance based envelopes: a theory of spatialized skins and the emergence of the integrated design professional*. [online] Available at: https://www.researchgate.net/publication/307671319/figure/fig2/AS:406346466906113@1473891955371/Water-Cube-Project-in-Beijing-China-ARUP-Associates-Courtesy-Terri-Boake-University.png [Date accessed 11.08.2025].

URL-1: https://www.zasa.com/york-engineering-2 [Date accessed 11.08.2025].

Vassilev, T. S. and Eades, B. (2013). Generalizations of the Voronoi Diagram. *American Journal of Computational and Applied Mathematics*, Vol. 3, No. 2, pp. 91–96. DOI: 10.5923/j.ajcam.20130302.06.

w.litour.cn (2018). *Water Cube, Beijing*. [online] Available at: https://w.litour.cn/img/beijing/water-cube/water-cube-1.jpg [Date accessed 11.08.2025].

Wood, B. (2020). *An apartment in Le Corbusier's iconic Villa Stein is for sale*. [online] Available at: https://thespaces.com/an-apartment-in-le-corbusiers-iconic-villa-stein-is-for-sale/ [Date accessed 12.08.2024].

Wordpress (2013). *Water Cube*. [online] Available at: https://wanba001.wordpress.com/wp-content/uploads/2013/11/e68d95e88eb7.jpg [Date accessed 10.08.2025].

Zhao, G., Denisova, K., Sehatpour, P., Long, J., Gui, W., Qiao, J., Javitt, D. C., and Wang, Z. (2016). Fractal dimension analysis of subcortical gray matter structures in schizophrenia. *PloS One*, Vol. 11, No. 5, e0155415. DOI: 10.1371/journal.pone.0155415.

Zou, P. X. W. and Leslie-Carter, R. (2010). Lessons learned from managing the design of the 'Water Cube' National Swimming Centre for the Beijing 2008 Olympic Games. *Architectural Engineering and Design Management*, Vol. 6, Issue 3, pp. 175–188. DOI: 10.3763/aedm.2010.0114.

АРХИТЕКТУРНЫЕ ПРОЕКТЫ, ВДОХНОВЛЕННЫЕ ПРИРОДОЙ И МАТЕМАТИЧЕСКИМИ МОДЕЛЯМИ

Аслы Таш[1]*, Гюнеш Мутлу Авинч[2]

[1]Университет Невшехир Хаджи Бекташ Вели, Невшехир, Турция
[2]Университет Муш Альпарслана, Муш, Турция

*E-mail: aslydz@gmail.com

Аннотация
Введение: в данной статье рассматривается применение математических моделей, вдохновленных природой, а также принципов, наблюдаемых в природе, в архитектурном проектировании и их вклад в разработку инновационных и рациональных решений. Архитектурные сооружения, задействующие математические модели, вдохновленные природой, широко изучаются в литературе. Однако исследований, рассматривающих связь между природой и математикой именно в контексте архитектуры, все еще сравнительно немного. С тем чтобы закрыть данный пробел, в данной статье исследуется взаимодействие математики и природы в архитектурном проектировании. В рамках работы выполнен комплексный анализ применения математических моделей в архитектуре. Были проанализированы пять примеров, в основу которых положены различные математические принципы. **Методы:** сооружения оценивались путем качественного контент-анализа, а математические модели выявлялись с помощью визуального контент-анализа. Полученные результаты представлены в виде таблицы. **Заключение:** архитектура формируется под глубоким влиянием взаимодействия природы и математики. Анализ математических закономерностей, присущих природе, и их применение в проектировании служат ориентиром для создания эстетически привлекательных, экологически рациональных и инновационных зданий.

Ключевые слова: математическая модель; архитектура, вдохновленная природой; золотое сечение; фрактальная геометрия; математика в архитектуре.

DOI: 10.23968/2500-0055-2025-10-3-15-27

METHODOLOGICAL ASPECTS OF INTEGRATING ARTIFICIAL INTELLIGENCE INTO THE ENERGY EFFICIENCY MANAGEMENT OF ALGERIA'S HOUSING STOCK

Hocine Sami Belmahdi[1]*, Marouane Samir Guedouh[2,3]

[1] Laboratory of Architecture, Urbanism and Transport: Habitat, Landscape and Urban Mobility (LAUTr), Institute of Architecture and Urbanism, University of Batna 1, Batna, Algeria
[2] Laboratory of Design and Modeling of Architectural Forms and Ambiances (LACOMOFA), University of Biskra, Biskra, Algeria
[3] Institute of Architecture and Urbanism, University of Batna 1, Batna, Algeria

*Corresponding author's email: hocine.belmahdi@univ–batna.dz

Abstract
Introduction: In Algeria, the housing sector accounts for a significant portion of the country's energy consumption, making creative solutions essential for improving energy efficiency. Artificial intelligence (AI) offers effective tools to optimize energy use and reduce the ecological footprint. **Purpose of the study:** This study examines the methodological aspects of integrating AI into the energy efficiency management system of Algeria's housing stock. **Methods:** The Six W's approach was employed to analyze AI integration in this context through two steps. First, the theoretical framework was established. Second, a case study was conducted to better understand the context and explore potential solutions from multiple perspectives. **Results:** The findings of AI integration in urban areas fall into two main categories. The first concerns the stakeholders involved, the methods of AI integration, and the spatio-temporal context. The second addresses the motivation and rationale for selecting specific AI integration strategies, as well as the aspects of AI technologies to be adopted.

Keywords: energy efficiency, Algerian housing, artificial intelligence (AI) integration, Six W's approach, smart city.

Introduction

Energy is one of the most important drivers of human progress and economic growth (Türkoğlu and Kardoğan, 2018). As humanity's contribution to climate change and sustainability challenges increases, improving energy efficiency has become urgent, particularly in highly energy-intensive sectors such as housing, which accounts for a major share of overall consumption. Energy efficiency practices and technologies make it possible to maximize the use of energy with minimal waste. This not only reduces dependence on conventional energy sources but also promotes more efficient resource use and helps mitigate greenhouse gas emissions to protect the environment.

Harnessing energy efficiency through artificial intelligence (AI) is increasingly becoming a policy priority in developed countries. AI has the capacity to accelerate progress by enabling faster knowledge generation and advancing technologies for energy conservation and cleaner production. According to Ahmad et al. (2022), AI can enhance the renewable energy sector in several ways, including through the creation of centralized and intelligent control centers, integration of micro-grids, improvements in system reliability and security, market expansion, and incorporation of AI-enabled storage into smart grids. The intersection of AI and smart city development is particularly promising, forming a strong alliance. Evidence shows that AI applications provide a solid foundation for advancing smart urban environments. Within smart cities, one of the key AI roles is to improve energy efficiency (Zamponi and Barbierato, 2022).

In Algeria, the introduction of the Smart City concept marks an important step toward sustainable urban development, yet its practical implementation remains complex and requires significant time and commitment. The Smart City initiative, which is an integral part of Algiers' development vision up to 2035, seeks to address the city's major challenges and transform it into a modern, attractive urban center. Although still in its early stages, this initiative provides a valuable case study in the ongoing evolution of Smart City practices (Aït–Yahia et al., 2019). Currently, there is a growing consensus on AI integration in the housing sector to improve energy efficiency — a critical issue given that residential

For citations: Belmahdi, H. S., Guedouh, M. S. (2025). Methodological aspects of integrating artificial intelligence into the energy efficiency management of Algeria's housing stock. Architecture and Engineering, No 3 (10), pp. 15–27.
DOI: 10.23968/2500-0055-2025-10-3-15-27.

buildings account for nearly 40 % of total energy consumption. Moreover, greenhouse gas emissions from this sector contribute approximately 10 % to the national climate change burden.

Recognizing the importance of optimizing energy consumption, researchers in the fields of energy and housing are increasingly exploring how AI can be applied to monitor and enhance energy efficiency in residential buildings. This perspective motivated us to investigate the issue within the Algerian context, using the Six W's framework — Who, What, Where, When, Why, and How. Such an approach requires not only a comprehensive review of the existing literature but also an analysis based on analogical reasoning specific to the study context.

Methods

The housing sector in Algeria is characterized by high energy consumption (Denker et al., 2014) and associated carbon emissions, leading to environmental degradation and financial pressure on households. Addressing these challenges makes the integration of AI solutions into the sector essential for fostering sustainable development. This paper examines the methodological aspects of incorporating AI into the energy efficiency management system of Algeria's housing stock. It begins with an analysis of energy consumption patterns across the main sectors — industry, transport, and housing — drawing on official reports and documents, with a particular focus on housing. Subsequently, the Six W's approach is applied to provide a structured framework for analyzing the nuances of AI integration (Fig. 1). The framework operates on two levels: the first considers the contextual application of AI for energy efficiency in housing, while the second identifies tailored AI integration solutions for the sector. The rationale for using this approach lies in the limited availability of studies applying such frameworks in comparable contexts. Its implementation therefore represents a significant step forward, offering a theoretical basis for practical approaches that account for infrastructure constraints and propose adaptive solutions.

Case Study Presentation

Algeria, the largest country in Africa and the Arab world, has a population of 44.6 million. Combined with its heavy reliance on fossil fuels, this has raised serious concerns about the sustainability of its energy production and consumption patterns. Such dependence not only accelerates environmental degradation but also creates economic vulnerabilities. To address these challenges, a re-evaluation of earlier energy initiatives was required, leading to the assessment of prospective urban development projects that prioritize energy efficiency and the transition toward clean, sustainable energy systems. Fig. 2 illustrates one such initiative: the development of technology districts in Algeria's new cities. These districts are strategically designed to serve as hubs of innovation, integrating digital infrastructure and advanced technologies to support national sustainable development goals.

The housing sector plays a particularly crucial role in this energy landscape, contributing significantly to both overall energy consumption and CO_2 emissions (Benharkat and Telilani, 2020). In the context of the new city initiative, and specifically within the housing sector, Algeria has introduced measures to develop digital infrastructure and adopt innovative technologies, including AI, to support its goal of increasing renewable energy capacity by 2030. These efforts aim to improve energy efficiency in residential buildings, optimize resource management, and enhance residents' quality of life.

Results and Discussion

Energy Consumption Patterns in Algeria

Energy efficiency directly impacts Algeria's economic and environmental development. According to the 2023 National Energy Report by Algeria's Ministry of Energy, Mines, and Renewable Energies, the country's total energy consumption (including losses) reached 72.2 Mtoe in 2023, representing a 3.2 % increase compared to the previous year. This

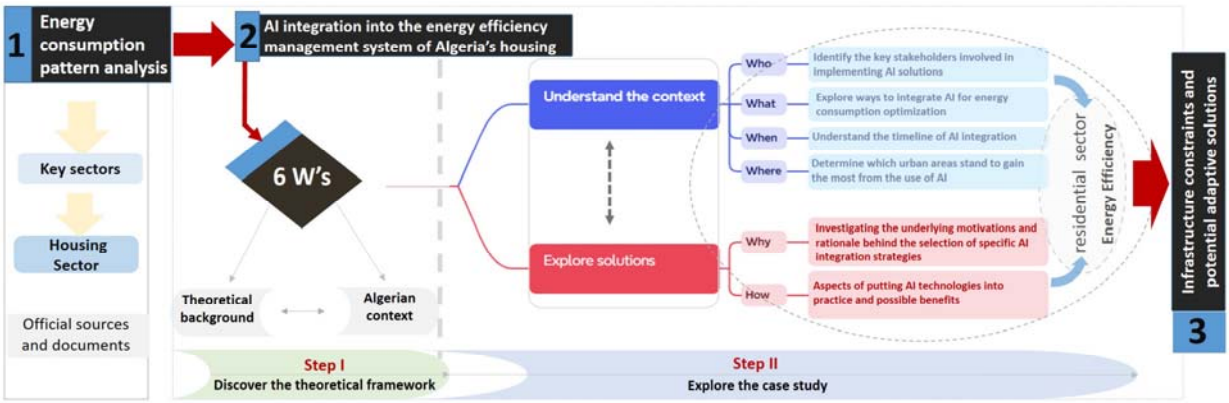

Fig. 1. Overview of the Research Framework and Steps

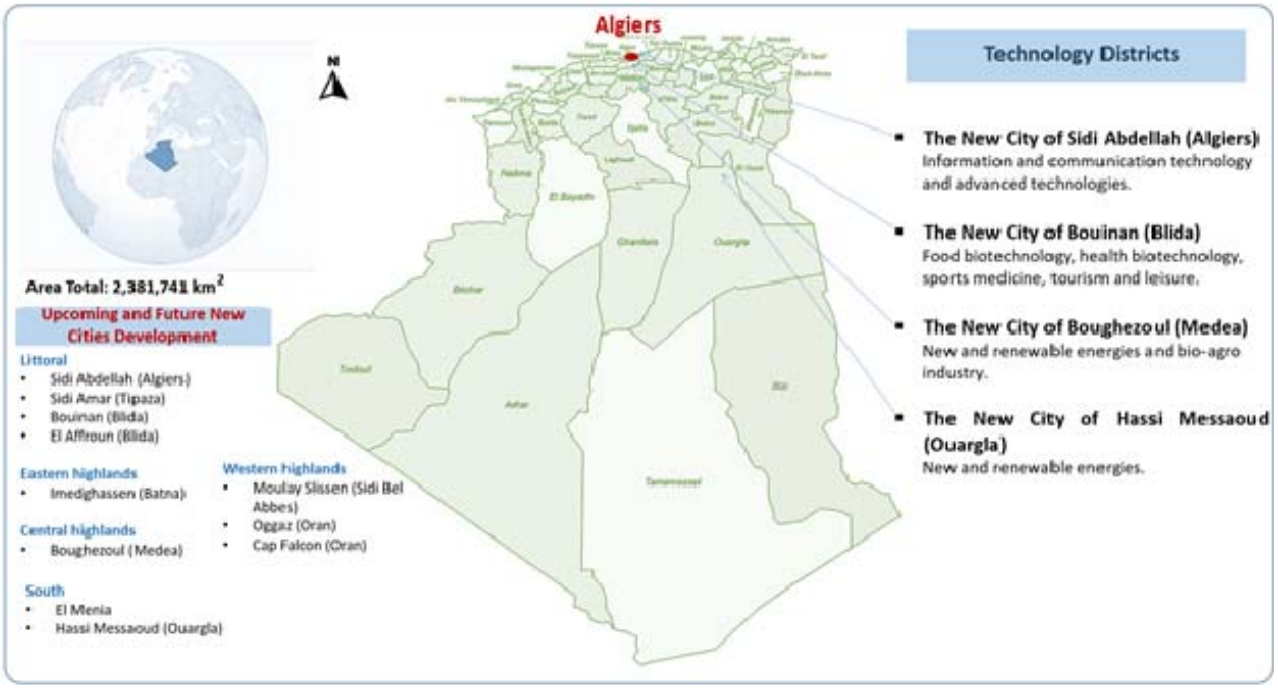

Fig. 2. Technology Districts in Algeria's New Cities (Source: National Territorial Development Plan 2030 and author's interpretation)

growth was primarily driven by final consumption (2.1 %), followed by energy industries (7.1 %), losses (11.5 %), and non-energy industries (2.5 %). As shown in Fig. 3a, natural gas dominates the national energy consumption mix at 39 %, followed by electricity (31 %) and liquid products (22 %). However, renewable energy's share in total final energy consumption remains minimal, as illustrated in Fig. 3b. In 1990, renewable energy accounted for only 0.2 % of consumption, gradually increasing to 0.4 % in 1995. The upward trend continued until it stabilized at 0.4–0.5 % between 2000 and 2005, peaking at 0.6 % in 2005. Thereafter, it gradually declined to 0.3 % by 2010 and fell further to around 0.1 % in 2015, stabilizing at 0.1–0.2 % with minor fluctuations until 2020. These findings indicate that renewable energy has not yet established a significant presence in actual consumption. A large portion of renewable energy produced does not reach end-users efficiently, due to losses during conversion and transmission or limitations in existing infrastructure. Consequently, Algeria continues to rely heavily on fossil fuels as its primary energy source.

Meanwhile, the structure of final energy consumption by sector is dominated by households and others (46 %), followed by transport (30 %) and industry (25 %) (Fig. 3c). As shown in Fig. 3d, energy intensity between 2000 and 2017 displays notable sectoral differences. In early 2005, intensity fell by 18 % in both agriculture and transport and by 16 % in industry, while the services sector remained stable. In contrast, the residential sector experienced a sharp increase of 80 % over this period, averaging approximately 3.6 % per year, particularly since 2010. This rise is mainly due to increased demand for heating and air conditioning and the growing use of electrical appliances.

According to Algeria's first updated annual report to the United Nations Framework Convention on Climate Change in 2023, published by the Ministry of the Environment and Renewable Energy, the residential sector is the largest energy consumer, along with the transport sector. As presented in Table 1, the residential sector comprises approximately 11.5 million housing units. Of these, individual houses account for around 65 %, while collective housing makes up the remaining 35 %. Energy consumption across the three primary energy sources is distributed as follows: 69 % from natural gas, 19 % from electricity, and 13 % from liquefied petroleum gas (LPG). A review of energy consumption data over the period 2007–2017 indicates an approximate increase of 1.38 % per year, equivalent to 15,003 million tons of oil equivalent (Mtoe). If this trend continues, consumption is projected to reach around 25,000 Mtoe by 2030.

The results also indicate that energy efficiency varies according to dwelling typology, urban form, and degree of insulation. Two main patterns are observed: 83 % for moderately insulated houses and 66 % for well-insulated houses. This variation across Algerian cities, combined with differences in urban form, highlights the need to reconsider approaches to energy efficiency management and carbon footprint assessment, emphasizing the importance of more in-depth studies.

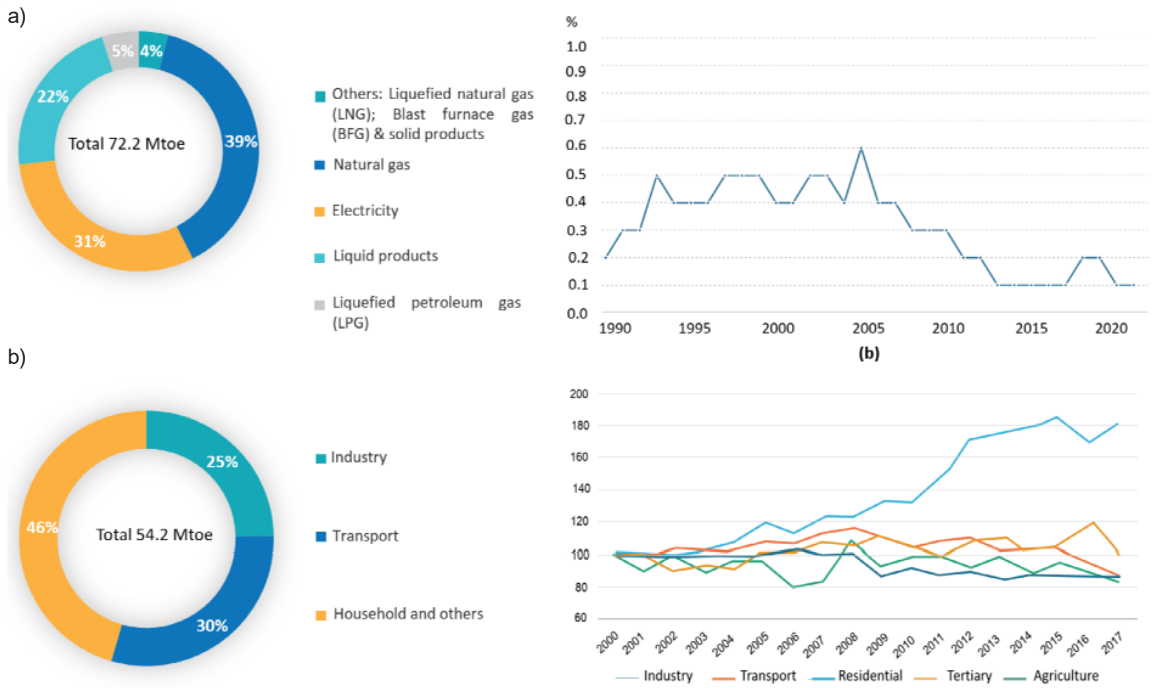

Fig. 3. Patterns and Trends in Energy Consumption across Sectors in Algeria: (a) structure of national energy consumption by energy form, (b) renewable energy consumption (% of total final energy consumption), (c) structure of final energy consumption by sector of activity, (d) evolution of final energy intensity by sector. Source: Redrawn according to the following data: (a, c) National Energy Report (Ministère de l'Energie et des Mines et des Energies Renouvelables, 2023); (b) World Bank (2023); (d) MeetMed (2020)

Table 1. **Patterns of Energy Consumption and Efficiency in the Housing Sector (Source: Algeria's first updated annual report to the United Nations Framework Convention on Climate Change (Ministère de l'Environnement et des Energies Renouvelables, 2023)**

Aspect	Details
Housing stock	Total: 11.5 million units - Individual houses: 65 % - Collective houses (apartments): 35 %
Primary energy sources	Natural gas (69 %), electricity (19 %), LPG (13 %)
Energy consumption growth	- 2007: 10,837 Mtoe - 2017: 15,003 Mtoe (avg. growth: 3.3 %/year) - 2030 (projected): 25,000 Mtoe
GHG emissions	- 2017: 41,487 tons CO_2 equivalent - 2030 (projected): 69,079 tons CO_2 equivalent
Energy consumption per house	- Average: 1.29 Mtoe/year (~15,000 kWh/year) Average permitted consumption - Moderately insulated house: 12,500 kWh/year - Well-insulated house: 10,000 kWh/year
Energy efficiency	- Compared to moderately insulated house: 83 % - Compared to well-insulated house: 66 %

Understanding the Context

Who?

In the development and implementation of AI systems, the involvement of stakeholders at all stages of the design and lifecycle process is crucial. A participatory approach should engage not only those directly affected by the project but also developers, operators, and even passive stakeholders, who must be actively involved in the process (Kunkel et al., 2023).

With regard to habitat energy issues, key actors such as developers and building owners play a decisive role in applying AI to housing projects. Technology companies using AI for environmental sustainability must therefore collaborate closely with these stakeholders to ensure successful project implementation (Kunkel et al., 2023; Yadav and Singh, 2023). The integration of AI into habitat energy management offers clear benefits, including enhanced efficiency and sustainability. However,

stakeholders in the energy services industry also bear responsibility for addressing ethical considerations such as data privacy, equitable access to energy, and the environmental impacts of AI-driven solutions.

Academic and research institutions act as key catalysts for applying AI in habitat energy, as they enable the development of environmentally friendly systems that improve energy value chains. The success of such energy management projects depends on several conditions: availability of resources, accountability, technological maturity, expertise, and the capacity for seamless integration (Holecska and Dineva, 2023). Another important factor is financial literacy, which helps stakeholders make informed decisions about the implementation of AI in energy systems (Stecyk and Miciuła, 2023).

The incorporation of AI for energy efficiency depends on several factors: the influence of stakeholders in decision-making, the level of financial commitment, responsibility for ensuring ethical use, the technological maturity needed for seamless integration, and the knowledge and capacity required to effectively manage and optimize AI systems.

In the Algerian context, some studies support AI integration to improve energy efficiency in the residential sector and explain the role of stakeholders, particularly the government. The government's involvement has been crucial in establishing energy efficiency standards, as illustrated by initiatives such as the Eco-Bat program (Sayed et al., 2022).

Table 2 presents our proposal in the form of a stakeholder matrix, showing the different levels of influence, financial commitment, responsibility, technological maturity, and knowledge among the actors involved in integrating AI into Algeria's residential sector. The government and regulatory agencies have strong influence since they set the rules and guidelines that govern how AI is applied in housing. However, variations in financial support and technological expertise may hinder the successful execution of policies. Technology companies, by contrast, are better positioned to drive the adoption of advanced AI solutions. They combine significant financial resources and technological maturity, even if their direct influence is more limited. Non-governmental organizations and energy service providers, although contributing less in terms of finance, influence, and technology, still play an essential role in raising public awareness and advocating for inclusive energy policies. Overall, effective collaboration among all stakeholders — leveraging their diverse capacities — will be critical for the successful integration of AI in Algeria's housing sector.

What?

The application of AI in the energy sector, also referred to as smart energy, aims to reduce its environmental impact by enhancing the efficiency of energy management, production, and consumption (Gil–González, 2022). This is achieved through advanced AI-based management technologies. For example, research in South Africa has demonstrated the potential of AI methods, such as support vector regression (SVR) and artificial neural networks (ANN), to improve electricity access and thereby enhance living standards (Mashapu et al., 2022).

At the same time, in the realm of smart homes, AI plays a crucial role in improving energy efficiency through advanced technologies, including smart meters, which facilitate monitoring of utility usage and regulation of indoor temperature (Rehman et al., 2020). Many countries are increasingly focusing on the housing sector as a major contributor to energy consumption, including Algeria, where research on AI technologies is still in early stages in terms of both study and practical application. For instance, the Intelligent Reasoning Rules for Home Energy Management (IRRHEM) system employs natural resources to inform residents about instances

Table 2. **Proposed Stakeholder Matrix for Enhancing Energy Efficiency in Algerian Residences through AI Integration**

Stakeholder	Level				
	Influence	Financial Engagement	Responsibility	Technological Maturity	Knowledge & Capacity
Government & Regulators	High	Variable	High	Medium	Variable
Technology Companies	Medium	High	Variable	High	High
Building Owners & Developers	Medium	High	High	Medium	Variable
Utilities	Medium	High	Medium	Medium	Medium
Research Institutions	Low	Medium	Low	Medium	High
Energy Service Companies	Low	Medium	Medium	Medium	Medium
Non-Governmental Organizations	Low	Low	Low	Low	Variable

of energy waste and coordinate related activities to achieve efficient electricity consumption (Saba et al., 2022). Additionally, the successful application of energy management techniques for off-grid solar households using artificial neural network algorithms has been demonstrated, enabling energy savings without compromising comfort (Chekired et al., 2019). These AI technologies show significant potential for optimizing energy efficiency in residential settings. Consequently, to identify the most effective solutions, it is necessary to adopt a systematic approach due to the diverse and complex nature of AI applications.

We therefore propose a straightforward four-part model (Fig. 4) to assess the critical elements influencing the success of energy-saving initiatives. The aim of this model is to facilitate well-informed decision-making by providing a structured methodology for evaluating AI initiatives, thereby ensuring a balance between effectiveness and practicality.

Firstly, managing technological development allows stakeholders and leaders to ensure that new technologies are effectively used and sustainable throughout the processes of energy generation, distribution, and consumption. In computer science, task management can be approached at three levels of algorithmic complexity: simple, medium, and complex. Secondly, data utilization refers to the collection, analysis, and application of data to guide strategic decisions and improve energy-related processes. This dimension can be considered at three scales: applications relying primarily on data from individual households or buildings, solutions using data from a broader urban area such as a city, and initiatives leveraging nationwide datasets. The third dimension concerns the degree of complexity associated with implementing the intervention. It evaluates the specific actions required for deployment and considers the necessary resources — financial, human, and time — across different organizational contexts. Three levels of intervention can be defined: low-complexity solutions that are easy to implement and require minimal infrastructure modifications; medium-complexity solutions requiring moderate infrastructure enhancements; and high-complexity solutions demanding substantial infrastructure changes or significant organizational adjustments. The fourth dimension relates to the impact and scope of the intervention, which can manifest across three

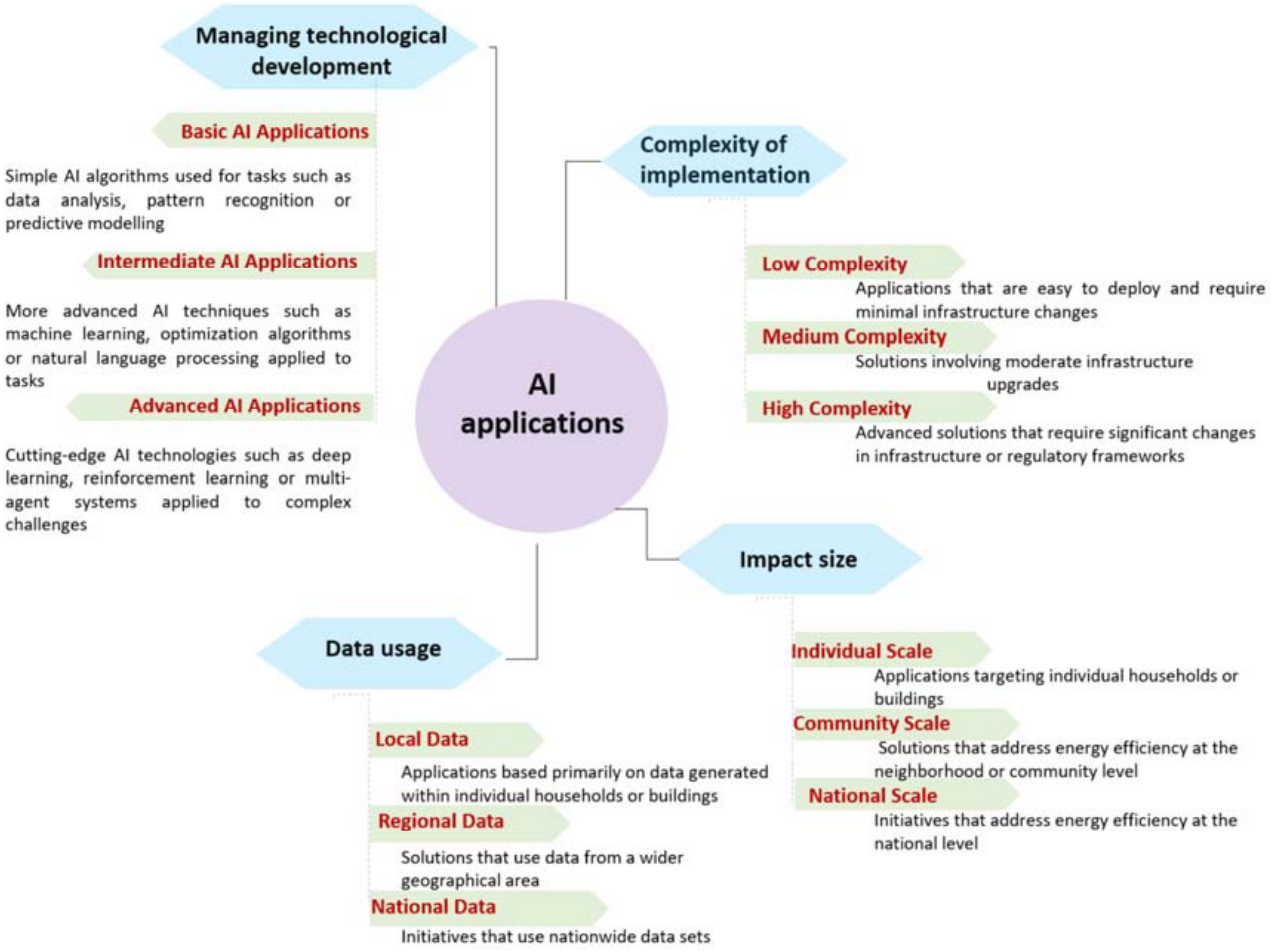

Fig. 4. Proposed Four-Dimensional Model for Integrating AI Applications to Optimize Energy Efficiency in the Algerian Housing Sector

sequential and overlapping scales: individual, city, and national levels, or as part of a general strategy for AI integration in energy management.

When?

The importance of understanding and evaluating progress in integrating AI into residential energy-saving strategies necessitates analyzing current advances and identifying future challenges and opportunities, as research in Algeria highlights that integration initiatives are still in their infancy, primarily in the realm of theoretical research. Initially, researchers focused on using AI to regulate electricity consumption in smart homes (Saba et al., 2022). It is projected that by 2030, Algeria could reduce its energy consumption by 15 %, primarily through improvements in window quality and enhanced thermal insulation (Sotehi et al., 2022). To facilitate this objective, policies such as the Eco–Bat program and revised thermal regulations have been implemented to improve energy efficiency within the construction sector, a significant energy consumer (Meftah and Mahri, 2022). Subsequently, AI algorithms have been deployed in on-grid photovoltaic homes to manage energy consumption effectively, demonstrating the ability to reduce energy usage while maintaining comfort levels (Chekired et al., 2019). Moreover, AI techniques, including artificial neural networks and case-based reasoning systems, have been employed to optimize building energy efficiency, enabling the design of single-family homes with minimal energy consumption (Węglarz, 2018). Furthermore, the integration of AI into the architectural design of low-energy residential buildings in Algerian Saharan conditions has led to significant energy savings, highlighting the importance of both passive and active design strategies (Haddam et al., 2019).

A thorough summary of the evolving use of AI in the housing sector is presented in Fig. 5, with a focus on improving energy efficiency. In the Algerian context, this integration can be divided into four major phases, each reflecting notable advancements and trends:

Prior to 2010: Initial conceptualization and exploration of theoretical frameworks and guiding principles, which laid the foundation for subsequent developments.

2010–2020: Implementation of proof-of-concept trials, allowing preliminary testing of AI-driven solutions. Simultaneously, a series of research initiatives was undertaken to evaluate the practical efficacy of AI.

2020–Present: Stakeholders have collectively worked to integrate AI solutions into established procedures, adopting advanced AI technologies, including machine learning and neural networks, for predictive maintenance, demand response, and energy optimization.

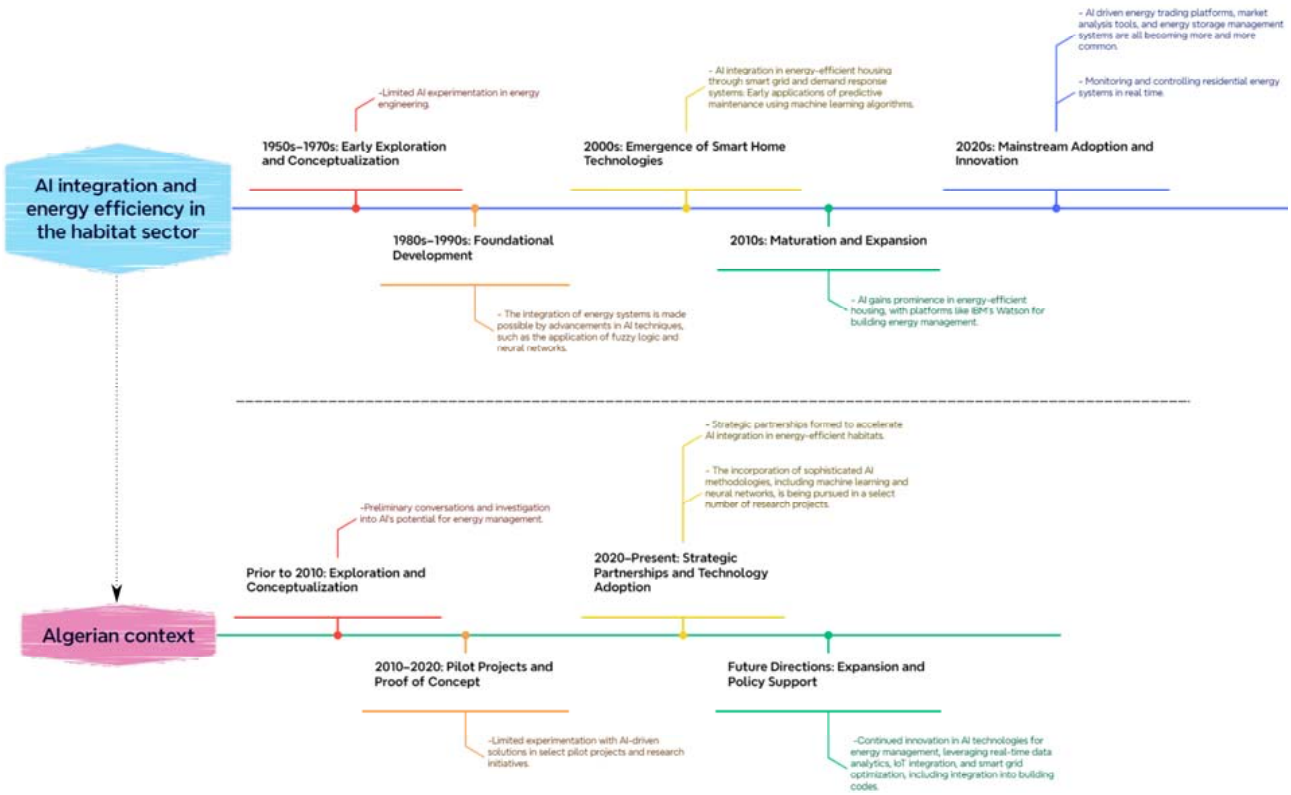

Fig. 5. Chronological Integration of AI for Energy-Efficient Housing: (a) Historical Evolution over Time, (b) Context in Algeria (suggested by the author).

Future Directions: With increasing recognition of AI's potential to support sustainability and climate objectives, there is a growing focus on the transition toward broader acceptance and institutional support for AI-driven energy-efficient housing. It is expected that policymakers and industry leaders will increasingly prioritize comprehensive regulations and guidelines to facilitate the widespread adoption of AI in the residential sector.

Despite these advances, significant challenges remain in the effective deployment of AI for energy management. Implementing new technologies often requires substantial financial resources, particularly when modernizing existing systems. Addressing these challenges will require further research to resolve technological and regulatory issues, with a clear emphasis on prioritizing AI integration in projects highlighted in government agendas.

Where?

The integration of AI technology is becoming increasingly prevalent in urban planning, particularly as a response to the challenges posed by rapid urbanization. This integration is critical for addressing various urban issues, including the need for energy-efficient housing solutions across diverse contexts. AI provides applications for optimizing energy consumption (Sanchez, 2023), identifying resilient and inclusive urban land-use strategies (Koutra and Ioakimidis, 2023), and facilitating efficient urban redevelopment initiatives (Ye et al., 2023).

In Algeria, the use of AI in housing projects involves analyzing specific factors to determine energy demand and consumption patterns. This includes spatial and temporal analyses to identify neighborhoods with high energy use due to factors such as aging infrastructure or operational inefficiencies. Large residential complexes and urban redevelopment projects, particularly in areas undergoing renovation or replacement of old buildings, should be prioritized to ensure compliance with energy efficiency standards and address neighborhoods with diverse income levels. Furthermore, aligning AI interventions with smart city initiatives ensures that AI-driven solutions not only optimize energy consumption in housing but also contribute to broader goals of sustainable urban development.

Exploring Solutions

Why?

The objective of selecting specific solutions for integrating AI into energy-efficient systems is to enhance reliability and generate technological and economic benefits (Danish, 2023). These solutions can contribute to reducing carbon emissions and combating climate change (Navarra, 2023), aiming for integrated building management and effective digital connections with users and smart grids (Mocerino, 2020). In the Algerian context, the use of AI in implementing energy-saving measures in the housing sector is expected to generate significant benefits. As illustrated in Fig. 6, five key benefits can be identified with their reliability and applicability explained:

1) innovation in construction — AI integration may inspire creativity by introducing new technologies for designing more efficient, sustainable, and durable buildings; 2) curbing carbon emissions — AI optimizes energy use and encourages adoption of clean energy sources; 3) enhanced efficiency — continuous monitoring and optimization improve building performance; 4) socio-economic advantages — AI creates new job opportunities, reduces household energy costs, and improves living standards; 5) data-driven decision-making — AI enables stakeholders to identify patterns, forecast energy needs, and implement targeted interventions for maximum impact.

How?

The integration of AI is central to achieving actual energy savings in the residential sector. Agent-based modeling and simulation, when applied to homes operating with hybrid renewable energy systems, can reduce energy usage without compromising occupant comfort. Furthermore, AI can enhance building energy management systems by enabling intelligent heating, ventilation, and air conditioning (HVAC) optimization, as well as predictive energy efficiency measures (Mocerino, 2020). As noted by Szczepaniuk and Szczepaniuk (2023), integrating AI along the energy value chain has the potential

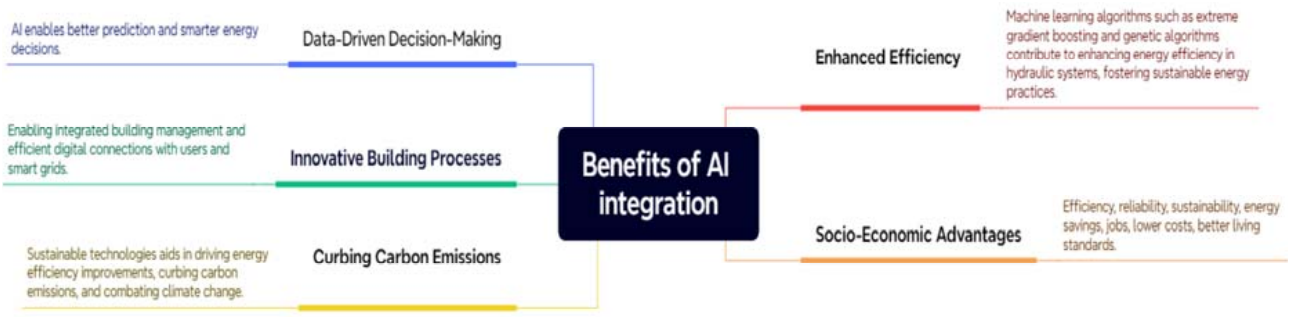

Fig. 6. Key Benefits of AI Integration in the Algerian Residential Sector

to promote sustainable energy practices, improve energy utilization, and reduce overall environmental impact. This can be achieved through techniques such as machine learning, metaheuristic algorithms, and intelligent fuzzy inference systems.

Several studies have identified key factors that facilitate AI integration in residential energy management. These factors can be broadly classified into two categories: those that enable automatic energy management and those that allow the anticipation of system failures, thereby reducing costs. The first category includes smart control systems, while the second encompasses predictive maintenance, machine learning, and data analytics, which collectively support more effective decision-making based on large datasets. Sensor networks and the Internet of Things (IoT) further enhance performance by providing real-time data collection.

To identify potential avenues for change in the Algerian context, we propose a model illustrating the integration of AI in the residential energy sector, as shown in Fig. 7. This model highlights five key factors, along with their associated methods, challenges, and opportunities. Areas of focus include smart grid integration, intelligent control systems, machine learning and data analytics, sensor networks and IoT, and predictive maintenance.

Infrastructure Constraints and Potential Adaptive Solutions

The integration of AI into residential energy management in Algeria demonstrates significant potential to enhance both efficiency and sustainability. However, based on the Six W's framework, several infrastructure challenges must be addressed before this technology can be widely deployed. These challenges can be categorized into technical, economic and environmental, social and legal constraints (see Table 3 for details).

Considering the Six W's framework, allocating resources to AI monetization through four adaptation mechanisms can enable smoother and more efficient integration of AI into Algeria's energy sector:

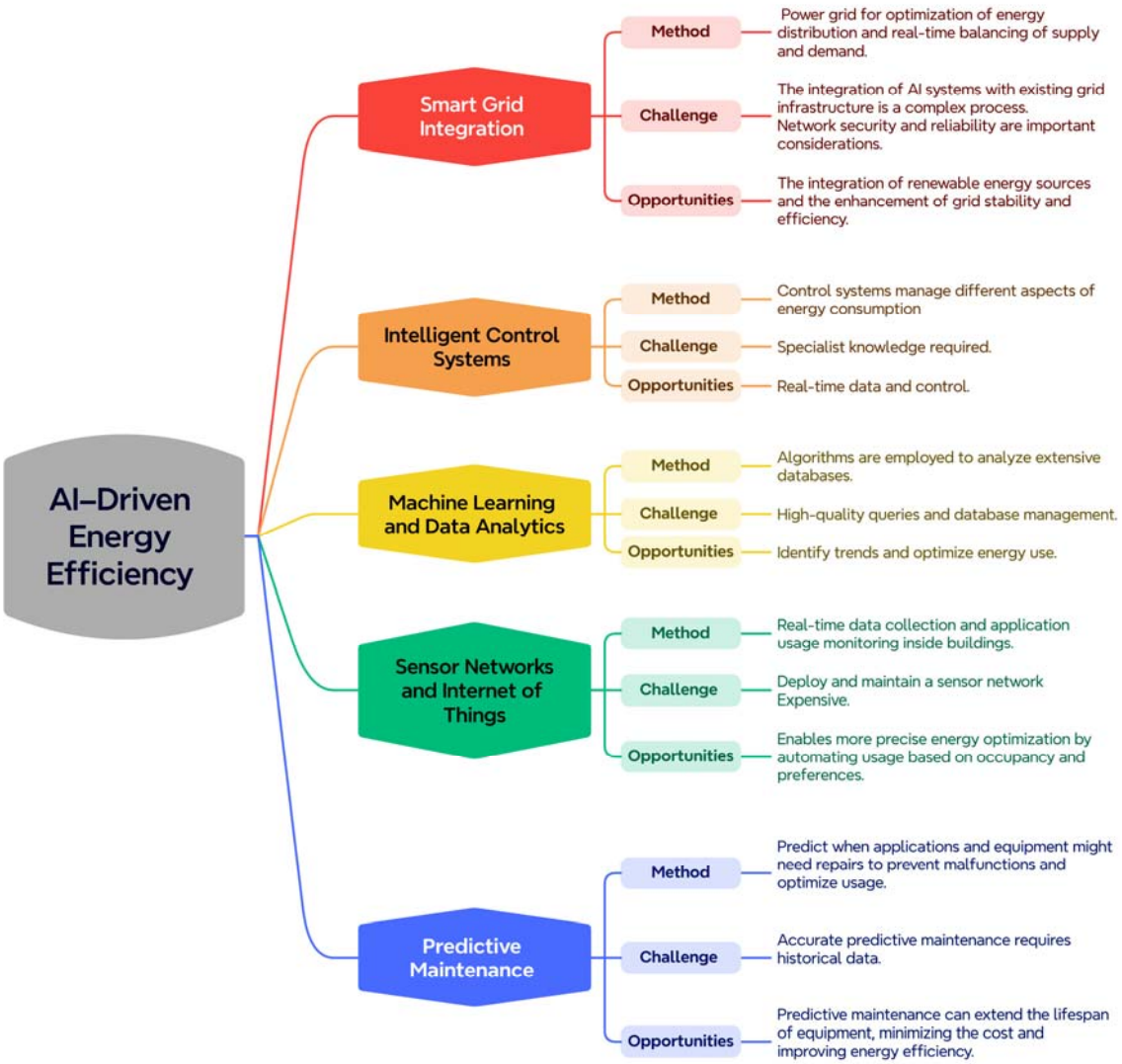

Fig. 7. AI-Driven Energy Efficiency in Algerian Housing: Methods, Challenges, and Prospects (suggested by the author)

Table 3. **Types of Infrastructure Constraints for AI Integration in Algeria**

Constraint Type		Details
Technical	Structure	- Difficulty of integration with traditional energy infrastructure, requiring major modifications. – Significant investments needed to modernize infrastructure and incorporate AI technologies.
	Data and Quality	- Unclear and inconsistent data availability policies hinder accurate analysis and predictions.
	Performance and Scalability	- High computational requirements for real-time data processing, leading to heavy technical resource consumption.
	Experience	- Implementation requires extensive multidisciplinary knowledge.
Economic and Environmental	Cost and Budget	- AI integration involves significant costs. - High costs and complexity of upgrading legacy systems make balancing budgets and AI performance challenging.
	Environmental	- Smart data centers consume large amounts of energy. - Dependence on non-renewable energy sources increases carbon emissions and negatively impacts the environment.
Social and Legal	Social	- Digital divide limits access to smart technologies for some groups, reducing overall efficiency.
	Legal	- Lack of clear policies and regulations for AI in energy management slows down implementation and adoption.

• *Infrastructure and Technology:* A robust digital architecture is needed, including upgrades to communication networks, investments in cloud computing, and enhanced data protection to safeguard sensitive information from cyber-attacks. Moreover, the synergy between AI and IoT enhances precision in data collection and analytics.

• *Policies and Management:* Modernizing laws and institutional frameworks is crucial to regulate the application of AI in governance and establish a clear legal basis for its use in energy management.

• *Skill Development and Training:* Specialized training programs in energy management should be developed to ensure professionals can effectively operate smart tools.

• *Balancing AI and Human Oversight:* AI cannot be entirely relied upon for critical decision-making. Human supervision remains essential to ensure accountability and legitimacy. Mechanisms should be established to review AI outputs and validate operational results, thereby minimizing errors or system failures that could have severe economic consequences.

Conclusion

The present study was conducted with the objective of investigating the potential of integrating artificial intelligence to enhance energy efficiency in Algerian housing. Using the Six W's methodology as a guiding framework, the key findings can be summarized as follows:

Who: A stakeholder matrix has been proposed as a practical instrument for identifying the most influential actors in AI integration, including government and regulators, technology companies, building owners and developers, utilities, research institutions, energy service companies, and non-governmental organizations. The matrix highlights their relative influence, financial commitment, responsibilities, and technological maturity.

What: The study aimed to provide a comprehensive evaluation of the critical factors that determine the success of AI interventions in the housing sector. Four key application areas were identified as particularly significant: the management of technological sophistication, the scope and scale of impact, the utilization of data, and the complexity of implementation.

When: Realizing the potential of AI in the housing sector requires continued research to address the technological and regulatory barriers that currently limit progress. The implementation of advanced technologies — particularly in the context of upgrading existing infrastructure — remains a costly endeavor.

Where: AI integration into the housing sector requires a detailed analysis of energy consumption patterns and the prioritization of large residential complexes and urban redevelopment projects. Neighborhoods with diverse income levels, aligned with broader smart city initiatives, represent an ideal

context for AI deployment since such integration not only optimizes energy consumption but also contributes to sustainable urban development goals.

Why: The motivations driving AI integration encompass environmental sustainability, resource optimization, regulatory compliance, cost efficiency, technological innovation, and positive societal impacts, which include improved public perception, enhanced health and well-being.

How: The identification of prospective alterations within the case study context requires an assessment of a number of factors, including: intelligent control systems, predictive maintenance, machine learning, data analytics, sensor networks, IoT integration, and smart grid integration.

Although this research topic has not been extensively explored, particularly within the case study context, the methodology employed herein represents an initial investigation that will facilitate future research by enabling a more comprehensive examination of each dimension. Moreover, the findings of this research will be invaluable for future studies, providing the basis for developing a comprehensive evaluation framework to assess potential AI integration for enhancing energy efficiency. It is envisaged that this framework could subsequently be applied to the development of future smart cities in Algeria.

References

Ahmad, T., Zhu, H., Zhang, D., Tariq, R., Bassam, A., Ullah, F., AlGhamdi, A. S., and Alshamrani, S. S. (2022). Energetics Systems and artificial intelligence: applications of industry 4.0. *Energy Reports*, Vol. 8, pp. 334–361. DOI: 10.1016/j.egyr.2021.11.256.

Aït–Yahia, K. G., Ghidouche, F., and N'Goala, G. (2019). Smart city of Algiers: defining its context. In: Anthopoulos, L. (ed.). *Smart City Emergence. Cases From Around the World*. New York: Elsevier, pp. 391–405. DOI: 10.1016/B978-0-12-816169-2.00019-5.

Benharkat, S. and Telilani, I. (2020). Impact of thermal insulation strategies on energy consumption of residential buildings in Constantine. *Journal of Fundamental and Applied Sciences*, Vol. 12, No. 2, pp. 865–874. DOI: 10.4314/jfas.v12i2.23.

Chekired, F., Berkane, S., Meflah, A., and Mahrane, A. (2019). Artificial neural network based controller for energy management in a solar home in Algeria. In: *2019 7th International Renewable and Sustainable Energy Conference (IRSEC)*, November 27–30, 2019, Agadir, Morocco. DOI: 10.1109/IRSEC48032.2019.9078172.

Danish, M. S. S. (2023). AI in energy: overcoming unforeseen obstacles. *AI*, Vol. 4, No. 2, pp. 406–425. DOI: 10.3390/ai4020022.

Denker, A., El Hassar, S. M. K., and Baradiy, S. (2014). *Guide pour une construction eco-énergétique en Algérie*. Born and Eschborn: Deutsche Gesellschaft für Internationale Zusammenarbeit, 288 p.

Gil–González, A. B. (2022). *Artificial intelligence in the energy industry.* Basel: MDPI AG., 146 p.

Haddam, M. A. C., Cherier, M. K., Bekkouche, S. M. E. A., Hamdani, M., Belgherras, S., Mihoub, R., and Benamrane, N. (2019). Efficient energy and financial solutions for residential buildings in Algerian Saharan climate. *Modelling Measurement and Control C*, Vol. 80, No. 2–4, pp. 79–87. DOI: 10.18280/mmc_c.802–406.

Holecska, D. and Dineva, A. (2023). Towards sustainable energy management: analyzing AI-based solutions for PV systems with battery in energy communities. In: *2023 IEEE 17th International Symposium on Applied Computational Intelligence and Informatics (SACI)*, May 23–26, 2023, Timișoara, Romania, pp. 000655–000660. DOI: 10.1109/SACI58269.2023.10158604.

Koutra, S. and Ioakimidis, C. S. (2023). Unveiling the potential of machine learning applications in urban planning challenges. *Land*, Vol. 12, Issue 1, 83. DOI: 10.3390/land12010083.

Kunkel, S., Schmelzle, F., Niehoff, S., and Beier, G. (2023). More sustainable artificial intelligence systems through stakeholder involvement?. *GAIA - Ecological Perspectives for Science and Society*, Vol. 32, Supplement 1, pp. 64–70. DOI: 10.14512/gaia.32.S1.1.

Mashapu, L. D., Eboule, P. S. P., and Pretorius, J.-H. C. (2022). The need for artificial intelligence for energy–efficiency management: a review. In: *2022 8th International Conference on Energy Efficiency and Agricultural Engineering (EE&AE)*, June 30 – July 2, 2022, Ruse, Bulgaria. DOI: 10.1109/EEAE53789.2022.9831359.

MeetMed Mitigation Enabling Energy Transition in the Mediterranean Region (2020). *Med'observeer. Fiche pays: Algérie.* [online] Available at: https://south.euneighbours.eu/wp-content/uploads/2022/07/A12_FICHE-PAYS_ALGERIE-2.pdf [Date accessed February 20, 2025].

Meftah, N. and Mahri, Z. L. (2022). Analysis of Algerian energy efficiency measures in buildings for achieving sustainable development goals. *Journal of Renewable Energies*, Vol. 1, No. 1, pp. 37–44. DOI: 10.54966/jreen.v1i1.1030.

Ministère de l'Energie et des Mines et des Energies Renouvelables (2023). *Bilan Énergétique National*. [online] Available at: https://www.energy.gov.dz/Media/galerie/bilan_energetique_2023_6763e8ed2d76d.pdf [Date accessed February 20, 2025].

Ministère de l'Environnement et des Energies Renouvelables (2023). *Premier rapport biennal actualise de l'algerie a la Convention cadre des Nations Unies sur le Changement Climatique*. [online] Available at: https://www.undp.org/sites/g/files/zskgke326/files/2024-01/BUR1%20Alg%C3%A9rie%20r%C3%A9vis%C3%A9%20VF%2022102023.pdf [Date accessed February 19, 2025].

Mocerino, C. (2020). The new integrated management of efficient buildings: an intelligent method approach and AI. *Journal of Civil Engineering and Architecture*, Vol. 14, pp. 207–213. DOI: 10.17265/1934–7359/2020.04.004.

Navarra, D. (2023). Integrating artificial intelligence and sustainable technologies in strategic renewable energy and Power–to–X projects: a review of global best practices, risks and future prospects. *Society and Economy*, Vol. 45, Issue 4, pp. 472–493. DOI: 10.1556/204.2023.00012.

Rehman, A. U., Tito, S. R., Ahmed, D., Nieuwoudt, P., Lie, T. T., and Vallès, B. (2020). An artificial intelligence-driven smart home towards energy efficiency: an overview and conceptual model. In: *2020 FORTEI-International Conference on Electrical Engineering (FORTEI-ICEE)*, September 23–24, 2020, Bandung, Indonesia, pp. 47–52. DOI: 10.1109/FORTEI-ICEE50915.2020.9249816.

Saba, D., Cheikhrouhou, O., Alhakami, W., Sahli, Y., Hadidi, A., and Hamam, H. (2022). Intelligent Reasoning Rules for Home Energy Management (IRRHEM): Algeria case study. *Applied Sciences*, Vol. 12, Issue 4, 1861. DOI: 10.3390/app12041861.

Sanchez, T. W. (2023). Planning on the verge of AI, or AI on the verge of planning. *Urban Science*, Vol. 7, Issue 3, 70. DOI: 10.3390/urbansci7030070.

Sayed, A., Himeur, Y., Bensaali, F., and Amira, A. (2022). Artificial intelligence with IoT for energy efficiency in buildings. In: Verma, A., Verma, P., Farhaoui, Y., and Lv, Z. (eds.). *Emerging Real-World Applications of Internet of Things*. Boca Raton: CRC Press, pp. 233–252.

Sotehi, O., Maifi, L., Belili, H., and Djebaili, I. (2022). Nano technology building insulation effect on the thermal behavior of building under different Algerian weather. *The International Journal of Multiphysics*, Vol. 16, No. 3, pp. 273–286. DOI: 10.21152/1750–9548.16.3.273.

Stecyk, A. and Miciuła, I. (2023). Harnessing the power of artificial intelligence for collaborative energy optimization platforms. *Energies*, Vol. 16, Issue 13, 5210. DOI: 10.3390/en16135210.

Szczepaniuk, H. and Szczepaniuk, E. K. (2023). Applications of artificial intelligence algorithms in the energy sector. *Energies*, Vol. 16, Issue 1, 347. DOI: 10.3390/en16010347.

Türkoğlu, S. P. and Kardoğan, P. S. Ö. (2018). The role and importance of energy efficiency for sustainable development of the countries. In: Fırat, S., Kinuthia, J., and Abu-Tair, A. (eds.). *Proceedings of 3rd International Sustainable Buildings Symposium (ISBS 2017)*. Lecture Notes in Civil Engineering, Vol. 7. Cham: Springer, pp. 53–60. DOI: 10.1007/978-3-319-64349-6_5.

Węglarz, A. (2018). Using artificial intelligence in energy efficient construction. *E3S Web of Conferences*, Vol. 49, 00125. DOI: 10.1051/e3sconf/20184900125.

World Bank (2023). *Renewable energy consumption (% of total final energy consumption) - Algeria*. [online] Available at: https://data.worldbank.org/indicator/EG.FEC.RNEW.ZS?end=2012&locations=DZ [Date accessed February 20, 2025].

Yadav, M. and Singh, G. (2023). Environmental sustainability with artificial intelligence. *EPRA International Journal of Multidisciplinary Research (IJMR)*, Vol. 9, Issue 5, pp. 213–217. DOI: 10.36713/epra13325.

Ye, X., Newman, G., Lee, C., Van Zandt, S., and Jourdan, D. (2023). Toward urban artificial intelligence for developing justice–oriented smart cities. *Journal of Planning Education and Research*, Vol. 43, Issue 1, pp. 6–7. DOI: 10.1177/0739456X231154002.

Zamponi, M. E. and Barbierato, E. (2022). The dual role of artificial intelligence in developing smart cities. *Smart Cities*, Vol. 5, Issue 2, pp. 728–755. DOI: 10.3390/smartcities5020038.

МЕТОДОЛОГИЧЕСКИЕ АСПЕКТЫ ИНТЕГРАЦИИ ИСКУССТВЕННОГО ИНТЕЛЛЕКТА В СИСТЕМУ УПРАВЛЕНИЯ ЭНЕРГОЭФФЕКТИВНОСТЬЮ ЖИЛОГО ФОНДА АЛЖИРА

Хосин Сами Бельмахди[1]*, Маруан Самир Геду[2,3]

[1]Лаборатория архитектуры, урбанизма и транспорта: жилье, ландшафт и городская мобильность, Институт архитектуры и урбанизма, Университет Батны 1, Батна, Алжир
[2]Лаборатория дизайна и моделирования архитектурных форм и обстановки (LACOMOFA), Университет Бискры, Бискра, Алжир
[3]Институт архитектуры и урбанизма, Университет Батны 1, Батна, Алжир

*E-mail: hocine.belmahdi@univ–batna.dz

Аннотация
Введение: жилищный сектор Алжира потребляет существенную часть энергии страны, вследствие чего становится необходимым поиск креативных решений для повышения энергоэффективности. Искусственный интеллект (ИИ) предлагает эффективные инструменты оптимизации потребления энергии и снижения экологического следа. **Цель исследования:** настоящее исследование направлено на изучение методологических аспектов интеграции ИИ в систему управления энергоэффективностью жилого фонда Алжира. **Методы:** для анализа интеграции ИИ был использован подход 6W, реализованный в два этапа. На первом этапе формировалась теоретическая основа. На втором — проводилось исследование конкретного кейса, позволяющее глубже понять контекст и проанализировать возможные решения с разных точек зрения. **Результаты:** результаты исследования разделены на две основные категории. Первая касается участников процесса, методов интеграции ИИ и пространственно-временного контекста. Вторая охватывает мотивацию и причины выбора конкретных стратегий интеграции ИИ, а также аспекты технологий ИИ, подлежащих внедрению.

Ключевые слова: энергоэффективность, жилищный фонд Алжира, интеграция искусственного интеллекта, подход 6W, умный город.

DOI: 10.23968/2500-0055-2025-10-3-28-39

IMPACT OF BREATHING FACADES AND BIOMIMICRY ON VENTILATION AND INDOOR AIR QUALITY

Ehsan M. Elhennawi[1]*, Hesham Sameh Hussein Sameh[2]

[1]Higher Technology Institute, 10th of Ramadan City, Egypt
[2]Cairo University, Egypt

*Corresponding author's email: ehsan.m.k.89@gmail.com

Abstract

Introduction: One of the most pressing challenges today is global warming, which has significantly increased building temperatures. Developing cost-effective solutions to mitigate indoor overheating is therefore a key architectural task. This paper examines the impact of breathing facades on ventilation and indoor air quality, with a particular focus on the relationship between biomimicry and facade design. It emphasizes how biomimicry can inspire architects to address environmental challenges and explores the concept of "breathing skins" through two case studies. **Purpose of the study**: The study aims to analyze the connection between biomimicry and breathing facades, and to evaluate their effectiveness in enhancing indoor air quality and reducing building temperatures. **Methods**: The methodology combines inductive and analytical approaches within the framework of a systematic literature review, complemented by comparative analysis to assess the performance of innovative facade systems. **Results** indicate that smart breathing facades have significant potential to reduce pollution levels and improve urban livability.

Keywords: breathing facades, sustainable architecture, biomimicry, ventilation, indoor air quality.

Introduction

Poor indoor air quality negatively affects the health, learning capacity, and productivity of building occupants. In existing structures, facade ventilation systems are commonly used to enhance indoor air quality; however, their effectiveness remains limited due to susceptibility to wind conditions and ambient temperature fluctuations. Breathing facades represent an innovative approach to building envelope design, aiming to improve energy efficiency, enhance indoor air quality, and support climate change mitigation (Omrany et al., 2016). By integrating intelligent systems, these facades can adapt to dynamic environmental conditions, thereby optimizing thermal comfort and sustainability (Moloney, 2006). This paper provides an overview of breathing facades, emphasizing their advantages and potential applications in contemporary architecture.

Objectives

The objective of this study is to examine the role of biomimicry in architecture, with particular attention to technologies that mitigate indoor temperature extremes by enhancing ventilation and air quality through the use of breathing facades. The research highlights six innovative facade systems: intelligent facades, climate adaptive building shells, vertical greenery systems, phase change materials, thermo-bimetals, and breathing walls. These systems are evaluated through a comparative analysis to identify their effectiveness and potential applications. The study specifically focuses on facade systems that integrate breathing mechanisms, both on the exterior and interior of buildings. Fig. 1 illustrates the main objectives of the research.

Issues and Challenges

The rise in indoor temperatures represents one of the major global challenges of the 21st century, with climate change expected to cause long-term impacts on the built environment. Recently, new generations of materials and treatments have been developed to reduce air pollutants. The key challenge, however, lies in ensuring that such materials and systems not only contribute to mitigating global warming but also effectively improve indoor air quality. Breathing facades, along with other innovative ventilation strategies, hold significant potential in addressing these challenges (Imbabi and Peacock, 2003).

Methods

This study employs inductive and analytical approaches within the framework of a systematic literature review, aiming to identify the most effective techniques for reducing indoor temperatures through the use of breathing facades. Particular attention is given to biomimicry-inspired concepts that contribute to environmental goals by establishing the relationship between natural systems and breathing facade design. The research also examines differences among innovative facade systems in this context. At an advanced stage, a comparative analysis was applied to evaluate the effectiveness of selected techniques.

For citations: Elhennawi, Eh. M. , Sameh, H. S. H. (2025). Impact of breathing facades and biomimicry on ventilation and indoor air quality. Architecture and Engineering, No 3 (10), pp. 28–39. DOI: 10.23968/2500-0055-2025-10-3-28-39.

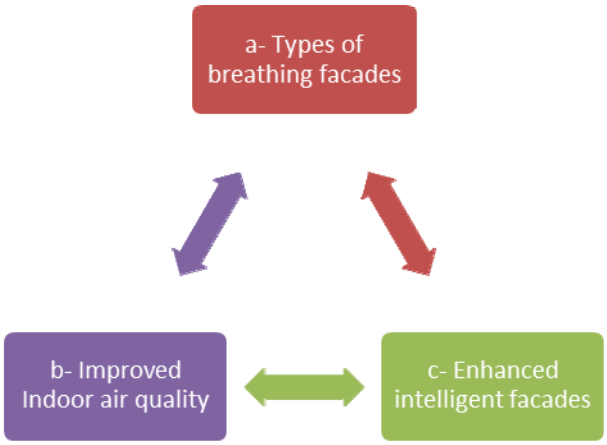

Fig. 1. Objectives of the study

A comprehensive review of relevant literature was conducted using academic databases such as Scopus, ScienceDirect, and Google Scholar. The search strategy relied on targeted keywords, including "breathing facades", "sustainable architecture", "biomimicry", "ventilation", and "indoor air quality".

Literature Selection Criteria

To ensure both relevance and academic rigor, a set of criteria was established to select studies included in the literature review. The selection process was guided by the following requirements:

- The study must directly address the relationship between biomimicry, architecture, and architectural technologies or applications.
- It must provide a clear critical or applied analysis that contributes to understanding the design or technical dimensions of the topic.
- It must be published in peer-reviewed scientific journals, preferably between 1997 and 2024.

Studies were excluded if they:

- Lacked analytical depth or relied on general descriptions without a direct connection to the research topic.
- Focused exclusively on technical aspects without considering the design or conceptual dimensions.
- Were not published in reliable academic sources or could not be verified.

According to the reviewed literature, the research methodology was divided into two complementary components:

Analytical Methodology

A thematic analysis approach was applied to classify the literature into conceptual themes that formed the analytical framework of the study: (i) an overview of biomimicry and its applications in architecture, (ii) an examination of breathing skin systems supported by two practical experiments, and (iii) a detailed analysis of the behavioral characteristics and methods of six innovative facade systems classified as "breathing facades".

Comparative Analysis

Following the thematic analysis, a comparative evaluation was conducted among the six identified facade systems. The comparison focused on identifying the strengths and weaknesses of each case, thereby extracting general trends. This comparative analysis was essential to achieving the research objective: reducing indoor temperatures and improving air quality through the implementation of breathing facades.

Biomimicry in Architecture

Biomimicry offers architects a framework for addressing environmental challenges by drawing inspiration from natural systems (Benyus, 1997). It is a science grounded in the study and simulation of nature, particularly the interactions of living organisms with their environments (Nkandu and Alibaba, 2018). From this perspective, the environment is understood as inherently balanced, and by applying its principles to building design, architects can develop effective solutions to various issues. Biomimicry is commonly categorized into three levels: organism, behavior, and ecosystem, as illustrated in Fig. 2.

An example of the organism level is the lotus flower, whose leaves possess a natural self-cleaning property. This characteristic has been adapted to develop self-cleaning paints for building surfaces (Ensikat et al., 2011) (Fig. 3). At the behavioral level, a well-known example is the ant colony, where ants construct vertical air channels that facilitate the expulsion of indoor air to the outside. This principle has been applied in architectural design to reduce heating and cooling energy demand by up to 10 % (Pawlyn, 2019), as illustrated in Fig. 4. Finally, the ecosystem level represents the integration of organismal and behavioral strategies, emphasizing

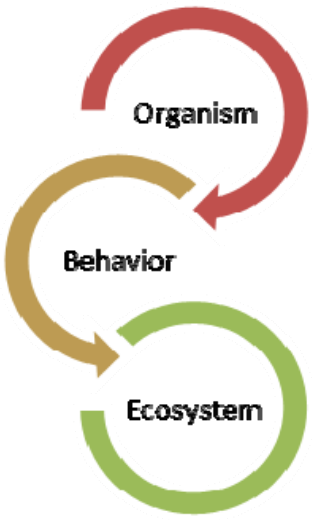

Fig. 2. Three levels of biomimicry

Fig. 3. The texture of lotus flower leaves

the interaction of sustainable designs with their surrounding environment.

Breathing Skin System

Extreme weather conditions, such as those found in the Arctic, present significant challenges to life; yet organisms like polar bears thrive in these environments. Their survival is largely due to thermoregulatory adaptations, such as dense white fur, which protects them from extreme cold. Thermoregulation is an internal response to external conditions, aiming to maintain thermal balance within the organism — a form of homeostasis. Homeostasis represents thermal stability, allowing the body to use minimal energy to regulate temperature (Craig, 2018). When applied to building envelopes, these principles inspire automatic thermoregulatory systems, enhancing energy efficiency. The body maintains internal homeostasis through a feedback loop (Becker, 2016; Turner, 2016). The neuroendocrine system detects deviations from normal conditions and transmits these signals to the brain, which then activates regulatory organs to respond to external changes, thereby restoring balance. This process represents the negative feedback loop of temperature regulation. Such biological mechanisms inspire the design of intelligent buildings, providing a model for energy-efficient, self-regulating systems.

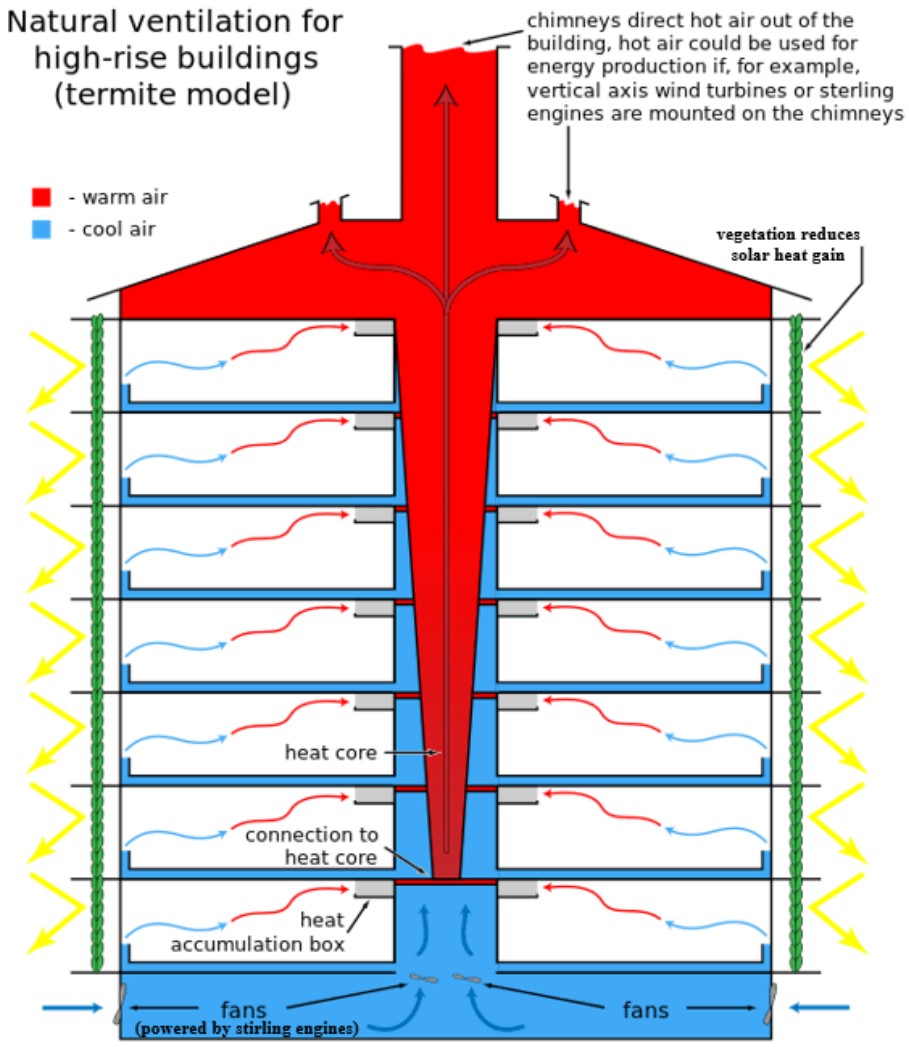

Fig. 4. A schematic showing the natural ventilation used in the Eastgate building, Harare

Human respiration also plays a critical role in sustaining life and thermoregulation. Lung-inspired experiments have demonstrated the ability to self-regulate temperature. Heat exchange in respiration occurs primarily in the diaphragm and alveoli, as illustrated in Fig. 5. Respiration consists of two main processes: external respiration, involving inhalation and exhalation, and internal respiration, which is the gas exchange between oxygen and carbon dioxide. Oxygen-rich air entering the lungs is transported via blood vessels to the alveoli, where internal respiration is closely linked to metabolism. Thus, biomimicry of respiration encompasses both external and internal mechanisms, offering valuable insights for the design of intelligent, energy-efficient building envelopes.

Pneumatic Design

The organic respiration process serves as a model for the breathing skin, a type of wall that employs passive or active ventilation. It can regulate environmental factors such as solar radiation, relative humidity, and surface temperature, as illustrated in Fig. 6, providing a comprehensive framework for environmental thermal evaluation.

The two case studies analyzed in this research applied different methodological approaches, both relying on pneumatic mechanisms to create favorable indoor environmental conditions.

Becker (2016) developed a breathing skin, illustrated in Fig. 7, in a showroom project inspired by organic skins that allow air to enter through small, tube-like apertures in the wall. The system regulates airflow, incident velocity, ambient temperature, and sound dispersion. Internal airspeed stabilizes naturally through the wall design. The wall features a reversed air duct mechanism that enables control over air volume, airspeed, and anticipated temperature variations, influenced by its morphological configuration. Solar transmittance is modulated through the color of the material: transparent and dark opaque polycarbonate sheets are used in the air ducts in two color variations (Laird, 2016). By adjusting the positioning of these colors relative to the Sun's orientation, the transparent wall can be rendered translucent or opaque, thereby managing solar gain while optimizing airflow through the air pockets.

The second case study focuses on a project that employed a light sensor to monitor changes in the external environment. This project was designed and implemented by a group of students from the Institute for Advanced Architecture of Catalonia (IAAC). The system, referred to as the adaptive pneumatic skin (Fig. 8), is an adaptive wall that actively regulates airflow in response to environmental conditions. The wall's breathing mechanism, inspired by the human nervous system, allows it to respond dynamically to external stimuli. According to the system's programming, when the light sensor detects a specific level of solar radiation, the air valve opens to activate the air compressor, releasing air through the pneumatic pipes. Each balloon inflates as the air flows through its apertures, mimicking the process of inhalation and exhalation observed in animals. Unlike the previous breathing skin project, this system incorporates a mechanical feedback loop that actively responds to environmental variables, adjusting the indoor environment accordingly. It regulates indoor conditions and light permeability by reacting to changes in both external light and temperature (IAAC, 2019). The materials used in the balloons further influence the internal environment. Constructed in multiple colors with varying visual transmittances, the membrane also functions as a dynamic solar shading device, as its transparency changes in response to air pressure levels (IAAC, 2019).

The two case studies discussed above are both inspired by biomimicry, particularly the influence of breathing and pneumatic mechanisms on indoor temperature regulation. Although both systems demonstrated favorable effects on internal conditions, their embedded control strategies differ. Since the breathing skin relies solely on external wind pressure, the fluctuations in internal conditions closely mirror those of the external environment. As a predominantly passive system, it lacks the capacity to self-correct and reach an optimal internal state. In contrast, the adaptive pneumatic skin incorporates automated control using light sensors to detect

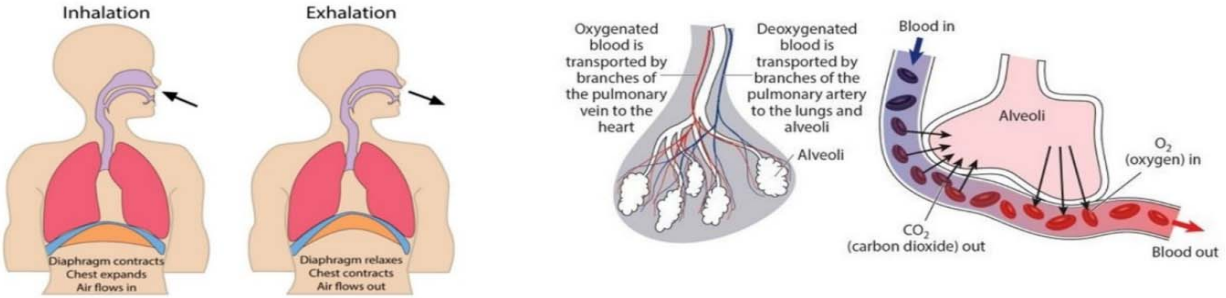

Fig. 5. External (left) and internal (right) respiration

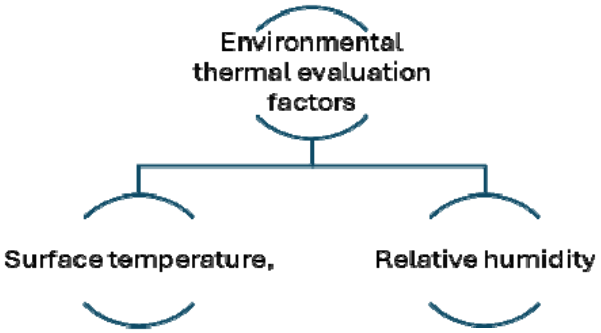

Fig. 6. Environmental thermal evaluation factors

environmental changes. This mechanical feedback system enables the indoor environment to adjust more precisely and maintain desired conditions.

Smart Materials Analysis

Enhancing energy efficiency in the building sector is one of the most effective strategies for ensuring sustainability and conserving natural resources for future generations. The energy performance of a building is closely linked to the condition of its envelope, as efficient envelopes minimize energy consumption for heating, cooling, and ventilation. Smart building skins are capable of responding to both the surrounding environment and external weather conditions (Beaven and Vincent, 2004). By incorporating environment-responsive materials and adaptive design strategies, energy consumption can be significantly reduced. Smart materials, which react dynamically to changes in their surroundings, play a crucial role in these adaptive systems (Addington and Schodek, 2005).

The following section provides a detailed analysis of behavioral traits and smart facade strategies, which can serve as a foundation for energy simulations and physical experiments. Six advanced facade technologies are examined: intelligent facades, phase change materials, vertical greenery systems, thermo-bimetals, breathing walls, and climate adaptive building shells. Each technology is evaluated based on its behavioral response to environmental changes and its potential to reduce energy consumption.

Intelligent Facade

Intelligent facades integrate a variety of technologies designed to reduce energy

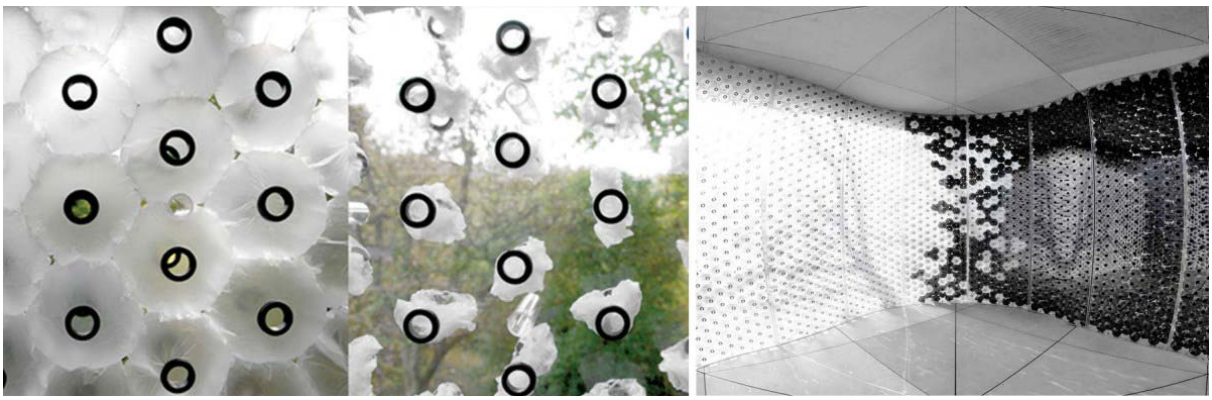

Fig. 7. Breathing skin

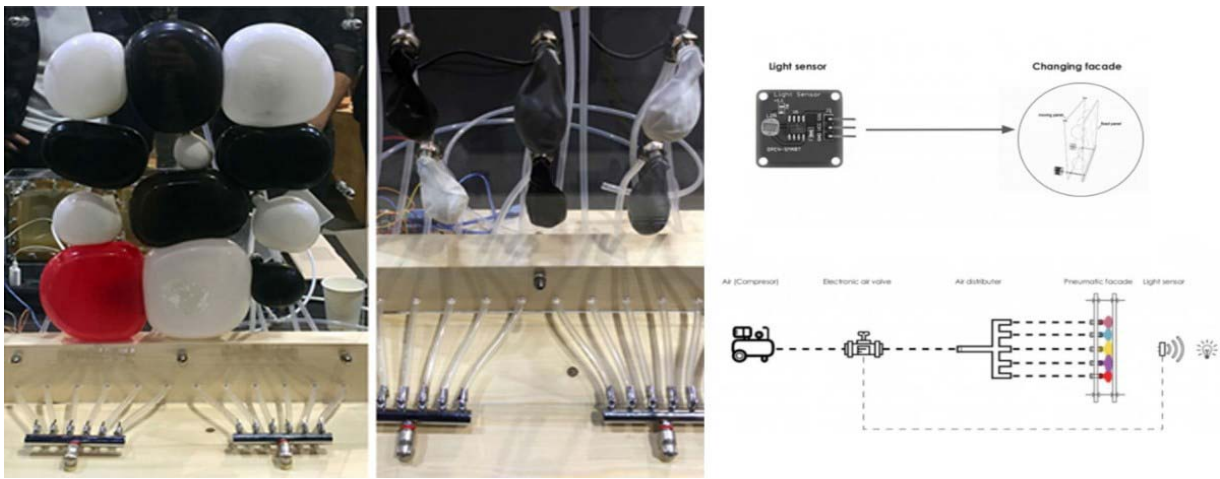

Fig. 8. Adaptive pneumatic skin

consumption and enhance indoor comfort (Omrany et al., 2016). The terms “smart materials“ and “intelligent facades” are often used interchangeably, as both involve interactive, responsive, and adaptive environmental functions. The development of intelligent envelopes increasingly relies on smart materials capable of generating energy and autonomously activating in response to environmental conditions (Velikov and Thün, 2013). Compared to traditional responsive systems, intelligent facades incorporate more sophisticated electronic control mechanisms to actively improve sustainability (Moloney, 2006). In this context, an intelligent facade refers to an integrated environmental control system that simultaneously aims to reduce energy consumption and enhance internal comfort (Fig. 9).

For an intelligent facade to be responsive, it must consider three key environmental parameters: the context, the occupant, and the weather (Omrany et al., 2016) (Fig. 10). External temperature is a critical factor in responding to fluctuating conditions, while the wall must also adapt to the preferences of individual occupants and the specific context of the building (Skelly, 2000).

An external wall system can be classified as a new functional wall if it achieves energy efficiency and indoor thermal comfort by responding to internal or external environmental conditions. If it additionally incorporates intelligent features that actively promote sustainability, it qualifies as an intelligent facade. The classification depends primarily on the behavioral and functional attributes of the wall rather than its material type or structural function. Reactivity and enhanced energy efficiency are two core characteristics of intelligent facades. According to Skelly, an intelligent facade embodies five distinct traits and responds to contextual factors, as illustrated in Fig. 11. By integrating these traits, an intelligent facade achieves two objectives: reducing energy use and improving internal thermal comfort while engaging dynamically with its surroundings.

Climate Adaptive Building Shells (CABS)

Similar to intelligent facades, climate adaptive building shells (CABS) are described using terms such as “adaptable”, “intelligent”, “smart”, “responsive”, and “kinetic”, but they possess distinct characteristics. The external structural components of the building shell, such as the roof and walls, provide a boundary between the interior and exterior environments (Loonen et al., 2013). CABS facades act as external shields, protecting interior spaces from environmental influences. A notable example is the Al Bahr Towers project in Abu Dhabi (Fig. 12), which incorporates an adaptive external shading system to respond to solar radiation. The Arup Group developed the external shading system and its operating mechanism, while AHR Architects designed the tower structure.

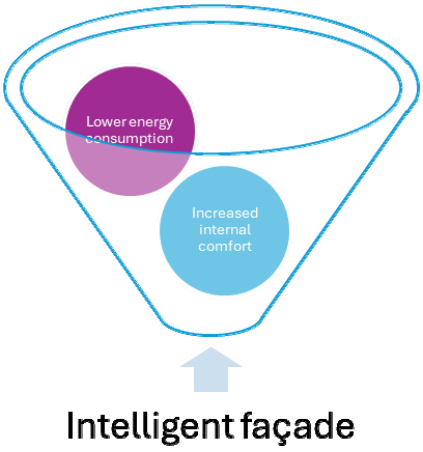

Fig. 9. Goals of an intelligent facade

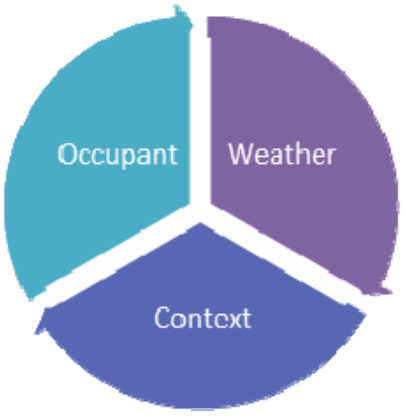

Fig. 10. Three environmental factors or parameters for responsiveness

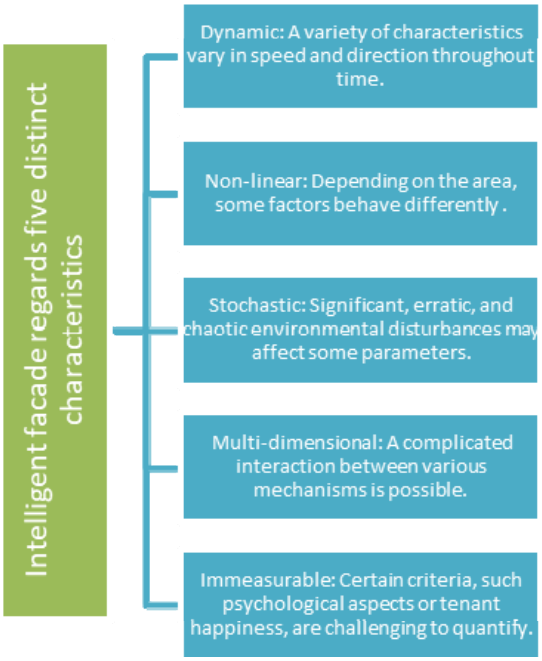

Fig. 11. Five distinct characteristics of an intelligent facade

The project features a two-layer facade, with movable shading elements attached to the exterior of the curtain wall surrounding the cylindrical tower. Solar tracking software controls the movement of these components, opening and closing them in response to the Sun's position, thereby optimizing the building's environmental performance (Autodesk, 2017). The primary advantage of this two-layer facade system is its ability to regulate energy flows and enhance indoor comfort by limiting solar heat gain. Similar to intelligent facades, CABS improve thermal comfort and energy efficiency. However, CABS distinguish themselves through three defining characteristics: adaptability, multi-functionality, and evolutionary capacity, making it possible to utilize dynamic facade elements more extensively than traditional intelligent walls.

Vertical Greenery System (VGS)

Vertical greenery systems (VGSs) can influence both surface and ambient temperatures, thereby enhancing the thermal performance of buildings. By reducing the demand for cooling energy, these systems contribute to environmental sustainability. VGSs, commonly referred to as green walls, vertical gardens, or green facades, have been widely adopted as a sustainable architectural practice worldwide (Fig. 13). The cooling effect of VGSs is achieved through a combination of plant shading, low solar absorbance, low-albedo surfaces, evapotranspiration, and the insulating properties of vegetation. These mechanisms collectively reduce the surface temperature of building walls (Pan and Chu, 2016). In tropical climates, VGSs reduce surface wall temperatures by up to 11.58°C (Wong et al., 2010). Furthermore, VGSs installed on south- and west-facing facades can reduce the building's cooling load by 1.4 % to 28.4 %, depending on the specific conditions of the building (Omrany et al., 2016).

Phase Change Materials (PCMs)

Phase change materials (PCMs) are widely used in thermal energy storage systems due to their ability to absorb heat under normal conditions and release it when needed. Over the past decade, PCM technology has attracted considerable attention for its energy efficiency, sustainability, and heat storage capabilities. When integrated with natural ventilation systems, PCMs can provide significant reductions in cooling loads. The key mechanism of PCMs is phase change, which occurs when materials repeatedly melt and solidify at specific ambient temperatures. This allows building envelope materials to transition between solid and liquid states, absorbing or releasing heat in the process. Paraffin wax, a common organic PCM, changes phase in response to temperature fluctuations, effectively storing or releasing thermal energy as needed (Faircloth et al., 2018). In building applications, PCMs help reduce HVAC sizing by utilizing thermal energy storage systems to offset peak energy loads. Studies in Germany have shown that integrating macro-encapsulated PCMs with building materials can lower indoor temperatures by up to 4°C (Schossig et al., 2005) (Fig. 14). PCMs represent a smart and environmentally friendly solution that enhances indoor thermal comfort, improves indoor air quality, and contributes to energy savings. Building envelopes with high heat-capacity materials utilize stored energy more efficiently during periods of deficit.

Thermo-bimetals

Thermo-bimetal is an innovative smart material. These materials can change shape and move in response to variations in temperature or humidity without requiring external energy. To control self-ventilation systems, thermo-bimetals have been experimented with as adaptive components capable of opening and closing pores autonomously (Sung, 2016) (Fig. 15). Incorporating these dynamic morphological elements into building envelopes enhances indoor comfort and energy efficiency. A thermo-bimetal consists of two layers of metal with different coefficients of thermal expansion; when heated, the material curls in a certain direction. The double-layered sheet metal, such as TM2 defined by

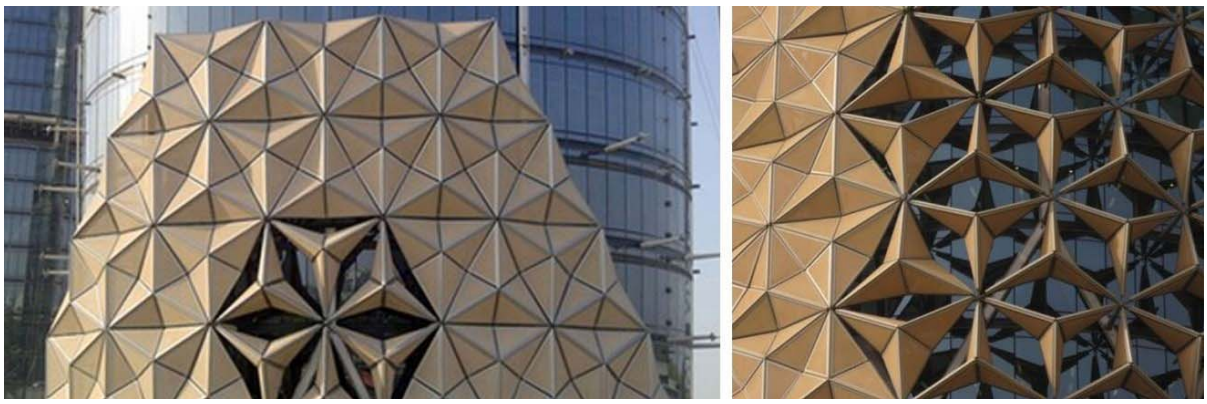

Fig. 12. Climate adaptive building shells

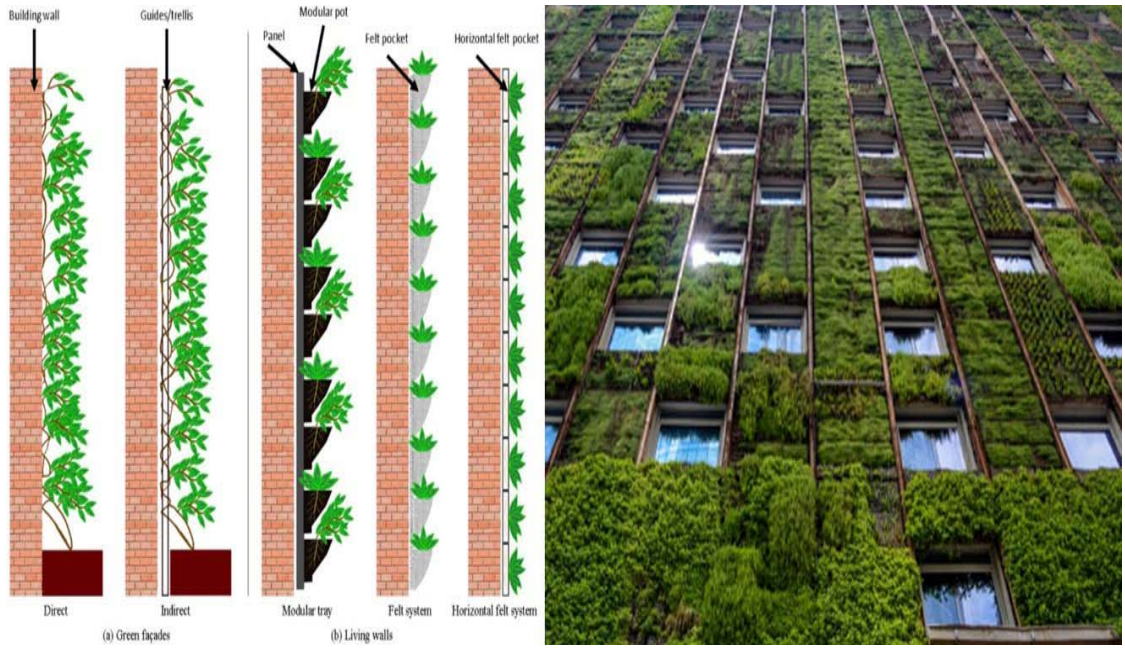

Fig. 13. Example of VGS types (left); VGS (right)

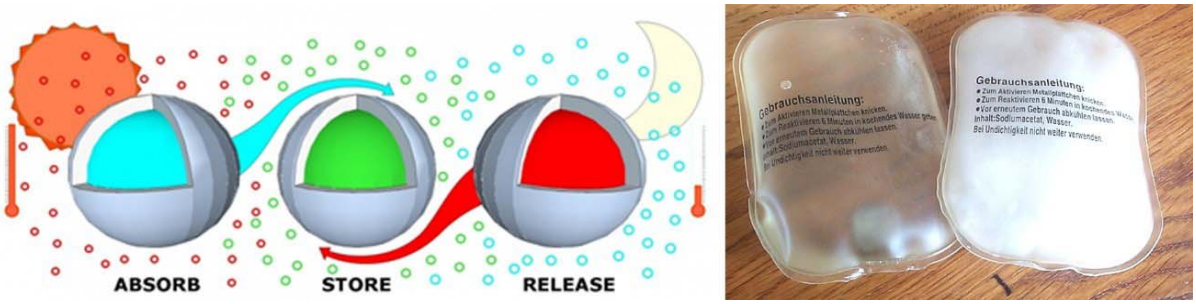

Fig. 14. Schematic diagram of macro-encapsulated PCMs (left); PCMs (right)

Fig. 15. Thermo-bimetals for natural ventilation effects

ASTM (American Society for Testing and Materials), typically includes an Invar layer with a low coefficient of expansion, while the outer layer expands more rapidly. In practical applications, such as the Pivot Shading System project, thermo-bimetals are used as shading devices. By curling in response to temperature changes, the system can regulate solar heat gain and control light penetration (Sung, 2011). Buildings incorporating thermo-bimetals benefit from reduced energy consumption and improved indoor air quality.

Breathing Walls

Breathing walls utilize natural ventilation to introduce outdoor air into the building. By employing

active or passive decompression, these systems draw clean air from the exterior, creating a dynamic insulating effect (Imbabi and Peacock, 2003). This approach combines natural ventilation with dynamic insulation, allowing the building envelope to “breathe” and providing two key benefits. The primary advantage of a breathing wall is the removal of indoor pollutants, delivering cleaner and filtered air to occupants. The secondary benefit is an increase in building energy efficiency, achieved through reduced thermal conductivity of the walls.

Natural Ventilation

Air ventilation is essential for maintaining proper indoor air quality, as it facilitates air movement and exchange. Building ventilation can occur through mechanical or natural means, both designed to regulate air cycles and enhance indoor air quality. Air leakage caused by differences in air pressure can produce a stacking effect within the building. Mechanical ventilation systems utilize components such as intake louvers, exhaust grilles, fans, and ductwork to purposefully circulate air into and out of the structure (ASHRAE, 2017).

Passive natural ventilation is commonly employed in breathing walls. A hollow gap in the double-layer walls allows wind pressure to induce air buoyancy, promoting airflow that removes indoor pollutants while supplying clean outdoor air. When outdoor air enters the wall system, it alters room airflow patterns and diffuses throughout the space. Two primary flow types are observed: displacement flow and entrainment flow (Fig. 16). Displacement flow utilizes buoyancy to move supplied air upward without turbulence, efficiently expelling indoor airborne contaminants through exhaust outlets. Entrainment flow combines indoor air with incoming clean air, creating a turbulent flux for distribution. However, effective mixing can be limited when air pressure is low or airflow velocity is insufficient. Maintaining appropriate air pressure and speed is crucial for the efficient removal of airborne pollutants. Proper indoor air quality and pressure management are essential to prevent the accumulation of indoor pollutants (ASHRAE, 2017).

Results

Based on the preceding discussion, all six innovative facade systems — climate adaptive building shells, vertical greenery systems, phase change materials, thermo-bimetals, intelligent facades, and breathing walls — demonstrate the capacity to respond to climate-related environmental changes. Table presents a comparative analysis of these technologies according to three criteria: response to climate change, electricity consumption, and impact on indoor air quality.

All six innovative facade systems are capable of responding to climate change to enhance environmental performance. Their passive or active responses can be evaluated using various metrics that reflect improvements in environmental conditions. Five of the six systems operate passively, requiring no electricity to adjust to environmental stimuli; only CABS rely on electrical power to actuate shape changes in response to solar movement.

Thermo-bimetals exhibit morphological changes triggered by ambient temperature, providing consistent adaptation to environmental variations. PCMs and VGSs also demonstrate passive responses through physical or thermal transformations.

Intelligent facades and CABS produce kinetic changes via physical motion, with CABS additionally responding to temperature through integrated sensors. In contrast, PCMs, thermo-bimetals, and breathing walls react spontaneously due to their intrinsic properties. Both breathing walls and PCMs, which actively respond to thermal variations, demonstrate the potential to influence energy flow within the building.

Conclusions

This research examined the relationship between biomimicry and breathing facades through an analysis of innovative facade systems. The results indicate that thermo-bimetals and breathing walls can reduce energy consumption and improve indoor air quality by moderating building temperatures.

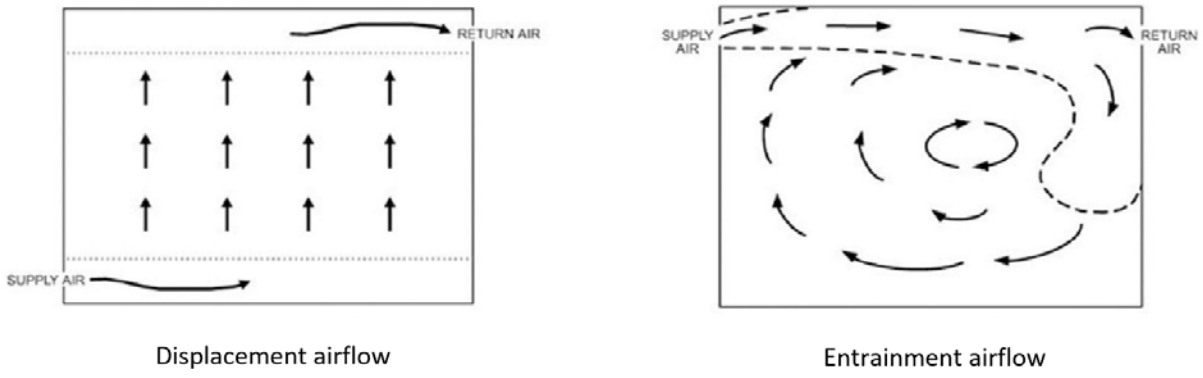

Fig. 16. Airflow movements

Comparative analysis of innovative facade technologies

		Intelligent Facade	Climate Adaptive Building Shells	Vertical Greenery System	Phase Change Materials	Thermo-bimetals	Breathing Walls
Response to climate change	Responsive	✓	✓	✓	✓	✓	✓
	Attributes	temperature sensors	solar movement	environmental adaptability	environmental adaptability	ambient air temperature	✓
Electricity consumption		×	✓	×	×	×	×
Impact on indoor air quality		×	×	×	×	✓	✓

In addition, breathing facades enhance indoor air quality through natural or mechanical ventilation, demonstrating significant potential to decrease inflow air temperatures. Proper building ventilation also contributes to lowering interior temperatures. These findings highlight the importance of integrating breathing facades into architectural design processes to optimize indoor air quality, user comfort, and energy efficiency. The study contributes to both the theoretical and applied understanding of architectural responses to changing environmental conditions.

Despite these insights, several limitations should be noted. The study focused primarily on humid tropical, Mediterranean, and temperate maritime climates, which may limit the generalizability of the results. In hot, dry desert climates, additional design considerations, such as double dust protection, would be necessary. Furthermore, the analysis was largely theoretical, lacking field testing, actual performance data, or user feedback. Future research should expand the climatic range, incorporate quantitative field measurements, and evaluate user experience to enhance the accuracy and applicability of the findings.

References

Addington, M. and Schodek, D. (2005). *Smart materials and new technologies. For the architecture and design professions*. Oxford: Architectural Press, 241 p.

ASHRAE (2016). ANSI/ASHRAE Standard 62.1-2019. *Ventilation for Acceptable Indoor Air Quality*. Atlanta: ASHRAE, 93 p.

ASHRAE (2017). Chapter 16. Ventilation and infiltration. In: *2017 ASHRAE handbook. Fundamentals* (pp. 16.1–16.38). Atlanta, GA: ASHRAE.

Autodesk (2017). *Making shade in Abu Dhabi: the Al Bahr Towers' adaptive architecture*. [online] Available at: https://www.cardiganrow.com/news/making-shade-abu-dhabi-al-bahr-towers%E2%80%99-adaptive-architecture [Date accessed November 28, 2024].

Beaven, M. and Vincent, J. (2004). Engineering Intelligence through nature. In: Clements-Croome, D. (ed.). *Intelligent buildings: design, management and operation*. London: Thomas Telford Limited, pp. 169–187.

Becker, T. (2016). *Innovation. The breathing skins. Tebe Berlin*. Available at: https://www.tebe.berlin/breathing-skins [Date accessed November 28, 2024].

Benyus, J. M. (1997). *Biomimicry: innovation inspired by nature*. New York: William Morrow, 308 p.

Craig, A. D. B. (2018). Central neural substrates involved in temperature discrimination, thermal pain, thermal comfort, and thermoregulatory behavior. In: Romanovsky, A. A. (ed.). *Handbook of Clinical Neurology*, Vol. 156, pp. 317–338. DOI: 10.1016/B978-0-444-63912-7.00019-9.

Ensikat, H. J., Ditsche-Kuru, P., Neinhuis, C., and Barthlott, W. (2011). Superhydrophobicity in perfection: the outstanding properties of the lotus leaf. *Beilstein Journal of Nanotechnology*, Vol. 2, pp. 152–161. DOI: 10.3762/bjnano.2.19.

Faircloth, B., Welch, R., Sinke, Y., Tamke, M., Nicholas, P., Ayres, P., Eherenbard, E., & Ramsgaard Thomsen, M. (2018). Coupled modeling and monitoring of phase change phenomena in architectural practice. In: Rakha, T., Turrin, M., Macumber, D., Meggers, F., and Rockcastle, S. (eds.). *2018 Proceedings of the Symposium on Simulation for Architecture and Urban Design*. San Diego: SCS, pp. 81–88.

IAAC (2019). *Adaptive pneumatic skin*. [online] Available at: http://www.iaacblog.com/programs/84626/ [Date accessed November 28, 2024].

Imbabi, M. S. and Peacock, A. (2003). Smart breathing walls for integrated ventilation, heat exchange, energy efficiency and air filtration. In: *ASHRAE/SIBSE Conference: Building Sustainability, Value and Profit*, September 24–26, 2003.

Laird, K. (2016). *Biomimetic plastic skin allows building façade to "breathe"*. [online] Available at: https://www.plasticstoday.com/building-construction/biomimetic-plastic-skin-allows-building-fa-ade-to-breathe- [Date accessed November 28, 2024].

Loonen, R. C. G. M., Trčka, M., Cóstola, D., and Hensen, J. L. M. (2013). Climate adaptive building shells: state-of-the-art and future challenges. *Renewable and Sustainable Energy Reviews*, Vol. 25, pp. 483–493. DOI: 10.1016/j.rser.2013.04.016.

Moloney, J. (2006). Between art and architecture: the interactive skin. In: Banissi, E., Burkhard, R. A., Ursyn, A., Zhang, J. J., Bannatyne, M. W. M., Maple, C., Cowell, A. J., Tian, G. Y., and Hou, M. (eds.). *Information Visualization*. London: IEEE Computer Society, pp. 681–686. DOI: 10.1109/IV.2006.28.

Nkandu, M. I. and Alibaba, H. Z. (2018). Biomimicry as an alternative approach to sustainability. *Architecture Research*, Vol. 8, No. 1, pp. 1–11. DOI: 10.5923/j.arch.20180801.01.

Omrany, H., Ghaffarianhoseini, A., Ghaffarianhoseini, A., Raahemifar, K., and Tookey, J. (2016). Application of passive wall systems for improving the energy efficiency in buildings: a comprehensive review. *Renewable and Sustainable Energy Reviews*, Vol. 62, pp. 1252–1269. DOI: 10.1016/j.rser.2016.04.010.

Pan, L. and Chu, L. M. (2016). Energy saving potential and life cycle environmental impacts of a vertical greenery system in Hong Kong: a case study. *Building and Environment*, Vol. 96, pp. 293–300. DOI: 10.1016/j.buildenv.2015.06.033.

Pawlyn, M. (2019). *Biomimicry in architecture*. London: Riba Publishing, 176 p.

Schossig, P., Henning, H.-M., Gschwander, S., and Haussmann, T. (2005). Micro-encapsulated phase-change materials integrated into construction materials. *Solar Energy Materials and Solar Cells*, Vol. 89, Issues 2–3, pp. 297–306. DOI: 10.1016/j.solmat.2005.01.017.

Skelly, M. (2000). Essay competition: the individual and the intelligent facade. *Building Research & Information*, Vol. 28, No. 1, pp. 67–69.

Sung, D. K. (2011). Skin deep: making building skins breathe with smart thermobimetals. In: Perez-Gomez, A., Cormier, A., and Pedret, A. (eds.). *99th ACSA Annual Meeting Proceedings, Where Do You Stand*. Washington, DC: ACSA Press, pp. 145–152.

Sung, D. (2016). Smart geometries for smart materials: taming thermobimetals to behave. *Journal of Architectural Education*, Vol. 70, No. 1, pp. 96–106.

Turner, J. S. (2016). Homeostasis is the key to the intelligent building. *Intelligent Buildings International*, Vol. 8, Issue 2, pp. 150–154. DOI: 10.1080/17508975.2015.1042958.

Velikov, K. and Thün, G. (2013). Responsive building envelopes: characteristics and evolving paradigms. In: Trubiano, F. (ed.). *Design and Construction of High-Performance Homes*. London: Routledge, pp. 75–92.

Wong, N. H., Tan, A. Y. K., Chen, Y., Sekar, K., Tan, P. Y., Chan, D., Chiang, K., and Wong, N. C. (2010). Thermal evaluation of vertical greenery systems for building walls. *Building and Environment*, Vol. 45, Issue 3, pp. 663–672. DOI: 10.1016/j.buildenv.2009.08.005.

ВЛИЯНИЕ «ДЫШАЩИХ» ФАСАДОВ И БИОМИМИКРИИ НА ВЕНТИЛЯЦИЮ И КАЧЕСТВО ВОЗДУХА В ПОМЕЩЕНИЯХ

Эхсан М. Эльхеннави[1]*, Хешам Самех Хуссейн Самех[2]

[1]Институт высших технологий, Город 10-го Рамадана, Египет
[2]Каирский университет, Египет

*E-mail: ehsan.m.k.89@gmail.com

Аннотация
Введение: Одной из наиболее актуальных проблем современности является глобальное потепление, которое существенно повышает температуру внутри зданий. Разработка экономически эффективных решений для снижения перегрева помещений представляет собой важную архитектурную задачу. В данной работе рассматривается влияние «дышащих» фасадов на вентиляцию и качество воздуха в помещениях, с особым акцентом на связь между биомимикрией и проектированием фасадов. Уделяется внимание тому, как биомимикрия вдохновляет архитекторов на решение экологических проблем. На ряде примеров исследуется концепция «дышащих оболочек». **Цель исследования** — анализ взаимосвязи между биомимикрией и «дышащими» фасадами, а также оценка их эффективности в улучшении качества воздуха в помещениях и снижении температуры в зданиях. **Методы**: используются индуктивный и аналитический подходы в рамках систематического обзора литературы, дополненного сравнительным анализом для оценки эффективности инновационных фасадных систем. **Результаты**: полученные данные свидетельствуют о том, что интеллектуальные «дышащие» фасады обладают значительным потенциалом снижения уровня загрязнения и повышения комфорта проживания в городской среде.

Ключевые слова: «дышащие» фасады, устойчивая архитектура, биомимикрия, вентиляция, качество воздуха в помещениях.

DOI: 10.23968/2500-0055-2025-10-3-40-52

EVOLUTION AND ADVANCEMENTS IN THERMAL COMFORT RESEARCH : A NARRATIVE LITERATURE REVIEW

Shivani Senthilkumar[1]*, Poulomee Ghosh[2]

[1]Research Scholar, NICMAR University, Pune, India – 411045
[2]School of Real Estate and Facilities Management, NICMAR University, Pune, India – 411045

*Corresponding author's email: shivani.phd2@pune.nicmar.ac.in

Abstract
Introduction: Climate change, heat waves, greenhouse gas emissions, and global warming have become a never-ending cycle, contributing to environmental degradation and causing discomfort to humans and other living beings. To address climate change, research on the thermal comfort of buildings has been conducted and developed since 1946, using both passive and active thermal comfort strategies. To understand the evolution of thermal comfort, this paper aims to establish the progression and principles of thermal comfort research. **Methodology:** A narrative literature review method was adopted to analyze the progress of thermal comfort research. A total of 122 selected articles examined concepts, models, architectural perspectives, standards, and policies related to thermal comfort. **Results and discussion:** Thermal comfort has evolved from the invention of air conditioning to the application of passive thermal comfort strategies in buildings. Thermal comfort research has consistently identified six key parameters that have improved our understanding of indoor thermal comfort. Moreover, the use of innovative technologies in thermal comfort studies can enhance occupant health and well-being. An interdisciplinary approach to thermal comfort research is therefore necessary. **Recommendations:** This study outlines the sequence of thermal comfort research, including innovations in models, simulation, prediction, and emerging challenges. As such, it will help future researchers, developers, and other stakeholders in the built environment to fill gaps and connect past findings with future directions.

Keywords: thermal comfort, chronology of thermal comfort, thermal comfort models, adaptive thermal comfort model.

Introduction

Climate change is a global concern. Human emissions become trapped in the atmosphere and release heat back into the environment. Carbon dioxide — one of the key greenhouse gases responsible for climate change — remains in the atmosphere for 300 to 1,000 years after it is initially produced, causing heat waves (NASA, 2019). As a result, the average global temperature has risen by 0.8°C compared to pre-industrial levels (NASA, 2011). Heat waves are becoming more frequent, severely affecting human survivability, especially in countries like India (Gupta, 2024). This climate scenario increases the demand for thermal comfort (TC) in living spaces, leading to the widespread installation of air conditioners in buildings and further contributing to emissions. It should be noted that approximately 30 % of all CO_2 emissions come from buildings, which accounts for nearly 40 % of global energy use (Lee et al., 2023).

Thermal comfort (TC) refers to the sensation of being hot or cold in a confined environment. It is essentially about how a person feels in a space, whether they perceive it as comfortable or not. Here, comfort is understood primarily in terms of temperature. The definition of TC is "the condition of mind that expresses satisfaction with the thermal environment" (ASHRAE, 2013). Several other studies have also provided definitions of TC. According to Emetere (2022), TC is a subjectively evaluated mental state that indicates contentment with the thermal environment. In addition to being a person's perception of the thermal atmosphere, TC is also described as a neutral sensation regarding a given thermal environment — that is, the ability to remain sweat-free. TC is a multifaceted phenomenon influenced by mean radiant heat, air velocity, relative humidity, and ambient temperature (Chatzidimitriou and Yannas, 2016). There are six main TC parameters: four environmental factors (air temperature, relative humidity, mean radiant temperature, and air velocity) and two personal factors (clothing insulation and metabolic rate). These parameters are universally recognized and adopted in research and practice.

Research on TC has continually progressed, evolving from the invention of air conditioning (active strategies) to a growing focus on passive strategies, with contemporary emphasis on climate change, energy consumption, and environmental impacts. However, the roots of TC extend back to human evolution, beginning when humans lived in caves. The invention of fire provided warmth during cold nights, marking one of the earliest concerns for TC. This historical perspective illustrates that humans have always sought ways to maintain thermal

For citations: Senthilkumar, Sh., Ghosh, P. (2025). Evolution and advancements in thermal comfort research : a narrative literature review. Architecture and Engineering, No 3 (10), pp. 40–52. DOI: 10.23968/2500-0055-2025-10-3-40-52.

satisfaction. Scientists studied TC on warships and gradually shifted their focus to indoor environments. Research advanced further with the introduction of computerization, simulation, and modeling. Modern TC research began in earnest in the 1930s, initially focusing on human metabolic activities (Stoops, 2006).

Typical areas of TC research can be categorized as follows: TC and energy efficiency, indoor environmental quality (IEQ) (Ma et al., 2021; Weng et al., 2023; Zuo et al., 2021), TC measurements (Nishi et al., 2017; Revel et al., 2014), passive strategies (Elshafei et al., 2021; Inusa and Alibaba, 2017; Pitts, 2017; Rana, 2021; Tungnung et al., 2023), active strategies (Gomez-Azpeitia et al., 2012; Han and Chen, 2017; International Energy Agency, 2018), TC bands (Faheem et al., 2023; Pal et al., 2024; Soflaei et al., 2020), adaptive TC (Manu et al., 2016; Rawal et al., 2022), personal TC (Luo et al., 2018), group comfort systems and analysis (Chowdhury et al., 2008; Kumar et al., 2022; Weng et al., 2023; Xie et al., 2014), simulation (Pragati et al., 2023; Thapa et al., 2023), and optimization (Alghamdi et al., 2024; Liu et al., 2024; Senthilkumar and Ayyathurai, 2022). As research has advanced, the complexity and scope of TC studies have also expanded. Understanding the chronological development and diverse areas of TC research is therefore crucial for new researchers. Given the breadth of the literature and the significance of the field, a clear understanding of TC evolution is especially important, particularly regarding its implications in India.

This study aims to identify the chronological progression of TC research, providing a comprehensive overview of its evolution over time. It seeks to explore key themes, trends, and debates within the literature, offering insights into the primary focus areas and ongoing discussions in the field. Finally, the study aims to highlight gaps and opportunities for future research, equipping researchers with a clearer understanding of TC studies and guiding them in selecting appropriate methodologies by building on existing models and approaches.

Method of Literature Review

This study adopted a narrative literature review approach, which is well-suited to the aim of understanding the chronological progression of TC research. The literature search was conducted using electronic databases such as Scopus, Google Scholar, ScienceDirect, and ProQuest. The timeline for the search was set from 1946 to 2024 (see Fig.1). Such an extensive time range was required to capture the chronology of TC studies. The starting year of 1946 was chosen because the earliest published evidence on Scopus dates from that year. The preliminary screening of papers was based on titles and abstracts. The keyword “thermal comfort” generated 39,847 papers in Scopus. Papers were selected according to three main criteria: 1) to understand the fundamental concepts of TC and its relationship with the environment; 2) to trace the evolution of TC, including its origins, early indicators, and applications in architecture; 3) to examine research domains focused on TC models, simulation and prediction, standards, and policies. Only papers written in English were considered. In total, 122 sources were reviewed for this study, including journal papers, reports, conference proceedings, book chapters, code books, standards, and web resources. Of these, 86 were cited directly.

Chronology of Thermal Comfort Research

The study of TC is inherently interdisciplinary. As discussed earlier, TC concerns the thermal

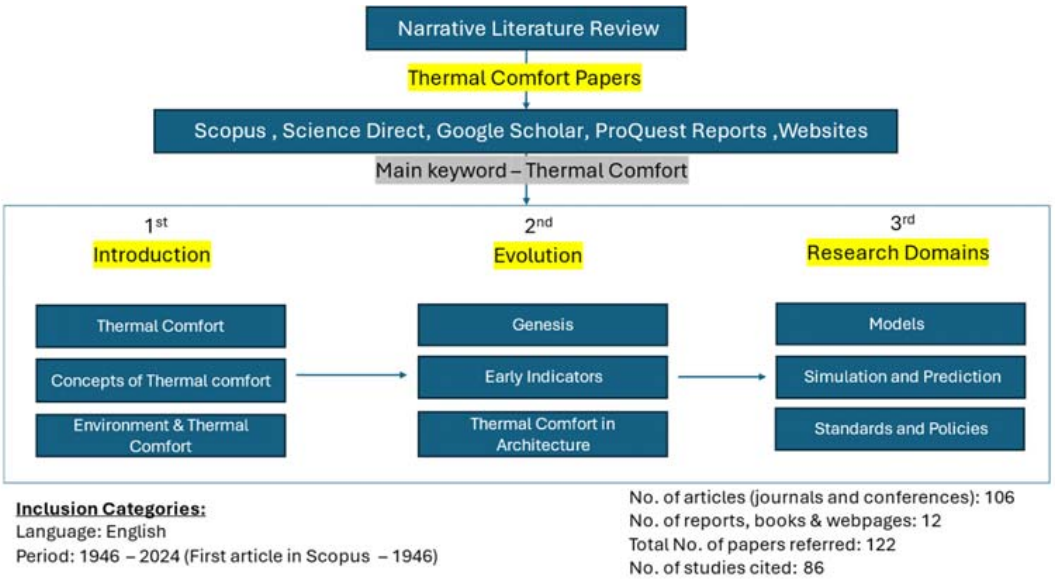

Fig. 1. Flowchart illustrating the literature review process for this study (Source: Author)

satisfaction of building occupants. Early TC research was primarily driven by military needs, focusing on innovations for warships, airplanes, and high-temperature environments. Research then shifted to indoor TC, examining physical, physiological, psychological, social, and cultural interactions, including the influence of human activity, clothing, architecture, and eating habits (Fabbri, 2015). Initially, TC studies concentrated on human physiology and physical factors. Over time, the focus evolved toward adaptive thermal comfort, exploring how people adjust their behavior to maintain comfort indoors. This transition also introduced the concept of space heating, which became a central concern in Western countries, where heating needs were particularly significant (de Dear et al., 2016).

Genesis of Thermal Comfort Research

This section identifies and discusses the key events and milestones in the history of TC research in chronological order.

The earliest stages of TC research focused on human comfort and the physiological effects of the environment. In 1850, American physician John Gorrie invented the first cooling machine, designed for hospitals to treat yellow fever patients. The device operated on a cold-air refrigeration process, emerging from attempts to reduce patient fevers by cooling indoor spaces. Fifty years later, in 1902, Willis Carrier — known as the father of modern air conditioning — developed the first true air conditioner. Carrier's system cooled air by passing it over coils filled with chilled water. Although the earliest air conditioners were large and expensive, the underlying principles remain the basis of today's systems. Early research at this stage primarily emphasized air temperature and air-related parameters. In the 1910s, synthetic air charts were introduced to represent vapor–liquid equilibria in the air. Building on this, Carrier made a major contribution in 1911 by presenting the psychrometric chart, a breakthrough that laid the foundation for modern air conditioning (McDowall, 2006) . This chart illustrated the relationships between temperature, humidity, and other air properties, becoming an essential tool for engineers, architects, and HVAC (Heating, Ventilation, and Air Conditioning) specialists. The application of psychrometrics quickly extended beyond building comfort to fields such as meteorology, agriculture, and industrial processes, significantly shaping the design and operation of air conditioning and refrigeration systems (Teitelbaum et al., 2023). At the core of these studies was the investigation of water–air vapor–liquid equilibrium, fundamental to understanding TC and the dynamic interplay between relative humidity and air temperature (Mark Crawford, 2012).

The studies "Determination of the Comfort Zone" and "Determining the Lines of Equal Comfort", published in 1923 by Houghten and Yaglou, introduced the empirical index of Effective Temperature (ET). ET for a given space is defined by the dry-bulb temperature of a thermo-equivalent environment with 50 % relative humidity and a specific uniform radiation condition. The term "thermo-equivalent conditions" refers to combinations that produce the same sensation of warmth or coldness (Roy Choudhury et al., 2011).

In 1936, Gagge developed the two-node model, a technique for predicting how the human body responds to temperature changes in its surroundings. This model has applications in thermal ergonomics, occupational health, and HVAC design, and is useful for evaluating human TC. According to the model, the human body is represented as two interacting thermal nodes: the core node, representing internal organs, and the skin node, representing the body's outer layer. This model is particularly important in environments where maintaining optimal temperatures is critical for human safety and comfort (van Hoof, 2008).

Simultaneously, the use of thermal manikins for TC research gained popularity in the 1940s. The United States Army was the first to adopt thermal manikins, subsequently using them to study indoor environments, clothing, and textiles (Simova et al., 2021). Thermal manikins are used to measure the Manikin-Based Equivalent Temperature (MBET), helping to determine tolerable temperatures and evaluate personal comfort systems (Luo et al., 2018; Mustakallio et al., 2017).

By the 1950s and 1960s, research increasingly focused on the impact of discomfort on health, giving rise to the term "Sick Building Syndrome" (Ganji et al., 2023; Nduka et al., 2021; Weng et al., 2023; Zuo et al., 2021). Many studies from this period were published in journals related to medicine, health, textiles, physiology, industrial medicine, toxicology, and industrial hygiene. The first documented building TC research in Scopus dates back to 1954, with a study by A. E. Moore on the thermal properties of concrete floors.

The 1960s and 1970s are often regarded as the golden era of TC research, during which numerous influential studies were conducted. Danish physiologist Ole Fanger focused on the correlation between environmental and physical factors and physiological responses, alongside subjective well-being reported by occupants (van Hoof, 2008). Building on this work, Fanger developed models such as the Predicted Mean Vote (PMV) to predict TC for groups of people (van Hoof, 2008). His contributions laid the foundation for adaptive TC research (Fabbri, 2015; Karyono et al., 2020). Later, Richard de Dear proposed an adaptive TC model, which was adopted in the ASHRAE 55 guidelines (Brager and de Dear, 1998).

Early Indicators of Thermal Comfort

In the 1950s, researchers including Constantine P. Yaglou and David Minard made a significant

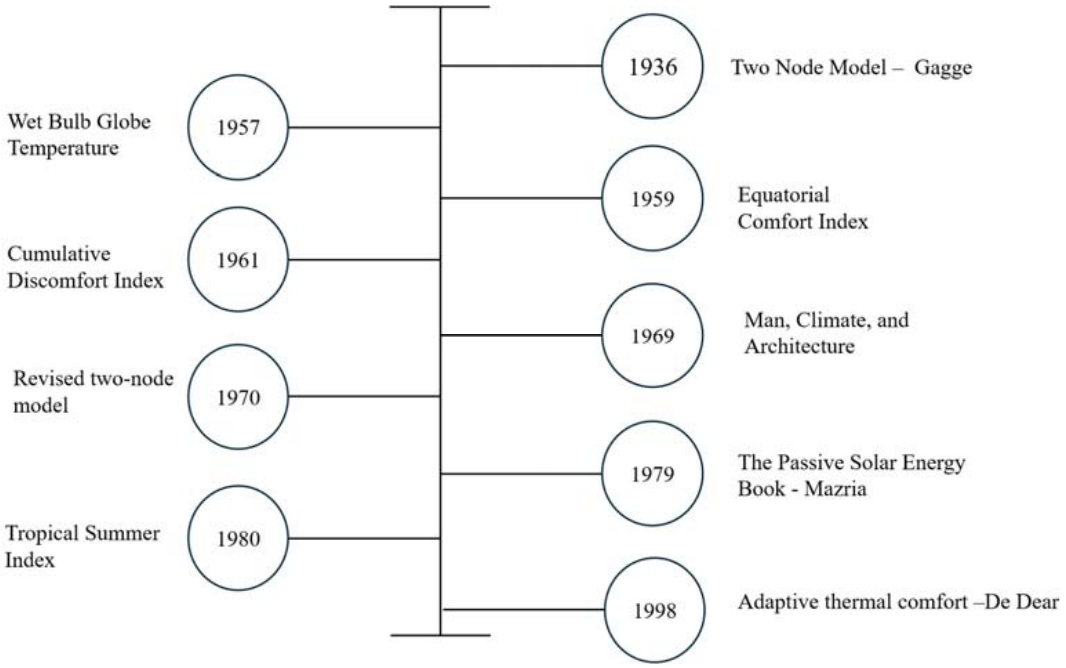

Fig. 2. Key milestones in the development of TC research (Source: Author)

contribution to the development of TC research (Fig. 2, Table). They introduced the Wet Bulb Globe Temperature (WBGT), a comprehensive index for assessing thermal discomfort that accounts for temperature, humidity, wind speed, and solar radiation. The WBGT is widely used to prevent heat-related illnesses and ensure safety in hot environments (Hensen Centnerová, 2018). Two other notable indices were subsequently developed: the Equatorial Comfort Index (ECI) in 1959 and the Cumulative Discomfort Index (CDI) in 1961. The ECI is used to assess TC in hot and humid climates by integrating temperature and humidity into a single measure. The CDI provides a practical method for evaluating the total amount of discomfort a person experiences over time due to environmental factors. It offers a comprehensive assessment of thermal stress by considering both the intensity and duration of exposure, helping to guide interventions and improve comfort and safety in various contexts (Fabbri, 2015). In 1980, researchers at the Central Building Research Institute, Roorkee, India, developed the Tropical Summer Index (TSI). This index measures the degree of tropical climatic characteristics, particularly during the summer, and is calculated using multiple meteorological parameters such as temperature, humidity, and precipitation. The TSI reflects both the severity and frequency of tropical conditions, representing an early effort to adapt TC research to local geographical and climatic conditions (Sharma and Ali, 1986).

Thermal Comfort in Architecture

Over time, TC research increasingly focused on the architectural aspects of buildings. While the use of vernacular materials and traditional designs was common, there was little documented evidence before the 1960s on the application of passive strategies to achieve TC. In 1963, Victor Olgyay published “Design with Climate”, introducing the concept of bioclimatic architecture, which examined the relationship between building form and climate. Similarly, in 1969, Baruch Givoni’s book “Man, Climate and Architecture” discussed human heat transfer and perspiration, emphasizing strategies to maintain comfort within built environments (Givoni, 1969).

Givoni discusses climate, human comfort, climate zones, architectural design, passive design strategies, building materials, thermal performance, and several case studies in his book. These works inspired Mazria’s 1979 “The Passive Solar Energy Book”, which developed architectural design principles for solar, passive, green, and bioclimatic architecture. Since then, researchers have explored and experimented with passive design strategies in buildings to enhance TC. Passive design strategies investigated include window-to-wall ratio (Abdullah and Alibaba, 2020), building envelope (Sharma and Chani, 2019; Surendran et al., 2023; Wang et al., 2020; Yamamoto, 2023), building insulation (Arumugam and Ramalingam, 2024), materials (Marey et al., 2024; Sen et al., 2014), glazing, building orientation (Kaushal et al., 2023; Sharma and Rakshit, 2017), form and shape, green and cool roofs, etc. (Jia et al., 2024; Kumar and Mahalle, 2016; Pragati et al., 2023). Researchers have also employed computer simulations to analyze and evaluate the performance of these passive strategies.

Key Milestones in TC Research (Source: Author)

Period	Focus	Key Developments	Key Researchers	Significance
Early research	Thermal regulation models	Two-node models	Gagge (1936)	Laid the foundation for understanding and modeling human thermal regulation.
1950s–1960s	Indoor TC, comfort zones	Comprehensive studies on Wet Bulb Globe Temperature (WBGT), Equatorial Comfort Index (ECI) and other thermal comfort indices, and comfort lines	Webb (1959), Yaglou and Minard (1957)	Identified indoor environment indices to measure and understand TC.
1960s–1970s	Developing TC models	Introduction of Predicted Mean Vote (PMV) and Predicted Percentage Dissatisfied (PPD) models to predict group TC	Fanger (1967)	Established a basis for predicting and quantifying TC in built environments.
1980s–present	Adaptive TC	Introduction of adaptive models; recognition of dynamic and personal variations in comfort	Brager and de Dear (1998)	Supported more flexible and energy-efficient building designs; influenced ASHRAE 55 and NBC.
Recent decades & ongoing	Passive and active strategies	Exploration of building orientation, materials, HVAC control, and PCM insulation	Ali et al. (2020), Dili et al. (2010), Elshafei et al. (2021), Figueiredo et al. (2020), Inusa and Alibaba (2017)	Advanced strategies for enhancing TC and energy efficiency in buildings.
Recent decades & ongoing	Simulations and computerization	Use of AI, ML, and genetic algorithms to optimize indoor TC and energy usage	Lu et al. (2019), Pragati et al. (2023), Silva et al. (2016), Soflaei et al. (2020), Xu et al. (2023)	Enhanced precision and control in building automation systems; improved energy efficiency.
1940–ongoing	Thermal manikins	Measurement of equivalent temperatures and evaluation of personal systems	Simova et al. (2021), Zasimova et al. (2023)	Provided accurate, detailed assessments of TC and supported ergonomic designs.
Recent & ongoing	Climate change and TC	Assessing climate change scenarios, mitigation strategies, and weather file usage	Dodoo and Ayarkwa (2019), Ferdyn-Grygierek et al. (2021), Tomrukcu & Ashrafian (2024)	Mitigation strategies for climate change scenarios.

Models of Thermal Comfort

This section discusses the main techniques and models used to measure and evaluate TC. Two widely recognized and universally accepted approaches are Fanger's PMV and PPD model and de Dear's adaptive comfort model.

(i) Fanger's model

Fanger made significant contributions to TC studies. He emphasized the relationship between physical environmental parameters, physiological indicators of occupants, and their subjective experience of well-being. In 1967, he published the paper "Calculation of Thermal Comfort: Introduction of Basic Comfort Equation", proposing a rating scale to assess reported sensations of comfort. In 1970, his book "Thermal Comfort" further highlighted the study of comfort and health in indoor environments. Fanger introduced the Predicted Mean Vote (PMV) to quantify an individual's perception of comfort based on four environmental and two personal factors. The PMV helps identify a comfort zone on psychrometric charts, setting optimal conditions for shared spaces such as theaters, hospitals, and shopping centers. However, the PMV alone does not indicate whether these conditions are universally acceptable. To address this limitation, Fanger proposed the Predicted Percentage of Dissatisfied (PPD) index, which estimates the proportion of individuals likely to feel discomfort under given conditions, even if the majority find them acceptable. For example, a PMV of –0.3 may appear slightly cold, but the PPD accounts for the 5 % of occupants who may find it unsatisfactory. The PPD–PMV diagram helps determine the percentage of dissatisfied individuals based on variations in the PMV, which depends on factors such as relative humidity, air velocity, temperature, metabolism, and clothing. Extreme PMV values, such as "very cold" or "very hot," exponentially increase dissatisfaction. Additional indicators, including stress indices and local

discomfort measures like heat stress, also reflect dissatisfaction caused by non-uniform environmental conditions. Architect Baruch Givoni introduced the Index of Thermal Stress (ITS) to assess thermal discomfort under such circumstances (Fabbri, 2015).

(ii) Adaptive TC

De Dear's adaptive thermal comfort model has significantly advanced our understanding and application of TC in building design. Unlike static models, it emphasizes the dynamic interaction between occupants and their surroundings by considering human adaptability to temperature variations. De Dear's research, particularly during the late 20th and early 21st centuries, provided robust empirical evidence and theoretical frameworks highlighting the importance of behavioral and contextual factors in TC. In collaboration with Gail Brager, de Dear developed a pioneering theory, presented in their 1998 paper "Developing an Adaptive Model of Thermal Comfort and Preference". This study demonstrated that occupants in naturally ventilated buildings could tolerate a wider range of indoor temperatures than those in mechanically controlled environments.

The model emphasizes the significance of occupants' actions, such as adjusting clothing, opening windows, and acclimating to seasonal temperature changes. According to the adaptive approach, comfort levels should be context-specific and flexible, rather than universally applicable. This approach highlights the dynamic and adaptive nature of human comfort in response to environmental changes. The model predicts comfort based on observed occupant behavior and preferences, demonstrating that people can feel comfortable across a wide range of temperatures. Empirical data from various climates and building types are used to define adaptive comfort ranges. The relationship between outdoor and indoor temperatures is established through regression analysis of the collected field data. The results of the adaptive model are typically presented as a comfort band graph, illustrating the acceptable range of indoor temperatures.

Subsequent research has further validated the applicability and robustness of the adaptive model. Its assumptions have been supported in diverse climate zones, including tropical, temperate, and continental regions. For example,Nicol and Humphreys (2002) observed comparable adaptive responses in European environments. These findings support a more occupant-centered approach to thermal regulation and building design, reducing reliance on HVAC systems and improving energy efficiency. Further adaptations of the model include work by Manu et al. (2016), who developed an adaptive thermal comfort model for air-conditioned, mixed-mode, and naturally ventilated commercial buildings. The approach was also incorporated into the National Building Code of India (Bureau of Indian Standards, 2016). More recently, Rawal et al. (2022) proposed a thermal comfort model specifically for Indian residential buildings.

Simulation and Prediction

Simulation in the built environment, often referred to as Building Performance Simulation (BPS), is a crucial tool for predicting the energy performance, thermal performance, and daylighting of buildings (Altan et al., 2016). A simulation tool typically requires input data such as climate, building envelope characteristics, lighting, equipment, occupancy patterns, ventilation, heating and cooling systems, fans, and occupant schedules. Based on these inputs, the tool generates outputs projecting building energy use and environmental performance across end-use categories such as cooling, lighting, heating, fans, plugs, and processes. Some simulation software can also estimate energy costs. The potential applications of building simulation include building design, Life Cycle Analysis (LCA), and retrofit assessments. Widely used tools include DesignBuilder, EnergyPlus, TRNSYS, Ecotect, and IES-VE. DesignBuilder, with its integrated EnergyPlus plugin and user-friendly interface, is particularly popular among researchers for rapid adoption. The main advantage of building simulation is its ability to test and compare different design solutions, optimize equipment efficiency, and predict building performance during the design phase. The duration of a simulation depends on the complexity of the building model (Altan et al., 2016).

Recognition of the limitations of older models through large-scale field studies involving actual building occupants has led to a better understanding of thermal interactions and overall satisfaction with the indoor environment, thereby informing improved design and operation of buildings and building services (de Dear et al., 2013). Recently, the use of computer-based technologies in TC research has expanded significantly. In addition to energy simulation, optimization techniques have gained popularity, including genetic algorithms, artificial neural networks (ANNs), and multi-objective optimization algorithms (Han and Chen, 2017; Liu et al., 2024; Sekartaji et al., 2023; Sen et al., 2014; Senthilkumar and Ayyathurai, 2022; Wang, 1990; Xu et al., 2023). These methods have also been applied to evaluate comfort hours and optimize set points in retail spaces in India.

Several studies have explored the use of machine learning (ML) and artificial intelligence (AI) in TC research. Researchers have experimented with AI models to estimate building temperatures based on external temperature and other environmental parameters. Most published studies have focused on model validation (Ngarambe et al., 2020). Additionally,

some studies have applied optimization algorithms, such as genetic and multi-objective algorithms, alongside sensitivity analysis to evaluate passive strategies, including building orientation, insulation, glazing, and materials, and their effects on TC.

Standards and Policies

Globally, standards for TC have evolved to incorporate both static and adaptive models, aiming to create interior spaces that enhance human health and productivity. The most widely recognized standard is ASHRAE Standard 55, developed by the American Society of Heating, Refrigerating, and Air-Conditioning Engineers. This standard integrates both the Predicted Mean Vote (PMV) and Adaptive Comfort Model and has undergone multiple revisions, allowing adjustments of TC parameters according to climate and occupant management (ASHRAE, 2013). Similarly, the ISO 7730 standard of the International Organization for Standardization provides guidelines for calculating TC based on the PMV and PPD indices (ISO, 2005).

The European Standard EN 16798-1, which replaced EN 15251, emphasizes the adaptive approach, allowing for greater temperature variations based on outdoor conditions and occupant behavior, particularly in naturally ventilated buildings. This standard reflects a growing recognition of the need for flexible comfort criteria to accommodate the wide climatic variations across Europe (European Committee for Standardization, 2019).

Due to India's diverse climate zones and increasing emphasis on sustainable building practices, TC standards have received growing attention. The National Building Code of India (NBC) incorporates the adaptive thermal comfort model. The Energy Conservation Building Code (ECBC) promotes energy-efficient building design that accounts for regional climate variations in commercial buildings (BEE, 2017; Bureau of Indian Standards, 2016). In addition to the ECBC, the ECBC-R (Residential), also known as Eco Niwas Samhita (ENS), addresses efficient building design for residential buildings in India. Research from Indian academic institutions, such as the Center for Advanced Research in Building Science and Energy (CARBSE) at CEPT University, has supported the inclusion of the adaptive model in national standards by validating its suitability for Indian climates (Manu et al., 2016; Rawal et al., 2022).

Indian policies such as the Affordable Housing Policy (Pradhan Mantri Awas Yojana) aim to provide housing for all while ensuring comfort for low-income populations. State-level policies, including the Tamil Nadu Affordable Urban Housing and Habitat Policy and the Punjab Affordable Housing Policy, encourage energy-efficient and eco-friendly building practices. Adaptation and sustainability are increasingly prioritized to meet both national and international requirements for TC. While international standards such as ISO 7730 and ASHRAE 55 provide broad frameworks, Indian standards adopt a more tailored approach, recognizing the country's unique climatic and cultural contexts.

Results and Discussion

According to de Dear et al. (2013), TC in buildings is essential for ensuring occupant well-being. Early researchers focused on the human factors of TC and demonstrated how environmental parameters influence human comfort. These pioneering studies laid the foundation for subsequent key contributions in the field. For example, the two-node models help identify and observe core body responses to environmental conditions and changes. Additionally, researchers developed tools such as the psychrometric chart, which remains a fundamental resource for understanding air-related environmental factors, as it comprehensively represents the interactions between temperature, humidity, and other atmospheric parameters. Following this, indices such as the Wet Bulb Globe Temperature (WBGT), Equatorial Comfort Index (ECI), Cumulative Discomfort Index (CDI), and Tropical Summer Index (TSI) were introduced, further linking TC to environmental parameters. Research on the architectural aspects of TC began in the 1960s with contributions from Givoni and other influential architects, including works such as "Man, Climate and Architecture", "The Passive Solar Energy Book", etc. To this day, research on architectural strategies for TC continues to evolve, driven by varying climatic conditions, climate change scenarios, urban agglomeration, urban heat islands, and other environmental challenges. However, very few studies have examined the cost implications of passive design strategies on TC. Adaptive TC and other TC models have been widely tested and adopted globally to measure TC levels. Standards such as ASHRAE 55 are internationally recognized, while EN 15251 is primarily applied in European contexts. Over time, researchers worldwide have also developed adaptive comfort models tailored to their local climates. Recent studies increasingly rely on simulation and computational tools to investigate TC. Tools such as EnergyPlus and DesignBuilder are commonly used for energy simulations, optimization, and TC modeling. These tools enable researchers to generate optimized results and prioritize desired parameters for TC. Recent research has explored passive strategies, optimization techniques, and energy simulation approaches. However, simulation tools have limitations: they primarily model building systems and environmental factors, while thermophysical, physiological, psychological, and human core responses are often excluded, except for clothing insulation. Emerging research areas include the effects of urban heat islands, personal

comfort systems, real-time mapping using AI and IoT, computational fluid dynamics (CFD), and sleep quality. Despite these advances, significant gaps remain, particularly in defining specific design requirements for different building spaces. Addressing these gaps is essential for optimizing energy use, enhancing environmental conditioning, and developing design guidelines that improve TC while reducing energy consumption across diverse building types.

On the other hand, existing comfort bands and standards often fail to account for regional climatic diversity. For instance, India, with its five distinct climatic zones, lacks an all-encompassing TC band. Consequently, architects, designers, and construction professionals face challenges in creating thermally comfortable environments tailored to local climates. Addressing these knowledge gaps is essential for improving energy efficiency, enhancing occupant satisfaction, and optimizing environmental conditioning in buildings. Given the rapidly evolving challenges posed by global warming, there is an urgent need for comprehensive design standards and adaptive models that integrate localized climatic variations and account for changing occupant behavior patterns. Furthermore, a significant gap exists in understanding TC at the project scale, as most existing studies focus on the unit level. Bridging this gap represents a critical and promising direction for future research.

Conclusion

This paper examines the historical trajectory of TC research, highlighting key milestones, innovations, and directions for future exploration. TC has evolved from the invention of air conditioning to the integration of passive design strategies in buildings. De Dear's adaptive thermal comfort model, now internationally recognized, has been incorporated into major standards such as ASHRAE 55 and the National Building Code of India. Over time, researchers have consistently identified six key parameters. In addition, complementary measures such as the Wet Bulb Globe Temperature (WBGT), the Cumulative Discomfort Index (CDI), and the Tropical Summer Index (TSI) have further advanced our understanding of indoor comfort. These indices provide a more nuanced basis for maintaining optimal indoor conditions across different settings. The integration of cutting-edge technologies into TC studies presents significant opportunities for enhancing building design and improving occupant well-being. At the same time, there is a growing need to examine the long-term impacts of TC on both health and productivity. Some of the key takeaways of this study are as follows:

- Evolution of TC research: Progressing from early physiological investigations to advanced adaptive models, reflecting a growing understanding of human–environment interactions.
- Passive strategies: Implementation of design measures such as insulation, building envelope improvements, phase-changing materials (PCM), orientation, window-to-wall ratios, and cool roofs can significantly enhance occupant satisfaction and well-being.
- Policy context in India: While policies encourage eco-friendly materials and native landscaping, explicit integration of TC performance into regulations remains limited.
- Technological advancements: AI, ML, AR, and IoT are transforming simulation and modeling tools, opening new opportunities for evaluating TC in dynamic and complex contexts.
- Design guidelines: There is a pressing need to develop context-specific guidelines that simultaneously improve TC and reduce electricity consumption in buildings.
- Research gaps: More integrated approaches combining optimization, simulation modeling, climate change considerations, and region-specific comfort models are required. Moreover, most studies focus on individual houses, whereas project-scale investigations remain underexplored but could yield significant societal benefits.

In conclusion, the critical contribution of this paper lies in summarizing the key areas of TC research that can be adopted in practice, while also providing insights into the chronological evolution of TC studies.

Acknowledgements

The authors would like to express their sincere gratitude to NICMAR University for its continuous support and encouragement throughout this research.

References

Abdullah, H. K. and Alibaba, H. Z. (2020). Window design of naturally ventilated offices in the Mediterranean climate in terms of CO_2 and thermal comfort performance. *Sustainability*, Vol. 12, Issue 2, 473. DOI: 10.3390/su12020473.

Alghamdi, S., Tang, W., Kanjanabootra, S., and Alterman, D. (2024). Optimising building energy and comfort predictions with intelligent computational model. *Sustainability*, Vol. 16, Issue 8, 3432. DOI: 10.3390/su16083432.

Ali, S. F., Sharma, L., Rakshit, D., and Bhattacharjee, B. (2020). Influence of passive design parameters on thermal comfort of an office space in a building in Delhi. *Journal of Architectural Engineering*, Vol. 26, Issue 3, 04020017. DOI: 10.1061/(asce) ae.1943-5568.0000406.

Altan, H., Padovani, R., and Hashemi, A. (2016). Building performance and simulation. In: Noguchi, M. (ed.). *ZEMCH: Toward the Delivery of Zero Energy Mass Custom Homes. Springer Tracts in Civil Engineering*. Cham: Springer, pp. 311–338. DOI: 10.1007/978-3-319-31967-4_11.

Arumugam, P. and Ramalingam, V. (2024). Thermal comfort enhancement of office buildings located under warm and humid climate through phase change material and insulation coupled with natural ventilation. *Sustainable Energy Technologies and Assessments*, Vol. 63, 103657. DOI: 10.1016/j.seta.2024.103657.

ASHRAE (2013). *ANSI/ASHRAE Standard 55-2013. Thermal Environmental Conditions for Human Occupancy*. Atlanta, GA: ASHRAE, 52 p.

BEE (2017). *Energy Conservation Building Code 2017*. New Delhi: Bureau of Energy Efficiency, 183 p.

Brager, G. S. and de Dear, R. J. (1998). Thermal adaptation in the built environment: a literature review. *Energy and Buildings*, Vol. 27, Issue 1, pp. 83–96. DOI: 10.1016/S0378-7788(97)00053-4.

Bureau of Indian Standards (2016). *National Building Code of India 2016 (NBC 2016):Volume 2.*

Chatzidimitriou, A. and Yannas, S. (2016). Microclimate design for open spaces: ranking urban design effects on pedestrian thermal comfort in summer.*Sustainable Cities and Society*, Vol. 26, pp. 27–47. DOI: 10.1016/j.scs.2016.05.004.

Chowdhury, A. A., Rasul, M. G., and Khan, M. M. K. (2008). Thermal-comfort analysis and simulation for various low-energy cooling-technologies applied to an office building in a subtropical climate. *Applied Energy*, Vol. 85, Issue 6, pp. 449–462. DOI: 10.1016/j.apenergy.2007.10.001.

De Dear, R. J., Akimoto, T., Arens, E. A., Brager, G., Candido, C., Cheong, K. W. D., Li, B., Nishihara, N., Sekhar, S. C., Tanabe, S., Toftum, J., Zhang, H., and Zhu, Y. (2013). Progress in thermal comfort research over the last twenty years. *Indoor Air*, Vol. 23, No. 6, pp. 442–461. DOI: 10.1111/ina.12046.

De Dear, R., Foldvary, V., Zhang, H., Arens, E., Luo, M., Parkinson, T., Du, X., Zhang, W., Chun, C., and Liu, S. (2016). Comfort is in the mind of the beholder: a review of progress in adaptive thermal comfort research over the past two decades. In: *The Fifth International Conference on Human-Environment System*, October 29 – November 2, 2016, Nagoya, Japan.

Dili, A. S., Naseer, M. A., and Zacharia Varghese, T. (2010). Passive control methods of Kerala traditional architecture for a comfortable indoor environment: comparative investigation during various periods of rainy season. *Building and Environment*, Vol. 45, Issue 10, pp. 2218–2230. DOI: 10.1016/j.buildenv.2010.04.002.

Dodoo, A. and Ayarkwa, J. (2019). Effects of climate change for thermal comfort and energy performance of residential buildings in a Sub-Saharan African climate. *Buildings*, Vol. 9, Issue 10, 215. DOI: 10.3390/buildings9100215.

Elshafei, G., Vilcekova, S., Zelenakova, M., and Negm, A. M. (2021). Towards an adaptation of efficient passive design for thermal comfort buildings.*Sustainability*, Vol. 13, Issue 17, 9570. DOI: 10.3390/su13179570.

Emetere, M. E. (2022). *Numerical methods in environmental data analysis*. Amsterdam, Netherlands; Elsevier, 240 p.

European Committee for Standardization (2019). *EN 16798-1:2019 (2019). Energy performance of buildings - Ventilation for buildings - Part 1: Indoor environmental input parameters for design and assessment of energy performance of buildings addressing indoor air quality, thermal environment, lighting and acoustics - Module M1-6.* [online] Available at: https://standards.iteh.ai/catalog/standards/cen/b4f68755-2204-4796-854a-56643dfcfe89/en-16798-1-2019?srsltid=AfmBOoqyRO8k7ngNVXq_R_xEb-JJAME8PZbXLcfBK2omvVWzyguGYWOW [Date accessed 07/06/2024].

Fabbri, K. (2015). Indoor thermal comfort perception: A questionnaire approach focusing on children. In Indoor Thermal Comfort Perception: A Questionnaire Approach Focusing on Children. Springer International Publishing. https://doi.org/10.1007/978-3-319-18651-1.

Faheem, M., Bhandari, N., and Tadepalli, S. (2023). Adaptive thermal comfort in naturally ventilated hostels of warm and humid climatic region, Tiruchirappalli, India. *Energy and Built Environment*, Vol. 4, Issue 5, pp. 530–542. DOI: 10.1016/j.enbenv.2022.04.002.

Fanger, P. O. (1967). Calculation of thermal comfort: introduction of a basic comfort equation. *ASHRAE Transactions*, Vol. 73, Part 2, pp. III4.1–III4.20.

Ferdyn-Grygierek, J., Sarna, I., and Grygierek, K. (2021). Effects of climate change on thermal comfort and energy demand in a single-family house in Poland. *Buildings*, Vol. 11, Issue 12, 595. DOI: 10.3390/buildings11120595.

Figueiredo, A., Rebelo, F., Castanho, R. A., Oliveira, R., Lousada, S., Vicente, R., and Ferreira, V. M. (2020). Implementation and challenges of the passive house concept in Portugal: lessons learnt from successful experience. *Sustainability*, Vol. 12, Issue 21, 8761. DOI: 10.3390/su12218761.

Gagge, A. P. (1936). The linearity criterion as applied to partitional calorimetry.*American Journal of Physiology*, Vol. 116, Issue 3, pp. 656–668. DOI: 10.1152/ajplegacy.1936.116.3.656.

Ganji, V., Kalpana, M., Madhusudhan, U., John, N. A., and Taranikanti, M. (2023). Impact of air conditioners on sick building syndrome, sickness absenteeism, and lung functions. *Indian Journal of Occupational and Environmental Medicine*, Vol. 27, Issue 1, pp. 26–30. DOI: 10.4103/IJOEM.IJOEM_23_22.

Givoni, B. (1969). Man, climate, and architecture (Cowan J. Henry, Ed.). Elsevier Publishing Company Limited. https://archive.org/details/manclimatearchit0000unse/page/n7/mode/2up.

Gomez-Azpeitia, G., Estrella, K., and Torres, M. (2012). Thermal comfort and health conditions in air-conditioned offices in a warm and sub-humid climate. In: *PLEA2012 - 28th Conference, Opportunities, Limits & Needs Towards an Environmentally Responsible Architecture*, November 7–9, 2012, Lima, Peru.

Gupta, J. (2024). *In South Asia, heat stress kills without a heatwave*. [online] Available at: https://www.preventionweb.net/news/south-asia-heat-stress-kills-without-heatwave [Date accessed 06/05/2024].

Han, M. and Chen, H. (2017). Effect of external air-conditioner units' heat release modes and positions on energy consumption in large public buildings. *Building and Environment*, Vol. 111, pp. 47–60. DOI: 10.1016/j.buildenv.2016.10.014.

Hensen Centnerová, L. (2018). *On the history of indoor environment and it's relation to health and wellbeing*. [online] Available at: https://www.rehva.eu/rehva-journal/chapter/on-the-history-of-indoor-environment-and-its-relation-to-health-and-wellbeing [Date accessed 12/06/2024].

International Energy Agency (2018). *The future of cooling. Opportunities for energy-efficient air conditioning*. [online] Available at: https://www.iea.org/reports/the-future-of-cooling [Date accessed 20/05/2024].

Inusa, M. and Alibaba, H. Z. (2017). Application of passive cooling techniques in residential buildings: a case study of Northern Nigeria. *International Journal of Engineering Research and Application*, Vol. 7, Issue 1, pp. 24–30. DOI: 10.9790/9622-0701012430.

ISO (2005). *ISO 7730:2005. Ergonomics of the thermal environment — Analytical determination and interpretation of thermal comfort using calculation of the PMV and PPD indices and local thermal comfort criteria*. [online] Available at: https://www.iso.org/standard/39155.html [Date accessed 06/05/2024].

Jia, S., Weng, Q., Yoo, C., Xiao, H., and Zhong, Q. (2024). Building energy savings by green roofs and cool roofs in current and future climates. *Npj Urban Sustainability*, Vol. 4, 23. DOI: 10.1038/s42949-024-00159-8.

Karyono, K., Abdullah, B. M., Cotgrave, A. J., and Bras, A. (2020). The adaptive thermal comfort review from the 1920s, the present, and the future. *Developments in the Built Environment*, Vol. 4, 100032. DOI: 10.1016/j.dibe.2020.100032.

Kaushal, A. A., Anand, P., and Aithal, B. H. (2023). Assessment of the impact of building orientation on PMV and PPD in naturally ventilated rooms during summers in warm and humid climate of Kharagpur, India. In: *BuildSys 2023 – Proceedings of the 10th ACM International Conference on Systems for Energy-Efficient Buildings, Cities, and Transportation*. New York: Association for Computing Machinery, pp. 528–533. DOI: 10.1145/3600100.3627034.

Kumar, V. and Mahalle, A. M. (2016). Investigation of the thermal performance of green roof on a mild warm climate. *International Journal of Renewable Energy Research*, Vol. 6, No. 2, pp. 487–493.

Kumar, S., Sheeja, R., Ajin, M., Chandrasekar, P., Sekar, S., and Sai Krishnan, G. S. (2022). Thermal performance analysis of PCM building for moderate climatic region in Bangalore City, India. *IOP Conference Series: Earth and Environmental Science*, Vol. 1100, 012003. DOI: 10.1088/1755-1315/1100/1/012003.

Lee, M., Ham, J., Lee, J.-W., and Cho, H. (2023). Analysis of thermal comfort, energy consumption, and CO_2 reduction of indoor space according to the type of local heating under winter rest conditions. *Energy*, Vol. 268, 126722. DOI: 10.1016/J.ENERGY.2023.126722.

Liu, M., Que, Y., Yang, N., Yan, C., and Liu, Q. (2024). Research on multi-objective optimization design of university student center in China based on low energy consumption and thermal comfort. *Energies*, Vol. 17, Issue 9, 2082. DOI: 10.3390/en17092082.

Lu, S., Wang, W., Lin, C., and Hameen, E. C. (2019). Data-driven simulation of a thermal comfort-based temperature set-point control with ASHRAE RP884. *Building and Environment*, Vol. 156, pp. 137–146. DOI: 10.1016/j.buildenv.2019.03.010.

Luo, M., Arens, E., Zhang, H., Ghahramani, A., and Wang, Z. (2018). Thermal comfort evaluated for combinations of energy-efficient personal heating and cooling devices. *Building and Environment*, Vol. 143, pp. 206–216. DOI: 10.1016/j.buildenv.2018.07.008.

Ma, N., Aviv, D., Guo, H., and Braham, W. W. (2021). Measuring the right factors: a review of variables and models for thermal comfort and indoor air quality. *Renewable and Sustainable Energy Reviews*, Vol. 135, 110436. DOI: 10.1016/j.rser.2020.110436.

Manu, S., Shukla, Y., Rawal, R., Thomas, L. E., and de Dear, R. (2016). Field studies of thermal comfort across multiple climate zones for the subcontinent: India Model for Adaptive Comfort (IMAC). *Building and Environment*, Vol. 98, pp. 55–70. DOI: 10.1016/j.buildenv.2015.12.019.

Marey, H., Kozma, G., and Szabó, G. (2024). Green concrete materials selection for achieving circular economy in residential buildings using system dynamics. *Cleaner Materials*, Vol. 11, 100221. DOI: 10.1016/j.clema.2024.100221.

McDowell, Ian, Measuring Health: A guide to rating scales and questionnaires, 3rd edn (New York, 2006; online edn, Oxford Academic, 1 Sept. 2009), https://doi.org/10.1093/acprof:oso/9780195165678.001.0001 [Date accessed: 16/05/2024].

Mustakallio, P., Bolashikov, Z., Rezgals, L., Lipczynska, A., Melikov, A., and Kosonen, R. (2017). Thermal environment in a simulated double office room with convective and radiant cooling systems. *Building and Environment*, Vol. 123, pp. 88–100. DOI: 10.1016/j.buildenv.2017.06.029.

NASA (2011). *Secrets from the past point to rapid climate change in the future*. [online] Available at: https://science.nasa.gov/earth/climate-change/secrets-from-the-past-point-to-rapid-climate-change-in-the-future/ [Date accessed 29/05/2024].

NASA (2019). *The atmosphere: getting a handle on carbon dioxide*. [online] Available at: https://science.nasa.gov/earth/climate-change/greenhouse-gases/the-atmosphere-getting-a-handle-on-carbon-dioxide/ [Date accessed 10/06/2024].

Nduka, D. O., Oyeyemi, K. D., Olofinnade, O. M., Ede, A. N., and Worgwu, C. (2021). Relationship between indoor environmental quality and sick building syndrome: a case study of selected student's hostels in Southwestern Nigeria. *Cogent Social Sciences*, Vol. 7, Issue 1, 1980280. DOI: 10.1080/23311886.2021.1980280.

Ngarambe, J., Yun, G. Y., and Santamouris, M. (2020). The use of artificial intelligence (AI) methods in the prediction of thermal comfort in buildings: energy implications of AI-based thermal comfort controls. *Energy and Buildings*, Vol. 211, 109807. DOI: 10.1016/j.enbuild.2020.109807.

Nicol, J. F., & Humphreys, M. A. (2002). Adaptive thermal comfort and sustainable thermal standards for buildings. Energy and Buildings, 34(6), 563–572. https://doi.org/10.1016/S0378-7788(02)00006-3.

Nishi, K., Demura, M., Miura, J., and Oishi, S. (2017). Use of thermal point cloud for thermal comfort measurement and human pose estimation in robotic monitoring. In: *2017 IEEE International Conference on Computer Vision Workshops (ICCVW 2017)*, October 22–29, 2017, Venice, Italy, pp. 1416–1423. DOI: 10.1109/ICCVW.2017.168.

Pal, C. L., Netam, N., Sanyal, S., and Manish, M. (2024). Exploring thermal comfort in rural houses of Chhattisgarh state, India: a comprehensive survey and adaptive model analysis. *Science and Technology for the Built Environment*, Vol. 30, Issue 5, pp. 523–545. DOI: 10.1080/23744731.2024.2312799.

Pitts, A. (2017). Passive house and low energy buildings: barriers and opportunities for future development within UK practice. *Sustainability*, Vol. 9, Issue 2, 272. DOI: 10.3390/su9020272.

Pragati, S., Shanthi Priya, R., Pradeepa, C., and Senthil, R. (2023). Simulation of the energy performance of a building with green roofs and green walls in a tropical climate. *Sustainability*, Vol. 15, Issue 3, 2006. DOI: 10.3390/su15032006.

Rana, K. (2021). Towards passive design strategies for improving thermal comfort performance in a naturally ventilated residence. *Journal of Sustainable Architecture and Civil Engineering*, Vol. 29, No. 2, pp. 150–174. DOI: 10.5755/j01.sace.29.2.29256.

Rawal, R., Shukla, Y., Vardhan, V., Asrani, S., Schweiker, M., de Dear, R., Garg, V., Mathur, J., Prakash, S., Diddi, S., Ranjan, S. V., Siddiqui, A. N., and Somani, G. (2022). Adaptive thermal comfort model based on field studies in five climate zones across India. *Building and Environment*, Vol. 219, 109187. DOI: 10.1016/j.buildenv.2022.109187.

Revel, G. M., Arnesano, M., and Pietroni, F. (2014). Development and validation of a low-cost infrared measurement system for real-time monitoring of indoor thermal comfort. *Measurement Science and Technology*, Vol. 25, No. 8, 085101. DOI: 10.1088/0957-0233/25/8/085101.

Roy Choudhury, A. K., Majumdar, P. K., and Datta, C. (2011). Factors affecting comfort: human physiology and the role of clothing. In: Song, G. (ed.). *Improving Comfort in Clothing*. Oxford: Woodhead Publishing, pp. 3–60. DOI: 10.1533/9780857090645.1.3.

Sekartaji, D., Ryu, Y., Novianto, D., Eto, K., and Gao, W. (2023). Energy-use and indoor thermal performance in junior high school building after air-conditioning installation with the private finance initiative. *Buildings*, Vol. 13, Issue 2, 455. DOI: 10.3390/buildings13020455.

Sen, R., Chattopadhyay, S., and Kandra, S. (2014). Investigation on the performance of alternative walling materials in an affordable housing unit situated in warm humid climate. In: *30th International PLEA Conference*, December 16–18, 2014, Ahmedabad, India.

Senthilkumar, S. and Ayyathurai, V. (2022). Energy efficiency management and setpoints optimisation strategy in retail store building, India. *Journal of Building Pathology and Rehabilitation*, Vol. 7, Issue 1, 99. DOI: 10.1007/s41024-022-00238-2.

Sharma, M. R. and Ali, S. (1986). Tropical summer index—a study of thermal comfort of Indian subjects. *Building and Environment*, Vol. 21, Issue 1, pp. 11–24. DOI: 10.1016/0360-1323(86)90004-1.

Sharma, A. and Chani, P. S. (2019). Adaptive thermal comfort for naturally ventilated buildings through building envelope retrofitting. In: Agrawal, A. and Gupta, R. (eds.). *Revisiting the Role of Architecture for 'Surviving' Development. 53rd International Conference of the Architectural Science Association 2019,Roorkee, India,* Architectural Science Association, pp. 391–400.

Sharma, P. and Rakshit, D. (2017). Quantitative assessment of orientation impact on heat gain profile of naturally cooled buildings in India. *Advances in Building Energy Research*, Vol. 11, Issue 2, pp. 208–226. DOI: 10.1080/17512549.2016.1215261.

Silva, A. S., Ghisi, E., and Lamberts, R. (2016). Performance evaluation of long-term thermal comfort indices in building simulation according to ASHRAE Standard 55. *Building and Environment*, Vol. 102, pp. 95–115. DOI: 10.1016/j.buildenv.2016.03.004.

Simova, I., Angelova, R. A., Markov, D., Velichkova, R., and Stankov, P. (2021). Thermal manikins – general features and applications. In: *2021 6th International Symposium on Environment-Friendly Energies and Applications (EFEA)*, March 24–26, 2021, Sofia, Bulgaria. DOI: 10.1109/EFEA49713.2021.9406231.

Soflaei, F., Shokouhian, M., Tabadkani, A., Moslehi, H., and Berardi, U. (2020). A simulation-based model for courtyard housing design based on adaptive thermal comfort. *Journal of Building Engineering*, Vol. 31, 101335. DOI: 10.1016/j.jobe.2020.101335.

Stoops, John L. Indoor Thermal Comfort, an Evolutionary Biology Perspective, article, April 15, 2006; Berkeley, California, University of North Texas Libraries, UNT Digital Library, https://digital.library.unt.edu; crediting UNT Libraries Government Documents Department,https://digital.library.unt.edu/ark:/67531/metadc901474/ [Date accessed 10/06/2026].

Surendran, V. M., Irulappan, C., Jeyasingh, V., and Ramalingam, V. (2023). Thermal performance assessment of envelope retrofits for existing school buildings in a hot–humid climate: a case study in Chennai, India. *Buildings*, Vol. 13, Issue 4, 1103. DOI: 10.3390/buildings13041103.

Teitelbaum, E., Miller, C., & Meggers, F. (2023). Highway to the Comfort Zone: History of the Psychrometric Chart. Buildings, 13(3). https://doi.org/10.3390/buildings13030797.

Thapa, S., Rijal, H. B., Pasut, W., Singh, R., Indraganti, M., Bansal, A. K., and Panda, G. K. (2023). Simulation of thermal comfort and energy demand in buildings of sub-Himalayan eastern India - impact of climate change at mid (2050) and distant (2080) future. *Journal of Building Engineering*, Vol. 68, 106068. DOI: 10.1016/j.jobe.2023.106068.

Tomrukcu, G. and Ashrafian, T. (2024). Climate-resilient building energy efficiency retrofit: evaluating climate change impacts on residential buildings. *Energy and Buildings*, Vol. 316, 114315. DOI: 10.1016/j.enbuild.2024.114315.

Tungnung, K., Varma, A., Kodama, Y., Takemasa, K., Pde, G., and Roy, S. (2023). Parametric strategies on passive heating techniques in cold-cloudy climate, Shillong towards net-zero energy. *AIP Conference Proceedings*, Vol. 2760, Issue 1, 020022. DOI: 10.1063/5.0149181.

Van Hoof, J. (2008). Forty years of Fanger's model of thermal comfort: comfort for all? *Indoor Air* , Vol. 18, Issue 3, pp. 171–258. DOI: 10.1111/j.1600-0668.2007.00516.x.

Wang, X.-L. (1990). A dynamic model for estimating thermal comfort. In: *Indoor Air Quality And Ventilation In Warm Climates*, April, 24–26, 1990, Lisbon, Portugal.

Wang, R., Lu, S., and Feng, W. (2020). A three-stage optimization methodology for envelope design of passive house considering energy demand,thermal comfort and cost. *Energy*, Vol. 192, 116723. DOI: 10.1016/j.energy.2019.116723.

Webb, C. G. (1959). An analysis of some observations of thermal comfort in an equatorial climate. *British Journal of Industrial Medicine*, Vol. 16, Issue 4, pp. 297–310.

Weng, J., Zhang, Y., Chen, Z., Ying, X., Zhu, W., and Sun, Y. (2023). Field measurements and analysis of indoor environment, occupant satisfaction, and sick building syndrome in university buildings in hot summer and cold winter regions in China. *International Journal of Environmental Research and Public Health*, Vol. 20, Issue 1, 554. DOI: 10.3390/ijerph20010554.

Xie, X., Liu, Y., and Hou, J. (2014). An analysis on behaviors of real estate developers and government in sustainable building decision making. *Journal of Industrial Engineering and Management*, Vol. 7, Issue 2, pp. 491–505. DOI: 10.3926/jiem.1042.

Xu, Y., Chen, J., Cai, J., Li, S., and He, Q. (2023). Simulation-based trade-off modeling for indoor infection risk of airborne diseases, energy consumption, and thermal comfort. *Journal of Building Engineering*, Vol. 76, 107137. DOI: 10.1016/j.jobe.2023.107137.

Yaglou, C. P. and Minard, D. (1957). Control of heat casualties at military training centers. *A.M.A. Archives of Industrial Health*, Vol. 16, No. 4, pp. 302–316.

Yamamoto, T. (2023). Evaluation of thermal comfort with and without fill using a thermal environment analysis method for building envelopes with thermally complex geometry: a case study in Hokkaido, Japan. *Buildings*, Vol. 13, Issue 7, 1646. DOI: 10.3390/buildings13071646.

Zasimova, M. A., Podmarkova, A. D., Ivanov, N. G., and Marinova, A. A. (2023). Evaluation of CFD-predicted thermal comfort uncertainties based on a seated thermal manikin test case. *IOP Conference Series: Earth and Environmental Science*, Vol. 1185, 012041. DOI: 10.1088/1755-1315/1185/1/012041.

Zuo, C., Luo, L., and Liu, W. (2021). Effects of increased humidity on physiological responses, thermal comfort, perceived air quality, and sick building syndrome symptoms at elevated indoor temperatures for subjects in a hot-humid climate. *Indoor Air*, Vol. 31, Issue 2, pp. 524–540. DOI: 10.1111/ina.12739.

ЭВОЛЮЦИЯ И ДОСТИЖЕНИЯ В ИССЛЕДОВАНИЯХ ТЕПЛОВОГО КОМФОРТА: НАРРАТИВНЫЙ ОБЗОР ЛИТЕРАТУРЫ

Шивани Сентилкумар[1]*, Пуломи Гош[2]

[1]Научный сотрудник, Университет NICMAR (Национальный институт управления и исследований в строительстве), Пуна, Индия – 411045
[2]Факультет недвижимости и управления объектами, Университет NICMAR (Национальный институт управления и исследований в строительстве), Пуна, Индия – 411045

*E-mail: shivani.phd2@pune.nicmar.ac.in

Аннотация
Введение. Изменение климата, аномальная жара, выбросы парниковых газов и глобальное потепление образуют бесконечный цикл, разрушающий окружающую среду и приводящий к дискомфорту человека и других живых существ. С 1946 года проводятся исследования в области теплового комфорта в зданиях, охватывающие как пассивные, так и активные стратегии. Настоящая статья направлена на изучение эволюции исследований в области теплового комфорта и принципов, на которых они основаны. **Методы.** Для анализа прогресса в области теплового комфорта использовался метод нарративного обзора литературы. В исследование были включены 122 статьи, рассматривающие концепции, модели, архитектурные подходы, стандарты и нормативные документы, связанные с тепловым комфортом. **Результаты и обсуждение.** Исследования в области теплового комфорта прошли путь от изобретения кондиционирования воздуха до внедрения пассивных стратегий в строительстве. В ходе этих исследований были выделены шесть ключевых параметров, способствующих более глубокому пониманию теплового комфорта в помещениях. Кроме того, использование инновационных технологий в исследованиях теплового комфорта позволяет улучшать самочувствие пользователей зданий. В связи с этим представляется необходимым междисциплинарный подход к изучению теплового комфорта. **Рекомендации.** В статье систематизируются основные этапы развития исследований в области теплового комфорта, включая инновации в моделировании и прогнозировании, а также сопутствующие проблемы. Данная работа может помочь будущим исследователям, разработчикам и другим специалистам строительной отрасли выявить имеющиеся пробелы и связать достижения прошлого с перспективными направлениями.

Ключевые слова: тепловой комфорт, хронология исследований в области теплового комфорта, модели теплового комфорта, адаптивная модель теплового комфорта.

DOI: 10.23968/2500-0055-2025-10-3-53-66

INVESTIGATING WINDOW DESIGN IMPACT ON OTTV THROUGH BIM MODELING IN WARM-HUMID CITIES

Rissa Syafutri[1]*, Yani Rahmawati[2], Jatmika Adi Suryabrata[2]

[1]Pontianak State Polytechnic University, Indonesia
[2]Gadjah Mada University, Indonesia

*Corresponding author's email: rissasyafutri@polnep.ac.id

Abstract

Introduction: Fenestration design is critical for building energy efficiency in warm-humid climates, where solar radiation through windows significantly affects the overall thermal transfer value (OTTV). Many buildings in Indonesia do not adequately address location-specific envelope design, potentially due to limited experimental research on appropriate designs for Indonesia's diverse climates. **Purpose of the study:** This study aims to examine the impact of different window design strategies on building thermal transfer across Indonesian cities. **Methods:** A sensitivity analysis was conducted to evaluate the influence of window design on the OTTV in three geographically distinct Indonesian cities: Banda Aceh (Northern Hemisphere), Pontianak (Equator), and Yogyakarta (Southern Hemisphere). Using a building information modeling (BIM)-based OTTV calculator in Autodesk Revit and Dynamo, 3,600 window variations were generated and represented in 180 line graphs. Variations included window-to-wall ratio (WWR), glazing properties, and shading devices. **Results:** The analysis indicates that WWR has a more significant effect on the OTTV than the shading coefficient (SC), with reductions of up to 46 W/m² when WWR decreased from 65 % to 25 %. Shading dimensions proved more influential on the OTTV than glazing properties, highlighting the critical role of shading configuration in thermal performance. Optimizing WWR and implementing standardized shading systems can significantly enhance energy efficiency and thermal comfort, especially in tropical climates with high solar exposure. These findings encourage early design-stage exploration of WWR and shading combinations to achieve compliance with energy standards while maintaining design flexibility.

Keywords: fenestration design, energy efficiency, OTTV, sensitivity analysis, warm-humid climate buildings, Indonesian buildings.

Introduction

The design of a building's envelope is critical to its energy consumption (Albatayneh, 2021; Mushtaha et al., 2021; Natephra et al., 2018; Tong et al., 2021). To avoid inefficient energy use and the subsequent need for costly retrofits, it is essential to prioritize the initial design phase. Therefore, a strategic and systematic approach during this phase is vital for optimal decision-making (Al-Homoud, 2005). In countries with warm and humid climates, building envelopes face unique challenges, as they require adequate fenestration for natural ventilation and daylighting, particularly in daytime-use buildings such as schools. Proper natural lighting is necessary not only to achieve energy efficiency but also to prevent mold growth due to high humidity. Although facade design is one of the most critical factors influencing building performance, not all elements of the building envelope contribute equally. According to the Indonesian National Standard (SNI) 6389:2020, three values represent the amount of heat transferred through the building envelope by conduction and radiation: conduction through opaque walls, conduction through glass, and solar radiation through glass (BSN, 2020). The SR value comprises solar factor (SF), window-to-wall ratio (WWR), shading coefficient (SC), and glass shading coefficient (SC_G). Previous studies in tropical climates showed that SR-related variables significantly impact the overall thermal transfer value (OTTV) (Chow and Chan, 1995; Gondal et al., 2019; Habibi, 2019; Kusumawati et al., 2021; Pathirana et al., 2019; Syafutri et al., 2023a).

Previous studies also revealed that many mid- to high-rise buildings in Indonesian cities exceed the OTTV standard of 35 W/m² set by SNI 6389:2020. For instance, research on educational buildings in Lampung (Sani et al., 2019) and Yogyakarta (Octarino and Feriadi, 2021; Syafutri et al., 2023a) demonstrated a trend of surpassing the maximum allowable value. The same trend was observed in other studies: a study focusing on a church in Jakarta (Imran, 2019; Widhayaka and Rilatupa, 2021), and a study addressing a church in Semarang (Purwanto and Tichelmann, 2021). Likewise, Rahmanda and Suriansyah (2020) investigated a hotel building in Lampung, providing further evidence that many buildings in Indonesia exceed the recommended OTTV values due to inadequate envelope design. Nasrullah et al. (2024) studied two hotels in Makassar and showed through simulation that proper building envelope design could significantly reduce energy

consumption. Collectively, these studies suggest applying a smaller WWR and using glazing with superior thermal properties. The findings indicate that the buildings analyzed were not designed to respond effectively to the SF specific to each city, which determines the intensity of solar radiation in different areas (BSN, 2020). Each building orientation in Indonesian cities experiences a distinct SF, requiring careful window design. Therefore, poorly designed building envelopes can increase the cooling load, leading to energy inefficiency.

The initial review of literature indicates a lack of specific window designs in many buildings across Indonesian cities, which could help reduce heat transfer through windows. Despite the thermal properties of the glass used, the diverse SF values across Indonesia significantly affect the OTTV. This study aims to address this issue by examining how window components influence the OTTV in three Indonesian cities: Banda Aceh, Pontianak, and Yogyakarta. The study focuses on factors such as window-to-wall ratio (WWR), shading device shading coefficient (SC), and glass shading coefficient (SC_G), as outlined in SNI 6389:2020. The analysis will be conducted using statistical models generated through BIM-based applications, namely Autodesk Revit and Autodesk Dynamo. This method accelerates the analysis process and reduces the risk of human error, as demonstrated in previous studies (Bahdad et al., 2021; Eid et al., 2022; Lim et al., 2019; Seghier et al., 2017, 2022; Syafutri et al., 2023b; Tantisevi and Sornsuriya, 2010). By analyzing building envelope variables using BIM-based applications, the study intends to provide practical design recommendations for architects and policymakers to improve building energy efficiency across different regions of Indonesia.

Methods

The objective of this research is to investigate the influence of window variables on the OTTV across different locations in Indonesia. Previous research on this specific topic remains limited; therefore, three geographically distinct cities were selected as case studies: Banda Aceh in the Northern Hemisphere, Pontianak on the Equator, and Yogyakarta in the Southern Hemisphere.

Table 1 presents the SF values according to SNI 6389:2020 for the case study cities. Banda Aceh, located in the Northern Hemisphere, exhibits a significantly higher SF on the south side compared to Pontianak and Yogyakarta. The south SF value of Banda Aceh is even higher than the east SF value of Pontianak, despite the east side generally experiencing high SF values. Fig. 1 illustrates the sun path diagrams of the three case study cities (Tukiainen and Gaisma.com, 2024).

To further analyze the performance of window design variables in relation to the OTTV, an experiment was conducted using an educational building: Nahdlatul Ulama University (Universitas Nahdlatul Ulama, UNU) in Yogyakarta, Indonesia, as shown in Fig. 2. Fig. 3 presents a simplified model of the building created using Autodesk Revit 2021. Tables 2 and 3 provide the variable data of the case study building extracted from the Revit model. The UNU building has nine floors, most of which are air-conditioned. Table 4 details the dimensions of the building's windows.

OTTV Equation

The OTTV equation, based on the SNI 6389:2020 standard, is employed to determine the value of thermal transfer through the building envelope. According to SNI 6389:2020, OTTV consists of three components: (a) heat conduction through opaque walls, (b) heat conduction through transparent walls, and (c) solar radiation through transparent walls. The equation is expressed as follows:

$$OTTV = [(\alpha \times (1 - WWR) \times U_W \times TD_{EQ}) \times A] + [WWR \times U_F \times \Delta T] + [WWR \times SF \times (SC \times SC_G)]. \quad (1)$$

In the equation, α represents the absorptance value of exterior paint. The term (1 – WWR) expresses the ratio of wall area to window area, accounting for heat conduction through opaque walls. U_W represents the thermal transmittance of the wall material, while TD_{EQ} is the equivalent temperature difference of the material. U_F denotes

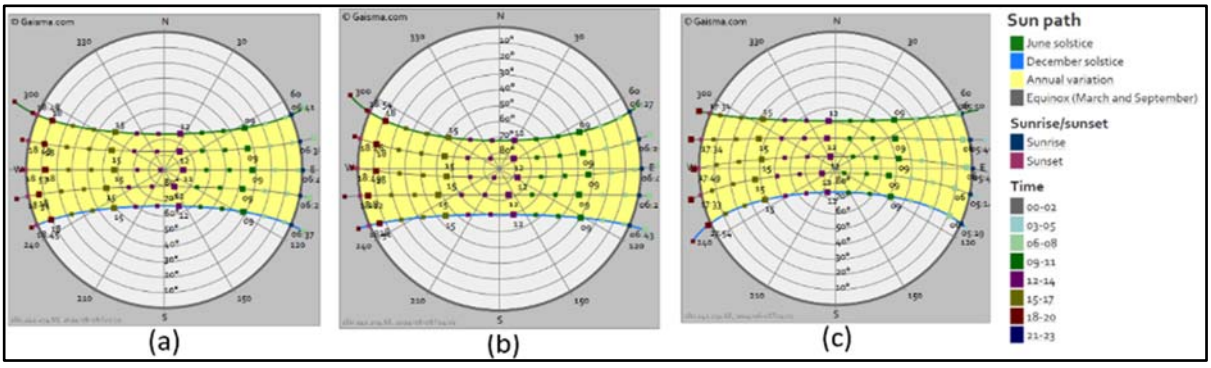

Fig. 1. Sun path diagrams for each city: (a) Pontianak, (b) Banda Aceh, and (c) Yogyakarta (Tukiainen and Gaisma.com, 2024)

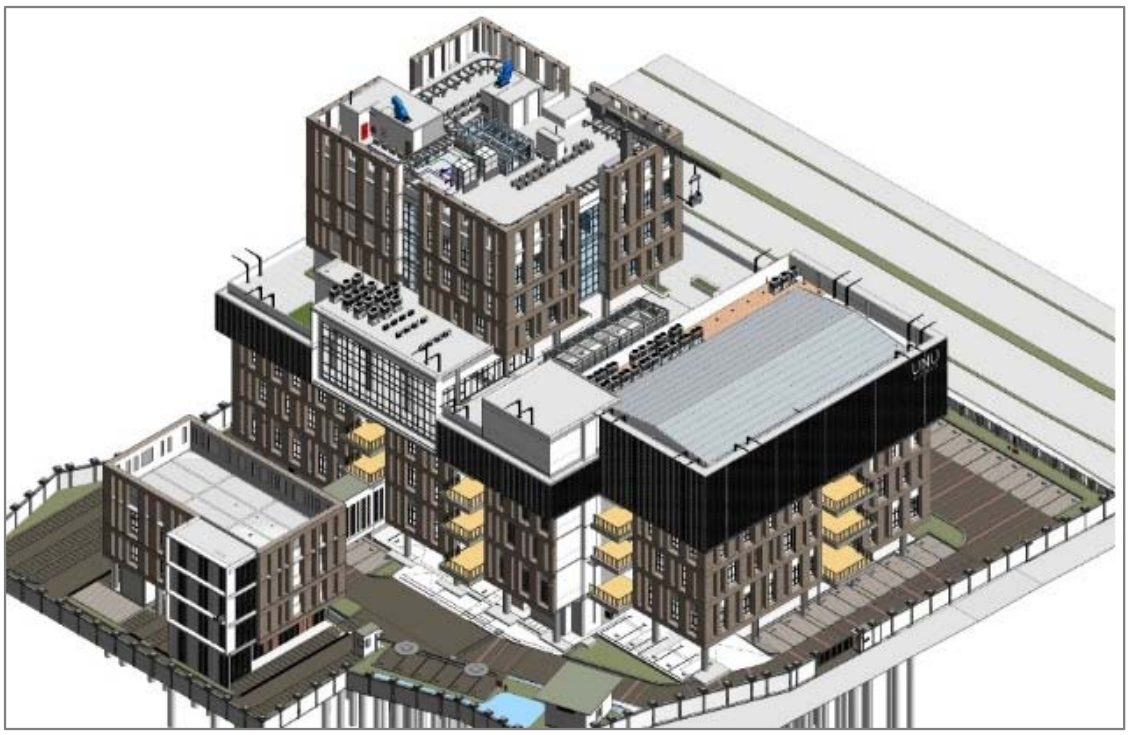

Fig. 2. Window area with minimal shading system on the west facade of the UNU building

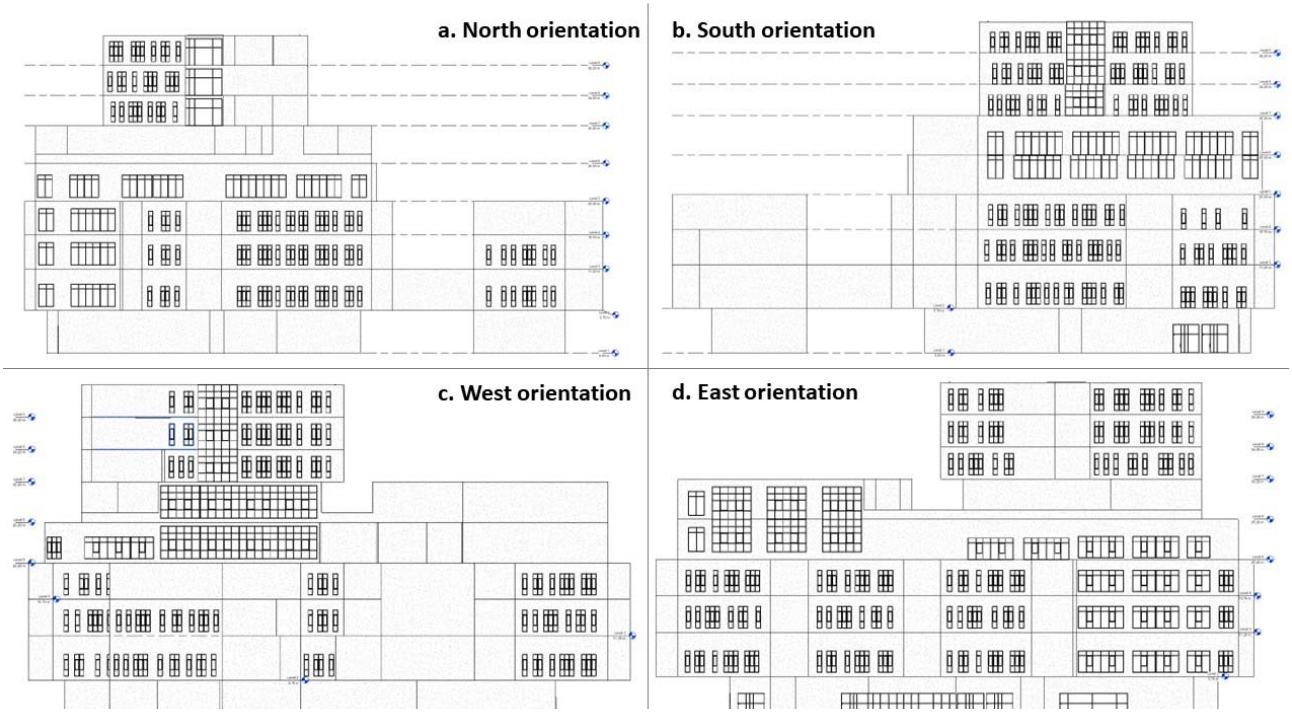

Fig. 3. Facades of the UNU building: (a) north, (b) south, (c) west, (d) east

Table 1. **Coordinates and solar factor of case study locations**

Location		Coordinates	Solar factor			
			North	South	East	West
Banda Aceh	Northern Hemisphere	5.5483° N, 95.3238° E	116	142	166	200
Pontianak	Equator	0.0263° S, 109.3425° E	125	120	139	186
Yogyakarta	Southern Hemisphere	7.8014° S, 110.3648° E	152	105	170	178

Table 2. **Facade and fenestration area, WWR of each orientation**

Orientation	Opaque wall area	Fenestration area	Total facade area	WWR
North	895.3 m²	499.1 m²	1,394.5 m²	36 %
South	992.2 m²	486.4 m²	1,478.6 m²	42 %
West	1,002.7 m²	742.2 m²	1,744.9 m²	34 %
East	1,519.4 m²	778.2 m²	2,295.6 m²	33 %

Table 3. **Variables of existing case study buildings for OTTV calculation**

Variables required for OTTV calculation	Data
Thermal absorptance value (α)	White exterior painting = 0.21
Thermal transmittance values (U_w & U_f)	• U-value of brick = 3.9 W/m²K • U-value of window glass = 5.7 W/m²K • U-value of door glass = 5.7 W/m²K
Equivalent temperature difference TD_{EQ}	10
Shading coefficient (SC)	• SC of window glass = 0.55 • SC of door glass = 0.55

Table 4. **Windows dimensions in the Nahdlatul Ulama University**

Window type		
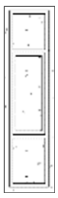 Window No. 1 Width = 0.6 m Length = 3.6 m	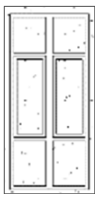 Window No. 2 Width = 1.2 m Length = 3.6 m	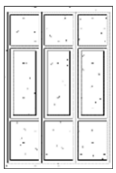 Window No. 3 Width = 1.8 m Length = 3.6 m
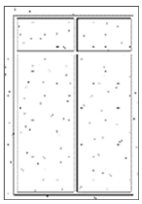 Window No. 4 Width = 2.8 m Length = 3.6 m	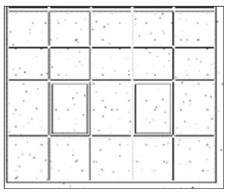 Window No. 5 Width = 4.8 m Length = 4.0 m	

the transmittance of window glass, and ΔT is a constant value that represents the difference between outdoor and indoor temperatures. This value is simplified to facilitate practical application. SF is the solar factor, SC is the shading coefficient of window glass, and SC_G is the shading coefficient of the shading system. The SC of the shading system depends on the shading system type and dimensions. SNI 6389:2020 defines three types of shading systems: (a) horizontal fins (HF), (b) vertical fins (VF), and (c) eggcrate fins (EF). The dimensions of each shading system determine the R value, which is used to calculate the SC. Fig. 4 shows the shading system types and the variables required to

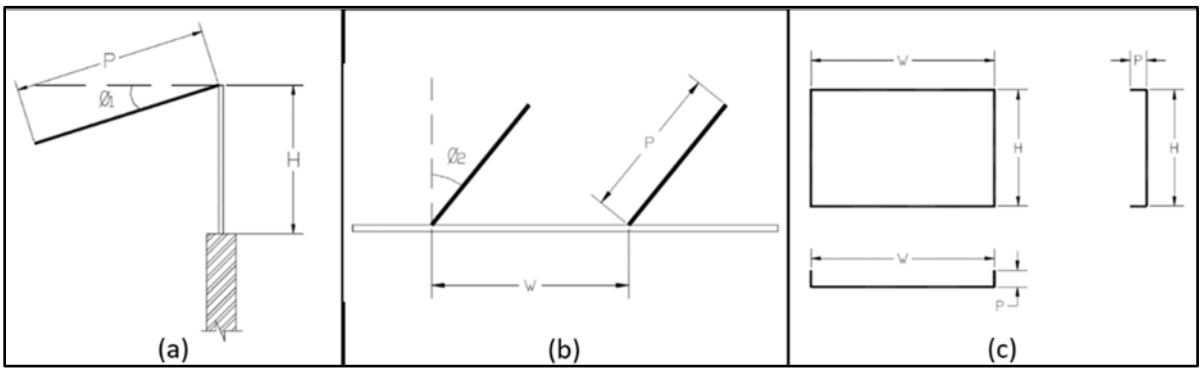

Fig. 4. Shading systems according to SNI 6389:2020: (a) horizontal fins, (b) vertical fins, (c) eggcrate fins

obtain the R value. The R value expresses the ratio between the dimension of the shading device and the corresponding dimension of the window. The calculation differs for horizontal and vertical fins. To obtain the R value of a horizontal fin, the length of the fin is divided by the height of the window frame, as shown in Fig. 4 ($R_1 = \frac{P}{H}$). To obtain the R value of a vertical fin, the width of the vertical shading system is divided by the width of the window ($R_2 = \frac{P}{W}$).

Calculating the OTTV of the existing building is essential for this research. The UNU building is originally located in Yogyakarta, Indonesia. However, for the purposes of this study, three locations were considered: Yogyakarta, Banda Aceh, and Pontianak, representing the Southern Hemisphere, Northern Hemisphere, and Equator, respectively. Accordingly, three sets of OTTV calculations were performed using the original building specifications, with the addition of the solar factor for Banda Aceh and Pontianak. Table 5 shows the OTTV for each case study location.

BIM-Based OTTV Calculator

To accelerate the experiment in this study, a BIM-based OTTV calculator was developed using Autodesk Dynamo within Autodesk Revit 2021. Several previous studies developed similar calculators based on SNI 6389:2020 (Syafutri et al., 2023b), MS 1525:2014 (Abass et al., 2020), and the GreenMark and Green RE rating systems (Seghier et al., 2017), while Lim et al. (2019) proposed a framework to automate decision-making for high-performance buildings. Fig. 5 illustrates the workflow of the OTTV calculator used in this study, based on the validated framework developed by Syafutri et al. (2023b). Furthermore, combinations of various window design elements were configured to conduct the experimental analysis.

In addition to the OTTV calculator, a framework for the experimental configuration was developed in this study using Autodesk Dynamo. This framework enables automation of the experiment. The variables tested included the window-to-wall ratio (WWR), the shading coefficient of glass (SC_G), and the shading coefficient (SC) of the shading systems. The experiment was conducted across three locations with different SF values. The WWR variations used in this study were 25 %, 35 %, 45 %, 55 %, and 65 %. The WWR values below 25 % were considered inadequate, as they restrict natural daylight penetration, while values above 65 % may lead to excessive OTTV (Sayadi et al., 2021). Table 6 presents the variations of the SC values for glass, and Table 7 presents the SC values of the shading systems used in the experiment. Fig. 6 illustrates the experimental framework. The automation tool was developed by implementing the OTTV equation and configuring it with the experimental variables, allowing automatic generation of results for sensitivity analysis.

Fig. 6 shows one of the frameworks used in this study to obtain the OTTV for analysis. The frameworks were adapted for each case study city and followed four stages: data input, data adjustment, experimentation, and result export to Microsoft Excel. At the data input stage, information extracted from the BIM model was compiled and written as a string in a code block to streamline the process. In Autodesk Dynamo, a string is a sequence of text characters used to store and manipulate information, while a code block is a flexible node that allows users to write and execute scripts for efficient data processing. The input data included the SF, WWR, U-value, absorptance (α), TDEQ, ΔT, SC, and SC_G for each building orientation in every city. At the data adjustment stage, the existing SC and SC_G values were multiplied by those corresponding to the glass types defined in Table 6. At the experimentation stage, the adjusted data were processed, and the results were categorized according to different WWR values (25 %, 35 %, 45 %, 55 %, and 65 %). Finally, the experimental results were exported to Microsoft Excel for further analysis. This framework was consistently applied across all cities included in the study.

Sensitivity Analysis Method

The BIM-based OTTV calculator developed for this research generated 3,600 OTTV values, each representing a different window design variation in terms of the WWR, SCG, SC, and SF, varying by location. To achieve the research objectives, a sensitivity analysis was applied to identify trends and synthesize the experimental results. Previous studies employed sensitivity analysis to investigate the impact of design variables on heating and cooling loads in residential buildings, for example in Hungary (Elhadad and Orban, 2021). Additionally, a review of sensitivity analysis methods for high-performance buildings, covering 96 studies from

Table 5. **Pre-experiment OTTV values for each case study location**

Location	OTTV (W/m²)			
	North	South	East	West
Banda Aceh	32.4	34.5	40.1	57.2
Pontianak	33.6	31.5	35.9	54.3
Yogyakarta	37.6	29.4	40.5	52.7

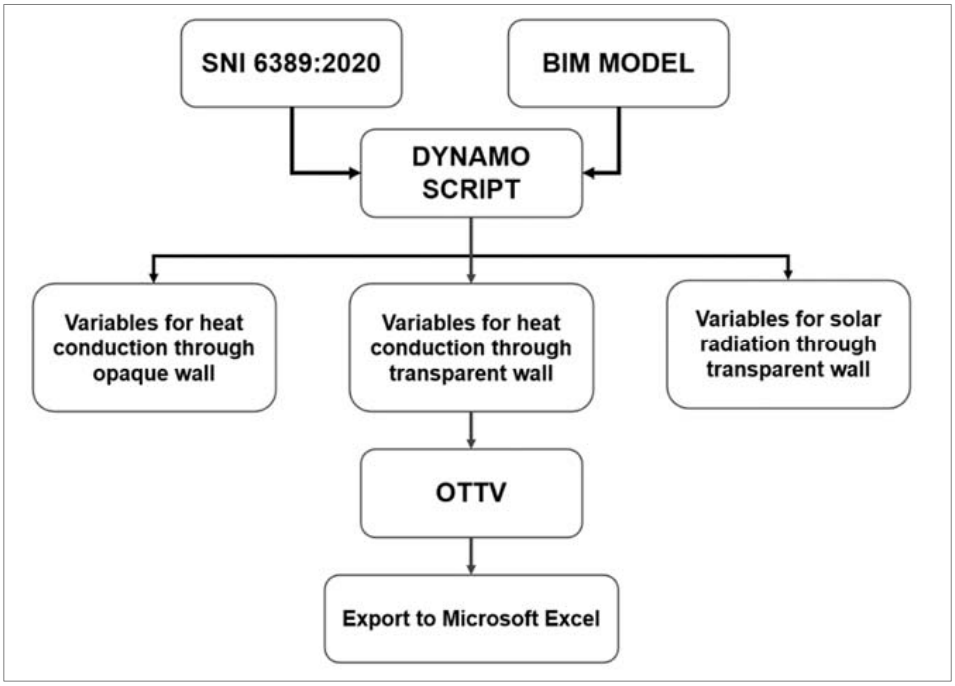

Fig. 5. BIM-based OTTV calculator

Table 6. **Variations of the SC values (PT Asahimas Flat Glass Tbk, 2022)**

Glass type	Thickness (mm)	SC value	U-value (W/m²K)	Image
Panasap *Bronze*	6	0.73	5.7	
T-Sunlux CS-150 #2	6	0.67	5.7	
Stopsol – *Eurogray*	6	0.56	5.7	
Stopsol – *Dark Blue*	8	0.39	5.7	

Table 7. **Shading coefficient for each R value of shading systems**

North–South orientation					
Horizontal fin		**Vertical fin**		**Eggcrate fin**	
R1 value	SC value	R2 value	SC value	R1/R2 value	SC value
0.2	0.87	0.2	0.91	0.2/0.2	0.81
0.4	0.76	0.4	0.81	0.4/0.4	0.68
0.6	0.7	0.6	0.75	0.6/0.6	0.66
0.8	0.69	0.8	0.73	0.8/0.8	0.66
1.0	0.68	1.0	0.71	1.0/1.0	0.66
East–West orientation					
Horizontal fin		**Vertical fin**		**Eggcrate fin**	
R1 value	SC value	R2 value	SC value	R1/R2 value	SC value
0.2	0.87	0.2	0.96	0.2/0.2	0.85
0.4	0.77	0.4	0.92	0.4/0.4	0.73
0.6	0.69	0.6	0.89	0.6/0.6	0.65
0.8	0.63	0.8	0.85	0.8/0.8	0.58
1.0	0.58	1.0	0.82	1.0/1.0	0.54

internationally indexed journals, identified the most frequently analyzed variables such as climate, building envelope components, ventilation, HVAC systems, and occupant behavior patterns (Pang et al., 2020).

Experimental Results

The experiment generated 3,600 OTTV values, each corresponding to a specific window design strategy. In this section, the results are discussed according to the variables examined in this study: (a) the impact of the SF and SC on the OTTV, and (b) the impact of the WWR on the OTTV. This division allows for a clear assessment of the influence of each variable on the OTTV. Finally, a synthesis of the results is presented to provide a comprehensive overview of the findings.

Impact of the Solar Factor and Shading Coefficient on the OTTV

The solar factor for the north and south orientations varies significantly depending on geographic location, as shown in Table 1. In Pontianak, located on the equator, the SF is 125 W/m² on the north side

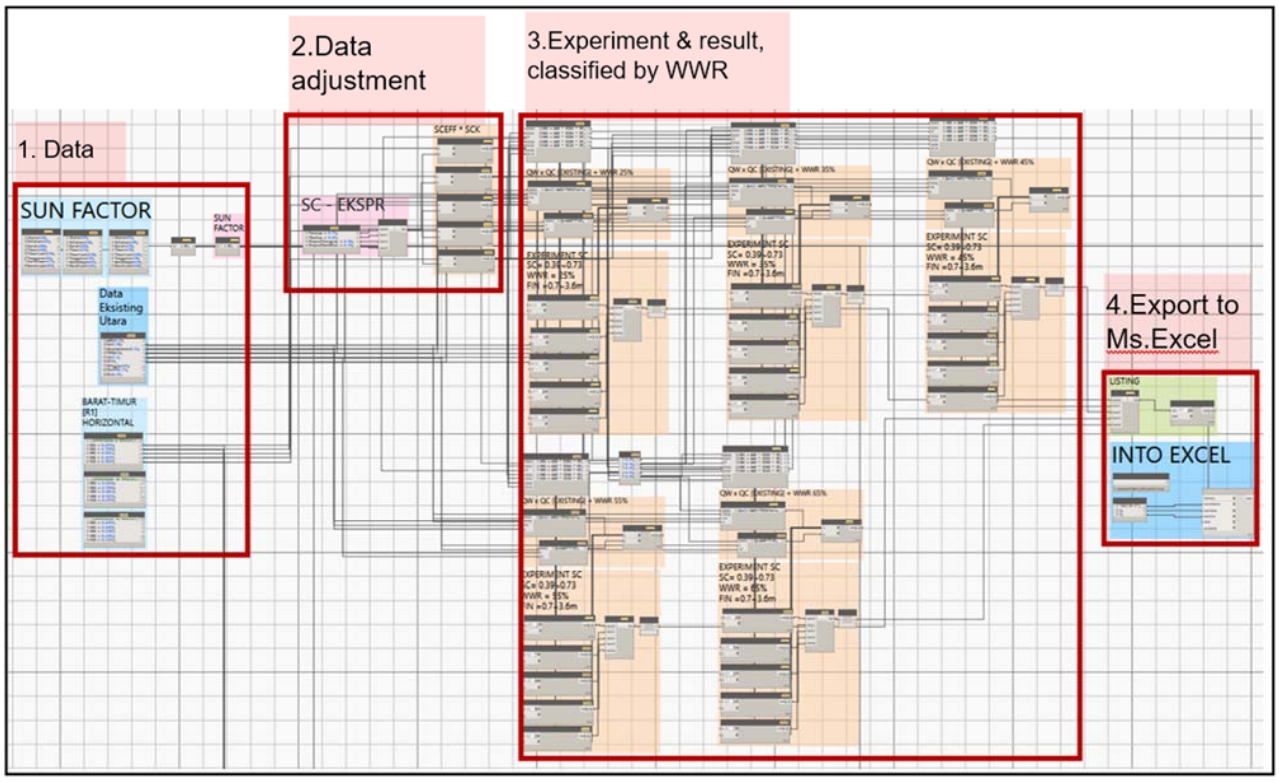

Fig. 6. One of frameworks of the BIM-based OTTV calculator

and 120 W/m² on the south side. In comparison, Yogyakarta exhibits a north SF of 152 W/m² and a south SF of 105 W/m², indicating a substantial variation in solar exposure between these orientations. Conversely, Banda Aceh shows an opposite pattern to Yogyakarta, with a north SF of 116 W/m² and a south SF of 142 W/m². As for the east and west sides, Banda Aceh has the highest SF values, with 200 W/m² on the west side and 166 W/m² on the east side. A similar imbalance is observed in Pontianak, where the east SF is 139 W/m² and the west SF is 186 W/m², which is significantly higher. In contrast, Yogyakarta exhibits more balanced SF values between the west (178 W/m²) and east (170 W/m²) orientations.

Yogyakarta stands out due to its substantial OTTV reduction, attributed to its higher SF on the north side. This higher SF indicates a greater influence of solar radiation, making the location more responsive to shading and glazing strategies aimed at reducing the OTTV. This sensitivity to thermal transfer reduction sets a benchmark for understanding the impact of solar exposure in locations with high SF. Similar trends are observed in other areas with high SF, including the west and east sides of Banda Aceh, the west side of Pontianak, and the east, west, and north sides of Yogyakarta. These variations suggest that higher SF values in specific orientations, such as west and east, amplify the OTTV reduction effect, highlighting the sensitivity of building thermal performance to shading and glazing characteristics.

OTTV Reduction Sensitivity to the Solar Factor and Shading Coefficient

The study further revealed that OTTV differences between Yogyakarta and Pontianak are more pronounced than those between Banda Aceh and Pontianak. A 27 W/m² difference in the SF between Yogyakarta and Pontianak resulted in an OTTV variation of up to 125 W/m² on the north side. Fig. 7 illustrates the substantial OTTV reduction observed across the three locations. This finding indicates that even relatively small increases in the SF can produce disproportionately large effects on the OTTV, highlighting the sensitivity of thermal transfer to solar exposure, particularly on north sides. High SF values also significantly affect the performance of high-quality glazing. As shown in Fig. 8, Stopsol Dark Blue glass with a thickness of 8 mm and an SC value of 0.39 performs differently depending on the location.

With regard to the OTTV calculation, the SF difference between Banda Aceh and Yogyakarta on the south side is similar to the SF difference between Banda Aceh and Pontianak on the west side (Table 8). This is notable because east and west orientations receive predominantly direct sunlight, while north and south orientations receive mainly diffuse sunlight. Typically, these differences in sunlight type would result in varying solar heat

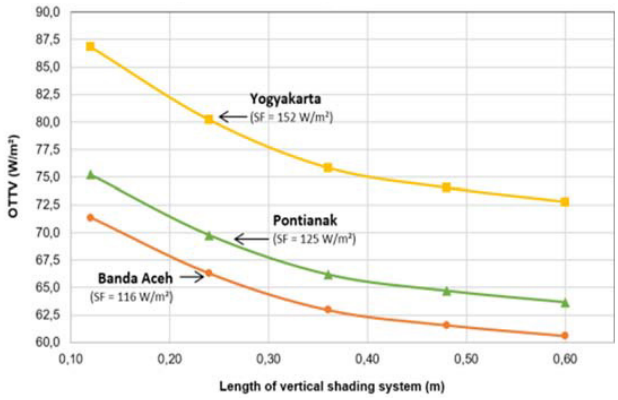

Fig. 7. Comparison of the OTTV in the north orientation of Pontianak, Banda Aceh, and Yogyakarta

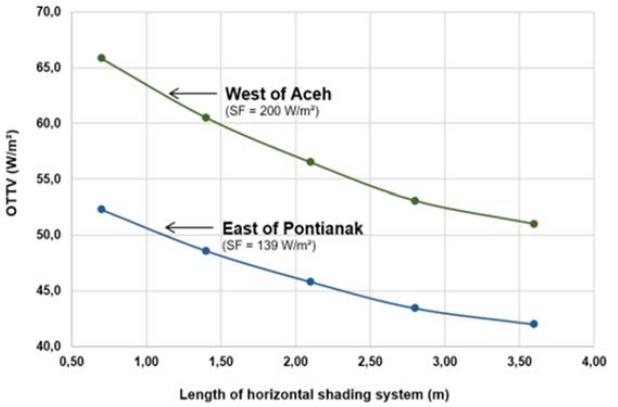

Fig. 8. Performance of high-quality glass (SC = 0.39) in the different locations (e.g the west side of Banda Aceh and the east side of Pontianak)

gains. However, in this case, the OTTV values are similar due to the consistent SC of the horizontal fin shading systems on all sides. The primary reason for this similarity is the uniform ratio of shading dimensions to window size across different orientations. Regardless of whether the orientation is north–south or east–west, maintaining the same shading ratio leads to comparable OTTV values despite variations in sunlight type and intensity. This trend is consistent for horizontal, vertical, and eggcrate shading systems.

In warm-humid climates, these findings suggest that shading devices can be standardized across orientations by maintaining a uniform ratio of shading dimensions to window size, achieving comparable OTTV results for all orientations. Although eggcrate shading systems exhibit larger SC differences between north–south and east–west orientations, they still follow a similar OTTV pattern as horizontal and vertical fins when the same shading-to-window ratio is applied. This insight provides a practical approach to shading device design for buildings in tropical regions, regardless of whether

Table 8. **Comparison of OTTV differences between west and south orientation for different locations**

WWR = 65 %; SC_G = 0.79									
West – horizontal fin	Location	SF (W/m²)	OTTV (W/m²)		South – horizontal fin	Location	SF (W/m²)	OTTV (W/m²)	
			Fin = 0.7 m	Fin = 3.6 m				Fin = 0.7 m	Fin = 3.6 m
	Banda Aceh	200	104.51	76.75		Banda Aceh	142	80.54	67.00
	Yogyakarta	178	95.37	70.67		Pontianak	120	71.39	59.94
	Difference	22	9.14	6.08		Difference	22	9.15	7.06
WWR = 65 %; SC_G = 0.79									
West – eggcrate fin	Location	SF (W/m²)	OTTV (W/m²)		South – eggcrate fin	Location	SF (W/m²)	OTTV (W/m²)	
			Fin = 0.7 m / 0.12 m	Fin = 3.6 m / 0.6 m				Fin = 0.7 m / 0.12 m	Fin = 3.6 m / 0.6 m
	Banda Aceh	200	101.94	72.81		Banda Aceh	142	76.20	65.77
	Yogyakarta	178	93.09	67.16		Pontianak	120	67.71	58.90
	Difference	22	8.85	5.65		Difference	22	8.48	6.87

they are located near the Equator, in the Northern Hemisphere, or in the Southern Hemisphere.

Moreover, the experiment demonstrated that OTTV reduction is less pronounced for lower SC values. For instance, on the south side of Banda Aceh, a combination of the highest WWR (65 %) and an SC value of 0.79 resulted in a 13.15 W/m² reduction in the OTTV when the fin R value increased from 0.2 to 1.0. In contrast, with the same WWR but an SC value of 0.39, the OTTV reduction was only 7 W/m². This comparison is summarized in Table 9. A similar pattern was observed across all orientations and locations. These findings indicate that using window glass with a lower SC value decreases the impact of shading system performance.

Substantial Role of the WWR Across Different Locations

A 25 % WWR configuration across the north–south orientation resulted in minimal OTTV variation between locations, as shown in Fig. 9. This consistency suggests that a 25 % WWR can serve as an effective baseline for minimizing thermal transfer across diverse Indonesian climates. The finding indicates that building envelopes respond consistently to this WWR configuration regardless of geographic or climatic variations, highlighting that specific WWR values can function as reliable performance standards across different environmental conditions. However, a WWR of 25 % on the north side of Yogyakarta, combined with an SCG of 0.79 and a vertical fin length of 0.6 m, yields an OTTV of 38.5 W/m², which exceeds the recommended limit according to SNI 6389:2020. None of the OTTV values in any orientation with a 65 % WWR configuration dropped below 35 W/m², even with the lowest SC value, as shown in Fig. 10. This indicates a performance limitation for high WWRs, regardless of other design interventions.

In terms of OTTV reduction, the WWR has a more significant impact than the SC value. The data indicate that, on the north side, OTTV reduction can reach up to 30 W/m² when comparing SC values of 0.79 and 0.39 at a 65 % WWR with vertical fins. The most substantial OTTV reduction, up to 46 W/m², occurs when decreasing the WWR from 65 % to 25 % at an SC of 0.79 with the same fin configuration. This finding highlights the critical impact of the WWR on thermal performance, suggesting that strategic adjustments to the WWR are more effective for energy efficiency than modifying the SC values. This trend is consistent across other orientations and locations, with varying reduction percentages. Furthermore, at a 25 % WWR configuration, variations in the SC and R values produce only minor differences in the OTTV across all studied cities.

Table 9. **OTTV margin comparison between vertical fin dimensions and various SC values**

Glass material characteristics			**OTTV by vertical fin dimensions**		**OTTV margin (a)–(b)**	**Percentage**
Glass material	**Thickness (mm)**	**SC value**	**0.12 m**	**0.6 m**		
			(a)	(b)		
Panasap Bronze	6	0.73	82.5 W/m²	69.4 W/m²	13.2 W/m²	16 %
T-Sunlux	6	0.67	77.5 W/m²	65.4 W/m²	12.1 W/m²	16 %
Stopsol Eurogray	6	0.56	68.3 W/m²	58.2 W/m²	10.1 W/m²	15 %
Stopsol Dark Blue	8	0.39	54.1 W/m²	47.1 W/m²	7 W/m²	13 %

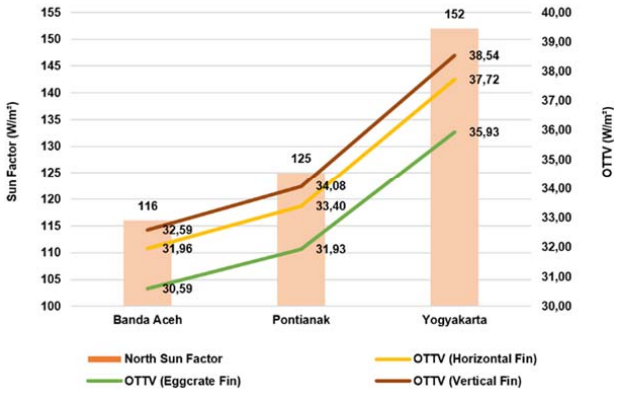

Fig. 9. Correlation of the OTTV with a 25 % WWR in the north orientation

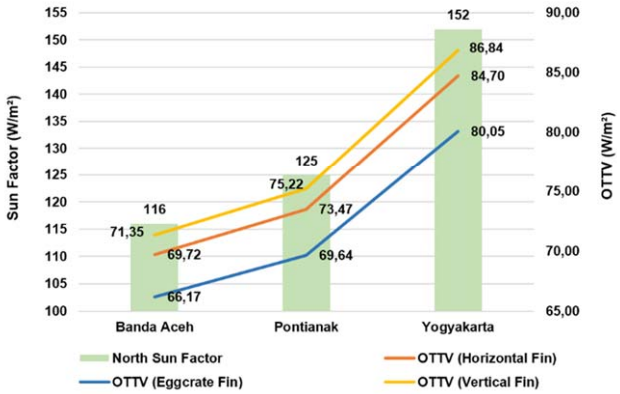

Fig. 10. Correlation of the OTTV with a 65 % WWR in the north orientation

For instance, in Yogyakarta, the OTTV difference in the north orientation (SF = 152 W/m²) with a 25 % WWR reaches up to 9 W/m², as shown in Fig. 9. However, this difference is considerably smaller compared to a 65 % WWR configuration, which exhibited variations of up to 30 W/m². These results indicate that as the WWR increases, the OTTV becomes more sensitive to changes in the SCG values and shading system dimensions, reinforcing the importance of optimizing the WWR for energy-efficient building design.

The finding shown in Fig. 11 indicate that the Overall Thermal Transfer Value (OTTV) decreases as the shading coefficient (SC) of the glass material is reduced. Among the tested glass types, Panasap Bronze, with the highest SC value of 0.79, produced the highest OTTV of approximately 85 W/m². Conversely, Stopsol Dark Blue, which has the lowest SC value of 0.39, achieved the most significant reduction in OTTV, reaching around 55 W/m². The intermediate glass materials, such as T-Sunlux CS-150 #2 (SC = 0.67) and Stopsol Eurogray (SC = 0.56), showed corresponding OTTV values that fell between these two extremes. This trend confirms that the use of glass materials with lower shading coefficients can substantially reduce OTTV and improve the thermal performance of building envelopes.

These findings collectively underscore the importance of tailored window design strategies that account for specific climatic and geographic conditions to maximize energy efficiency. By understanding the nuanced interactions among the WWR, SC values, and shading systems, architects and designers can make informed decisions that significantly reduce thermal transfer and improve the overall energy performance of buildings in warm-humid climates.

Discussion and Synthesis

This study highlights the critical impact of the solar factor on key building performance parameters, including the WWR, SCG, and SC. The solar factor, representing the intensity of solar radiation on wall surfaces, significantly affects heat transfer through windows, especially in orientations with high SF values. This effect is exemplified by the UNU building case study. As shown in Table 5, the existing OTTV for each city and orientation indicates that only the west orientation in all three locations fails to meet

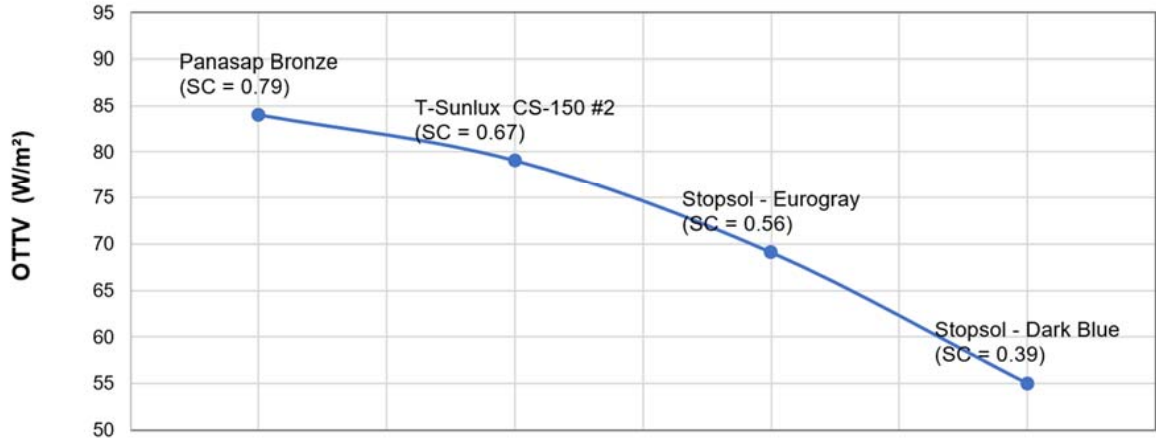

Fig. 11. OTTV reduction with different types of glass materials and SC values

the OTTV standard set by SNI 6389:2020, despite a relatively low WWR of 34 %. The elevated OTTV on the west side of the UNU building results from a combination of the highest SF values among all locations, inadequate shading system, and glass with an SCG value of 0.55. Fig. 12 shows the case study building with an eggcrate shading system, which has a high SC value of 0.877, indicating that approximately 87 % of solar radiation passes through the window. An SC_G value of 0.55 is not optimal for the west orientation in any location. The experimental results demonstrate that glass with an SC value of 0.39 can achieve OTTV values compliant with the SNI standard of 35 W/m².

Table 8 further highlights how orientation-specific shading dimensions yield different OTTV values. In tropical regions such as Indonesia, OTTV variations are relatively consistent between north–south and east–west orientations due to similar distributions of solar heat gain. Among the shading types analyzed, eggcrate systems perform most effectively, corroborating previous research (Sari and Rauzi, 2021), as they efficiently block both direct and diffuse solar radiation. In contrast, vertical and horizontal shading systems demonstrate lower effectiveness.

The study also finds that a high WWR, such as 65 %, is impractical for any orientation in Indonesia, as it fails to meet OTTV standards even when using low-SC glass. Conversely, reducing WWR to 25 % enables compliance with the standards even with an SC of 0.79, while applying an SC of 0.39 at this WWR further minimizes the OTTV. These findings encourage architects to consider WWR and shading system combinations early in design, providing flexibility to achieve energy performance standards without imposing rigid design constraints.

Recommendation as Best Practice

By analyzing building envelope variables using BIM-based applications, the study intends to provide practical design recommendations for architects and policymakers to improve building energy efficiency across different regions of Indonesia. Table 10 summarizes the best-practice window design strategies derived from this study. Orientation and solar exposure are critical factors, with higher WWRs permissible for orientations with lower solar heat gains. For instance, in Pontianak, north-facing windows with SC_G values between 0.67 and 0.73 are recommended to have a WWR below 25 %, reflecting the high solar exposure in that orientation. Conversely, lower SC_G values (0.39–0.56) allow for higher WWRs, such as 35–45 % for north-facing windows in Pontianak and Banda Aceh, indicating reduced heat gain. This table aids in optimizing building energy performance by minimizing unwanted solar heat gain while allowing daylight, tailored to the specific climate and solar exposure of each city.

Conclusion

This study investigates the impact of window design on the OTTV across three geographically distinct Indonesian cities — Banda Aceh, Pontianak, and Yogyakarta — covering a range of latitudes. The analysis

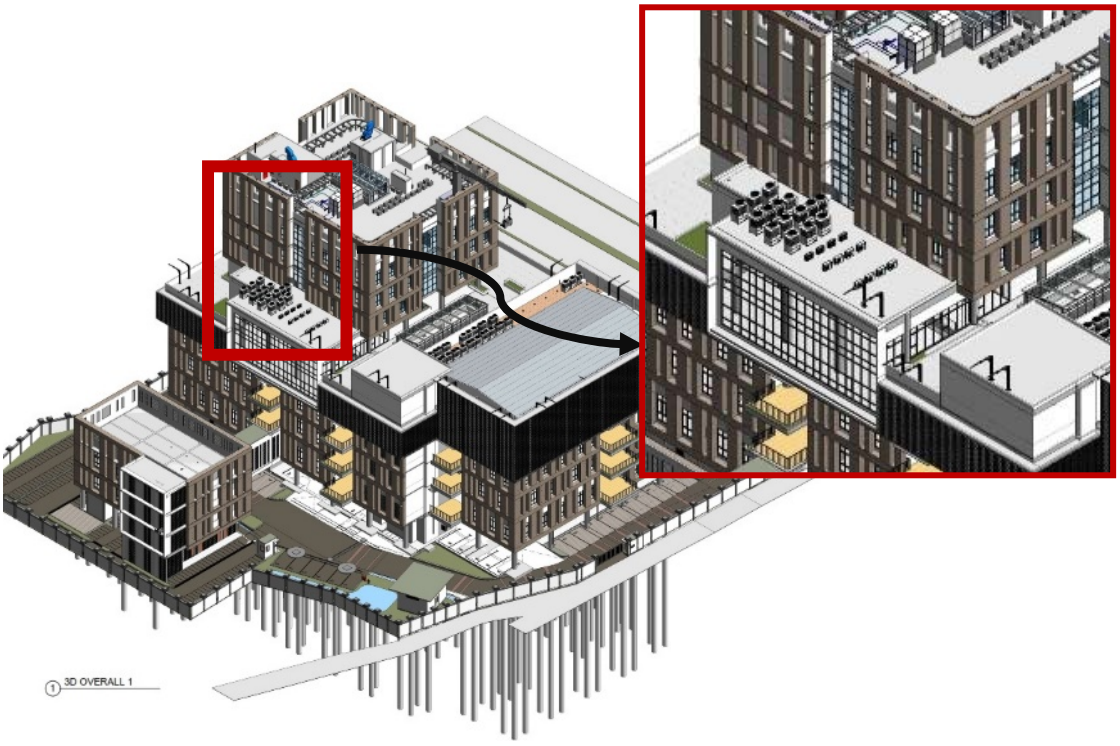

Fig. 12. Window area with minimal shading system on the west facade of the UNU building

Table 10. **Recommended window design strategies in Pontianak, Yogyakarta, and Banda Aceh**

City	Orientation & SF	SC_G	Recommended WWR for all shading systems
PONTIANAK	North *SF = 125 W/m²*	$0.67 \le SC_G \le 0.73$	WWR ≤ 25 %
		$0.39 \le SC_G \le 0.56$	35% < WWR < 45 %
	South *SF = 120 W/m²*	$0.67 \le SC_G \le 0.73$	WWR ≤ 30 %
		$0.39 \le SC_G \le 0.56$	35 % < WWR < 45 %
	East *SF = 139 W/m²*	$0.67 \le SC_G \le 0.73$	WWR < 25 %
		$0.39 \le SC_G \le 0.56$	30 % < WWR < 40 %
	West *SF = 186 W/m²*	$0.67 \le SC_G \le 0.73$	15 % < WWR < 20 %
		$0.39 \le SC_G \le 0.56$	23 % < WWR < 30 %
YOGYAKARTA	North *SF = 152 W/m²*	$0.67 \le SC_G \le 0.73$	23 % < WWR < 25 %
		$0.39 \le SC_G \le 0.56$	30 % < WWR < 40 %
	South *SF = 105 W/m²*	$0.67 \le SC_G \le 0.73$	WWR < 3 3%
		$0.39 \le SC_G \le 0.56$	40 % < WWR < 50 %
	East *SF = 170 W/m²*	$0.67 \le SC_G \le 0.73$	20% < WWR < 23%
		$0.39 \le SC_G \le 0.56$	30% < WWR < 33%
	West *SF = 178 W/m²*	$0.67 \le SC_G \le 0.73$	WWR < 20 %
		$0.39 \le SC_G \le 0.56$	25 % < WWR < 33 %
BANDA ACEH	North *SF = 116 W/m²*	$0.67 \le SC_G \le 0.73$	25 % < WWR < 35 %
		$0.39 \le SC_G \le 0.56$	35 % < WWR < 45 %
	South *SF = 142 W/m²*	$0.67 \le SC_G \le 0.73$	WWR < 25 %
		$0.39 \le SC_G \le 0.56$	33 % < WWR < 40 %
	East *SF = 166 W/m²*	$0.67 \le SC_G \le 0.73$	WWR < 20 %
		$0.39 \le SC_G \le 0.56$	25 % < WWR < 30 %
	West *SF = 200 W/m²*	$0.67 \le SC_G \le 0.73$	25 % < WWR < 20 %
		$0.39 \le SC_G \le 0.56$	23 % < WWR < 30 %

focused on key factors such as the window-to-wall ratio (WWR), solar factor (SF), glass shading coefficient (SCG), and shading system coefficient (SC), based on the OTTV framework outlined in SNI 6389:2020. The BIM-based OTTV calculator, developed using Autodesk Revit and Dynamo, generated over 3,600 window design variations for this study.

The results indicate that the WWR has a more pronounced effect on the OTTV than the SC, with reductions of up to 46 W/m² observed when the WWR decreased from 65 % to 25 %, regardless of orientation. The influence of the SC was minimal, especially at lower WWR values. Moreover, shading system dimensions had a greater impact on the OTTV than glazing properties alone, emphasizing the critical role of shading configurations in thermal performance. A key insight from the study is that maintaining a consistent shading fin-to-window ratio produces uniform OTTV reductions across all orientations, offering a reliable solution for energy-efficient design in tropical climates. Overall, optimizing the WWR and implementing standardized shading systems can enhance thermal comfort and reduce energy demand in warm-humid regions.

Future Research

A limitation of this study is the exclusion of energy cost calculations associated with the OTTV of the experimental window designs. Future research should incorporate these calculations to better understand the implications of applying different window design elements across diverse locations. Incorporating this analysis would provide a more comprehensive analysis of how the OTTV affects energy consumption and costs, offering valuable insights for optimizing window designs to improve energy efficiency and reduce operational expenses across diverse climatic contexts.

References

Abass, F., Ismail, L. H., Wahab, I. A., and Elgadi, A. A. (2020). Development of a model for OTTV and RTTV based on BIMVPL to optimize the envelope thermal performance. *IOP Conference Series: Materials Science and Engineering*, Vol. 713, 012009. DOI: 10.1088/1757-899X/713/1/012009.

Albatayneh, A. (2021). Sensitivity analysis optimisation of building envelope parameters in a sub-humid Mediterranean climate zone. *Energy Exploration & Exploitation*, Vol. 39, Issue 6, pp. 2080–2102. DOI: 10.1177/01445987211020432.

Al-Homoud, M. S. (2005). A systematic approach for the thermal design optimization of building envelopes. *Journal of Building Physics*, Vol. 29, Issue 2, pp. 95–119. DOI: 10.1177/1744259105056267.

Bahdad, A. A. S., Fadzil, S. F. S., and Onubi, H. O. (2021). Assessment of the thermal performance of vertical green walls using overall thermal transfer value based BIM simulation method: case study of residential buildings in sub-tropics. *Journal of Daylighting*, Vol. 8, Issue 2, pp. 294–312. DOI: 10.15627/JD.2021.23.

BSN (2020). *SNI 6389:2020. Standar Nasional Indonesia Konservasi energi selubung bangunan pada bangunan gedung*. [online] Available at: www.bsn.go.id [Date accessed: May 3rd 2024].

Chow, W. K. and Chan, K. T. (1995). Parameterization study of the overall thermal-transfer value equation for buildings. *Applied Energy*, Vol. 50, Issue 3, pp. 247–268. DOI: 10.1016/0306-2619(94)00023-8.

Eid, A. S., Aboulnaga, M. M., and Mahmoud, A. H. (2022). VPL-based code compliance checking for building envelope design using OTTV calculation. *IOP Conference Series: Earth and Environmental Science*, Vol. 1056, 012033. DOI: 10.1088/1755-1315/1056/1/012033.

Elhadad, S. and Orban, Z. (2021). A sensitivity analysis for thermal performance of building envelope design parameters. *Sustainability*, Vol. 13, Issue 24, 14018. DOI: 10.3390/su132414018.

Gondal, I. A., Syed Athar, M., and Khurram, M. (2019). Role of passive design and alternative energy in building energy optimization. *Indoor and Built Environment*, Vol. 30, Issue 2, pp. 278–289. DOI: 10.1177/1420326X19887486.

Habibi, S. (2019). Improving building envelope performance with respect to thermal, sound insulation, and lighting: a case study. *Building Acoustics*, Vol. 26, Issue 4, pp. 243–262. DOI: 10.1177/1351010X19877280.

Imran, M. (2019). Analisa hemat energi terhadap gedung GPIB Kelapa Gading melalui pendekatan OTTV. *Jurnal Linears*, Vol. 2, No. 2, pp. 79–91. DOI: 10.26618/j-linears.v2i2.3127.

Kusumawati, L., Setyowati, E., and Purnomo, A. B. (2021). Practical-empirical modeling on envelope design towards sustainability in tropical architecture. *Sustainability*, Vol. 13, Issue 5, 2959. DOI: 10.3390/su13052959.

Lim, Y.-W., Seghier, T. E., Harun, M. F., Ahmad, M. H., Samah, A. A., and Majid, H. A. (2019). Computational BIM for building envelope sustainability optimization. *MATEC Web of Conferences*, Vol. 278, 04001. DOI: 10.1051/matecconf/201927804001.

Mushtaha, E., Salameh, T., Kharrufa, S., Mori, T., Aldawoud, A., Hamad, R., and Nemer, T. (2021). The impact of passive design strategies on cooling loads of buildings in temperate climate. *Case Studies in Thermal Engineering*, Vol. 28, 101588. DOI: 10.1016/j.csite.2021.101588.

Nasrullah, N., Hamdy, M. A., Mustamin, M. T., and Faharuddin, A. (2024). Energy management model for air conditioning energy conservation in hotel buildings of Makassar City, Indonesia. *Civil Engineering and Architecture*, Vol. 12, No. 4, pp. 2755–2771. DOI: 10.13189/cea.2024.120419.

Natephra, W., Yabuki, N., and Fukuda, T. (2018). Optimizing the evaluation of building envelope design for thermal performance using a BIM-based overall thermal transfer value calculation. *Building and Environment*, Vol. 136, pp. 128–145. DOI: 10.1016/j.buildenv.2018.03.032.

Octarino, C. N. and Feriadi, H. (2021). Evaluasi kinerja selubung bangunan gedung agape universitas kristen duta wacana yogyakarta. *Langkau Betang: Jurnal Arsitektur*, Vol. 8, No. 2, pp. 86–97. DOI: 10.26418/lantang.v8i2.45436.

Pang, Z., O'Neill, Z., Li, Y., and Niu, F. (2020). The role of sensitivity analysis in the building performance analysis: a critical review. *Energy and Buildings*, Vol. 209, 109659. DOI: 10.1016/j.enbuild.2019.109659.

Pathirana, S., Rodrigo, A., and Halwatura, R. (2019). Effect of building shape, orientation, window to wall ratios and zones on energy efficiency and thermal comfort of naturally ventilated houses in tropical climate. *International Journal of Energy and Environmental Engineering*, Vol. 10, Issue 1, pp. 107–120. DOI: 10.1007/s40095-018-0295-3.

PT Asahimas Flat Glass Tbk. (2022). *Architectural glass*. [online] Available at: https://luminoindonesia.com/wp-content/uploads/2022/11/katalog-asahi.pdf [Date accessed November 5, 2024].

Purwanto, L. M. F. and Tichelmann, K. (2021). Effects of heat transfer through the walls of a catholic church in Semarang Indonesia simulated with Psi-Therm software and OTTV. *Civil Engineering and Architecture*, Vol. 9, No. 3, pp. 799–806. DOI: 10.13189/cea.2021.090321.

Rahmanda, A. P. and Suriansyah, Y. (2020). Upaya penurunan nilai ottv untuk penghematan energi pada hotel emersia lampung sesuai kriteria greenship. *Riset Arsitektur (RISA)*, Vol. 5, No. 0), pp. 18–35, DOI: 10.26593/risa.v5i01.4415.18-35.

Sani, A. A., Matondang, A. E., Kurniawan, G. K., and Mardiyanto, A. (2019). Kinerja termal selubung gedung kuliah kota bandar lampung ITERA. *Jurnal Arsitektur ARCADE*, Vol. 3, No. 3, pp. 267–273. DOI: 10.31848/arcade.v3i3.303.

Sari, L. H. and Rauzi, E. N. (2021). An evaluation of shading device in tropics utilising the sun-path diagram. ARTEKS: Jurnal Teknik Arsitektur, Vol. 6, No. 3, pp. 373–382. DOI: 10.30822/arteks.v6i3.877.

Sayadi, S., Hayati, A., and Salmanzadeh, M. (2021). Optimization of window-to-wall ratio for buildings located in different climates: an IDA-indoor climate and energy simulation study. *Energies*, Vol. 14, Issue 7, 1974. DOI: 10.3390/en14071974.

Seghier, T. E., Lim, Y. W., Ahmad, M. H., and Samuel, W. O. (2017). Building envelope thermal performance assessment using visual programming and BIM, based on ETTV requirement of Green Mark and GreenRE. *International Journal of Built Environment and Sustainability*, Vol. 4, Issue 3, pp. 227–235. DOI: 10.11113/ijbes.v4.n3.216.

Seghier, T. E., Lim, Y.-W., Harun, M. F., Ahmad, M. H., Samah, A. A., and Majid, H. A. (2022). BIM-based retrofit method (RBIM) for building envelope thermal performance optimization. *Energy and Buildings*, Vol. 256, 111693. DOI: 10.1016/j.enbuild.2021.111693.

Syafutri, R. F., Suryabrata, J. A., and Rahmawati, Y. (2023a). *Analisis sensitivitas elemen dinding selubung bangunan terhadap OTTV dengan kalkulator berbasis kerangka kerja BIM-VPL*. MSc Thesis in Architecture.

Syafutri, R. F., Suryabrata, J.A., and Rahmawati, Y. (2023b). Developing the building envelope thermal transfer value calculator based on BIM-VPL framework. *International Journal of Application on Sciences, Technology and Engineering*, Vol. 1, Issue 1, pp. 343–349. DOI: 10.24912/ijaste.v1.i1.343-349.

Tantisevi, K. and Sornsuriya, K. (2010). Building information model for evaluating the building energy performance: a case study. In: Tizani, W. (ed.). *Computing in Civil and Building Engineering, Proceedings of the International Conference*, June 30 – July 2, Nottingham, UK. Nottingham: Nottingham University Press, 84.

Tong, S., Wen, J., Wong, N. H., and Tan, E. (2021). Impact of façade design on indoor air temperatures and cooling loads in residential buildings in the tropical climate. *Energy and Buildings*, Vol. 243, 110972. DOI: 10.1016/j.enbuild.2021.110972.

Tukiainen, M. and Gaisma.com (2024). *Indonesia - sunrise, sunset, dawn and dusk times*. [online]. Available at: https://www.gaisma.com/en/dir/id-country.html [Date accessed June 6, 2024].

Widhayaka, S. A. and Rilatupa, J. E. D. (2021). Optimalisasi kinerja termal selubung bangunan unit hunian di rusunawa cibesut jakarta timur. *MODUL*, Vol. 21, No. 1, pp. 43–50. DOI: 10.14710/mdl.21.1.2021.43-50.

ИССЛЕДОВАНИЕ ВЛИЯНИЯ ДИЗАЙНА ОКОН НА ОБЩИЙ КОЭФФИЦИЕНТ ТЕПЛОПЕРЕДАЧИ С ПОМОЩЬЮ BIM-МОДЕЛИРОВАНИЯ В ГОРОДАХ С ТЕПЛЫМ И ВЛАЖНЫМ КЛИМАТОМ

Рисса Сяфутри[1]*, Яни Рахмавати[2], Джатмика Ади Сурьябрата[2]

[1]Политехнический университет Понтианака, Индонезия
[2]Университет Гаджа Мада, Индонезия

*E-mail: rissasyafutri@polnep.ac.id

Аннотация
Введение: Проектирование оконных конструкций имеет решающее значение для энергоэффективности зданий в теплом и влажном климате, где солнечное излучение через окна существенно влияет на общий коэффициент теплопередачи. Во многих зданиях в Индонезии особенности проектирования ограждающих конструкций с учетом местного климата не учитываются должным образом, что, вероятно, связано с ограниченным экспериментальным исследованием подходящих проектов в разнообразных климатических условиях страны. **Цель исследования:** изучить влияние различных стратегий проектирования окон на теплопередачу зданий в индонезийских городах. **Методы:** для оценки влияния конструкций окон на общий коэффициент теплопередачи был проведен анализ чувствительности в трех географически различающихся индонезийских городах: Банда-Ачех (северное полушарие), Понтианак (экватор) и Джокьякарта (южное полушарие). При помощи BIM-калькулятора общего коэффициента передачи в Autodesk Revit и Dynamo было сгенерировано 3600 вариантов оконных конфигураций, представленных на 180 графиках. Варьировались следующие параметры: соотношение площади окна к площади стены, характеристики остекления и тип затеняющего устройства. **Результаты:** анализ показал, что соотношение площади окна к площади стены оказывает более существенное влияние на общий коэффициент теплопередачи, чем коэффициент затенения, причем при снижении соотношения с 65 % до 25 % уменьшение общего коэффициента теплопередачи составило до 46 Вт/м². Размеры элементов затенения оказали большее влияние на общий коэффициент теплопередачи, чем характеристики остекления, что подчеркивает важность конфигурации затенения для теплоэффективности здания. Оптимизация соотношения площади окна к площади стены и внедрение стандартизированных систем затенения могут существенно повысить энергоэффективность и комфорт, особенно в тропических климатических условиях с высокой инсоляцией. Результаты исследования подчеркивают необходимость изучения комбинаций соотношения площади окна к площади стены и систем затенения на ранних стадиях проектирования для достижения соответствия энергетическим стандартам при сохранении гибкости проектных решений.

Ключевые слова: проектирование оконных конструкций, энергоэффективность, общий коэффициент теплопередачи, анализ чувствительности, здания в теплом и влажном климате, индонезийские здания.

DOI: 10.23968/2500-0055-2025-10-3-67-75

PERFORMANCE OF A HIGH-RISE REINFORCED CONCRETE BUILDING WITH A SLIDING BELT, TAKING INTO ACCOUNT THE NONLINEAR CHARACTER OF DEFORMATION

Oleg V. Mkrtychev, Salima R. Bulusheva*

Moscow State University of Civil Engineering, Moscow, Russia

*Corresponding author's email: salima.mingazova@yandex.ru

Abstract

Introduction: The relevance of seismic isolation is driven by the need to improve the safety of buildings and structures in conditions of high seismic activity. Earthquakes pose a serious threat to human life and can result in significant economic and material losses. With the development of urbanization and increasing building density in earthquake-prone regions, there is growing demand for methods that effectively mitigate the destructive impact of seismic waves on structures. **Purpose of the study**: The study aims to analyze the performance of a high-rise reinforced concrete building with a sliding belt, taking into account the nonlinear nature of deformation. **Methods**: Calculations were performed using the LS-DYNA software through the direct dynamic method with explicit schemes for direct integration of the equations of motion, employing a nonlinear model of concrete and reinforcement. Foundation–structure interaction was modeled using the substructure method, while the nonlinear behavior of the soil foundation was described by the Mohr–Coulomb model. **Results and discussion**: The analysis shows a decrease in the effectiveness of seismic isolation in the form of a sliding belt at the foundation level of high-rise buildings. Considering all structural characteristics, it is possible to select optimal parameters for the seismic isolation sliding belt to effectively protect the building from seismic loads.

Keywords: seismic isolation, sliding belt, high-rise buildings, nonlinear behavior, soil foundation.

Introduction

Earthquakes are powerful natural phenomena that can cause extensive damage to buildings and infrastructure, as well as pose a serious threat to human life and safety. Ensuring the seismic resistance of buildings is therefore one of the key priorities of modern construction, particularly in regions with high seismic activity (Dzhinchvelashvili and Bulushev, 2014). To date, a variety of methods and technologies have been developed and implemented to improve the resistance of structures to seismic loads (Gorshkov and Kuznetsov, 2020). Among them, seismic isolation has become one of the most effective approaches (Pan et al., 2012; Uzdin et al., 2022). There are several types of seismic isolation (Eisenberg, 2004). Rubber-metal bearings (RMBs) (Mkrtychev and Bunov, 2014) and pendulum sliding bearings (PSBs) (Figs. 1, 2) (Mkrtychev and Arutyunyan, 2016) have been extensively used

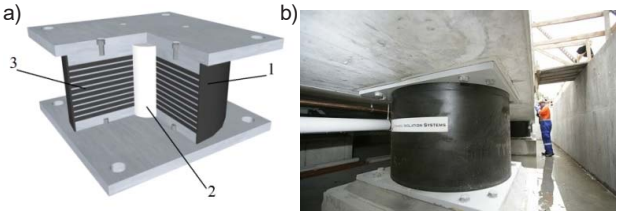

Fig. 1. RMB device (a): 1 — rubber; 2 — lead core; 3 — internal steel plates with rubber layers; Installation of an RMB at a construction site (b)

Fig. 2. PSB device (a): 1 — housing plate; 2 — articulated slider; 3 — sliding coating; 4 — concave plate; 5 — stainless steel concave surface; Installation of a PSB at a construction site (b)

For citations: Mkrtychev, O. V., Bulusheva, S. R. (2025). Performance of a high-rise reinforced concrete building with a sliding belt, taking into account the nonlinear character of deformation. Architecture and Engineering, No 3 (10), pp. 67–75.
DOI: 10.23968/2500-0055-2025-10-3-67-75.

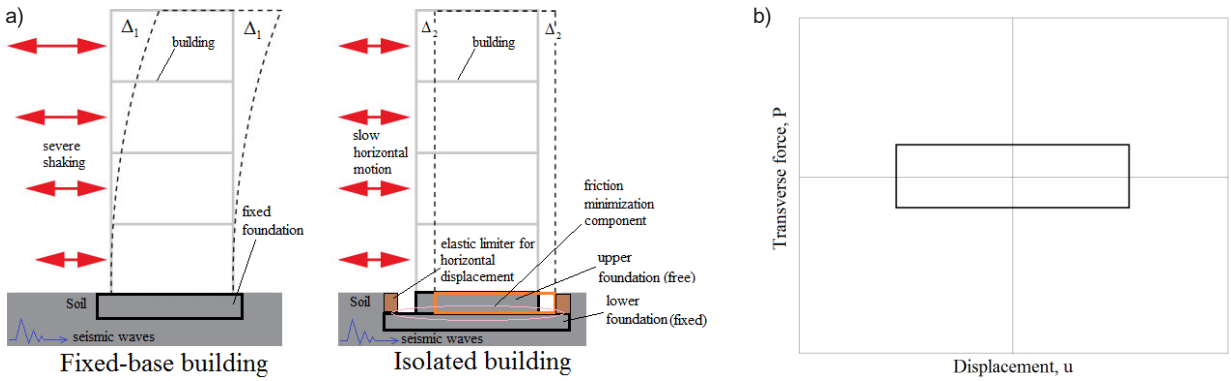

Fig. 3. Operating principle of the seismic isolation sliding belt at the foundation level (a); Functional scheme of the seismic isolation sliding belt (b)

in construction practice, which makes them the most widespread and sought-after solutions. In comparison, the sliding belt system, installed at the foundation level, represents a simpler seismic isolation solution than RMBs and PSBs (Kuznetsov and Chen, 2011). Its structural simplicity reduces both the installation time and the associated costs, which makes it an attractive alternative to more complex isolation devices.

The seismic isolation sliding belt consists of several key components, each performing a specific function to ensure effective protection of the structure from seismic impacts (Fig. 3). The primary elements are sliding supports, which enable the building to move freely in the horizontal plane relative to the foundation. These supports are made of low-friction materials, such as Teflon, to minimize friction between contact surfaces. In some designs, displacement limiters are incorporated to control excessive horizontal movements. Such limiters help regulate the amplitude of displacements and ensure that the building returns to its initial position after a seismic event (Mirzaev and Turdiev, 2021).

In the 1970s and 1980s, seismic protection in the form of an earthquake-isolating sliding belt became one of the research priorities in the USSR in the field of earthquake-resistant buildings and structures, as well as in experimental design and construction. The developed system was intended to reduce seismic loads on the superstructure of buildings. To evaluate the operability and effectiveness of the seismic isolation sliding belt, a wide range of experimental studies was carried out on seismic platforms. These included investigations of different material pairs for sliding elements, tests of elastic limiters made of spring steel, experimental studies of a nine-story building model with seismic isolation, and design developments for buildings of three, five, and nine stories. In addition, three-story buildings with a specially developed sliding belt construction technology were built in Frunze (Polyakov et al., 1989).

Seismic isolation in the form of a sliding belt at the foundation level is therefore relatively well established and has found practical application. However, currently, the design justifications for this type of seismic isolation remain incomplete, particularly with regard to the interaction of the building, the isolation system, the foundation, and the soil base. This gap continues to limit its broader implementation in modern construction practice.

Methods

The study examined the performance of a 24-storey monolithic reinforced concrete building with a seismic isolation sliding belt, considering the nonlinear nature of deformation under the action of an intense earthquake and accounting for the deformability of the soil base (Fig. 4).

The building employs a cross-wall structural system. The load-bearing elements are made

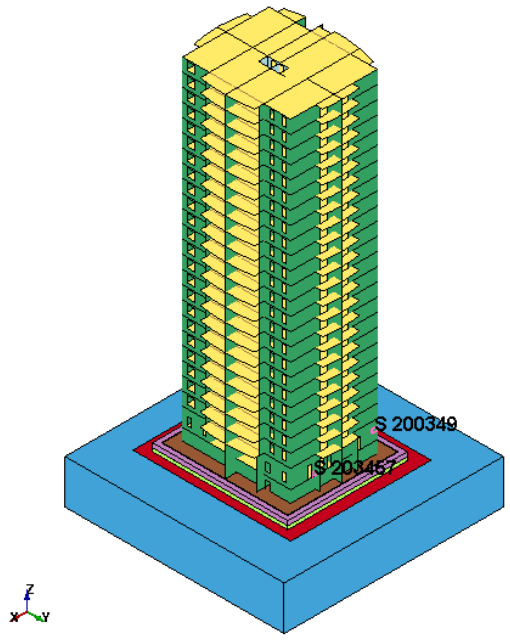

Fig. 4. Design scheme of a building with seismic isolation on a soil base

of concrete of class C20/25. The building dimensions in plan are 24.7 × 19.8 m, with a typical floor height of 3.0 m. Wall thicknesses are 0.20 and 0.25 m, while floor slabs are 0.22 m thick. Floor beams have a cross-section of 0.40 × 0.56 m.

The configuration of the seismic isolation sliding belt is shown in Fig. 5. Fluoroplastic plates (PTFE + PTFE) with friction coefficient $\mu_P = 0.05$ are used as friction-reducing elements.

The elastic limiter for large horizontal displacements is represented by sand (ρ=1,680 kg/m^3, E = 100 MPa), placed along the perimeter of the upper foundation slab at a distance of 15 cm. The sand layer is assumed to have a height and width of 1.0 m. The coefficient of friction between concrete and sand is taken as $\mu_s = 0.3$.

A two-component accelerogram of the external seismic excitation, corresponding to an earthquake intensity of 9 points on the MSK-64 scale, is shown in Figs. 6 and 7.

The study was conducted using the LS-DYNA software package. The analysis employed the direct dynamic method with explicit schemes for direct integration of the equations of motion, incorporating a nonlinear model for concrete and reinforcement.

The interaction between the structure and the soil base was modeled using the substructure method (soil–structure interaction (SSI)) (Fig. 8) (Herrera and Bielak, 1997; LSTC, 2018; Mkrtychev et al., 2013).

Using this approach, the equations of motion in the time domain for the structure–soil system can be expressed as follows:

$$\mathbf{M}\ddot{\mathbf{u}} + \mathbf{C}\dot{\mathbf{u}} + \mathbf{K}\mathbf{u} = \mathbf{m}_{ef} \cdot \ddot{\mathbf{u}}_f^{\,0} + \mathbf{k}_{ef} \cdot \mathbf{u}_f^{\,0}, \qquad (1)$$

where: **M** is the mass matrix of the entire system, including the structure, foundation, and soil:

$$\mathbf{M} = \begin{bmatrix} M_{ss} & M_{sb} & 0 \\ M_{bs} & M_{bb} + M_{ff} & M_{fe} \\ 0 & M_{ef} & M_{ee} \end{bmatrix}, \qquad (2)$$

C is the damping matrix of the construction materials and the soil:

$$\mathbf{C} = \begin{bmatrix} C_{ss} & C_{sb} & 0 \\ C_{bs} & C_{bb} + C_{ff} & C_{fe} \\ 0 & C_{ef} & C_{ee} \end{bmatrix}, \qquad (3)$$

K is the stiffness matrix of the system:

$$\mathbf{K} = \begin{bmatrix} K_{ss} & K_{sb} & 0 \\ K_{bs} & K_{bb} + K_{ff} & K_{fe} \\ 0 & K_{ef} & K_{ee} \end{bmatrix}, \qquad (4)$$

$\mathbf{m}_{ef}$ is the auxiliary mass vector of the soil base:

$$\mathbf{m}_{5f} = \begin{bmatrix} 0 \\ m_{ff} \\ m_{ef} \end{bmatrix}, \qquad (5)$$

$\mathbf{k}_{ef}$ is the auxiliary stiffness vector of the soil foundation:

$$\mathbf{k}_{ef} = \begin{bmatrix} 0 \\ k_{ff} \\ k_{ef} \end{bmatrix}, \qquad (6)$$

$\mathbf{u}$ is the vector of relative displacements, and $\mathbf{u}_f$, $\ddot{\mathbf{u}}_f^{\,0}$ represent the external seismic excitation in the form of a seismogram and accelerogram.

The nonlinear behavior of the soil under intense seismic loading is described using the Mohr–Coulomb model (Mkrtychev and Busalova, 2014, Mkrtychev, Dzhinchvelashvili and Busalova, 2014, Mkrtychev and Dudareva, 2018).

The soil base consists of medium-density sand (Table 1).

For numerical modeling, rod elements (672 FE), plate elements (36,596 FE), and volumetric finite elements (200,896 FE) were used.

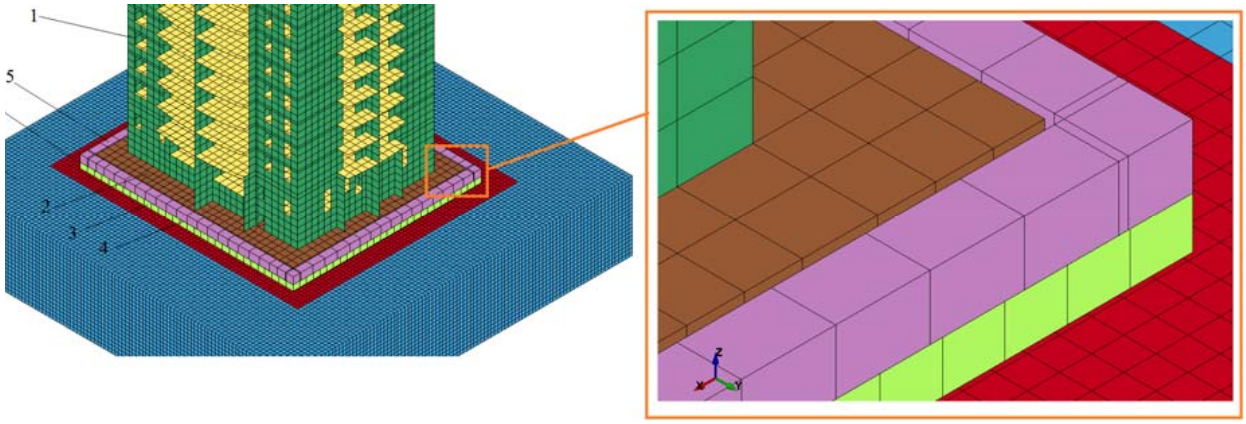

Fig. 5. Fragment of the design scheme of a building with a seismic isolation sliding belt: 1 — building; 2 — upper slab of the foundation; 3 — lower slab of the foundation; 4 — friction-reducing component; 5 — elastic limiter for horizontal displacements (sand); 6 — soil; 7 — soil with PML layer

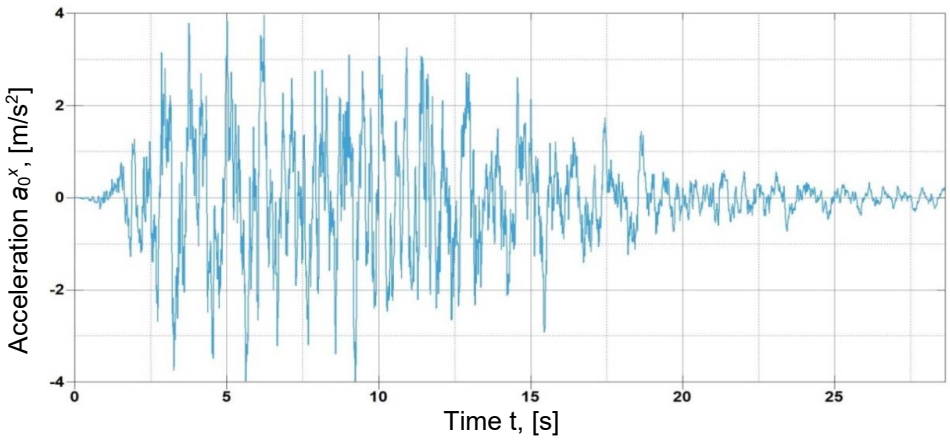

Fig. 6. Component of an earthquake's accelerogram along the *X*-axis for a 16-storey building

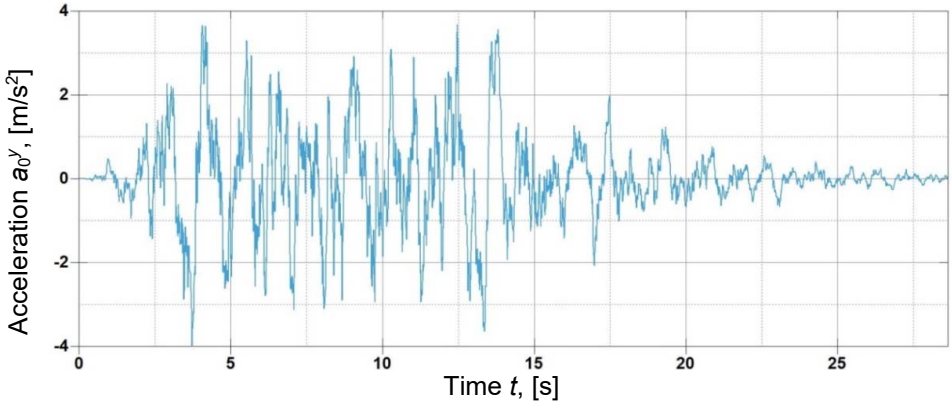

Fig. 7. Component of an earthquake's accelerogram along the *Y*-axis for a 16-storey building

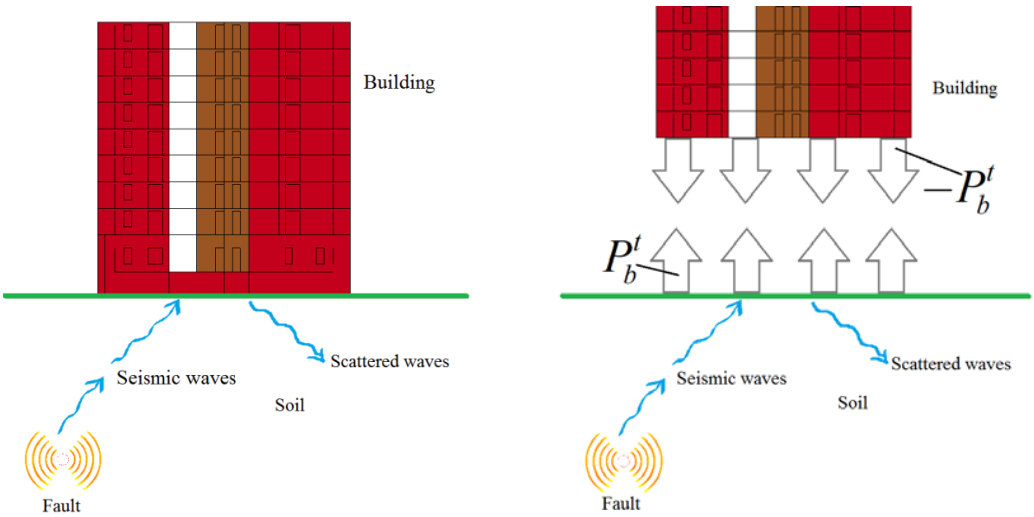

Fig. 8. Structure–soil system under seismic loading

Table 1. **Physical and mechanical properties of the soil base**

Medium-density sand				
Material density ρ, [kg/m^3]	**Standard value of specific cohesion C_s, [kPa]**	**Internal friction angle γ_s, [°]**	**Modulus of deformation E, [MPa]**	**Poisson's ratio v**
1,600	2	38 (31)*	40 (320)*	0.3

* Note: Dynamic values are shown in parentheses.

Results

The calculation results are presented below.

Fig. 9 shows the intensity of plastic deformations in a wall element of the 1st floor of a building without and with seismic isolation.

Figs. 10 and 11 show isofields of the intensity of plastic deformations in a building without seismic isolation at specific moments in time.

Fig. 12 shows the intensity of plastic deformations in a wall element of the 1st floor of a building without and with seismic isolation.

Figs. 13 and 14 show isofields of the intensity of plastic deformations in a building without seismic isolation at specific moments in time.

Figs. 15 and 16 present the absolute displacement of the top point of the building along the X and Y axes, with and without seismic isolation.

The results of the study demonstrate the effectiveness of the seismic isolation sliding belt in protecting the building from external seismic effects. From the graphs of the intensity of plastic deformations in the wall elements of the 1st floor (Figs. 9 and 12), it is evident that in the building without seismic isolation, structural damage begins after approximately six seconds of earthquake excitation, whereas in the building with seismic isolation, damage occurs after about ten seconds. When selecting a specific type of seismic protection, the parameters and structural features of the building must be considered. The analysis of the 24-storey building with seismic isolation in the form of a sliding belt at the foundation level indicates that the effectiveness of the sliding belt decreases as the number of stories increases. By accounting for all structural characteristics, it is possible to determine the optimal parameters for the seismic isolation belt to ensure adequate building protection during seismic events.

Acknowledgments

This research was funded by the Ministry of Science and Higher Education of the Russian Federation, grant number FSWG-2023-0004.

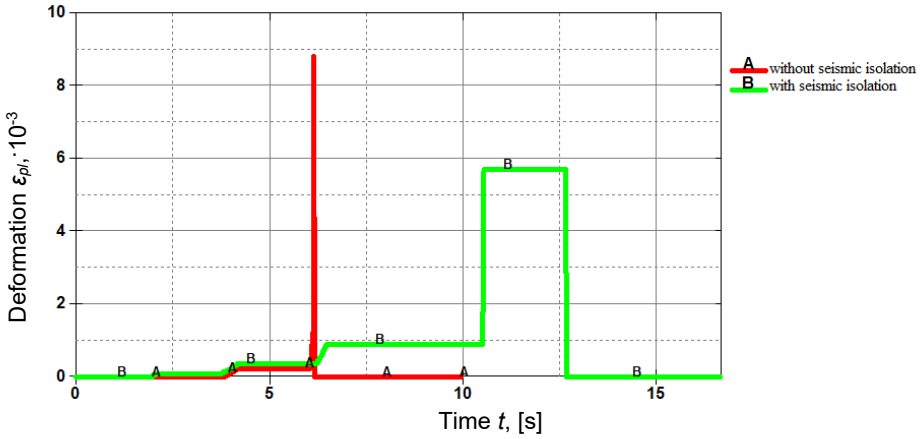

Fig. 9. Intensity of plastic deformations in wall element No. 200349 of the 1st floor of a building without and with seismic isolation

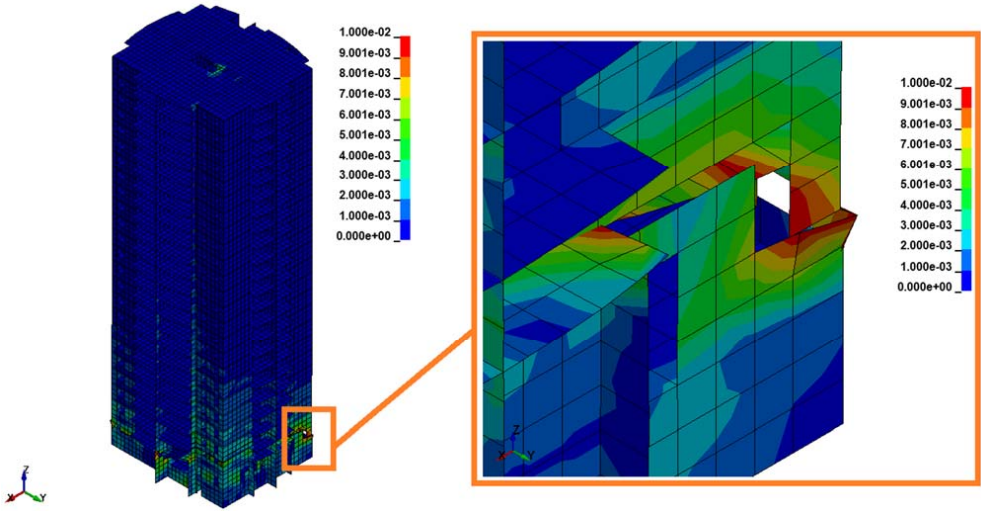

Fig. 10. Isofields of the intensity of plastic deformations in a building without seismic isolation at t = 6.53 s

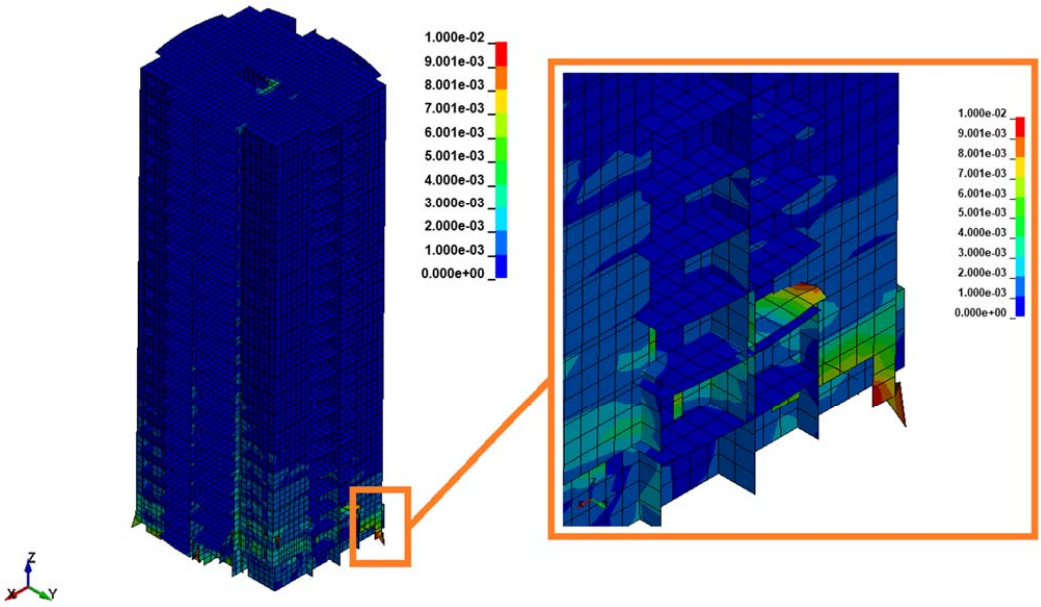

Fig. 11. Isofields of the intensity of plastic deformations in a building without seismic isolation at t = 7.35 s

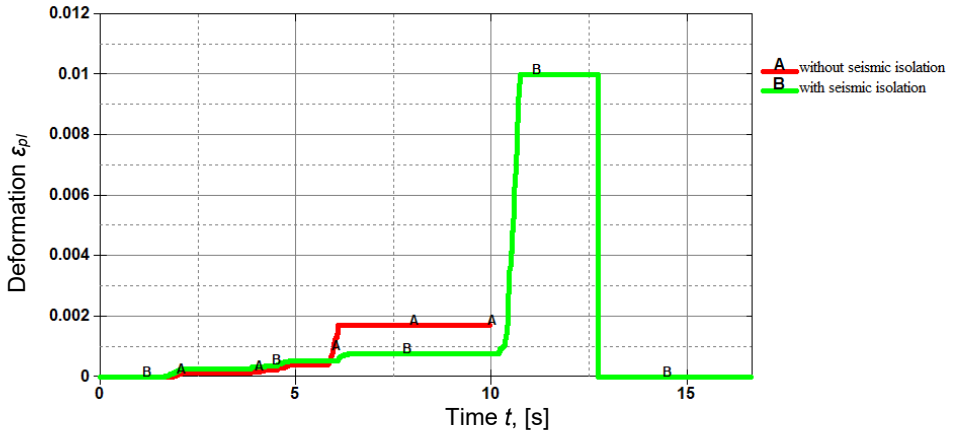

Fig. 12. Intensity of plastic deformations in wall element No. 203457 of the 1st floor of a building without and with seismic isolation

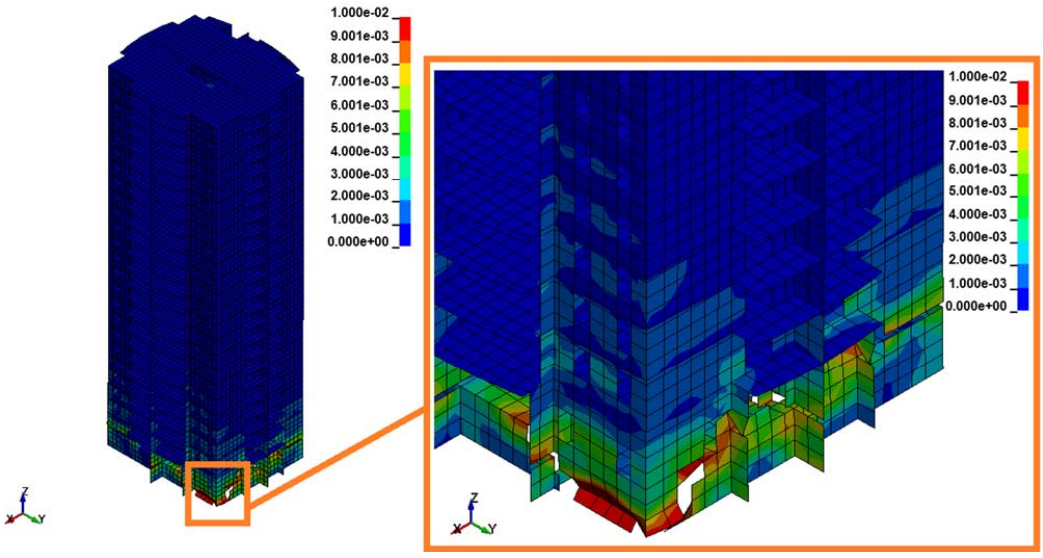

Fig. 13. Isofields of the intensity of plastic deformations in a building with seismic isolation at t = 10.89 s

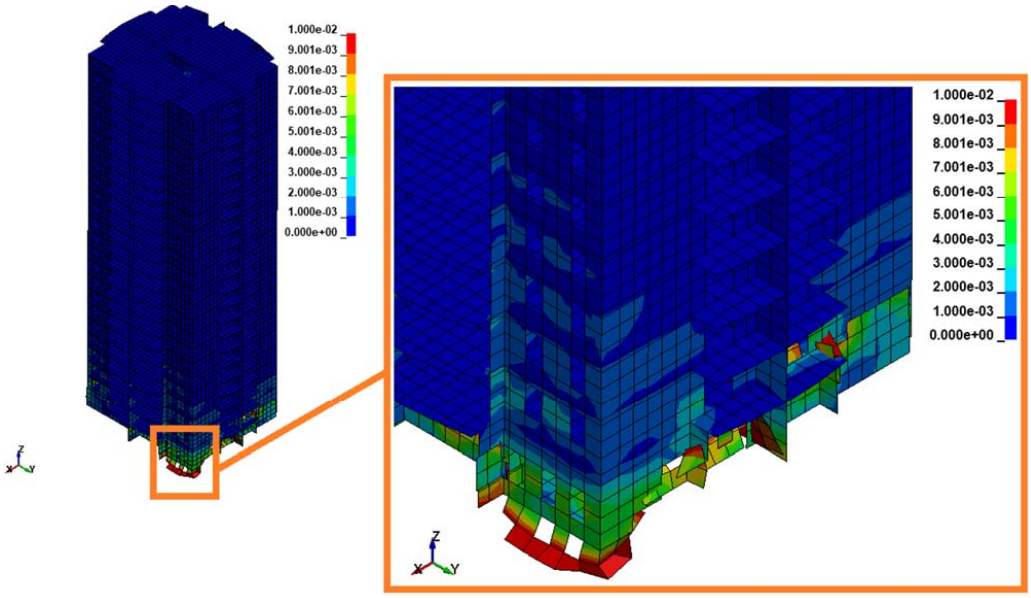

Fig. 14. Isofields of the intensity of plastic deformations in a building with seismic isolation at t = 11.55 s

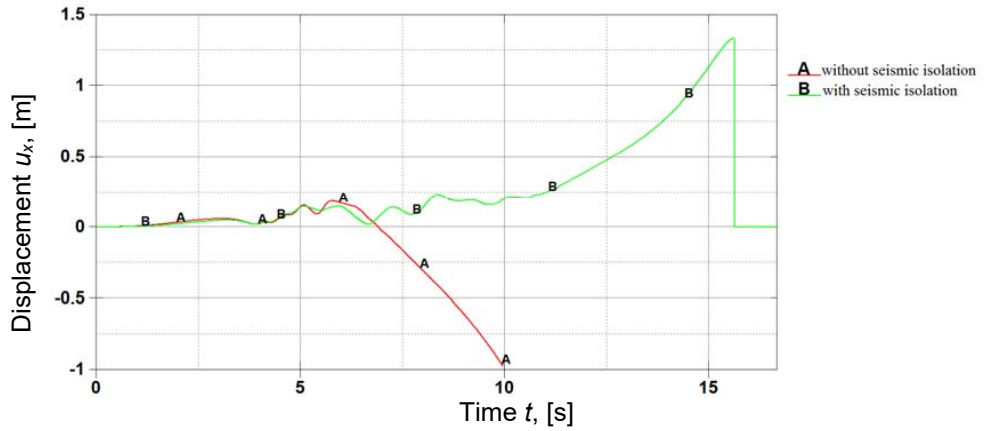

Fig. 15. Absolute displacement of the top point of the building along the X axis, [m]

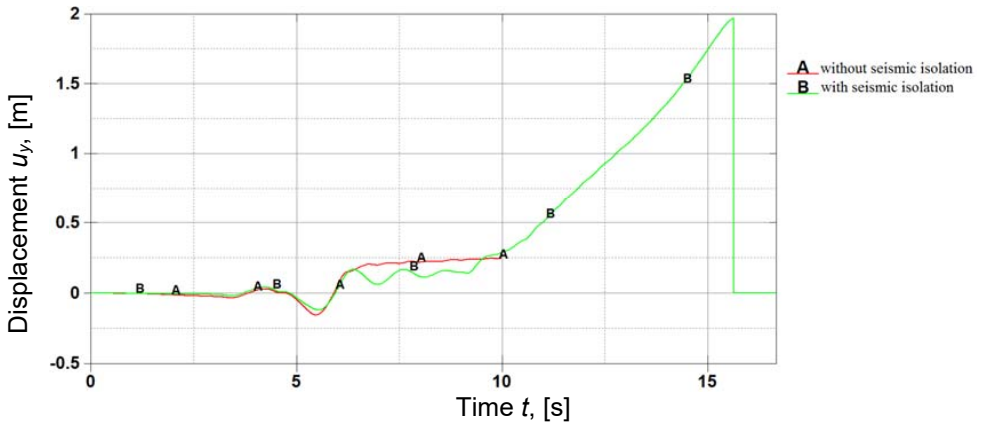

Fig. 16. Absolute displacement of the top point of the building along the Y axis, [m]

References

Dzhinchvelashvili, G. A. and Bulushev, S. V. (2014). Oscillations of high-rise buildings under seismic influence considering physical and geometric nonlinearity. *Construction: Science and Education*, No. 2, 1.

Eisenberg, Ya. M. (2004). Basic seismic isolation. Columns of lower floors as an element of seismic isolation of a building. *Earthquake Engineering. Constructions Safety*, No. 1, pp. 28–32.

Gorshkov, E. V. and Kuznetsov, S. V. (2020). Protection of underground parts of buildings from flat seismic waves. *Construction Production*, No. 1, pp. 77–81.

Herrera, I. and Bielak, J. (1977). Soil-structure interaction as a diffraction problem. In: *Proceedings of the 6th World Conference on Earthquake Engineering*, January 10–14, 1977, New Delhi, India. Vol. 2, pp. 1467–1472.

Kuznetsov, V. D. and Chen, X. (2011). Sliding belt with fluoroplast in an earthquake-resistant building. *Magazine of Civil Engineering*, No. 3, pp. 53–58.

LSTC (2018). *LS-DYNA Keyword User's Manual.* Vol. I, II. Livermore: Livermore Software Technology Corporation (LSTC), 3186 p.

Mirzaev, I. and Turdiev, M. S. (2021). Vibrations of buildings with sliding foundations under real seismic effects. *Construction of Unique Buildings and Structures*, Vol. 94, 9407. DOI: 10.4123/CUBS.94.7.

Mkrtychev, O. V. and Arutyunyan, L. M. (2016). Research of work of seismic isolation friction pendulum bearing at periodic influence. *Earthquake Engineering. Constructions Safety*, No. 4, pp. 38-43.

Mkrtychev, O. V. and Bunov, A. A. (2014). The analysis of influence of soil conditions on efficiency of seismic isolation in the form of lead-rubber bearings. *Industrial And Civil Engineering*, No. 6, pp. 71–74.

Mkrtychev, O. V. and Busalova, M. S. (2014). Calculation of a multistoried building on the intensive earthquake taking into account the possibility of foundation soil fluidifying. *Vestnik MGSU*, No. 5, pp. 63–69.

Mkrtychev, O. V. and Dudareva, M. S. (2018). Accounting the combined action of the reinforced concrete building with foundation soil in case of strong ground shaking. *Construction: Science and Education*, Vol. 8, No. 2 (28), pp. 28–42. DOI: 10.22227/2305-5502.2018.2.3.

Mkrtychev, O. V., Dzhinchvelashvili, G. A., and Busalova, M. S. (2013). Simulation of structure interaction with the base in case of earthquake. *Vestnik MGSU*, No. 12, pp. 34–40.

Mkrtychev, O. V., Dzhinchvelashvili, G. A., and Busalova, M. S. (2014). Calculation accelerogram parameters for a "construction-basis" model, nonlinear properties of the soil taken into account. *Procedia Engineering*, Vol. 91, pp. 54–57. DOI: 10.1016/j.proeng.2014.12.011.

Pan, P., Ye L.-P., Shi, W., and Cao, H.-Y. (2012). Engineering practice of seismic isolation and energy dissipation structures in China. *Science China Technological Sciences*, Vol. 55, Issue 11, pp. 3036–3046. DOI: 10.1007/s11431-012-4922-6.

Polyakov, V. S., Kilimnik, L. S., and Cherkashin, A. V. (1989). *Modern methods of seismic protection of buildings.* Moscow: Stroyizdat, 320 p.

Uzdin, A. M., Mozzhuhin, A. S., and Sorokina, G. V. (2022). Some questions of nonlinear seismic isolation behavior. *Earthquake Engineering. Constructions Safety*, No. 3, pp. 8–19.

РАБОТА ЖЕЛЕЗОБЕТОННОГО ЗДАНИЯ ПОВЫШЕННОЙ ЭТАЖНОСТИ СО СКОЛЬЗЯЩИМ ПОЯСОМ С УЧЕТОМ НЕЛИНЕЙНОГО ХАРАКТЕРА ДЕФОРМИРОВАНИЯ

Мкртычев Олег Вартанович, Булушева Салима Рафиловна*

НИУ МГСУ, Москва, Россия

*E-mail: salima.mingazova@yandex.ru

Аннотация
Введение: Актуальность применения сейсмоизоляции обусловлена необходимостью повышения безопасности зданий и сооружений в условиях высокой сейсмической активности. Землетрясения представляют серьезную угрозу для жизни людей, а также могут привести к значительным экономическим и материальным потерям. С развитием урбанизации и увеличением плотности застройки в сейсмоопасных регионах возрастает спрос на методы, которые эффективно снижают разрушительное воздействие сейсмических волн на здание. **Целью исследования** является анализ работы железобетонного здания повышенной этажности со скользящим поясом с учетом нелинейного характера деформирования. **Методы**: расчет выполнен в программном комплексе LS-DYNA прямым динамическим методом с явными схемами прямого интегрирования уравнений движения с использованием нелинейной модели бетона и арматуры; взаимодействие основания с сооружением задается методом субструктур, нелинейная работа грунтового основания описывается моделью Мора-Кулона. **Анализ результатов** показывает снижение эффективности работы сейсмоизоляции в виде скользящего пояса в уровне фундамента при повышенной этажности здания. С учетом всех характеристик здания можно подобрать наиболее подходящие параметры сейсмоизолирующего скользящего пояса, позволяющие эффективно защитить его от сейсмических нагрузок.

Ключевые слова: сейсмоизоляция, скользящий пояс, повышенная этажность, нелинейная работа, грунтовое основание.

DOI: 10.23968/2500-0055-2025-10-3-76-85

ASSESSMENT OF THE INFLUENCE OF BUILDING FACADE FACETING ON THE ACCURACY OF WIND LOAD SIMULATION

Olga Poddaeva[1]*, Oleg Kudinov[2], Kamil Mustafin[2]

[1]Moscow State University of Civil Engineering (MGSU), Moscow, Russia
[2]Research Institute of Concrete and Reinforced Concrete named after A. A. Gvozdev, JSC Research Center of Construction, Moscow, Russia

*Corresponding author's email: poddaevaoi@gmail.com

Abstract

Introduction: The influence of the level of building facade detail (protruding and recessed balconies, fins, and other facade elements) — referred to as facade faceting — on the results of wind load simulations has been examined in various studies. It has been established that a higher level of facade faceting in models improves the consistency of computational fluid dynamics (CFD) results with results of wind tunnel experiments. However, in order to simplify calculations, under certain conditions, some details may be neglected. Nevertheless, clear recommendations regarding the degree to which such simplifications affect the final accuracy of simulation are rarely found. **Purpose of the study**: In this study, the influence of facade faceting detail on the distribution of wind flows around the investigated object was assessed using computational and experimental modeling. **Methods**: Physical testing of scale models of unique buildings and structures in a wind tunnel, as well as numerical simulation of wind effects, were carried out. **Results**: The study demonstrated a significant impact of facade faceting detail on the distribution of wind loads around the investigated building model. It is recommended to design facade structures with consideration of the turbulence effects of wind flow associated with their actual geometry. At the same time, the design of load-bearing structures should account for the maximum possible wind loads without incorporating facade faceting detailing.

Keywords: high-rise buildings, wind simulation, CFD, wind tunnel, facade detailing, faceting.

Introduction

Predicting wind loads on high-rise buildings is a critical stage in their design. Architectural facades, including balconies, mullions, shading boards, and ribs, are widely used in high-rise building design for both aesthetic and functional purposes. In this paper, facade faceting refers to various facade elements such as balconies, ribs, mullions, fins, etc. The influence of facade faceting on the aerodynamics of airflow is substantial, particularly at high wind speeds. Facade faceting significantly affects the distribution of velocities and stresses in the boundary layer. However, the requirements regarding the level of facade faceting detail in physical and numerical modeling of wind effects remain insufficiently studied.

In the study by Lalin et al. (2021), the necessity of accounting for facade details in wind load simulations was examined using numerical modeling. The paper presented the influence of recessed balconies on a building facade on pressure distribution using computational fluid dynamics (CFD). The results show that in all cases the pressure on a building facade without recessed balconies is higher, therefore, a building can be modeled without recessed balconies, for example, in structural strength calculations. However, there are certain areas where pressure values differ significantly.

Dagnew and Bitsuamlak (2013) summarized the main aspects of numerical wind load modeling for buildings and structures and concluded that more research is needed on transient inlet boundaries and near-wall modeling-related issues.

Li et al. (2023) presented a detailed comparison of CFD simulations with multiple Level of Detail (multi-LoD) geometric models in predicting wind pressure on a complex high-rise wooden tower. It was shown that the higher LoD model makes CFD results more consistent with those following the wind tunnel tests, especially on the leeward of the tower. Components affecting the shape of the structure (e.g., railings, ridges, and columns) have a significant impact on the wind flow. Fu et al. (2024) demonstrated that the level of detail in tree models significantly affects the accuracy of simulating wind flows in urban areas. Zheng et al. (2020) showed that the geometrical details of a facade can substantially influence the near-facade airflow patterns and pressures. This is especially relevant for building balconies as their presence can lead to multiple separation and recirculation areas near facades. Tieleman et al. (1981) compared wind-tunnel and full-scale wind pressure measurements. Based on the full-scale/model comparisons, it was shown that the non-stationary character of the natural wind has a significant effect on the mean, RMS and peak

For citations: Poddaeva, O., Kudinov, O., Mustafin, K. (2025). Assessment of the influence of building facade faceting on the accuracy of wind load simulation. Architecture and Engineering, No 3 (10), pp. 76–85. DOI: 10.23968/2500-0055-2025-10-3-76-85.

pressure coefficients. Under non-stationary wind conditions, the full-scale extreme peak coefficients may be as much as five times the wind-tunnel values. The authors concluded that the complex terrain is responsible for increased turbulence intensities of the horizontal velocity components as a result of increased low-frequency spectral energy. Xu et al. (2020) demonstrated that detailed BIM-based geometric models of buildings allow for significantly different predictions of wind load compared to simplified CAD models. Chen et al. (2022) showed that facade appurtenances significantly influence the fluctuating wind pressure on tall buildings but have a smaller effect on the mean wind pressure. Quan et al. (2016) investigated the effects of grid curtains on the local and overall wind loads of a high-rise building. The results showed that grid curtains increase the mean and fluctuating windward aerodynamic forces and reduce the fluctuating aerodynamic torsions. Agakhanov et al. (2017) examined the influence of building geometry on wind load modeling and found that buildings with complex spatial shapes require finite element analysis for accurate prediction of comfort parameters and wind pressures. Moravej (2018) emphasized that large-scale testing of low-rise buildings or components of tall buildings is essential as it provides more representative information about the realistic wind effects than the typical small scale studies, but as the model size increases, relatively less large-scale turbulence in the upcoming flow can be generated. This results in a turbulence power spectrum lacking low-frequency turbulence content. This deficiency is known to have significant effects on the estimated peak wind loads. Quan et al. (2017) investigated the influence of vertical ribs protruding from facades on the wind loads of super high-rise buildings and concluded that vertical ribs significantly decrease the most unfavorable suction coefficients in the corner recession and edge regions of facades and increase the mean and fluctuating along-wind overall aerodynamic forces. Liu et al. (2023) reached similar conclusions, showing that facade ribs can significantly affect the wind field and reduce the wind force on high-rise buildings.

The work of Rao (2018) is of particular value since it is essentially the only study to specify the exact degree of facade faceting that can be neglected without compromising accuracy. The author compared the flow around a smooth cylindrical profile with that around profiles having increasingly large facet sizes. The air flow patterns and dynamic pressure profiles at the surface were used as a means of comparison of the different geometric types. The experiments explored the effects of faceting for a circular geometry, with a radius of 20 m. The results showed that at 128 divisions (i.e., a facet size of 0.98 m), the effects of faceting are not consequential. This size can be rounded up to 1.0 m for similar results. At 256 divisions (i.e., a facet size of 0.49 m), the surface behaves almost exactly like its circular counterpart. In conclusion, it was shown that a completely smooth geometry can be faceted without noticeable impacts on air flows near the surface. Converting these lengths into a percentage value of the circumference, it showed that the facet size needs to be at least equal to or lesser than approximately 0.79 % of the length of the circumference. It must be noted that the length of the facet needs to be considered in conjunction with the angle between two adjacent facets, especially when the geometry is completely circular. Zdanchuk et al. (2022) modeled wind effects on a building with and without ledge to compare peak wind loads. They discussed the possibility of simplifying the geometry of a building in numerical modeling, namely, ignoring the protrusions on the facades of buildings when calculating the wind pressure. The investigation showed that when studying peak wind loads, facades with small protrusions could be considered as smooth facades.

Thus, existing studies demonstrate that building facade faceting, especially protruding and recessed balconies, has a significant impact on the distribution of wind loads. However, for the purpose of simplifying calculations, certain details may be neglected under specific conditions. Nevertheless, clear recommendations regarding the degree to which such simplifications affect the overall accuracy of modeling are lacking.

In this study, computational and experimental modeling was employed to assess the influence of facade faceting on the distribution of wind flows around the investigated object, as well as on the deformability of the structural system, taking into account its actual stiffness.

Materials and Methods

As the object of study, a high-rise multi-functional complex (Fig. 1) located in a dense urban environment was selected. The complex consists of two high-rise residential buildings located on a shared substructure.

These high-rise buildings have 50 above-ground and 3 underground floors each. The total building height is 181 m. The structural system is a frame-wall system made of cast-in-place reinforced concrete.

Two facade design options were considered (Fig. 2):

1) with open balconies and vertical partitions between them;

2) with smooth facades.

Experimental studies were conducted using a unique research setup — the Large Gradient Wind Tunnel, courtesy of the National Research Moscow State University of Civil Engineering. Considering the dimensions of the working section of the wind tunnel, the maximum possible model scale of 1:270 was

Fig. 1. Object under study

selected to minimize flow blockage effects (Fig. 3). Each model had pressure measurement points on its surface. Pressure from each opening was transmitted through copper — and then silicone — tubes to differential pressure sensors.

In addition, numerical simulations were performed using the ANSYS CFD software to complement the experimental research. The experimental data on mean pressure distribution at drainage points were used for verification and validation of the applied numerical modeling approach (Fig. 4).

Results and Discussion

A comparison of the obtained results demonstrates a significant influence of faceting on the facade of the studied object on the distribution of wind loads across the facades. The difference is most clearly visible in the isofields of the distribution of aerodynamic external pressure coefficients on the facades of the studied object (Fig. 5).

Analysis of the isofields shows that, in addition to quantitative changes in the values of aerodynamic coefficients, the overall pattern of wind load distribution across the facades also changes. This results from the altered behavior of the flow around the buildings. The presence of facade elements introduces additional turbulence into the wind flow in the immediate vicinity of the facades and even shifts the position of the “separation point” As a consequence, substantial differences in wind load values are observed in corresponding zones, including changes in the sign from (+) to (−).

As an example, Table 1 presents the percentage ratio of wind load values for specific zones on the building facades with a wind direction of 45°.

From the perspective of the practical applicability of the obtained results, the greatest interest lies in comparing the integral (total) wind load on the supporting structures of the object under study. This comparison is presented in Table 2.

As can be seen from Table 2, without accounting for faceting due to the presence of balconies, the total wind load on building C1 at a wind direction of 45° increases by 28 %, or 1.39 times, compared to the design scheme in which such faceting was considered. For building C2, the total wind load

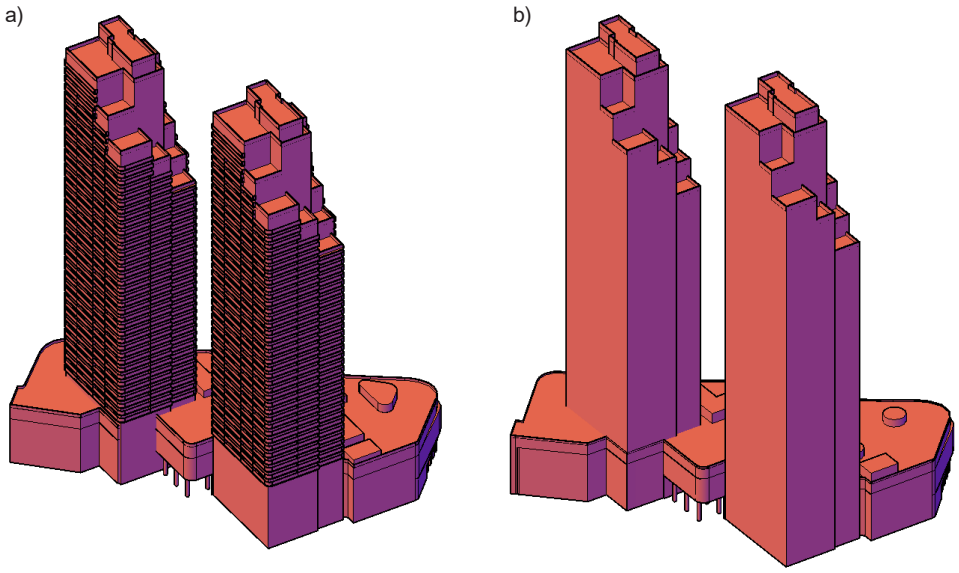

Fig. 2. Facade configurations: a — facades with balconies; b — smooth facades

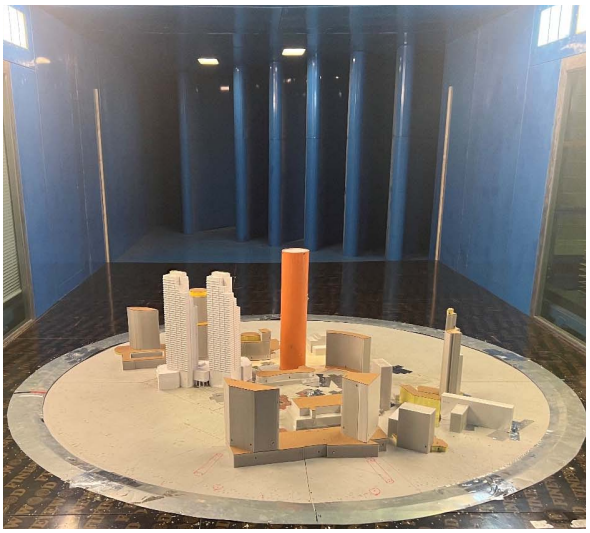

Fig. 3. Model of the studied object in the working section of the wind tunnel

increase at a wind direction of 15° reached 40 %. The ratio of change in integral wind loads for cases with and without balconies is 1.39 for C1 and 1.67 for C2.

Based on the results of the conducted studies, it can be concluded that detailing of facade structures in wind load modeling has a significant impact on both the qualitative distribution of wind loads across the facades and their quantitative values.

Moreover, increasing the level of detail in modeling of facade elements (increasing faceting detail) reduces the integral wind load acting on the facades of the entire building across different wind directions by approximately 30–40 %.

For individual floors (10^{th}, 20^{th}, 30^{th}) within different height zones of the buildings, differences in wind loads between models with and without facade faceting can vary from 1.3 to 2.0 times or more. Figs. 6 and 7 show the ratio of change in the total wind load per floor, comparing cases with and without faceting, for buildings C1 and C2, respectively.

Thus, accounting for facade faceting in experimental studies of wind effects reduces the calculated horizontal loads on the building and may negatively affect the reliability of the structural system as a whole.

When performing wind load modeling, it is important to pay attention to the installation sequence of facade structures. If elements that generate faceting (e.g., fins and other decorative components) are installed after the primary facade systems (such as curtain wall glazing or suspended facades), it may be advisable to conduct studies using models with smooth facades and determine the maximum possible wind loads on the studied object (with a safety margin).

Calculations

To assess the influence of facade faceting, when determining wind loads based on the results of aerodynamic tests, on the deformability of the structural system of high-rise buildings, taking into account its actual stiffness, a calculation model for the complex with balconies on high-rise buildings as well as a separate calculation model for the complex without balconies on high-rise buildings were developed.

The structural analysis of the designed complex was performed using the finite element method in a three-dimensional setting, taking into account the mutual interaction between the structural system, foundations, and base under vertical and horizontal loads, using the STARK ES 2025 software.

The average component of the wind load on the buildings was determined based on aerodynamic coefficients obtained from the wind tunnel tests. The pulsation component of the wind load was calculated using dynamic analysis of the buildings' natural vibrations, considering the first vibration modes of the system. The formation of these loads was carried out in accordance with the main provisions of Code of Practice SP 20.13330.2016. For high-rise building C1, the critical directions of 45°, 150°, 195°, 345° were adopted as the design wind loads.

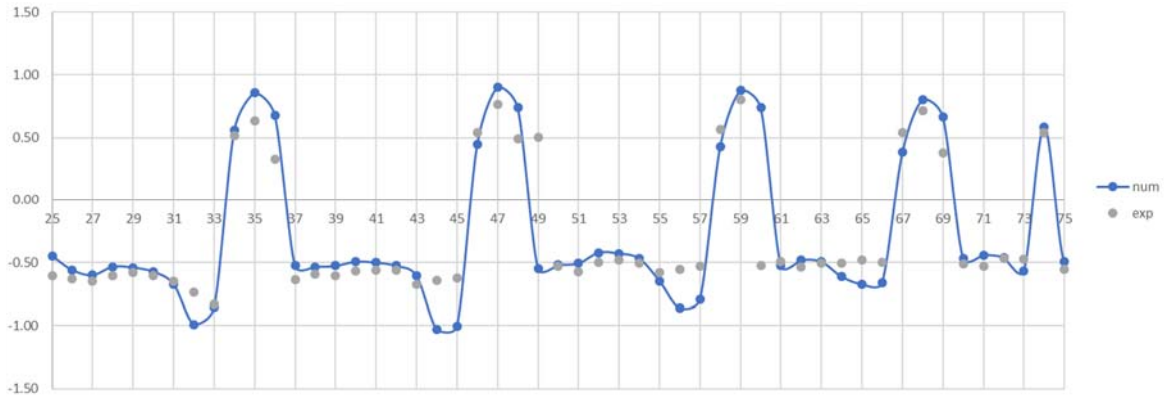

Fig. 4. Validation of numerical modeling results

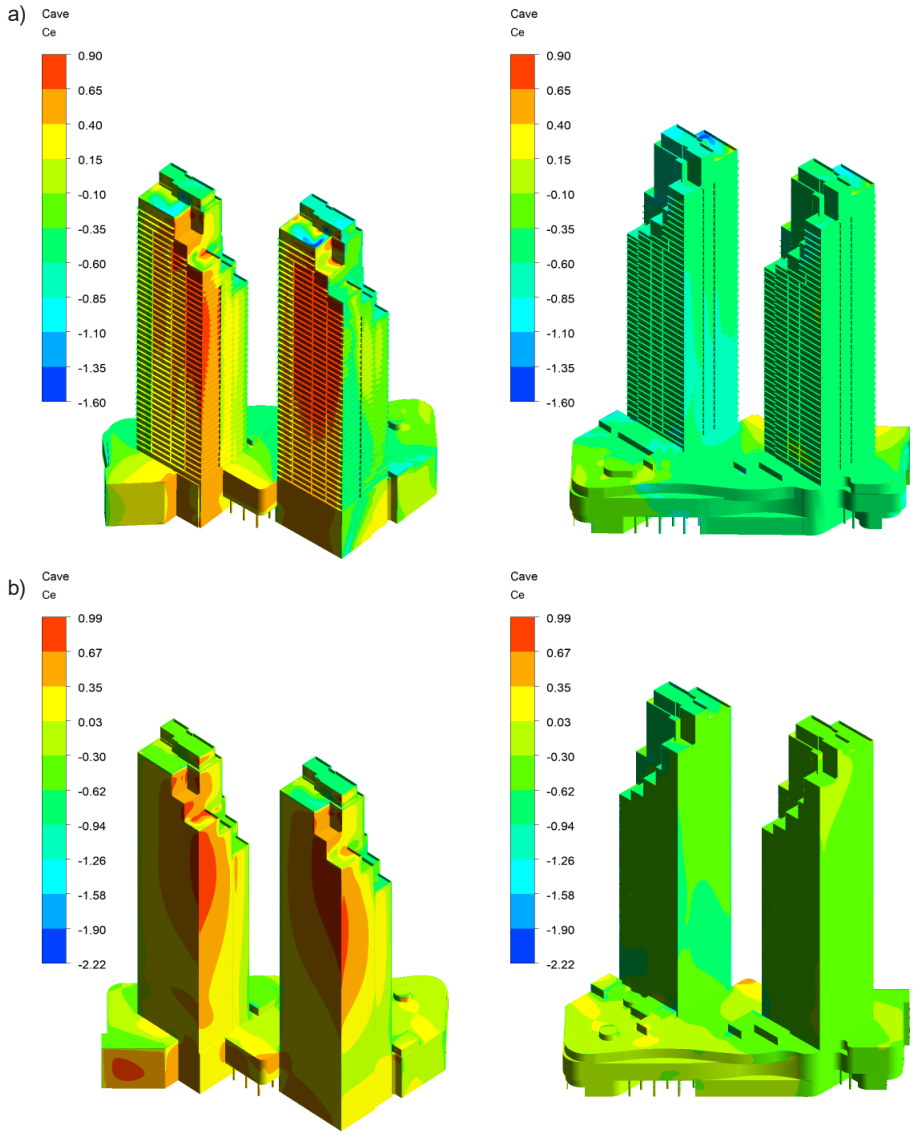

Fig. 5. Distribution of aerodynamic external pressure coefficients on the facades of the studied object: a — facades with balconies, b — smooth facades. Flow direction: 45°

Table 1. **Comparison of wind loads on specific facade zones of the studied object for different facade configurations**

Smooth facade (w_1)												
Belt/Zone	1	2	3	4	5	6	7	8	9	10	11	12
1	–157	–197	–82	–12	27	66	74	–6	–239	–173	–153	–173
2	–159	–164	–59	81	181	181	119	–33	–226	–228	–235	–176
3	–186	–210	–73	134	296	320	218	–8	–245	–237	–272	–183
Facade with balconies (w_2)												
Belt/Zone	1	2	3	4	5	6	7	8	9	10	11	12
1	–99	–108	–70	–78	–96	59	113	31	–152	–146	–124	–101
2	–115	–118	–76	–85	–132	90	152	33	–172	–170	–160	–122
3	–117	–117	–67	–41	–96	144	169	34	–170	–167	–169	–130
Ratio (w_2/w_1)												
Belt/Zone	1	2	3	4	5	6	7	8	9	10	11	12
1	0.63	0.55	0.85	6.53	3.56	0.90	1.53	5.16	0.64	0.84	0.81	0.59
2	0.72	0.72	1.29	1.05	0.73	0.50	1.28	0.99	0.76	0.74	0.68	0.69
3	0.63	0.56	0.93	0.31	0.32	0.45	0.78	4.22	0.69	0.70	0.62	0.71

Table 2. **Comparison of integral wind loads for critical wind flow directions**

Facade configuration	C1			C2		
	45°			15°		
	Fx	Fy	Rxy	Fx	Fy	Rxy
Facade with balconies	1,649	613	1,759	1,640	417	1,692
Facade without balconies	2,152	1,173	2,451	2,727	728	2,822
			28.23 %			40.04 %

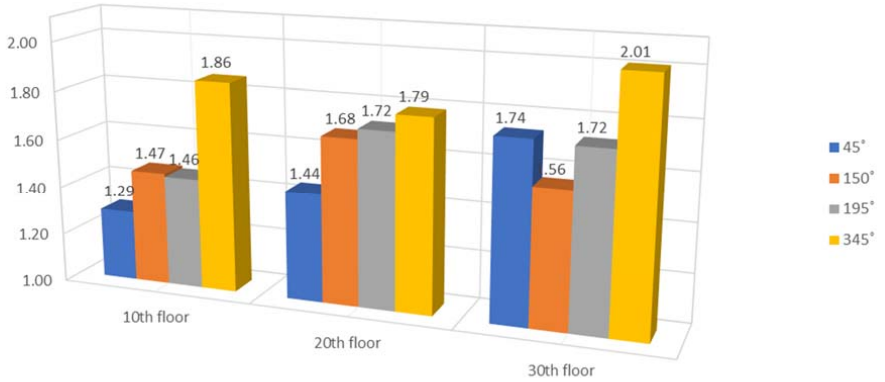

Fig. 6. Change in the total wind load with and without faceting due to the presence of balconies, depending on the height of the floor location and wind direction for building C1

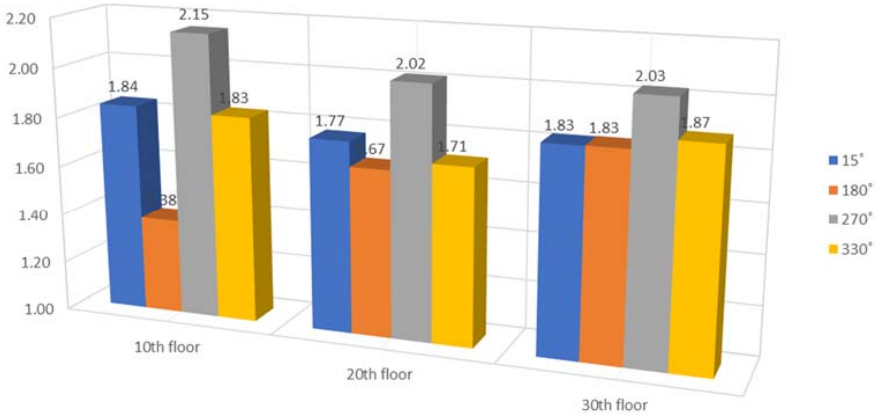

Fig. 7. Change in the total wind load with and without faceting due to the presence of balconies, depending on the height of the floor location and wind direction for building C2

For high-rise building C2, the critical directions were 15°, 180°, 270°, and 330°.

At the first stage, the structural system of the buildings was analyzed under standard wind loads only. The results showed that horizontal displacements for building C1 without balconies along the design directions exceed those for the building with balconies by a factor of 1.32–1.58.

The largest displacements under wind loads only occur in both cases at a wind direction of 45°. An increase in horizontal displacements at 45° wind direction was 1.32 times, corresponding to an increase in the integral wind load by 1.39 times. Table 3 presents the results of the calculation and comparison of the horizontal displacements of the C1 structure due to wind load.

For building C2, horizontal displacements increased by a factor of 1.47 to 1.65. The largest displacements under wind loads only occur in both cases at a wind direction of 15°. An increase in horizontal displacements at 15° wind direction was 1.57 times, corresponding to an increase in the integral wind load by 1.67 times. Table 4 presents the results of the calculation and comparison of the horizontal displacements of the C2 structure due to wind load.

The actual deformability of the building complex structural system was assessed in accordance with Code of Practice SP 430.1325800.2018 under standard combinations of vertical and horizontal loads. For instance, for building C1 without balconies, the largest horizontal displacements were observed

Table 3. **Comparison of the horizontal displacements of the C1 structure under wind loads (excluding vertical loads) for wind directions 45°, 150°, 195°, and 345°, with and without consideration of facade faceting due to the presence of balconies**

Wind direction	Facade without balconies			Facade with balconies			Ratio U_{xy1}/U_{xy2}
	Along X axis U_{x1}, mm	Along Y axis U_{y1}, mm	Total horizontal U_{xy1}, mm	Along X axis U_{x2}, mm	Along Y axis U_{y2}, mm	Total horizontal U_{xy2}, mm	
45°	95.5	35.9	102.0	75.8	14.8	77.2	1.32
150°	–77.5	13.8	78.7	–51	30.1	59.6	1.32
195°	–89.7	–26	93.4	–67	–16.1	69.1	1.35
345°	90.4	22	93.0	55.9	18.9	59.0	1.58

at the design wind direction of 195° and amounted to 162 mm in the X direction and 36 mm in the Y direction, with total horizontal displacements of 166 mm. Fig. 8 shows the horizontal displacements of the C1 structure under the standard load combination (considering both vertical and horizontal loads) for a wind direction of 195°, without accounting for facade faceting due to the presence of balconies.

For the structural system of building C1 with balconies, the largest horizontal displacements considering horizontal and vertical loads also occurred at a design wind direction of 195°. However, the maximum values were 138 mm in the X direction and 23 mm in the Y direction, totaling 140 mm.

Fig. 9 shows the horizontal displacements of the C1 structure under the standard load combination (considering both vertical and horizontal loads) for a wind direction of 195°, with accounting for facade faceting due to the presence of balconies.

Thus, accounting for balconies in wind load modeling reduces the horizontal displacements under the standard full load combination for building C1 in the critical direction by 16 %. For horizontal displacements under wind loads only, the reduction is 26 %.

The obtained horizontal displacements for buildings with and without balconies do not exceed the allowable limit specified in Code of Practice SP 20.13330.2016 (1/500 of the building height, or 362 mm), indicating sufficient stiffness of the structural system. However, the relatively large horizontal displacements indicate significant horizontal loads on the structural system, which necessitates their consideration when providing additional strength reserves for load-bearing vertical structures, and generally increases the material consumption during construction.

Conclusions

Based on the results of the computational and experimental studies, it is recommended, in order to ensure the required reliability of the building structural system, to carry out design under the maximum possible wind loads with no account for facade faceting detail. The design of facade structures should consider the turbulence effects of the wind flow when accounting for their actual geometry.

Table 4. **Comparison of the horizontal displacements of the C2 structure under wind loads (excluding vertical loads) for wind directions 15°, 180°, 270°, 330°, with and without consideration of facade faceting due to the presence of balconies**

Wind direction	**Facade without balconies**			**Facade with balconies**			**Ratio U_{xy1}/U_{xy2}**
	Along X axis U_{x1}, mm	**Along Y axis U_{y1}, mm**	**Total horizontal U_{xy1}, mm**	**Along X axis U_{x2}, mm**	**Along Y axis U_{y2}, mm**	**Total horizontal U_{xy2}, mm**	
15°	119	24	121.7	77.2	8.9	77.7	1.57
180°	–95.2	7.7	95.5	–64.2	9.6	64.9	1.47
270°	33	–60	68.6	12.5	–43.4	45.2	1.52
330°	108	–41	115.3	58.9	–37.5	69.8	1.65

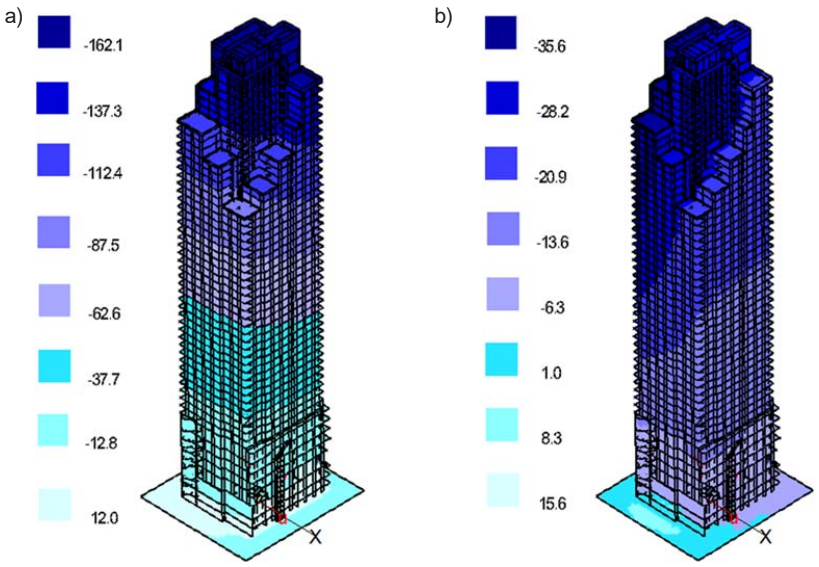

Fig. 8. Horizontal displacements of the C1 structure under the standard load combination (considering both vertical and horizontal loads) for a wind direction of 195°, without accounting for facade faceting due to the presence of balconies: a — displacements along x, b — displacements along y

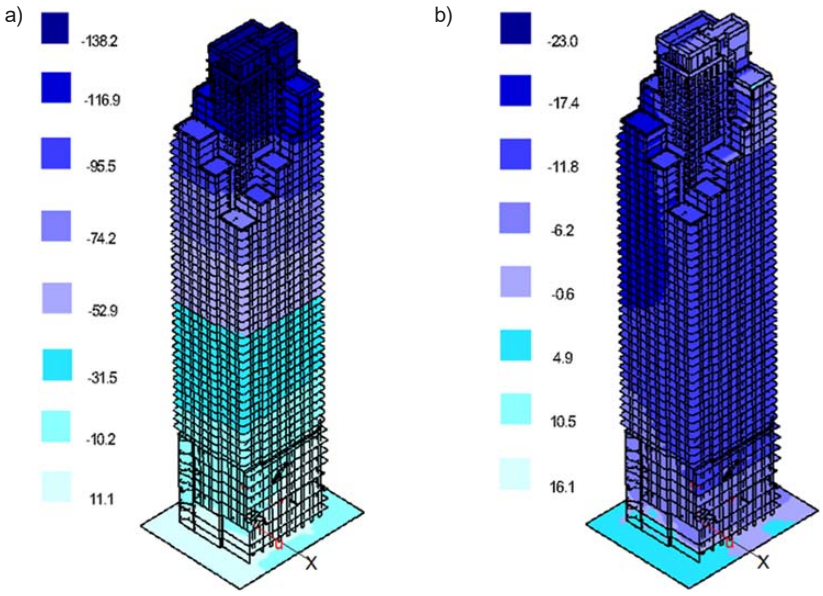

Fig. 9. Horizontal displacements of the C1 structure under the standard load combination (considering both vertical and horizontal loads) for a wind direction of 195°, with accounting for facade faceting due to the presence of balconies: a — displacements along x, b — displacements along y

References

Agakhanov, E. K., Kravchenko, G. M., Osadchiy, A. S., and Trufanova, E. V. (2017). Calculation of buildings with complex geometric shapes for withstanding wind impact. *Herald of Dagestan State Technical University. Technical Sciences*, Vol. 44, No. 2, pp. 8–17. DOI: 10.21822/2073-6185-2017-44-2-8-17.

Chen, F. B., Liu, H. M., Chen, W., Shu, Z. R., Li, Y., Li, Q. S., and Han, Y. (2022). Characterizing wind pressure on CAARC standard tall building with various façade appurtenances: an experimental study. *Journal of Building Engineering*, Vol. 59, 105015. DOI: 10.1016/j.jobe.2022.105015.

Dagnew, A. K. and Bitsuamlak, G. T. (2013). Computational evaluation of wind loads on buildings: a review. *Wind and Structures*, Vol. 16, No. 6, pp. 629–660. DOI: 10.12989/was.2013.16.6.629.

Fu, R., Pađen, I., and García-Sánchez, C. (2024). Should we care about the level of detail in trees when running urban microscale simulations? *Sustainable Cities and Society*, Vol. 101, 105143. DOI: 10.1016/j.scs.2023.105143.

Lalin, V., Orlovich, R., Zdanchuk, E., and Babaev, F. (2021). CFD simulation of pressure distribution on the facade with loggias. In: Vatin, N., Borodinecs, A., Teltayev, B. (eds.). *Proceedings of EECE 2020. EECE 2020. Lecture Notes in Civil Engineering*, Vol. 150. Cham: Springer, pp. 316–324. DOI: 10.1007/978-3-030-72404-7_31.

Li, Y., Deng, Y., Li. A., and Xu, T. (2023). Comparative studies of computational fluid dynamic geometric models at multiple levels of details in evaluating wind action on Asian ancient wooden tower. International *Journal of Architectural Heritage*, Vol. 17, Issue 6, pp. 970–987. DOI: 10.1080/15583058.2021.2003911.

Liu, J., Hui, Y., Yang, Q., and Wang, G. (2023). Numerical study of impact of façade ribs on the wind field and wind force of high-rise building under atmospheric boundary layer flow. *Journal of Wind Engineering and Industrial Aerodynamics*, Vol. 236, 105399. DOI: 10.1016/j.jweia.2023.105399.

Moravej, M. (2018). *Investigating scale effects on analytical methods of predicting peak wind loads on buildings*. PhD Thesis in Civil Engineering.

Quan, Y., Hou, F., and Gu, M. (2017). Effects of vertical ribs protruding from facades on the wind loads of super high-rise buildings. *Wind and Structures*, Vol. 24, No. 2, pp. 145–169. DOI: 10.12989/WAS.2017.24.2.145.

Quan, Y., Kuang, J., Gu, M., and Wang, S. (2016). Effects of grid curtains on the wind loads of a high-rise building. *The Structural Design of Tall and Special Buildings*, Vol. 25, Issue 5, pp. 245–262. DOI: 10.1002/tal.1256.

Rao, A. (2018). Impact of geometry faceting on air flows at the surface of building facades. International *Journal of Engineering Research & Technology (IJERT)*, Vol. 7, Issue 08, pp. 143–146. DOI: 10.17577/ijertv7is080050.

Tieleman, H. W., Akins, R. E., and Sparks, P. R. (1981). A comparison of wind-tunnel and full-scale wind pressure measurements on low-rise structures. *Journal of Wind Engineering and Industrial Aerodynamics*, Vol. 8, Issues 1–2, pp. 3–19. DOI: 10.1016/0167-6105(81)90003-9.

Xu, F., Yang, J., and Zhu, X. (2020). A comparative study on the difference of CFD simulations based on a simplified geometry and a more refined BIM based geometry. *AIP Advances*, Vol. 10, Issue 12, 125318. DOI: 10.1063/5.0031907.

Zdanchuk, E., Nikitina, O., Galyamichev, A., and Serdjuks, D. (2022). Influence of protrusions on building facades on the distribution of peak wind loads. In: Manakov, A. and Edigarian, A. (eds.). *International Scientific Siberian Transport Forum TransSiberia - 2021. TransSiberia 2021. Lecture Notes in Networks and Systems*, Vol. 403. Cham: Springer, pp. 1390–1398. DOI: 10.1007/978-3-030-96383-5_155.

Zheng, X., Montazeri, H., and Blocken, B. (2020). CFD simulations of wind flow and mean surface pressure for buildings with balconies: comparison of RANS and LES. *Building and Environment*, Vol. 173, 106747. DOI: 10.1016/j.buildenv.2020.106747.

ОЦЕНКА ВЛИЯНИЯ «ШЕРОХОВАТОСТИ» ФАСАДА ЗДАНИЯ НА ТОЧНОСТЬ МОДЕЛИРОВАНИЯ ВЕТРОВЫХ ВОЗДЕЙСТВИЙ

Ольга Игоревна Поддаева[1]*, Олег Кудинов[2], Камиль Мустафин[2]

[1]Национальный исследовательский московский государственный строительный университет (НИУ МГСУ), Москва, Россия
[2]Научно-исследовательский, проектно-конструкторский и технологический институт бетона и железобетона им. А. А. Гвоздева (НИИЖБ), Москва, Россия

*E-mail: poddaevaoi@gmail.com

Аннотация
Введение: Влияние степени детализации фасада зданий (балконов, лоджий, ламелей и других элементов фасада) – «шероховатость» фасада – на результаты моделирования ветровой нагрузки было изучено в различных исследованиях. Было установлено, что более высокий уровень «шероховатости» моделей повышает согласованность результатов вычислительной гидродинамики с испытаниями в аэродинамической трубе, однако для упрощения расчетов, при определенных условиях, можно пренебречь некоторыми деталями, но четких рекомендаций по степени влияния введенных упрощений на конечную точность моделирования практически не встречается. **Цель исследования:** В настоящей работе с помощью расчетно-экспериментального моделирования выполнена оценка влияния детализации «шероховатости» фасада здания на распределение ветровых потоков на исследуемый объект. **Методы**: физические испытания макетов уникальных зданий и сооружений в аэродинамической трубе, численное моделирование ветровых воздействий. **В результате** показано существенное влияние степени детализации «шероховатости» фасадов исследуемой модели здания на распределение ветровой нагрузки. Проектирование фасадных конструкций рекомендуется выполнять с учетом эффекта турбулизации ветрового потока при учете их фактической геометрии, а проектирование несущих конструкций необходимо осуществлять с учетом максимально возможных ветровых нагрузок без учета детализации «шероховатости» фасадных элементов.

Ключевые слова: высотные здания, моделирование ветра, вычислительная гидродинамика, аэродинамическая труба, детализация фасадов, шероховатость.

DOI: 10.23968/2500-0055-2025-10-3-86-95

DAMPING SEISMIC VIBRATIONS IN HIGH-RISE BUILDINGS USING CONTROLLED REACTIVE DAMPERS

Alexander Shein[1]*, Mikhail Zaitsev[1], Ashot Tamrazyan[2], Tatiana Matseevich[2]

[1]Penza State University of Architecture and Civil Engineering, Penza, Russia
[2]National Research Moscow State University of Civil Engineering, Moscow, Russia

*Corresponding author's email: shein-ai@yandex.ru

Abstract

Introduction. The paper investigates the dependence of seismic displacements of high-rise buildings on the control parameters of a reactive damper (vibration absorber). A frequency-vector analysis of a building's finite element model is performed. The building's response to non-stationary seismic loads is analyzed with respect to changes in damper parameters: the specified control displacement, the ejection velocity of the reactive jet, and the duration of a single reactive impulse. An algorithm for optimizing the controlled damper parameters is presented. The effectiveness of using a reactive damper to reduce the amplitude of oscillations in a high-rise building is evaluated. Reactive vibration dampers are installed at either one or two levels along the building's height. **Methods.** A mathematical model of the "high-rise building – reactive damper" system under non-stationary (seismic) loading was studied using a software suite based on the finite element method (FEM). The dynamic response of the structure was determined by numerically solving the system of differential equations of motion using Newmark's step-by-step method, implemented by the authors in the Matrix Laboratory environment as a software package. **Results.** The effectiveness of the reactive damper in reducing the amplitude of oscillations in mechanical systems (high-rise buildings) under non-stationary loads is demonstrated. It is assumed that under seismic loading, the damper activates when the displacement of one of the structural nodes exceeds a predetermined value, and the velocity vector of that node determines the direction of the reactive force. Equations of motion for the finite element model of a plate-rod system with an active damper operating on the reactive jet principle are presented. In the Matrix Laboratory interactive numerical computing environment, a software package was developed to solve the system of differential equations describing the motion of the plate-rod FE model of a high-rise building with a damping system. Graphs are provided showing how the effectiveness of the damper varies depending on such parameters as the velocity and duration of the reactive jet ejection (V_{gas} and T_{gas}) as well as the allowable deviation (displacement threshold for damper activation, δ_{max}) The influence of these parameters on damper performance was studied. It was found that the use of a reactive damper with optimally selected parameters reduces the amplitude range of oscillations by 50–80 %, i.e., the reactive system effectively suppresses mechanical vibrations of buildings and structures. A software package was developed to select optimal reactive damper parameters for a given high-rise building.

Keywords: high-rise building, seismic loading, oscillatory motion, reactive damper, vibration level, displacements.

Introduction

Buildings and structures of high criticality, constructed in regions with high seismic activity, require special protection methods. The development of new and the improvement of existing methods for protecting these structures from collapsing is an important and relevant task in construction research. Damping of oscillations allows for effective control over the development of oscillation amplitudes in mechanical systems, and, due to its effectiveness, this method is starting to be widely used in modern construction. Reducing vibration levels in mechanical systems is achieved through various methods, including the use of roller mechanisms (Burtseva et al., 2015), composite polymers (Lasowicz and Jankowski, 2017), friction dampers (Seong and Min, 2011), as well as innovative technological developments (Abramyan at el., 2022).

Modern vibration damping systems encompass a wide range of dampers adapted and optimized for various applications. In high-rise construction, the most widely used are dynamic vibration dampers such as tuned mass dampers (Etedali and Rakhshani, 2018; Marano et al., 2007; Owji et al., 2011) and tuned mass column dampers (Adam et al., 2017; Altay et al., 2017). Several studies (Tamrazyan and Chernik, 2021; Tamrazyan and Matseevich, 2024) provide assessments of the damageability and impact strength coefficients of high-rise building frames, affecting the oscillatory process under seismic disturbances. Other studies (Shein et al., 2022; Shein and Chumanov, 2021) proposed and analyzed innovative approaches to damping of oscillations in various structures. One such solution is a cable mechanism with a hydraulic cylinder operating in a single direction, for which a calculation algorithm was developed. A liquid damper was described in the work by Shein and Shmelev (2014), and the operating principle of a damper using the reactive impulse from burning fuel was presented in the study

For citations: Shein, A., Zaitsev, M., Tamrazyan, A., Matseevich, T. (2025). Damping seismic vibrations in high-rise buildings using controlled reactive dampers. Architecture and Engineering, No 3 (10), pp. 86–95. DOI: 10.23968/2500-0055-2025-10-3-86-95.

of Shein and Zaytsev (2023). To improve the seismic resistance of buildings, foundation seismic isolation is sometimes used. In particular, Amanollah et al. (2023) examined the effectiveness of rubber-metal supports with a lead core under various earthquake scenarios. The effectiveness of the supports was analyzed using specialized software.

Due to the reactive nature of the force resisting motion, high damping efficiency in high-rise buildings can be achieved at minimal cost. For instance, to reduce the risk of Taipei 101 skyscraper collapsing during earthquakes, a massive 660-ton tuned mass damper is used, which, utilizing the inertia of its own movement, suppresses building's oscillations.

The aim of this study was to develop a mathematical model and calculation algorithm for a high-rise building equipped with reactive dampers for seismic protection and assess the effectiveness of this damping method.

This system generates alternating impulses at specified time intervals, which counteract bending deformations and oscillations of the structure arising from non-stationary seismic loads.

Subject, Objectives, and Methods

The effectiveness of using reactive dampers to reduce the vibration levels of the FE model of a high-rise building under seismic loading was investigated. The dampers were installed at either one or two levels along the building's height. The building is square in plan (Fig. 1, a–b) with dimensions of 18 × 18 m and a height of 150 m (50 floors).

The load-bearing elements of the reinforced concrete frame of the building are columns, the core of rigidity, and cast-in-place slabs. The columns have square cross-sections measuring 50 × 50 and 70 × 70 cm in the lower and upper parts (halves) of the building, respectively, and are made of heavy concrete of grade M450. The main reinforcement of the columns consists of steel bars Ø32 A400 with a spacing of 100 mm. The cross-section of the core of rigidity is box-shaped, measuring 6 × 6 m, with a wall thickness of t = 250 mm. The core material is heavy concrete of grade M450. The main reinforcement elements of the walls are steel bars Ø12 A400 arranged in meshes with a cell size of 200 × 200 mm. The reinforcement of the slabs and roof, made of heavy concrete grade M400, consists of meshes of steel bars Ø10 A400 with a spacing of 200 mm. The thickness of the elements is t = 200 mm. The reinforcement of the building's load-bearing elements is shown in Fig. 1c.

The seismic load was applied in accordance with the accelerogram of the earthquake that occurred in Loma Prieta, USA, on October 18, 1989, which is characterized by a pronounced peak in translational accelerations (Fig. 2).

The peak values of the seismic impact characteristics are presented in Table.

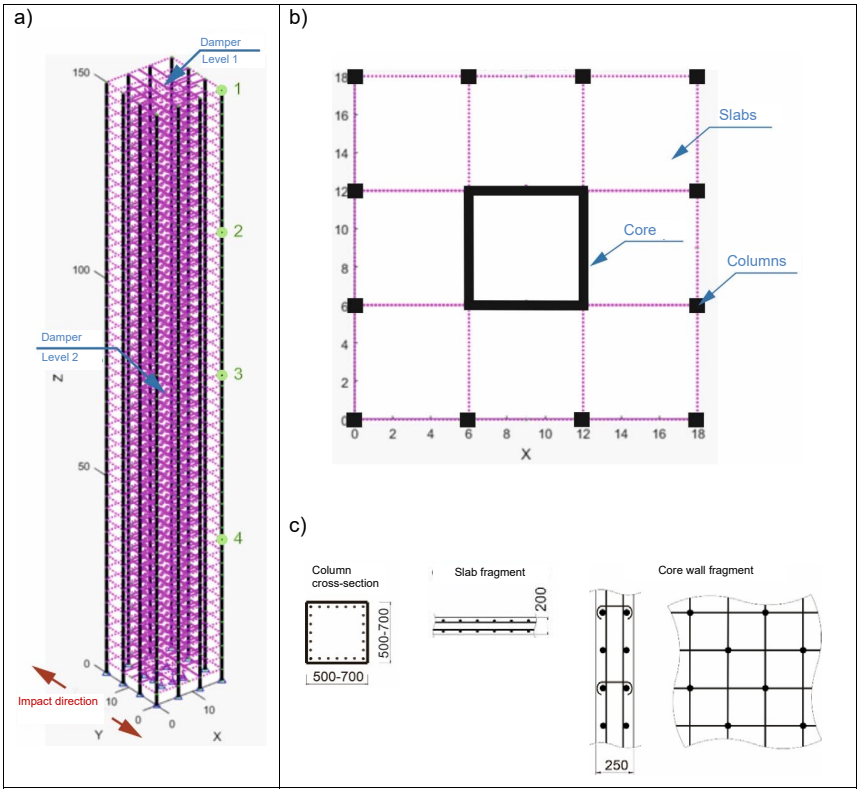

Fig. 1. Modeling of a high-rise building in the software package: (a) design mode; (b) layout of frame elements; (c) reinforcement of load-bearing elements

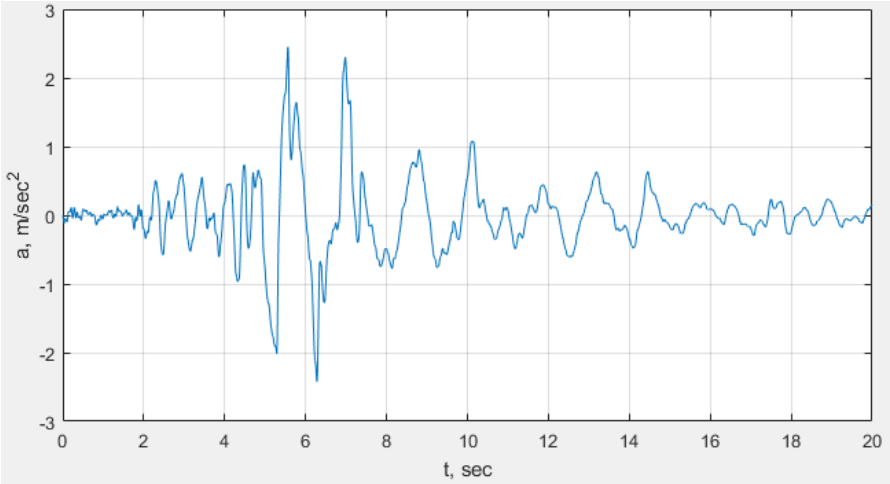

Fig. 2. Design accelerogram

Maximum values of the main seismic impact characteristics

Characteristic	Value (max)	Time t, s
Acceleration	2.451 m/s^2	5.56
Speed	0.427 m/s	5.35
Displacement	0.116 m	12.48

The studies were carried out using a software package developed by the authors in the Matrix Laboratory interactive numerical computing environment, which solves the system of differential equations describing the motion of the plate-rod FE model of the high-rise building with a damping system. The rectangular finite element of a thin plate used in the calculation of the plate-rod model is characterized by one linear (perpendicular to the FE plane) and two rotational displacements (rotations around the local axes of the FE out of its plane) at the node. The rod finite element has six degrees of freedom at the node. In this study, the direction of the seismic load was chosen along one of the axes of the global coordinate system (*OY* axis). The disturbance was created by converting the kinematic effect into a force effect. Fig. 1a shows the FE model of the investigated high-rise building. The results of determining the displacements of the control nodes of the plate-rod model under the considered seismic impact are presented in Fig. 3.

Reducing the amplitude of oscillations at a certain moment will be achieved by alternating reactive impulses of the gas jet ejected at high velocity from the damper nozzles.

The damper represents a block consisting of two oppositely directed reactive units (Fig. 4).

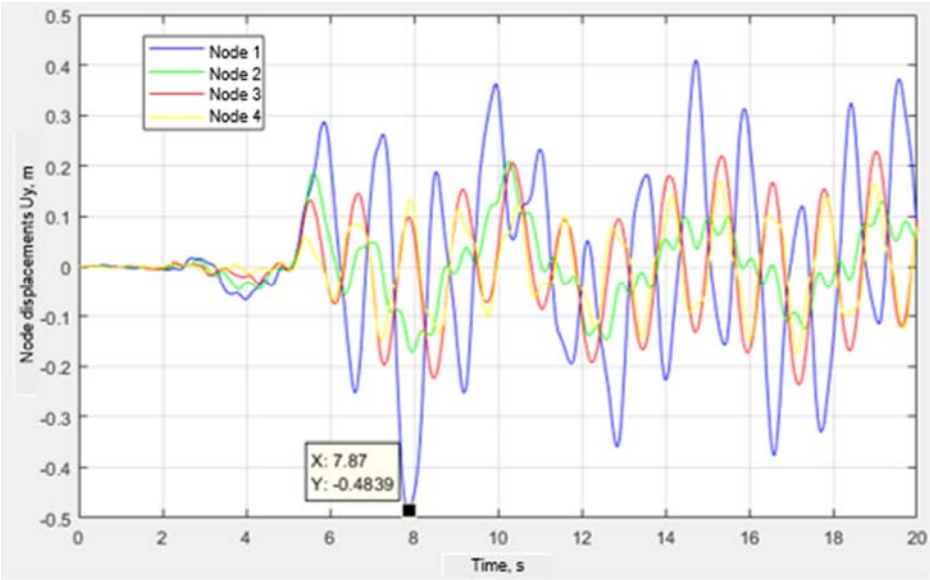

Fig. 3. Linear displacements along the *Y*-axis of nodes 1–4 of the design model of the building without damping

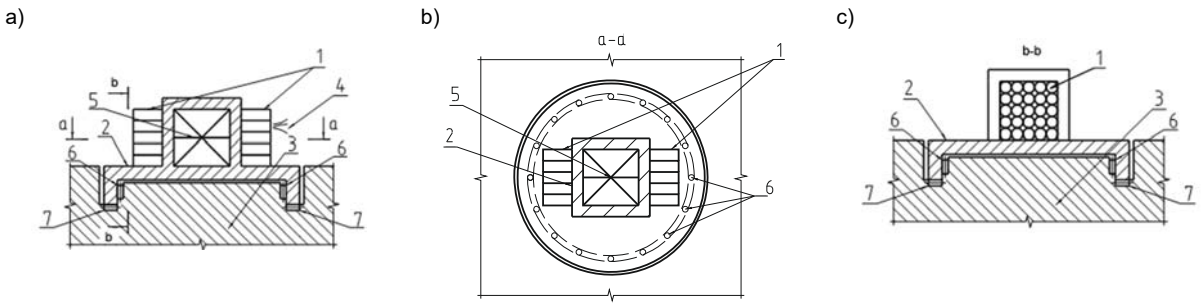

Fig. 4. Reactive vibration damper: (a) side view; (b) view a–a; (c) view b–b. 1 — sequentially operating reactive unit, 2 — support-rotating block, 3 — support surface, 4 — reactive impulses, 5 — stop to ensure the stiffness of the support block, 6 — vertical cylindrical rolling bearings, 7 — horizontal conical rolling bearings for horizontal orientation of the block

In the proposed studies, the dampers were installed at two levels along the height of the finite element model of the building (Fig. 1a). The reactive forces from the dampers were applied to the central node of the upper cross-section of the core of rigidity (level 1) and to the central node of the cross-section of the core of rigidity (level 2), the height position of which was determined based on the calculation of natural frequencies and mode shapes using the Frequencies module of the aforementioned software, which solves systems of equations of the following form:

$$\left|M^{-1}K-\omega^2 E\right|=0\,, \qquad (1)$$

where M is the mass matrix, K is the stiffness matrix, and ω is the natural frequency.

The effectiveness of both a single damper installed at level 1 and its operation in combination with a damper installed at level 2 was evaluated.

The dampers are activated when the displacement of one of the characteristic nodes 1 or 3, located at the damper installation level (Fig. 1a), exceeds the value δ_{max}. The vector of the damper reactive force is directed opposite to the velocity vector of the characteristic node.

The reactive force of the burning fuel is represented by the following relationship:

$$R=V_e\cdot\frac{dm}{dt}, \qquad (2)$$

where V_e is the gas jet ejection velocity, and $\dot{m}$ is the fuel consumption rate.

The equation of motion for a node of the finite element model of the high-rise building with an operating damper is as follows:

$$(M_i+m_i)\ddot{u}_i+\sum_{j=1}^{n}k_{ij}u_j=P_i\mp v_e\cdot\dot{m}_i, \qquad (3)$$

where m_i is the variable mass of the damper.

The mass matrix of the moving system and the external force vector can be represented as:

$$M=diag\left[M_1\ M_2\ \ldots M_i+m_{i,t+\Delta t}\ \ldots M_n\right], \qquad (4)$$

$$P=\left[P_1\ P_2\ \ldots P_i\mp V_e(m_{i,t+\Delta t}-m_{i,t})\ \big/\ (\Delta t)\ldots P_n\right]^T. \qquad (5)$$

The main parameters of the damper affecting its performance are:

- gas jet velocity V_{gas}, m/s;
- operating time per activation T_{gas}, m/s;
- maximum displacement limit for the nodes of the damped structure δ_{max}, m.

The study analyzed the influence of these reactive damper characteristics on the effectiveness of reducing the vibration levels of the high-rise building.

Results and Discussion

Frequency-vector analysis

Fig. 5 shows the results of determining the first three frequencies and mode shapes of the investigated system using the developed software package.

The obtained results show that placing dampers at the roof level according to the first mode shape and at mid-height of the building according to the third mode shape will lead to more effective suppression of oscillations.

Suddenly applied load from the reactive damper (Fig. 6)

Let us assume that the velocity of the damper's reactive jet is constant:

$$V_e=\text{const}, \qquad (6)$$

and the function of fuel mass loss is given as:

$$m=m_0(1-\beta t), \qquad (7)$$

where β is a constant factor, $[s^{(-1)}]$.

1.1. Damping of oscillations using a damper *placed at one level*

Fig. 7 presents the results of determining the displacements of characteristic nodes 1 and 3 of the high-rise building model upon the operation of a damper with specified parameters.

Graphs of the maximum displacements of nodes 1–4 of the design building model (Fig. 1a) as functions of the main damper characteristics are presented in Figs. 8–10.

1.2. Damping of oscillations using dampers *placed at two levels*

The results of the calculations over the time interval 5 s ≤ t ≤ 10 s, where a pronounced peak of translational accelerations is observed on the

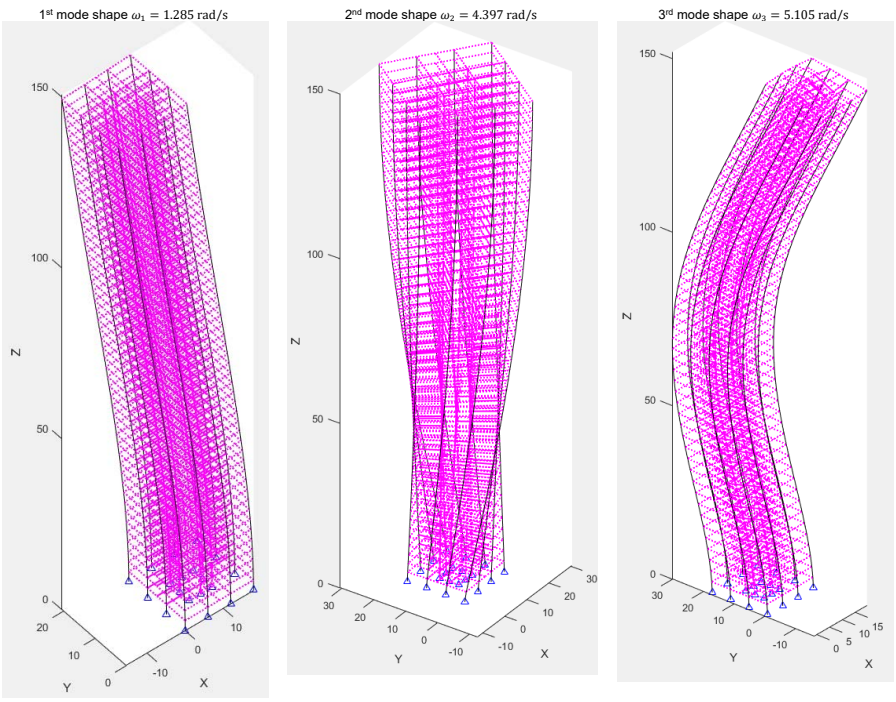

Fig. 5. Results of the frequency-vector analysis of the high-rise building model

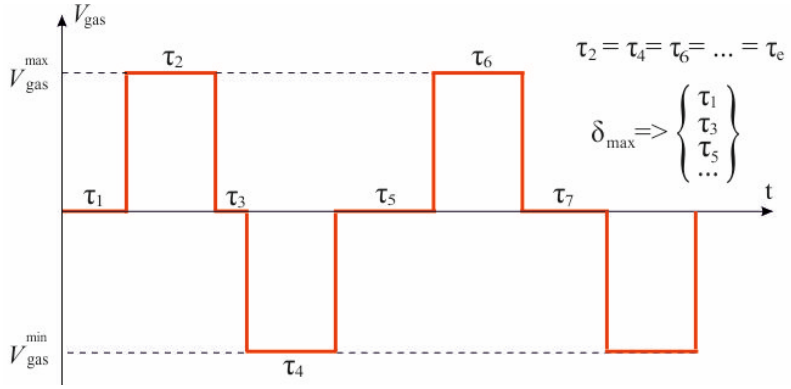

Fig. 6. Gas jet velocity under a suddenly applied load

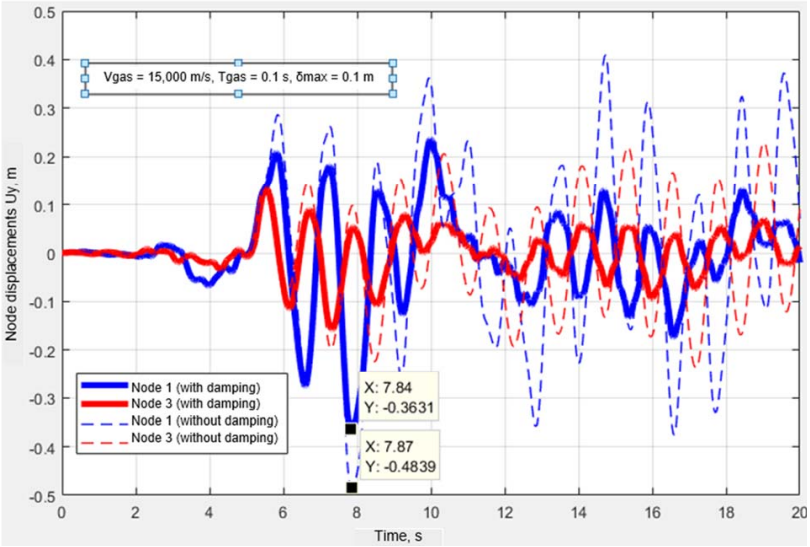

Fig. 7. Displacements of characteristic nodes 1 and 3 during oscillation damping

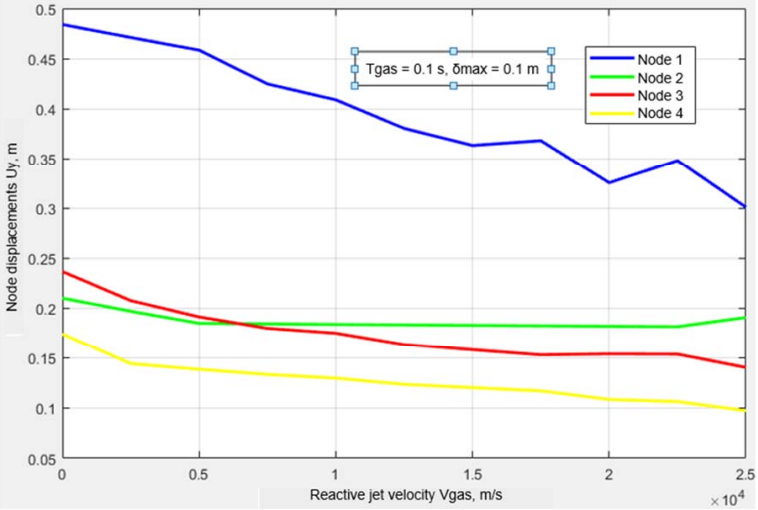

Fig. 8. Graph of the maximum displacements of nodes 1–4 of the building model depending on the damper parameter V_{gas}

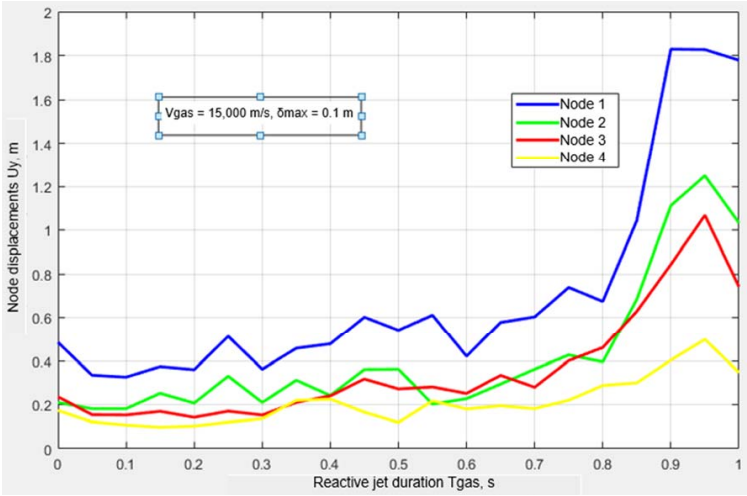

Fig. 9. Graph of the maximum displacements of nodes 1–4 of the building model depending on the damper parameter T_{gas}

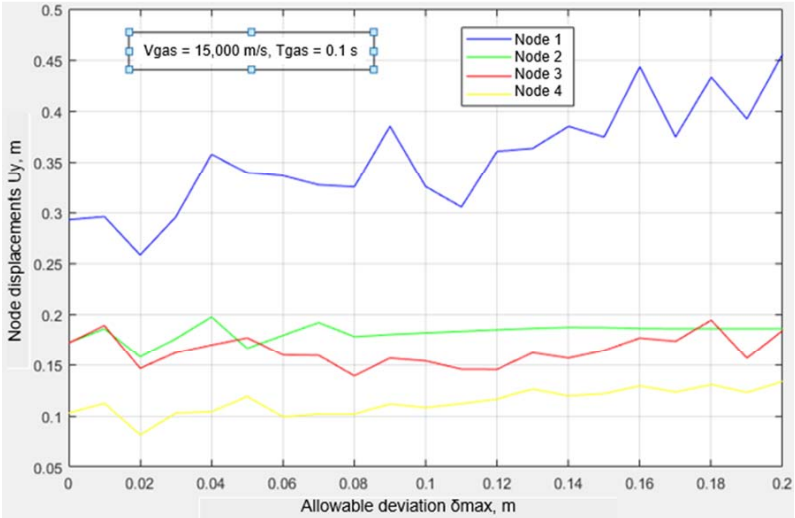

Fig. 10. Graph of the maximum displacements of nodes 1–4 of the building model depending on the damper parameter δ_{max}

accelerogram (Fig. 2), are presented in Fig. 11. In this case, the reactive force from the damper at level 2 was applied to the central node of the cross-section of the core of rigidity, located at mid-height of the building according to the results of the frequency-vector analysis. The direction of the force was taken opposite to the velocity vector of the node. The evaluation of damper efficiency was carried out based on the kinematic characteristics of nodes 1 and 3 of the building model, located in the planes of action of the corresponding reactive forces (Fig. 1a).

Optimization of Damper Parameters

Using the developed software package, a table was compiled showing the dependence of the maximum displacement of node 1 on the parameters V_{gas} and T_{gas} of the reactive damper located at level 1 (a function of two variables). By applying spline interpolation, the objective function was obtained in analytical form (Fig. 12):

$$U_{\max}(V_{gas}, T_{gas}) \to \min.$$

The software package makes it possible to determine the minima of the objective function of the damper's variable parameters (Fig. 13).

Fig. 14 presents the results of the calculation with selected optimal damper characteristics, when four charges are activated simultaneously: V_{gas} = 8,368 m/s (4 * 8268 = 33,472 m/s), T_{gas} = 0.051 s.

Conclusions

The process of active damping of vibrations in high-rise buildings, caused by non-stationary natural impacts, has been studied. The practical

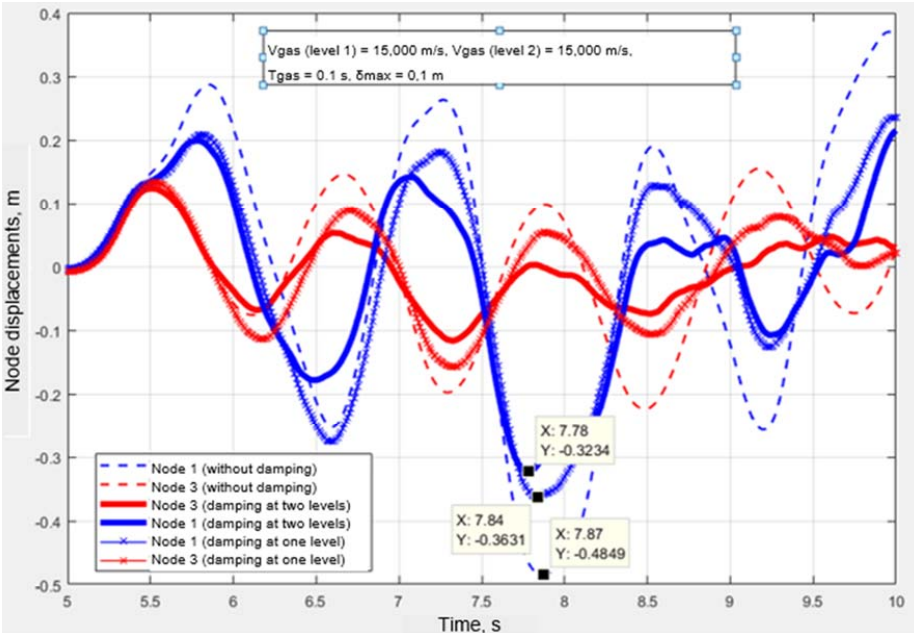

Fig. 11. Displacements of nodes 1 and 3 with dampers operating at two levels

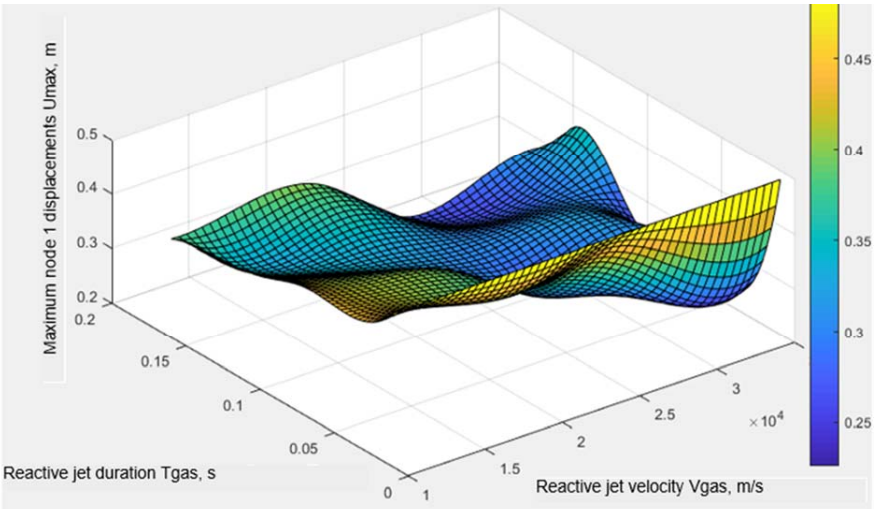

Fig. 12. Objective function of two variable parameters of the reactive damper

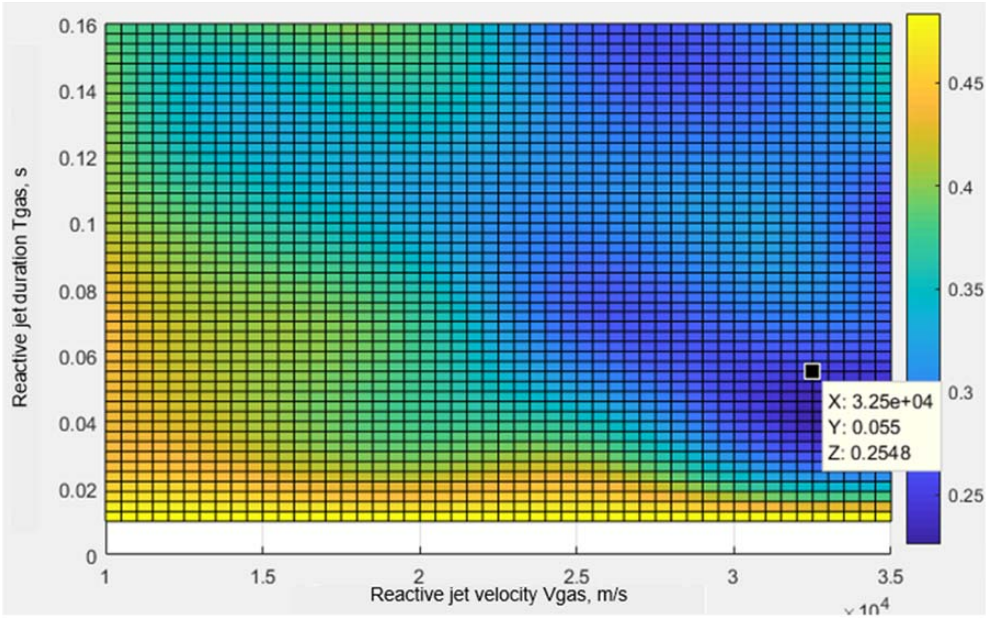

Fig. 13. Determination of local minima of the objective function of the maximum displacements of node 1

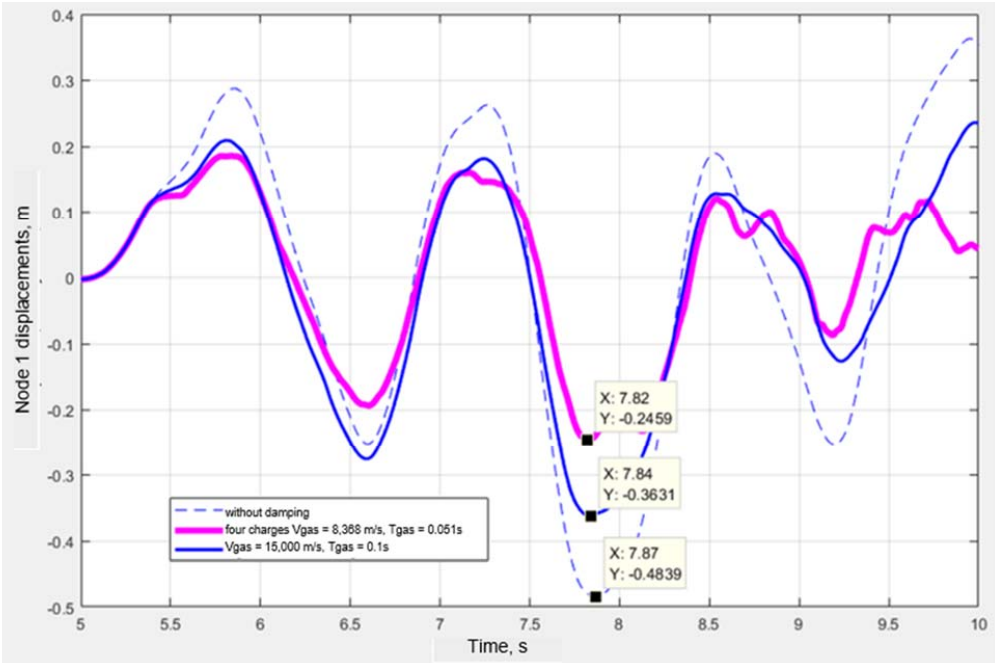

Fig. 14. Analysis of the displacements of node 1 with the obtained optimal characteristics of the reactive damper

suppression of vibrations in the mathematical model "building – damper" was carried out using controlled reactive impulses, which act as generators of resistance forces to motion. It has been shown that the proposed damping system makes it possible to reduce vibration amplitudes by more than half.

Funding

This research was carried out with the financial support of the National Research Moscow State University of Civil Engineering within the framework of the 2025 competition for conducting fundamental and applied research (R&D) by scientific teams of organizations acting as members and strategic partners of the Industry Consortium "Construction and Architecture" (Agreement No. PGUAS/K-25 dated 20.05.2025), in order to implement the Development Program of the National Research Moscow State University of Civil Engineering for 2021–2030 as part of the Strategic Academic Leadership Program "Priority-2030".

References

Abramyan, S. G., Burlachenko, O. V., Oganesyan, O. V., Burlachenko, A. O., Archakov, I. B., and Pleshakov, V. V. (2022). Technological solutions ensuring reliable operation of steel vertical reservoirs in seismic areas. *Construction Materials and Products*, Vol. 5, No. 5, pp. 5–16. DOI: 10.58224/2618-7183-2022-5-5-5-16.

Adam, C., Di Matteo, A., Furtmüller, T., and Pirrotta, A. (2017). Earthquake excited base-isolated structures protected by tuned liquid column dampers: design approach and experimental verification. *Procedia Engineering*, Vol. 199, pp. 1574–1579. DOI: 10.1016/j.proeng.2017.09.060.

Altay, O., Nolteernsting, F., Stemmler, S., Abel, D., and Klinkel, S. (2017). Investigations on the performance of a novel semi-active tuned liquid column damper. *Procedia Engineering*, Vol. 199, pp. 1580–1585. DOI: 10.1016/j.proeng.2017.09.061.

Amanollah, F., Ostrovskaya, N., Rutman, R. (2023). Structural and parametric analysis of lead rubber bearings and effect of their characteristics on the response spectrum analysis. *Architecture and Engineering*, Vol. 8, No. 1, pp. 37–43. DOI: 10.23968/2500-0055-2023-8-1-37-43.

Burtseva, O. A., Tkachev, A. N., and Chipko, S. A. (2015). Roller seismic impact oscillation neutralization system for high-rise buildings. *Procedia Engineering*, Vol. 129, pp. 259–265. DOI: 10.1016/j.proeng.2015.12.046.

Etedali, S. and Rakhshani, H. (2018). Optimum design of tuned mass dampers using multi-objective cuckoo search for buildings under seismic excitations. *Alexandria Engineering Journal*, Vol. 57, Issue 4, pp. 3205–3218. DOI: 10.1016/j.aej.2018.01.009.

Lasowicz, N. and Jankowski, R. (2017). Investigation of behaviour of metal structures with polymer dampers under dynamic loads. *Procedia Engineering*, Vol. 199, pp. 2832–2837. DOI: 10.1016/j.proeng.2017.09.540.

Marano, G. C., Greco, R., Trentadue, F., and Chiaia, B. (2007). Constrained reliability-based optimization of linear tuned mass dampers for seismic control. *International Journal of Solids and Structures*, Vol. 44, Issues 22–23, pp. 7370–7388. DOI: 10.1016/j.ijsolstr.2007.04.012.

Owji, H. R., Shirazi, A. H. N., and Hooshmand Sarvestani, H. (2011). A comparison between a new semi-active tuned mass damper and an active tuned mass damper. *Procedia Engineering*, Vol. 14, pp. 2779–2787. DOI: 10.1016/j.proeng.2011.07.350.

Seong, J. Y. and Min, K. W. (2011). An analytical approach for design of a structure equipped with friction dampers. *Procedia Engineering*, Vol. 14, pp. 1245–1251. DOI: 10.1016/j.proeng.2011.07.156.

Shein, A. I. and Chumanov, A. V. (2021). Belt vibration damping system for closed-type domes. In: Klyuev, S. V. and Klyuev, A. V. (eds.). *Environmental and Construction Engineering: Reality and the Future. Lecture Notes in Civil Engineering*, Vol. 160. Cham: Springer, pp. 245–252. DOI: 10.1007/978-3-030-75182-1_33.

Shein, A., Chumanov, A., Malkov, A., and Laskov, N. (2022). New vibration dampers for buildings and structures. *AIP Conference Proceedings*, Vol. 2503, Issue 1, 050065. DOI: 10.1063/5.0100292.

Shein, A. I. and Shmelev, D. A. (2014). Performance evaluation of active liquid vibration damper for high-rise buildings at the non-stationary impacts. *Structural Mechanics and Analysis of Constructions*, No. 1 (252), pp. 59–63.

Shein, A. I. and Zaytsev, M. B. (2023). Mathematical modeling of the operation of a reactive vibration dampener of a cooling tower. *Modeling and Mechanics of Structures*, No. 17, pp. 1–10.

Tamrazyan, A. and Chernik, V. (2021). Equivalent viscous damping ratio for a RC column under seismic load after a fire. *IOP Conference Series: Materials Science and Engineering*, Vol. 1030, 012095. DOI: 10.1088/1757-899X/1030/1/012095.

Tamrazyan, A. and Matseevich, T. (2024). Seismic resistance of reinforced concrete building frames based on interval assessment of the coefficient of permissible damage. *Buildings*, Vol. 14, Issue 12, 3776. DOI: 10.3390/buildings14123776.

ГАШЕНИЕ СЕЙСМИЧЕСКИХ КОЛЕБАНИЙ ВЫСОТНЫХ ЗДАНИЙ С ПОМОЩЬЮ УПРАВЛЯЕМЫХ РЕАКТИВНЫХ ДЕМПФЕРОВ

Александр Иванович Шеин[1]*, Михаил Борисович Зайцев[1], Ашот Георгиевич Тамразян[2], Татьяна Анатольевна Мацеевич[2]

[1]Пензенский государственный университет архитектуры и строительства, г. Пенза, Россия.
[2]НИУ Московский государственный строительный университет, г. Москва, Россия.

*E-mail: shein-ai@yandex.ru

Аннотация

Введение. Исследуется зависимость величины сейсмических перемещений высотных зданий от параметров управления реактивным демпфером (гасителем) колебаний. Выполнен частотно - векторный анализ конечно-элементной модели здания. Анализируется реакция здания, подверженного нестационарным сейсмическим воздействиям, на изменение параметров демпфера: заданной величины контрольного перемещения, скорости выбрасывания реактивной струи, времени однократного реактивного импульса. Представлен алгоритм оптимизации управляемых параметров демпфера. Оценивается эффективность применения реактивного демпфера для уменьшения размаха колебаний высотного здания. Реактивные демпферы колебаний устанавливаются как в одном, так и в двух уровнях по высоте здания. **Методы:** исследовалась математическая модель системы «высотное здание - реактивный демпфер» при нестационарном (сейсмическом) воздействии с использованием программного комплекса, основанного на методе конечных элементов (МКЭ). Динамический отклик конструкции определялся численным решением системы дифференциальных уравнений движения с помощью шагового метода Ньюмарка, реализованного авторами в среде «Matrix Laboratory» в виде программного комплекса. **Результаты:** Доказана эффективность применения реактивного демпфера для снижения размаха колебаний механических систем (высотных зданий) при нестационарных нагрузках. Принято, что при сейсмическом воздействии на сооружение демпфер активируется в случае, когда перемещение одного из узлов конструкции превышает наперед заданное значение, а вектор скорости этого узла определяет направление реактивной силы. Представлены уравнения движения конечно-элементной модели пластинчато-стержневой системы с активным демпфером, работающим на принципе реактивной струи. В интерактивной среде для численных вычислений «Matrix Laboratory» разработан программный комплекс для решения системы дифференциальных уравнений, описывающих движение пластинчато-стержневой КЭ модели высотного здания с системой демпфирования. Получены графики, показывающие, как изменяется эффективность работы демпфера в зависимости от таких параметров, как скорость и время выброса реактивной струи (V_{gas} и T_{gas}), а также от допустимого отклонения (ограничения по перемещениям для включения гасителя δ_{max}). Проведено исследование влияния указанных параметров на эффективность работы демпфера. Установлено, что применение реактивного демпфера с оптимально подобранными параметрами снижает размах амплитуд колебаний на 50–80 %, т.е. реактивная система эффективно гасит механические колебания зданий и сооружений. Разработан программный комплекс, позволяющий подобрать оптимальные, для данного высотного здания, параметры реактивного демпфера.

Ключевые слова: высотное здание, сейсмическое воздействие, колебательное движение, реактивный демпфер, уровень колебаний, перемещения.

DOI: 10.23968/2500-0055-2025-10-3-96-110

WHITE CEMENT-BASED BINDER FOR SELF-CLEANING FINE-GRAINED CONCRETE

Valeria Strokova, Yulia Ogurtsova, Ekaterina Gubareva*, Natalia Khmara, Alexandra Bukovtsova, Viktoria Ivanova, Margarita Skorokhodova

Shukhov Belgorod State Technological University, Belgorod, Russia

*Corresponding author's email: 43448504@mail.ru

Abstract

Introduction. The production of concrete products with complex shapes that are thin-walled, durable, and resistant to environmental influences — while retaining their decorative appearance during service and maximizing the use of industrial (secondary) mineral raw materials — poses a significant challenge. This challenge is particularly pronounced when producing white-colored products, as the range of suitable raw materials becomes severely limited. Additionally, reducing the Portland cement content in such concretes is essential. Therefore, a pressing task is the development of modern binders and concretes with reduced Portland cement content based on white-colored mineral components. **Materials and methods.** White Portland cement without mineral additives (PCB 1-500-D0 Cemix ProWhite, Cemix LLC, Republic of Bashkortostan) was used as the binder; expanded perlite sand (pozzolanic additive), microcalcite (carbonate additive), and anatase (photocatalytic additive), as well as their mixtures, were considered as additives; and polycarboxylate-based plasticizer Melflux 1641 F was employed to improve workability. The main physical and mechanical properties of the binder and the resulting cement stone — including normal consistency, mini-cone spread, and compressive strength — were evaluated according to standard procedures. Workability of the mixtures was assessed using rheological measurements, and the rate of heat release during cement stone hydration was determined calorimetrically. The study also examined the microstructural features of the resulting cement stone. **Results.** Replacing 40 % of cement with a complex of mineral additives in combination with a plasticizer mitigates the negative impact of fine components on the water demand of the mixture. This modification promotes intensified hydration, enhanced uniformity and density of the cement stone, and a reduction in the specific surface area and total nanopore volume of the cement stone by 39 % and 36 %, respectively. The presence of mineral additives enables the production of a binder achieving a compressive strength of 65.2 MPa after 28 days of standard curing.

Keywords: white Portland cement, perlite sand, complex additive, microstructure, hydration, concrete.

Introduction

In recent years, the production of modern high-performance construction materials has demonstrated new trends. Both manufacturers and consumers are increasingly focusing on the rational use of natural resources, with particular attention given to the recycling of industrial waste and the search for ways to reduce the energy intensity of production. Consequently, in the development, design, and implementation of composites, economic considerations are now taken into account alongside environmental ones. At the same time, modern construction materials are required to meet a wide range of performance criteria reflecting the high level of technological advancement, including workability, enhanced strength, frost resistance, corrosion resistance, self-cleaning capabilities, etc. Achieving an optimal balance of these properties is made possible through the development of multicomponent systems, in which the processes of phase and structure formation are controlled through the rational selection of raw materials, including modern additives, as well as by-products and industrial waste (Abouelnour et al., 2024; Cherkasov et al., 2015; Ledyaykina and Ledyaykin, 2024; Luo et al., 2024; Pogorelov, 2010; Tarasov et al., 2018).

In the modern construction industry, the production and use of binder systems with reduced Portland cement clinker content, in which a portion of clinker is replaced with mineral additives of various origins, are expanding. Such binders demonstrate enhanced environmental performance and efficiency by utilizing either industrial waste or locally available materials. At the same time, they maintain their operational properties while offering reduced energy consumption and cost, achieved through the rational design of the composition and the use of chemical admixtures.

The application of these advanced binders is particularly relevant for producing non-standard decorative and architectural concretes, which can be used in the manufacture of thin-walled elements as well as other non-standard products with complex geometries, coloring, surface texturing, etc. (Bazhenova and Bazhenova, 2016; Kalashnikov, 2011; Kalashnikov et al., 2023; Loganina and

For citations: Strokova, V., Ogurtsova, Yu., Gubareva, E., Khmara, N., Bukovtsova, A., Ivanova, V., Skorokhodova, M. (2025). White cement-based binder for self-cleaning fine-grained concrete. Architecture and Engineering, No 3 (10), pp. 96–110. DOI: 10.23968/2500-0055-2025-10-3-96-110.

Fokin, 2019; Moroz et al., 2016; Mousavinejad and Pourjamali, 2024; Stenechkina, 2023; Tolstoy et al., 2018).

The analysis of the challenges associated with producing thin-walled products from fine-grained white-cement-based concrete (Fig. 1) has identified rational approaches that can improve production efficiency and the durability of the resulting products, thereby contributing to the enhancement of the architectural appearance of the urban environment.

The solution to the specific challenges associated with concretes intended for thin-walled products — such as ensuring high resistance to environmental effects and achieving complex product geometries, which require good workability of the mix and high matrix strength — lies in the development and use of a binder based on white Portland cement and white-colored mineral additives. This approach reduces cement content while maintaining the rheological properties of the binder composition as well as the physical and mechanical characteristics of the hardened system. To impart self-cleaning ability and preserve the decorative appearance over extended periods under aggressive environmental conditions, the use of a photocatalytic additive, pre-immobilized on one of the binder components, is advisable. This strategy minimizes leaching (weathering) of the photocatalyst from the surface, ensures uniform distribution of the photocatalyst in the surface layer of the product, and enhances its self-cleaning performance.

The proposed set of measures, forming a comprehensive technological solution, enables the production of white fine-grained concrete with high physical and mechanical performance and resistance to environmental, man-induced, and biological impacts. This is achieved through reduced porosity of the cement matrix as well as physical and chemical immobilization of the photocatalyst within the cement-sand matrix.

The specific characteristics of white Portland cement, particularly its high degree of whiteness, significantly limit the range of mineral additives, including pozzolanic ones, that can be used in the binder composition, since changes in the concrete color would reduce the aesthetic appeal of the products. The use of mineral additives, fillers, and aggregates with colors substantially different from white together with white cement is economically impractical, as the cost of the latter is higher than that of ordinary Portland cement due to stricter raw material requirements and higher clinker sintering temperatures. Considering these primary criteria (color and inherent reactivity), expanded perlite sand was selected as one of the additives to partially replace cement (Ayubov et al., 2024; Grzeszczyk and Janus, 2021; Natsievsky, 2006; Shirina and Zagorodnyuk, 2007).

Expanded perlite used in cementitious materials is commonly addressed as a lightweight filler and aggregate (Berov et al., 2006; Kharitonov et al., 2023; Kotwica et al., 2017; Miryuk and Zagorodnyuk, 2022; Sidorova, 2024). However, its application as a pozzolanic additive and a carrier for a photocatalyst has received limited attention in the literature. Therefore, the objective of this stage

DEVELOPMENT OF FINE-GRAINED CONCRETE FOR THIN-WALLED PRODUCTS		
CHALLENGES	**SOLUTIONS**	**RESULTS**
High cost of white Portland cement and the carbon footprint of the global cement industry	Partial replacement of white Portland cement with mineral additives, including industrial by-products	Reduced production costs. Lower carbon footprint. Expanded raw material base for fine-grained concrete production.
Demand for white and light-colored concrete products and structures to create a favorable architectural environment	Use of binders, mineral additives, fillers, and aggregates of white color	Products exhibit high decorative qualities. Ability to produce products in a wide range of colors.
Increased water demand of the binder when using finely dispersed mineral additives	Control of rheological parameters of the binder through rational use of mineral and plasticizing additives	Improved workability of the mixture without increasing water content, enabling production of thin-walled products with complex shapes.
Loss of decorative appearance during long-term operation due to man-induced and biological impacts	Use of a photocatalyst immobilized on a mineral additive	Products gain properties of photocatalytic self-cleaning against organic contaminants, remaining resistant to environmental effects (weathering).
Difficulty achieving high performance and durability in thin-walled products with complex shapes	Control of the particle size distribution of components at the nano-, micro-, and macro-levels of fine-grained concrete to create a high-density structure	Products exhibit high strength and frost resistance, reduced water absorption, and resistance to environmental impacts and biological aggressions.

Fig. 1. Challenges and approaches to improving the efficiency of fine-grained concretes for thin-walled products

of the study was to evaluate the potential use of expanded perlite sand as an active (pozzolanic) additive to white Portland cement by examining its properties, the dependence of these properties on surface preparation (activation), and the influence of its composition and typomorphic features on the properties of the cement system.

Accordingly, the research aims to establish the properties — workability, strength, and durability — of fine-grained concrete for light-colored thin-walled products with reduced white Portland cement content. This reduction is achieved through the combined action of siliceous (expanded perlite) and carbonate (microcalcite) components at an optimal granulometric composition and content within the binder. Additionally, the leaching of nanosized photocatalyst during the service life of the products is prevented by pre-immobilizing it on the particles of the siliceous component of the binder.

Methods

A binder mixture consisting of white Portland cement without mineral additives PCB 1-500-D0 Cemix ProWhite produced by Cemix LLC, Republic of Bashkortostan (used as the control composition), and a binder mixture with the partial replacement of cement with mineral additives, were the object of the study. Ground expanded perlite sand (GEPS) produced by Oskolsnab JSC, Stary Oskol, was used as a pozzolanic additive; microcalcite (MC) produced by MramorPro LLC, Yekaterinburg, served as a carbonate additive; and nanosized titanium dioxide in the anatase modification (An) produced by Hangzhou Wanjing New Material Co., Ltd., China, was used as a photocatalytic additive. Additionally, a multifunctional composite material (MCM) of the “expanded perlite sand – nanosized anatase” (EPS–An) system was employed. It was produced by co-grinding expanded perlite sand pre-treated in a 2.0 % aqueous solution of oxalic acid with anatase in a 1:1 ratio.

To study the features of phase and structure formation in the binder, the influence of the additives on the normal consistency of the cement paste was evaluated according to GOST 30744-2001 using a Vicat apparatus.

A plasticizing admixture was selected with account for the requirement to maintain the white color of the mixture and the presence of highly dispersed components. Due to its well-documented effectiveness in such systems, polycarboxylate-based plasticizer Melflux 1641 F (BASF Construction Additives, Germany) was chosen. The dosage range of the admixture was determined based on the manufacturer’s recommendations. The admixture was introduced in equal increments of 0.05 % until no further increase in mini-cone spread was observed.

The influence of the nature of mineral additives on the rheological characteristics (viscosity and shear stress) of the binder systems was assessed using a Rheotest RN4.1 rotational viscometer with a cylindrical measuring system under shear deformation at a gradient of 0–150 s^{-1}.

To evaluate the effect of mineral additives on the early hydration of cement, isothermal calorimetry was performed using a ToniCAL 7339 differential calorimeter. The water-to-binder ratio for all mixtures was 0.5. Differential and integral heat release curves of the binder systems were recalculated per 1 g of white Portland cement.

The study of phase formation in the binder with various additives was carried out by determining the mineral composition of the resulting cement stone using X-ray diffraction patterns obtained with an ARL X’TRA diffractometer in the 4–56° range.

The effect of mineral additives on the strength properties (flexural and compressive strength) of the cement stone was evaluated according to GOST 30744-2001 after 3, 7, and 28 days of curing of 40×40×160 mm test beams.

The structural features of the cement stone based on binders with different additives were investigated through micrographs obtained using a TESCAN MIRA scanning electron microscope after preliminary chromium coating of the specimen surfaces.

The specific surface area and nanopore distribution in the cement stone based on binders with different additives were determined using BET (Brunauer–Emmett–Teller) and BJH (Barrett–Joyner–Halenda) methods based on low-temperature nitrogen adsorption on the specimen surface.

Results and Discussion

The results of normal consistency measurements of the cement paste show that replacing 20 % of white Portland cement with EPS–An increases the water demand of the binder by 21 %, while replacement with microcalcite reduces it by 9 %. A 40 % replacement of cement with a mixture of the above additives is accompanied by a 15 % increase in water demand compared to pure Portland cement (Table 1). The increase in normal consistency observed in all compositions is attributed to the physical sorption of water by highly dispersed and porous particles and their aggregates.

Accordingly, the next stage in the development of the binder was the rational selection of a plasticizing admixture. Traditionally, a plasticizer is introduced at the stage of concrete mix preparation, often regardless of the type of cement used. However, due to the multicomponent composition of the proposed binder and the high fineness of its components, conventional concrete mix designs may not ensure the required workability and may lead to excessive consumption of plasticizer or mixing water.

The obtained mini-cone spread results (Fig. 2) generally demonstrate an increase in the water

Table 1. **Normal consistency of binders depending on composition**

No.	Component content, %				Normal consistency, %
	Mixture composition	White Portland cement (WPC), %	EPS–An	Microcalcite (MC)	
1.	WPC	100	–	–	33
2.	WPC + EPS–An	80	20	–	40
3.	WPC + MC	80	–	20	30
4.	WPC + EPS–An + MC	60	20	20	38

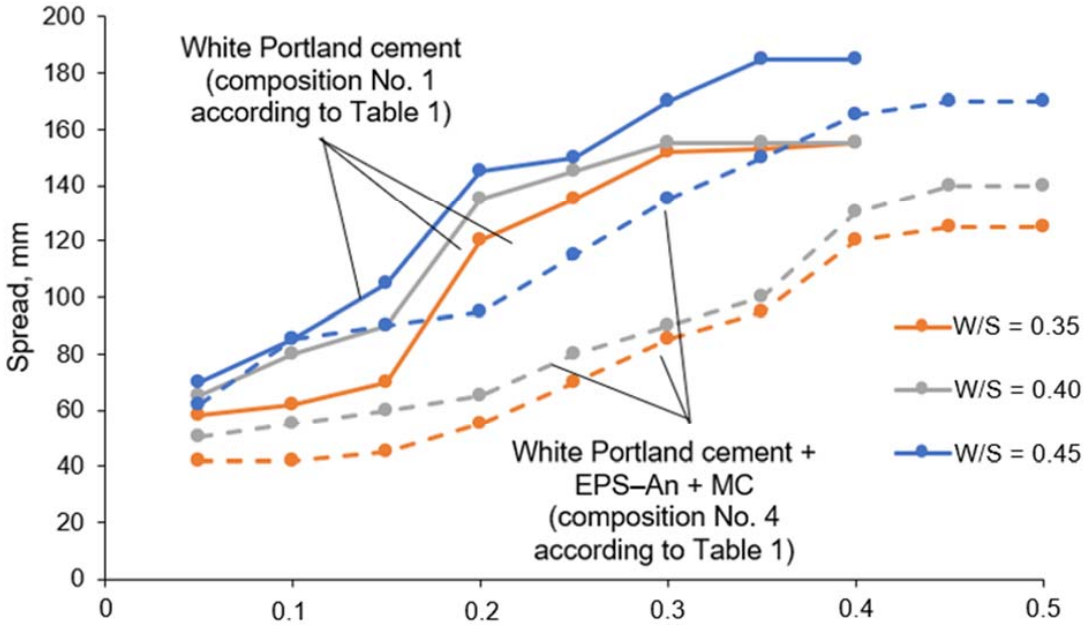

Fig. 2. Dependence of mini-cone spread of binders on the water-solid ratio and plasticizer dosage

demand of the binder when 40 % of Portland cement is replaced with finely dispersed additives, which is attributed to the excessive absorption of water from the mixture. Increasing the water-solid ratio from 0.35 to 0.45 allowed for greater mini-cone spreads in both binders: the maximum spread for white Portland cement was 185 mm, while that of the investigated composition reached 170 mm. The optimal dosage of the polycarboxylate-based plasticizer was determined, enabling a mini-cone spread diameter close to that of white Portland cement paste without mineral additives: at a water-solid ratio of 0.45, the dosage was 0.4 %.

The influence of each binder component on its rheological characteristics was determined for several mixture compositions (Table 2). The additives were introduced at their established optimal dosages.

For the systems containing only one type of additive with Portland cement (Table 2, Nos. 2–4), the influence of nanosized anatase was observed. Its presence leads to a significant increase in viscosity and shear stress of the system compared with unmodified Portland cement (Figs. 3, 4). This effect is attributed to the high specific surface area of anatase particles, the presence of numerous aggregates and agglomerates, and the difficulty of wetting the particles with water, all of which collectively hinder the flow of the mixture.

An increase in viscosity was also observed when ground expanded perlite sand was used. Its particles have irregular shapes and a highly developed surface morphology, leading to uneven water distribution in the system and hindering mixture flow.

In contrast, the use of microcalcite reduces the viscosity of the suspension, which is explained by the well-known enhancement of the dispersing effect of polycarboxylate superplasticizers in the presence of positively charged carbonate particles (Balykov et al., 2018; Martins et al., 2024; Xu et al., 2025).

The study of a suspension containing a mixture of all the components mentioned above (WPC + GEPS + + An + MC) still showed very high viscosity and shear stress values, primarily due to the presence of nanosized anatase, but these effects were slightly mitigated by the presence of microcalcite.

The negative influence of nanosized anatase on the rheological characteristics of the cement paste

Table 2. **Compositions of binder mixtures**

No.	Mixture composition	Component content, %					Content relative to binder mixture components, %	
		White Portland cement (WPC)	Ground expanded perlite sand (GEPS)	Nanosized anatase (An)	Microcalcite (MC)	EPS–An	Superplasticizer Melflux 1641 F	Water
1.	WPC	100	–	–	–	–	0.4	45
2.	WPC + GEPS	90	10	–	–	–		
3.	WPC + An	90	–	10	–	–		
4.	WPC + MC	80	–	–	20	–		
5.	WPC + GEPS + An + MC	60	10	10	20	–		
6.	WPC + EPS–An	80	–	–	–	20		
7.	WPC + EPS–An + MC	60	–	–	20	20		

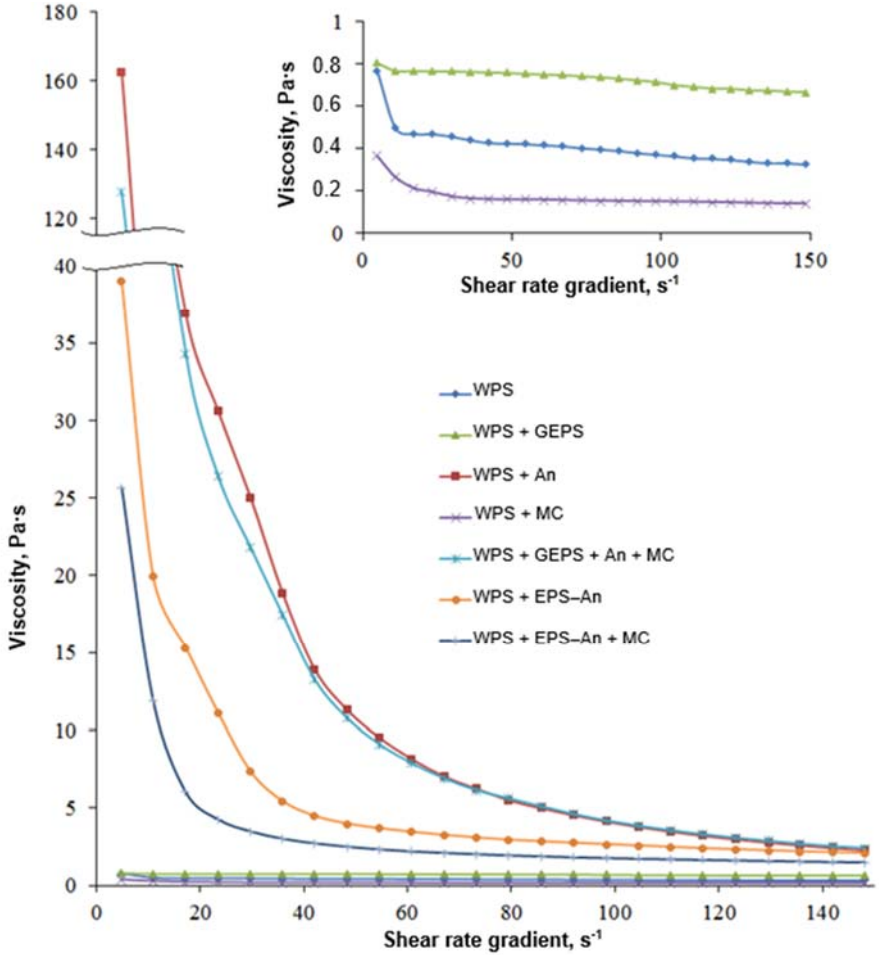

Fig. 3. Dependence of binder mixture viscosity (compositions according to Table 2) on shear rate gradient

was effectively reduced by using a product obtained through co-grinding expanded perlite sand and anatase (EPS–An). The co-grinding process allowed the breakdown of aggregates and agglomerates of the initial products, uniform distribution of individual particles, partial reduction of particle surface activity by deposition onto perlite particles, and smoothing of the perlite particle shape. This facilitated the flow of the suspension, reducing both its viscosity and shear stress.

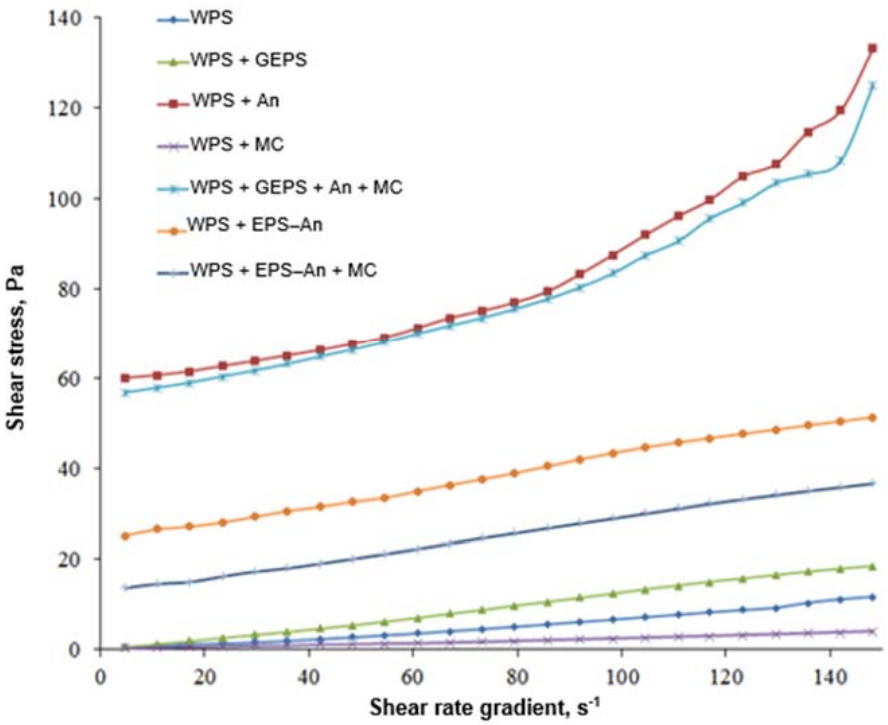

Fig. 4. Dependence of shear stress of binder mixtures on shear rate gradient (compositions according to Table 2)

In combination with microcalcite (WPC + EPS–An + MC), the viscosity and shear stress of the suspension are further reduced, which is attributed to the enhanced efficiency of the polycarboxylate plasticizer in the presence of carbonate particles. This allowed a reduction in water demand to achieve the required workability of the concrete mixture and resulted in a denser composite matrix.

Comparative analysis of differential heat release curves shows that the use of ground expanded perlite sand slightly slows down cement hydration, as evidenced by a shift of the main peak, corresponding to calcium silicate hydration, by 1 h 40 min relative to white Portland cement (Table 3). However, in the perlite-containing mixture, this peak is more intense, reaching 21 J/g cement·h compared to 18 J/g cement·h for cement without additives. Additionally, the perlite system exhibits a distinct shoulder and secondary peak following the main peak, which may be associated with ettringite formation (Taylor, 1996) or indicate a more gradual hydration process, including related to the pozzolanic reaction — a secondary hydration process (Voronov and Glagolev, 2020). The initial retardation of hydration is caused by limited water access to cement particles due to the developed morphology and high specific surface area of ground expanded perlite sand particles. The subsequent intensification and smoothing of the hydration process are related to the provision of additional surface area for new phase growth (the “crystallization seeding” effect) and gradual water release at later stages of hydration and the pozzolanic reaction.

The use of the EPS–An additive, obtained by co-grinding expanded perlite sand with nanosized anatase, led to several effects. First, a slight acceleration of the onset of the main hydration stage was observed, reflected in a leftward shift of the rising edge of the peak by several minutes (Fig. 5a). Second, the intensity of the main peak is higher compared with cement without additives, indicating an enhancement of silicate hydration. Third, the main heat release peak is more extended in time, which, as in the case of expanded perlite, may indicate the contribution of the pozzolanic reaction to the exothermic effect. The acceleration and intensification of the main hydration stage with the EPS–An additive are attributed to a reduction in the activation energy of the hydration process and an increase in the number of crystallization centers, which accelerates the formation and growth of hydration products — a well-known effect of using mineral additives (Beregovoy et al., 2023; Kuznetsova et al., 2015; Li et al., 2024; Stoyanov et al., 2024). Meanwhile, the effect of temporary water retention and hydration retardation observed when using pure expanded perlite sand is mitigated due to the partial coverage of perlite surfaces by anatase particles.

The application of the additive complex (EPS–An + MC) results in a 27-minute shift of the main heat release peak during hydration and a 21 % increase in heat release intensity compared with the

Table 3. **Heat release characteristics during hydration depending on binder mixture composition**

Mixture composition	Main hydration peak			Heat release over 72 h, J/g
	Time, h:min	dQ/dt (J/g cement·h)	Q(t) (J/g cement)	
WPC — 100 %	8:35	18.1	104.8	350.1
WPC — 90 % GEPS — 10 %	10:06	21.0	94.5	377.5
WPC — 80 % EPS–An — 20 %	8:35	20.5	118.4	395.6
WPC — 60 % EPS–An — 20 % MC — 20 %	8:08	21.9	125.0	417.6

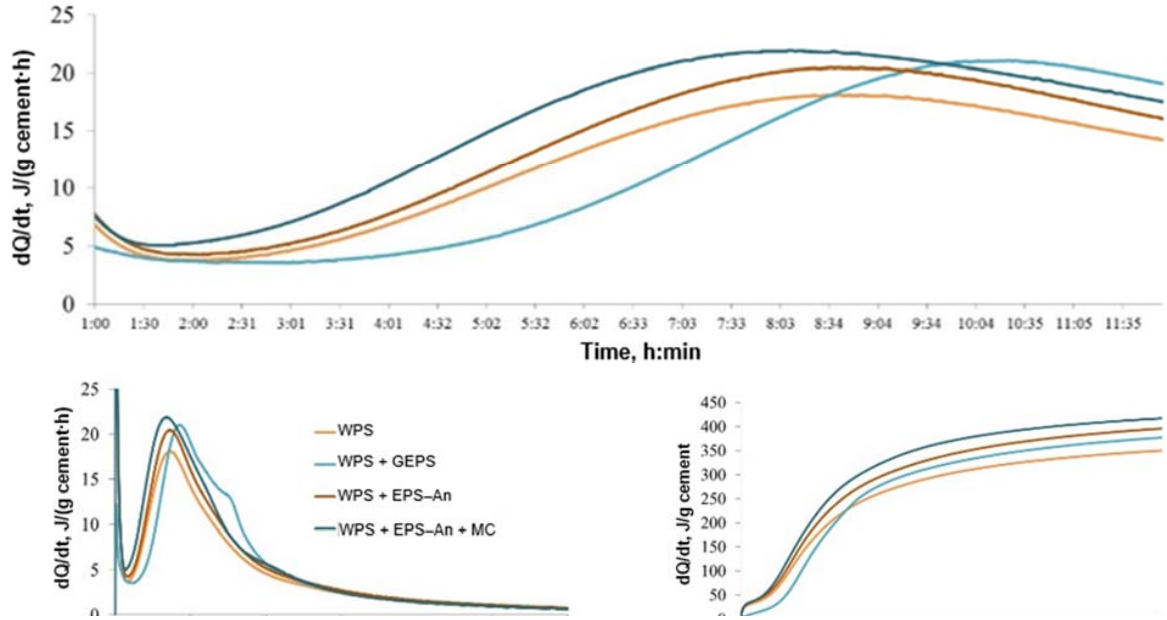

Fig. 5. Differential (*a, b*) and integral (*c*) heat release curves during hydration depending on binder mixture composition (calculated per 1 g of white Portland cement)

composition without additives (Figs. 5a, 5b). This is attributed to the nucleation effect provided by the highly dispersed particles and the progression of the pozzolanic reaction. Microcalcite may additionally participate in cement hydration reactions, forming calcium aluminum hydrocarbonates and calcium hydrocarbonates (Kulikova et al., 2019; Kopanitsa et al., 2023; Zhao et al., 2023).

Thus, all the aforementioned effects for the additives used contribute to an increase in the total heat release over 72 hours of binder hydration (Fig. 5b, Table 3). Based on the increase in heat release, the additives can be ranked as follows:

GEPS → EPS–An → EPS–An + MC.

A comparison of strength measurements for various binder mixture compositions (Table 4) also shows that the use of GEPS and EPS–An is less effective than EPS–An combined with microcalcite.

Replacing 10 % of white Portland cement with ground expanded perlite sand leads to a slowdown in strength development, manifested as a reduction in compressive strength by 12.5 % and 13.2 % at 3 and 7 days, respectively, compared with cement without additives. By 28 days, this difference decreases to 4.7 %. After steam curing, the strength of the GEPS-containing composition exceeds that of the control one by 4.2 %. These trends are attributed: first, to a slight retardation of hydration during the first few days in the presence of EPS, as observed in the heat release study; second, to the reduced Portland cement content; and third, to the enhanced pozzolanic reaction at elevated temperature.

For the composition with EPS–An, despite an even lower Portland cement content, the strength at 3 and 7 days remains almost equal to that of the GEPS-containing composition. This is due to the contribution of nanosized anatase particles, which accelerate hydration and early hardening. At 28 days, compressive strength decreases by 5.9 % compared with cement without additives, which is attributed

Table 4. **Strength of the binder depending on mixture composition**

No.	Mixture composition	Compressive/flexural strength, MPa at testing age			Specific compressive strength at 28 days	Compressive/flexural strength after steam curing, MPa
		3 days	7 days	28 days		
1.	WPC — 100 %	43.1 6.0	49.2 6.8	67.3 7.7	0.115	47.2 6.7
2.	WPC — 90 % GEPS — 10 %	37.7 5.3	42.7 5.9	64.1 7.3	0.122	49.3 6.9
3.	WPC — 80 % EPS–An — 20 %	37.4 5.2	43.1 6.1	63.3 7.1	0.135	47.0 6.6
4.	WPC — 60 % EPS–An — 20 % MC — 20 %	39.3 5.5	47.1 6.7	65.2 7.5	0.185	48.2 6.8

both to the reduced Portland cement content and possibly to a slight decrease in pozzolanic reaction intensity due to partial shielding of the perlite particle surfaces. After steam curing, the strength of EPS–An specimens is practically equal to that of the control ones, reflecting the progression of the pozzolanic reaction.

The determination of strength characteristics for the composition with EPS–An and microcalcite showed that, in this case, with a significant replacement of white Portland cement by the additive complex (Table 4, No. 4), there is no substantial loss of compressive or flexural strength at any of the tested curing ages (at 28 days, a decrease of 3 % in compressive strength and 2.5 % in flexural strength), while after steam curing, compressive strength exceeds that of the control specimen by 2 % and flexural strength — by 1.5 %.

Analysis of the specific strength of the specimens, i.e., the strength per 1 kg of cement relative to the total mass of solid components, revealed that despite the reduced white cement content, its contribution to overall strength increases. The achievement of high strength when using the additive combination may be attributed to the formation of a more monolithic and dense structure of hydration products on fine mineral particles, including those produced by the pozzolanic reaction, as well as the filling of micro- and nanopores with inert components.

Thus, based on the results of studying heat release during hydration and strength development kinetics, it can be concluded that the use of EPS–An together with microcalcite leads to a faster onset of the main cement hydration reactions, their more complete progression accompanied by the pozzolanic reaction, resulting in more intensive heat release, increased early strength, and the retention of 28-day strength even with a 40 % replacement of Portland cement by additives.

These findings are consistent with the results of mineralogical analysis of the hardened cement stone at 28 days (Fig. 6). In the cement stone from white Portland cement, both unreacted clinker minerals — alite and belite — and hydration products — C–S–H, portlandite, and ettringite — can be observed.

The use of ground expanded perlite sand (WPC + GEPS) led to hydration retardation, as evidenced by more pronounced peaks corresponding to alite, belite, and ettringite. The slightly reduced portlandite content may also be attributed to hydration retardation or to the pozzolanic reaction.

The use of ground expanded perlite sand with anatase (WPC + EPS–An) accelerated hydration, which reflected in a reduction of peaks associated with clinker minerals. No significant changes in portlandite content were observed. Peaks corresponding to anatase can also be noted.

When ground expanded perlite sand with anatase was combined with microcalcite (WPC + EPS–An + MC), low contents of alite, belite, and ettringite were observed, which can be attributed to the substantial reduction in Portland cement content, but may also reflect intensified hydration. The presence of mineral additives is confirmed by reflections of anatase and calcite. Peaks of the hydrosilicate phase — tobermorite — are also detected. The reduced portlandite content may result both from the lower Portland cement fraction and the ongoing pozzolanic reaction.

Investigation of the microstructural features of cement stone with different compositions revealed a decrease in microporosity and matrix densification upon the use of mineral additives (Fig. 7). In general, all specimens exhibit similar newly formed structures of varying size and morphology, including needle-like, columnar, layered, and dendritic forms. On GEPS particles, growths with a well-developed surface are observed, indicating reactions with cement hydration products and the formation of a developed but less compact interfacial zone.

A denser microstructure is observed when using EPS–An (Fig. 7). In the fracture, pores on the surface of EPS–An particles show active growth of newly formed structures with various morphologies. The addition of microcalcite to the system, despite an even greater reduction in the cement fraction, did not significantly alter the nature of the microstructure: it

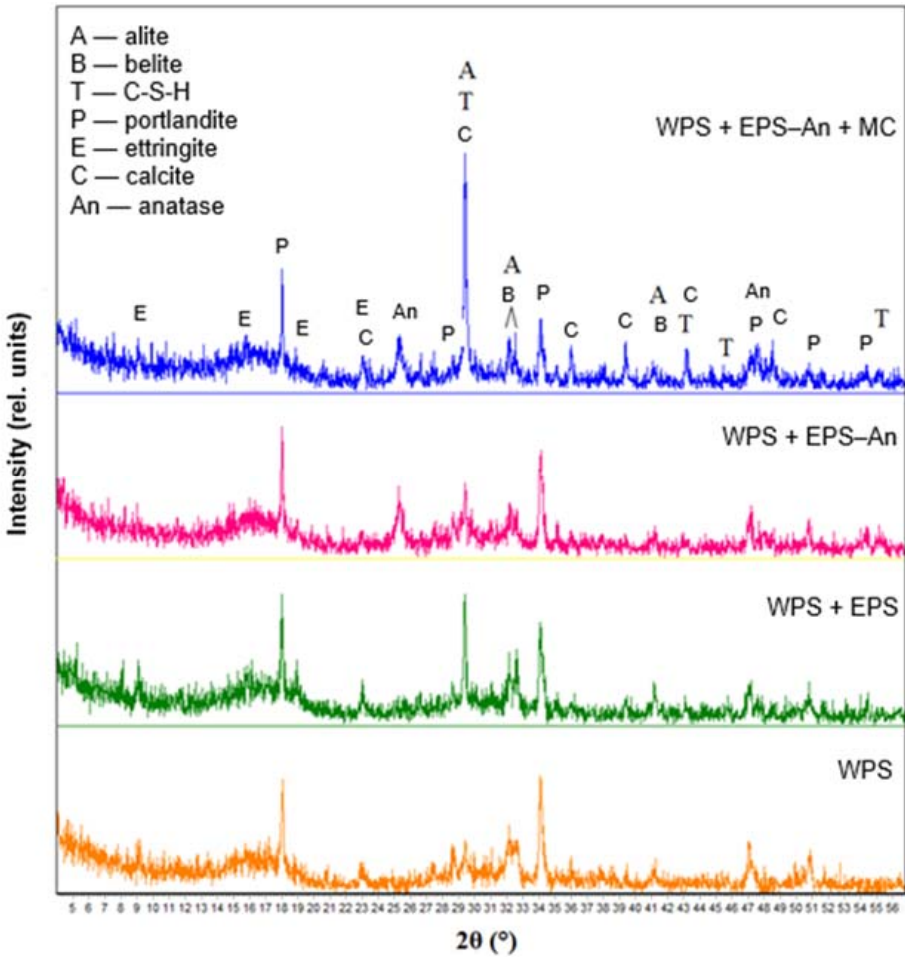

Fig. 6. X-ray diffraction patterns of cement stone at 28 days depending on binder mixture composition

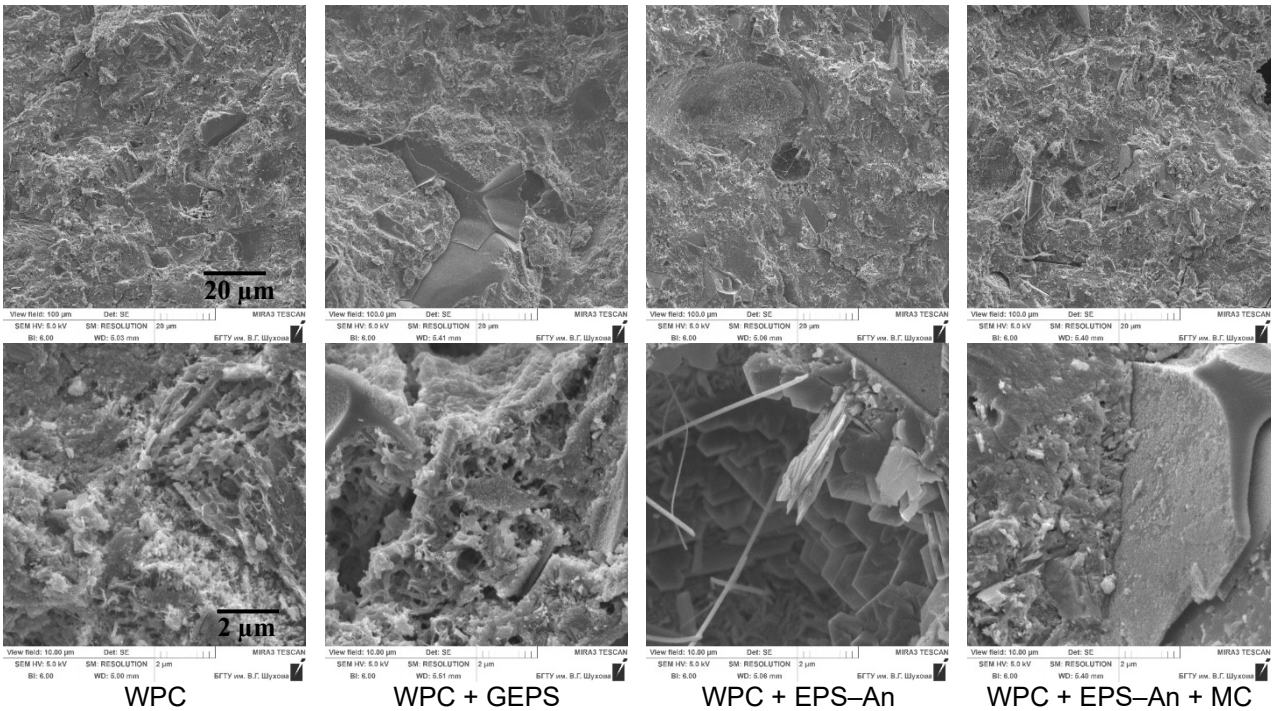

Fig. 7. Microstructure of cement stone at 28 days depending on binder mixture composition

remains dense, well-developed, with clearly defined boundaries of irregularly shaped perlite particles, partially interacting with cement components.

At higher magnification, the interfacial zone of the cement stone with EPS–An and MC (Fig. 8) shows a well-developed rough surface of the acid-pretreated expanded perlite sand, as well as accumulations of spherical particles smaller than 100 nm, corresponding to anatase.

Chemical element mapping of the WPC + EPS–An + MC specimen indicates a uniform distribution of titanium throughout the matrix, with accumulation near the surface of the perlite particles (Fig. 9).

The determination of specific surface area and nanopore distribution using BET and BJH methods (Table 5, Fig. 10) showed a higher specific surface area and greater nanopore volume for the specimen without additives. The lowest values were observed for the GEPS-containing specimen. The low specific surface area in this case may indicate incomplete hydration of Portland cement, consistent with results obtained by other methods for the GEPS specimen. The presence

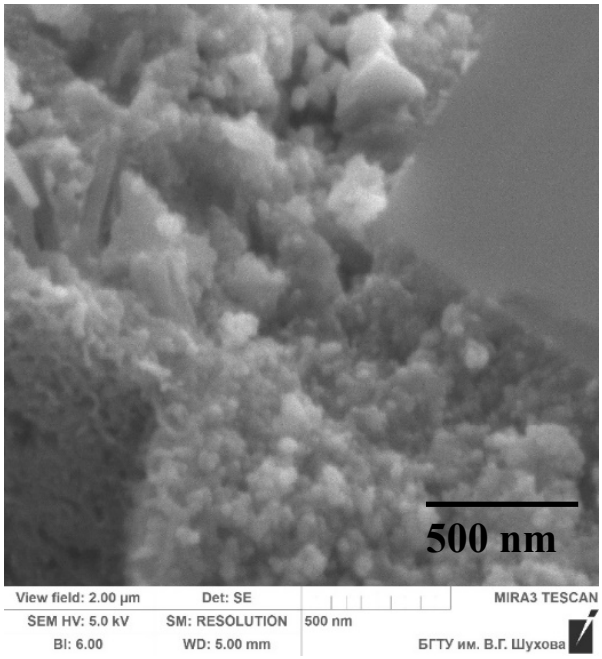

Fig. 8. Interfacial zone of cement stone with EPS–An and MC

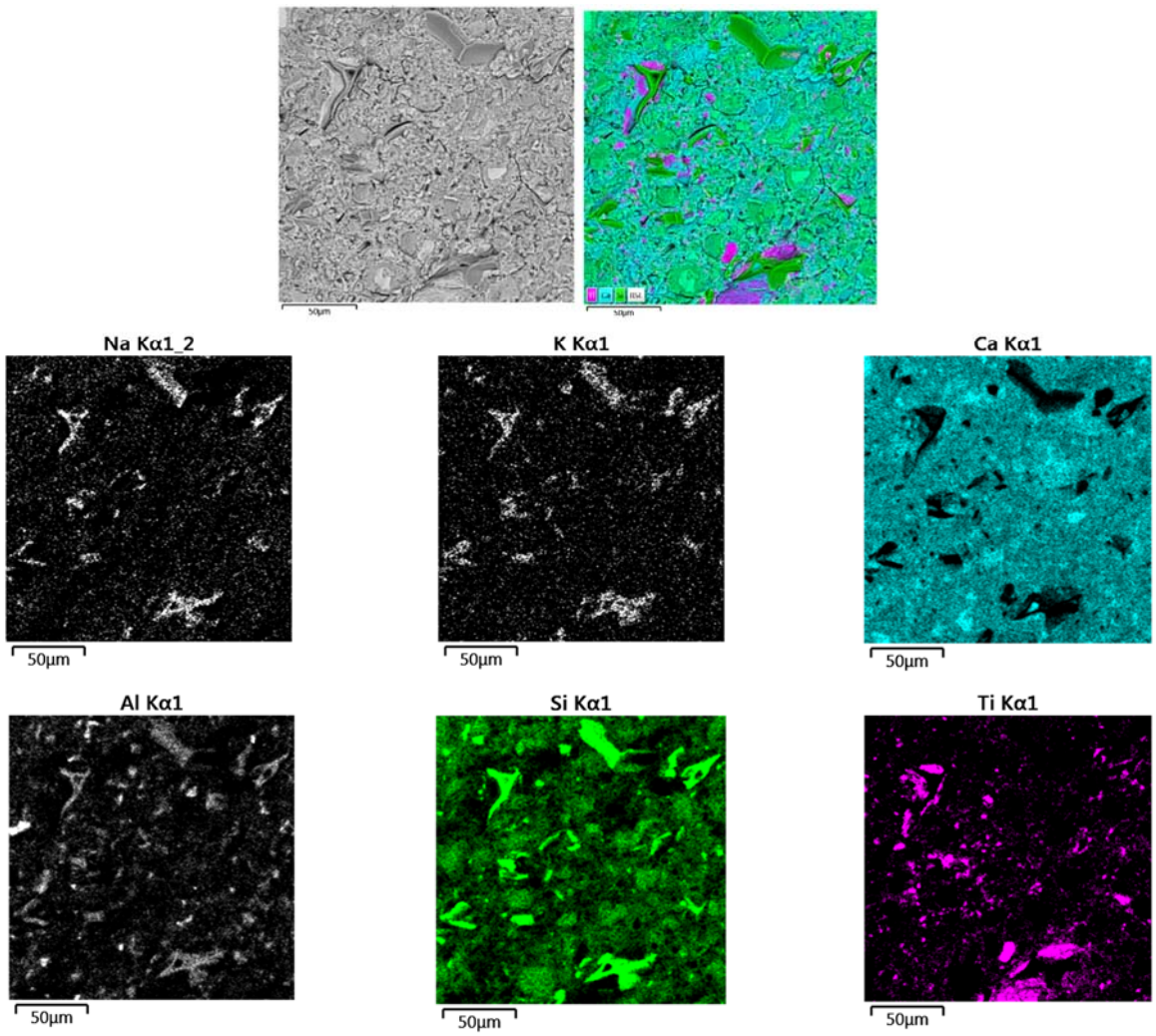

Fig. 9. Chemical element mapping of cement stone for the WPC + EPS–An + MC composition at 28 days

Table 5. **Dependence of specific surface area (BET) and nanoporous structure of cement stone at 28 days on binder mixture composition**

No.	Mixture composition	Specific surface area of the material, m^2/g	Total pore volume, cm^3/g	Average pore diameter, nm
1.	WPC — 100 %	62.06	0.078	5.02
2.	WPC — 90 % GEPS — 10 %	22.93	0.030	5.21
3.	WPC — 80 % EPS–An — 20 %	41.12	0.053	5.20
4.	WPC — 60 % EPS–An — 20 % MC — 20 %	37.84	0.050	5.25

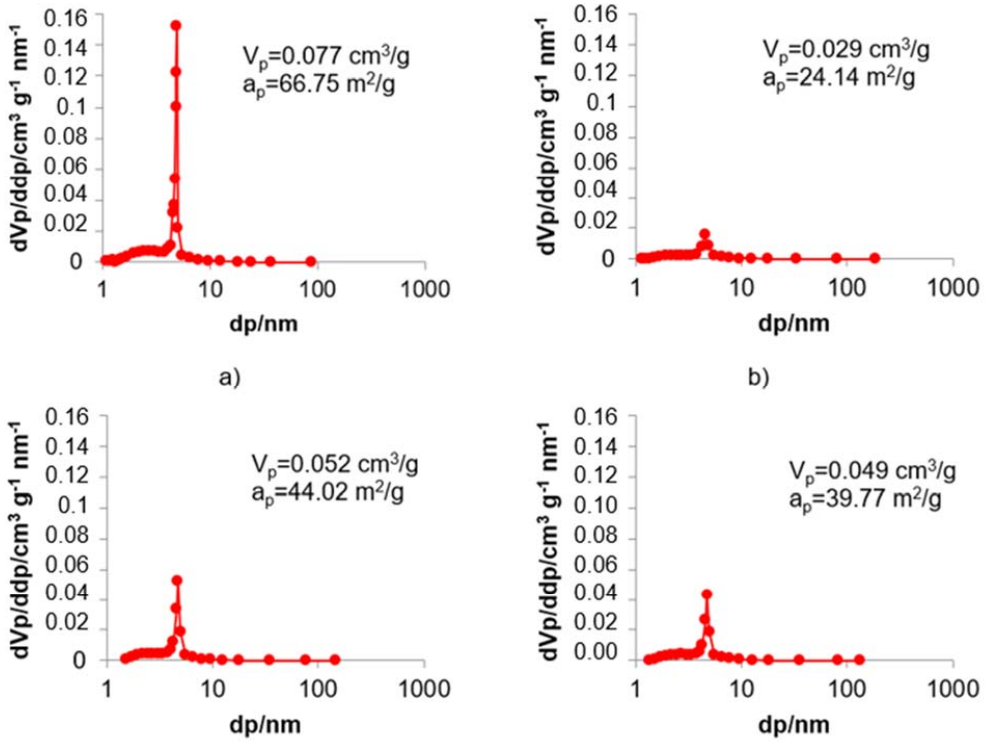

Fig. 10. Specific surface area values and pore size distribution (Barrett–Joyner–Halenda method) in cement stone at 28 days depending on binder mixture composition: a) WPC, b) WPC + GEPS, c) WPC + EPS–An, d) WPC + EPS–An + MC

of anatase on the surface of GEPS particles (Table 5, No. 3) mitigated hydration retardation, reflected in intermediate values of specific surface area and total pore volume between the specimen without additives and the GEPS-containing specimen. Slightly lower and similar values were observed for the EPS–An + + MC specimen. The decrease in specific surface area (by 39 %) and total nanopore volume (by 36 %) compared with the composition without additives indicates the clogging of pore space by both newly formed structures and additive components acting as microfillers.

Conclusion

It has been found that the combined use of a multifunctional composite material EPS–An, produced by co-grinding acid-pretreated expanded perlite sand with anatase, poly-dispersed microcalcite, and a plasticizer in a white Portland cement-based binder allows mitigating the negative impact of fine mineral additives on the water demand of the mixture. This effect is attributed to the improved particle size distribution of the multicomponent binder as well as to the enhanced efficiency of the polycarboxylate plasticizer in the presence of carbonate particles.

Analysis of the phase composition and microstructural features demonstrated that the application of the EPS–An + MC additive complex promotes accelerated hydration, reduces microporosity, and increases the homogeneity and density of cement stone. Low-temperature nitrogen adsorption showed a decrease in specific surface

area and total nanopore volume of cement stone by 39 % and 36 %, respectively, compared with the composition without additives, indicating a higher degree of cement hydration and pore space clogging by reaction products in the presence of reactive components.

It has been established that replacing 40 % of white Portland cement with the fine mineral additive complex EPS–An + MC (1:1 ratio) allows obtaining a binder with a compressive strength of 65.2 MPa at 28 days of standard curing. The presence of mineral additives shifts the main hydration peak by 27 minutes and increases the heat release intensity by 21 % compared with the additive-free composition due to the nucleation effect on the surface of highly dispersed particles and the pozzolanic reaction. After steam curing, the compressive and flexural strength of the binder exceeds that of the control specimen by 2 % and 1.5 %, respectively.

The study has established patterns of influence of the mineral additive complex on the rheological properties, heat release kinetics, phase composition, and microstructure of cement stone. Optimal dosages and particle size distribution of the mineral additive complex have been proposed, ensuring: production of highly workable cement pastes with reduced water demand, acceleration of the main hydration period onset, intensification of phase and structure formation processes, formation of dense homogeneous cement stone, and high photocatalytic activity.

It has been established that the combined use of the proposed mineral additive complex, with reduced cement content, provides high physical and mechanical performance of the cement system and can be applied to produce white decorative fine-grained concretes suitable for thin-walled products.

Financing

This work was carried out as part of the implementation of the state assignment of the Ministry of Science and Higher Education of the Russian Federation No. FZWN-2023-0006 using the equipment of the High Technology Center at Shukhov Belgorod State Technological University.

References

Abouelnour, M. A., Abd El-Aziz, M. A., Osman, K. M., Fathy, I. N., Tayeh, B. A., and Elfakharany, M. E. (2024). Recycling of marble and granite waste in concrete by incorporating nano alumina. *Construction and Building Materials*, Vol. 411, 134456. DOI: 10.1016/j.conbuildmat.2023.134456.

Ayubov, N. A., Fomina, E. V., Ageeva, M. S., Antoshina, N. V., Sabitov, L. S., and Sibgatullin, E. S. (2024). The use of expanded perlite waste in the composition of a composite binder. *Engineering Journal of Don*, No. 8 (116), pp. 577–590.

Balykov, A. S., Nizina, T. A., Korovkin, D. I., Volodin, V. V., Smakaev, R. M., and Gajiyeva, U. M. (2018). Study of reotechnological properties of cement and mineral suspensions for self-compacting concrete mixtures development. *Ogarev-Online*, Vol. 6, No. 9, 3.

Bazhenova, O. Yu. and Bazhenova, S. I. (2016). Features of structure of decorative concrete. *Advances in Modern Science*, Vol. 3, No. 6, pp. 21–23.

Beregovoy, V. A., Snadin, E. V., Inozemtsev, A. S., and Pilipenko, A. S. (2023). High-performance concretes for machine building with nano and micro-scale raw materials. *Nanotechnologies in Construction*, Vol. 15, No. 3, pp. 200–210. DOI: 10.15828/2075-8545-2023-15-3-200-210.

Berov, Ya. I., Petrov, S. P., Nasedkin, V. V., and Dudko, P. G. (2006). Some aspects of perlite concrete use in construction. *Construction Materials*, No. 6, pp. 82–83.

Cherkasov, V. D., Buzulukov, V. I., Tarakanov, O. V., and Yemelyanov, A. I. (2015). Structure formation of cement composites with addition of modified diatomite. *Construction Materials*, No. 11, pp. 75–77.

Grzeszczyk, S. and Janus, G. (2021). Lightweight reactive powder concrete containing expanded perlite. *Materials*, Vol. 14, Issue 12, 3341. DOI: 10.3390/ma14123341.

Kalashnikov, V. I. (2011). Terminology of the science of new generation concrete. *Construction Materials*, No. 3, pp. 103–106.

Kalashnikov, V. I., Tarakanov, O. V., Volodin, V. M., Erofeeva, I. V., and Abramov, D. A. (2023). Concretes of transitional and new generations. Status and prospects. *Concrete Technologies*, No. 2 (187), pp. 33–38.

Kharitonov, A. M., Sidorova, A. S., and Andreev, D. M. (2023). Expanded perlite additive for modification of properties of cement composites. *Cement and its Applications*, No. 4, pp. 72–75.

Kopanitsa, N. O., Demyanenko, O. V., and Kulikova, A. A. (2023). Complex additives based on secondary resources for modification of cement composites. *Bulletin of the Tomsk Polytechnic University. Geo Assets Engineering*, Vol. 334, No. 1, pp. 136–144.

Kotwica, Ł., Pichór, W., Kapeluszna, E., and Różycka, A. (2017). Utilization of waste expanded perlite as new effective supplementary cementitious material. *Journal of Cleaner Production*, Vol. 140, Part 3, pp. 1344–1352. DOI: 10.1016/j.jclepro.2016.10.018.

Kulikova, A. A., Dem'yanenko, O. V., Sorokina, E. A., and Kopanitsa, N. O. (2019). Complex modifying additives for cement construction mixes. *Journal of Construction and Architecture*, Vol. 21, No. 6, pp. 140–148. DOI: 10.31675/1607-1859-2019-21-6-140-148.

Kuznetsova, T. V., Nefed'ev, A. P., and Kossov, D. Yu. (2015). Kinetics of hydration and properties of cement with metakaolin addition. *Construction Materials*, No. 7, pp. 3–4.

Ledyaykina, O. V. and Ledyaykin, N. V. (2024). Study of the influence of modified additives on the properties of concrete. *Bulletin of BSTU named after V. G. Shukhov*, No. 4, pp. 8–15. DOI: 10.34031/2071-7318-2024-9-4-8-15.

Li, L., Sun, W., Feng, Z., Li, Y., Feng, T., and Liu, Z. (2024). Hydration kinetics and apparent activation energy of cement pastes containing high silica fume content at lower curing temperature. *Construction and Building Materials*, Vol. 435, 136881. DOI: 10.1016/j.conbuildmat.2024.136881.

Loganina, V. I. and Fokin, G. A. (2019). Ensuring the quality of the external type of varnish and paint coatings of cement concrete. *Regional Architecture and Engineering*, No. 3 (40), pp. 68–72.

Luo, H., Aguiar, J., Wan, X., Wang, Y., Cunha, S., and Jia, Z. (2024). Application of aggregates from construction and demolition wastes in concrete: review. *Sustainability*, Vol. 16, Issue 10, 4277. DOI: 10.3390/su16104277.

Martins, J. R., Rocha, J. C., Hotza, D., and Senff, L. (2024). Rheological and stability analysis of cement pastes incorporating silica-based wastes. *Particuology*, Vol. 89, pp. 144–152. DOI: 10.1016/j.partic.2023.11.005.

Miryuk, O. A. and Zagorodnyuk, L. H. (2022). Granular materials based on expanded sands and their production waste. *Complex Use of Mineral Resources*, Vol. 321, No. 2, pp. 14-21. DOI: 10.31643/2022/6445.13.

Moroz, M. N., Kalashnikov, V. I., and Suzdalsev, O. V. (2016). Classification criteria for the formation of the surface of architectural and decorative concretes. *Modern Scientific Researches and Innovations*, No. 10 (66), pp. 114–117.

Mousavinejad, S. H. G. and Pourjamali, M. (2024). Determining the mechanical behavior of thin-walled cylindrical shells of cement composite containing graphene oxide and glass fibers with the help of fuzzy logic model and artificial neural network. *Innovative Infrastructure Solutions*, Vol. 9, Issue 8, 332. DOI: 10.1007/s41062-024-01644-w.

Natsievsky, S. Yu. (2006). Perlite in modern concrete, dry building mixes, and non-combustible heat insulation products. *Construction Materials*, No. 6, pp. 78–81.

Pogorelov, V. A. (2010). Influence of concrete mixture grading on the structural transformation of concrete strength. *Vestnik MGSU*, No. 1, pp. 200–206.

Shirina, N. V. and Zagorodnyuk, L. H. (2007). Perlite dust — an effective filler for dry building mixes. *Construction Materials*, No. 5, pp. 44–45.

Sidorova, A. S. (2024). Analysis of perlite additive as internal cure agent in cement concrete system. *Bulletin of BSTU named after V. G. Shukhov*, No. 7, pp. 25–34. DOI: 10.34031/2071-7318-2024-9-7-25-34.

Stenechkina, K. S. (2023). The use of decorative concrete for finishing buildings and structure. *Engineering Journal of Don*, No. 3 (99), pp. 418–428.

Stoyanov, V., Petkova, V., Mihaylova, K., and Shopska, M. (2024). A study of the influence of thermoactivated natural zeolite on the hydration of white cement mortars. *Materials*, Vol. 17, Issue 19, 4798. DOI: 10.3390/ma17194798.

Tarasov, V. N., Gusev, B. V., Petrunin, S. Yu., Korotkova, N. P., and Garnovesov, A. P. (2018). Performance assessment of polycarboxylate superplasticizers for concrete manufacturing. *Journal of Science and Education of North-West Russia*, Vol. 4, No. 1, pp. 29–40.

Taylor, H. F. W. (1996). *Cement Chemistry*. Moscow: Mir, 560 p.

Tolstoy, A. D., Lesovik, V. S., and Milkina, A. S. (2018). Improving new generation concretes (NGCs) by introducing technogenic materials. *IOP Conference Series: Materials Science and Engineering*, Vol. 463, Issue 2, 022095. DOI: 10.1088/1757-899X/463/2/022095.

Voronov, V. V. and Glagolev, E. S. (2020). Polymineral composite binders for foam concrete: features of hydration and hardening. *The Russian Automobile and Highway Industry Journal*, Vol. 17, No. 1 (71), pp. 122–135. DOI: 10.26518/2071-7296-2020-17-1-122-135.

Xu, K., Yang, J., He, H., Wei, J., and Zhu, Y. (2025). Influences of additives on the rheological properties of cement composites: a review of material impacts. *Materials*, Vol. 18, Issue 8, 1753. DOI: 10.3390/ma18081753.

Zhao, D., Williams, J. M., Li, Z., Park, A. H. A., Radlińska, A., Hou, P., and Kawashima, S. (2023). Hydration of cement pastes with calcium carbonate polymorphs. *Cement and Concrete Research*, Vol. 173, 107270. DOI: 10.1016/j.cemconres.2023.107270.

ВЯЖУЩЕЕ НА ОСНОВЕ БЕЛОГО ЦЕМЕНТА ДЛЯ САМООЧИЩАЮЩЕГОСЯ МЕЛКОЗЕРНИСТОГО БЕТОНА

Валерия Строкова, Юлия Огурцова, Екатерина Губарева* , Наталия Хмара, Александра Буковцова, Виктория Иванова, Маргарита Скороходова

Белгородский государственный технологический университет им. В.Г. Шухова, Белгород, Россия

*E-mail: 43448504@mail.ru

Аннотация

Введение. Проблема получения бетонных изделий сложных форм, тонкостенных, прочных и устойчивых к атмосферным воздействиям, способных сохранять декоративный вид в процессе эксплуатации, при максимальном вовлечении в их производство техногенного (вторичного) минерального сырья, заключается в том, что при необходимости получения изделий белого цвета диапазон возможного сырья резко сокращается. Также необходимым является снижение содержания портландцемента в бетонах. В связи с этим, актуальной задачей является разработка современных вяжущих и бетонов с пониженным содержанием портландцемента на основе минеральных компонентов белого цвета. **Материалы и методы.** В качестве вяжущего вещества использован белый портландцемент без минеральных добавок ПЦБ 1-500-Д0 Cemix ProWhite производства ООО «Цемикс», респ. Башкортостан; в качестве добавок рассмотрены: вспученный перлитовый песок (пуццолановая добавка), микрокальцит (карбонатная добавка) и анатаз (фотокаталитическая добавка), а также их смеси; в качестве пластифицирующей добавки использован пластификатор на поликарбоксилатной основе Melflux 1641 F. Оценка основных физико-механических свойств вяжущего и цементного камня на его основе (нормальная густота, расплыв мини-конуса, предел прочности) проведена по стандартным методикам, удобоукладываемость смесей анализирована по результатам реотехнологических показателей, показатели интенсивности тепловыделения при гидратации цементного камня получены методом калориметрии. Также в работе отражены особенности микроструктуры получаемого цементного камня. **Результаты.** Выявлено, что замена 40 % цемента на комплекс минеральных добавок при использовании пластификатора позволяет нивелировать негативное влияние тонкодисперсных компонентов на водопотребность смеси. Отмечается интенсификация процессов гидратации, повышение однородности и плотности цементного камня, а также снижение удельной поверхности и суммарного объема нанопор цементного камня на 39 % и 36 % соответственно. Присутствие минеральных добавок позволяет получить вяжущее с прочностью на сжатие 65,2 МПа в возрасте 28 суток нормального твердения.

Ключевые слова: белый портландцемент, перлитовый песок, комплексная добавка, микроструктура, гидратация, бетон.

Guide for Authors
for submitting a manuscript for publication
in the «Architecture and Engineering»

The journal is an electronic media and accepts the manuscripts via the online submission. Please register on the website of the journal http://aej.spbgasu.ru/, log in and press “Submit article” button or send it via email aejeditorialoffice@gmail.com.

Please ensure that the submitted work has neither been previously published nor has been currently submitted for publication in another journal.

Main topics of the journal:

1. Architecture
2. Civil Engineering
3. Geotechnical Engineering and Engineering Geology
4. Urban Planning
5. Technique and Technology of Land Transport in Construction

Title page

The title page should include:

The title of the article in bold (max. 90 characters with spaces, only conventional abbreviations should be used); The name(s) of the author(s); Author’s(s’) affiliation(s); The name of the corresponding author.

Abstract and keywords

Please provide an abstract of 100 to 250 words. The abstract should not contain any undefined abbreviations or unspecified references. Use the IMRAD structure in the abstract (introduction, methods, results, discussion).

Please provide 4 to 6 keywords which can be used for indexing purposes. The keywords should be mentioned in order of relevance.

Main text

It should have the following structure:
1) Introduction,
2) Scope, Objectives and Methodology (with subparagraphs),
3) Results and Discussion (may also include subparagraphs, but should not repeat the previous section or numerical data already presented),
4) Conclusions,
5) Acknowledgements (the section is not obligatory, but should be included in case of participation of people, grants, funds, etc. in preparation of the article. The names of funding organizations should be written in full).

General comments on formatting:

- Subtitles should be printed in Bold,
- Use MathType for equations,
- Tables should be inserted in separate paragraphs. The consecutive number and title of the table should be placed before it in separate paragraphs. The references to the tables should be placed in parentheses (Table 1),
- Use “Top and Bottom” wrapping for figures. Figure captions should be placed in the main text after the image. Figures should be referred to as (Fig. 1) in the text.

References

The journal uses Harvard (author, date) style for references:
- The recent research (Kent and Park, 1990)...
- V. Zhukov (1999) stated that…

Reference list

The list of references should only include works that are cited in the text and that have been published or accepted for publication. Personal communications and unpublished works should only be mentioned in the text. Do not use footnotes or endnotes as a substitute for a proper reference list. All references must be listed in full at the end of the paper in alphabetical order, irrespective of where they are cited in the text. Reference made to sources published in languages other than English or Russian should contain English translation of the original title together with a note of the used language.

Peer Review Process

Articles submitted to the journal undergo a double blind peer-review procedure, which means that the reviewer is not informed about the identity of the author of the article, and the author is not given information about the reviewer.
On average, the review process takes from one to five months.